2023-01-17

Age-induced errors in DNA replication and repair in Saccharomyces cerevisiae

Mair, Nicola

UNIVERSITY OF CALGARY

Age-induced errors in DNA replication and repair in *Saccharomyces cerevisiae*

by

Nicola Mair

A THESIS

SUBMITTED TO THE FACULTY OF GRADUATE STUDIES

IN PARTIAL FULFILMENT OF THE REQUIREMENTS FOR THE

DEGREE OF DOCTOR OF PHILOSOPHY

GRADUATE PROGRAM IN BIOCHEMISTRY AND MOLECULAR BIOLOGY

CALGARY, ALBERTA

JANUARY, 2023

ABSTRACT

Aging is a multifactor process that leads to a widespread decrease in cellular function. The single most significant risk factor for developing cancer is age. Cancer is a disease of genome instability, and much of this genomic damage accumulates during DNA replication and inefficient repair. Although DNA replication and repair mechanisms have been extensively studied, little is known about whether these processes are altered with age. Accordingly, **my thesis aims to define age-related differences in DNA replication and repair** in the model organism budding yeast (*Saccharomyces cerevisiae).* By employing budding yeast as a model system, I have developed a protocol to isolate large quantities of precisely aged cells, thus allowing molecular comparisons between young and old cells. The results indicate that during cellular aging, there is a reduction in the efficiency of replication initiation. There is a reduction in the recruitment of polymerases and MCM helicases to the origins of replication. This coincides with a decrease in origin firing and DNA synthesis. I have also shown that double-strand break (DSB) repair becomes highly mutagenic as yeast cells age. The efficiency of homologous recombination and non-homologous end joining decreases, and the incidence of repair through alternative end-joining increases. Aged cells have an overall lower level of repair, and the recruitment of repair proteins to DSBs is impaired. Altogether, my work has identified mechanisms of DNA replication and repair that become increasingly dysregulated with age.

PREFACE

This thesis is presented in five major parts; in Chapter 1, I give a general overview of cellular aging, DNA replication, DNA damage, and DNA damage repair pathways. In Chapter 2, I discuss the need for a new method to enrich old yeast cells and how I developed a technique allowing large-scale molecular biology and biochemical studies. The content of Chapter 3 is being prepared as a manuscript for submission in collaboration with the Brown Laboratory (University of Toronto), where I am a co-first author and investigated DNA replication during aging. Chapter 4 contains a published manuscript titled *"Changes in DNA double-stand break repair during aging correlate with an increase in genomic mutations,"* where I am a co-first author. Finally, Chapter 5 summarises general conclusions and explores future directions.

ACKNOWLEDGEMENTS

Firstly, I would like to thank my supervisor, Dr. Jennifer Cobb, for her mentorship throughout my doctoral studies. I am fortunate to have been supported by such a great scientist and genuinely kind person. I am also grateful to my committee members, Dr. Aaron Goodarzi, Dr. Gareth Williams, and Dr. Dave Schriemer, for all their guidance and valuable technical advice, which helped me complete my Ph.D. project.

I express gratitude to the members of the Cobb Lab for their scientific discussions and support. Special thanks to Dr. Aditya Mojumdar for his consistent mentorship throughout my Ph.D., answering my never-ending list of questions and helping me become the scientist I am today. Thank you to Dr. Sarah Moradi-Fard, and Dr. Nancy Adam for all your help and the many coffee breaks to keep us fueled. Thank you to Laura Sosa for all your encouragement, joy and singing that got me through many long lab days. I also want to thank Carin Pihl, Shilpa Salgia and King Hsieh for keeping the lab organized and running daily. You all made the Cobb lab a genuinely wonderful place, and I am thankful for our shared experiences.

I want to thank everyone in my family, especially my siblings, Alex, Max and Rachel, and my granny Isobel, for their unwavering support and love. I would also like to thank Sammy and Christina for their friendship, encouragement, and laughter through the years. Finally, I would like to thank my husband, Michael, for his patience and support, but most of all, for pushing me forward through every obstacle and always having unwavering faith in me.

DEDICATION

I dedicate this thesis to the loving memory of my parents, Alex and Catherine, my grandparents, Sandy, Bill, Maria, and my aunt Trisha. I wish you had been here to see how far I have come, and I hope I have made you proud.

TABLE OF CONTENTS

LIST OF TABLES

LIST OF ILLUSTRATIONS, FIGURES AND GRAPHICS

GLOSSARY OF TERMS, SYMBOLS AND ABBREVIATIONS

TERM	DEFINITION
4C	Chromosome conformation capture on chip
ABF	ARS-Binding factor
ACS	ARS consensus sequence
ADE	Adenine
AGP	High-affinity glutamine permease
ALT	Alternative lengthening of telomeres
ALT-EJ	Alternative end-joining
AMP	Adenosine monophosphate
AMPK	AMP-activated protein kinase
ARS	Autonomously replication sequences
ATP	Adenosine 5’-triphosphate
BER	Base excision repair
BIR	Break induced replication
Bp	Base pairs
BRDU	Bromodeoxyuridine
BSA	Bovine serum albumin
CDC	Cell division cycle
CDK	Cyclin dependant kinase
CDT	Chromatin licensing and DNA replication factor
CFP	Cyan fluorescent protein
ChIP	Chromatin immunoprecipitation
ChIP-Seq	ChIP-sequencing
CHK	Checkpoint kinase
CLB	Cyclin B
CLS	Chronological lifespan
CMG	Cdc45-MCM-GINS complex
cNHEJ	Classical non-homologous end joining
CPT	Camptothecin
CRISPR	Clustered regularly interspaced short palindromic repeats
CTF4	Chromosome transmission fidelity
CTIP	CtBP interacting protein
DBF	Dumb bell former
DDC	DNA damage checkpoint
ddH20	Double distilled water

DDK	Dbf4-dependant kinase
DDR	DNA damage response
dHJ	Double Holliday junction
DIA2	Digs into agar
DNA	Deoxyribonucleic acid
DNL	DNA ligase
dNTPs	Deoxyribonucleotide triphosphate
DPB	DNA polymerase B
DRC	DNA replication checkpoint
DSB	Double strand break
dsDNA	Double-stranded DNA
EC	Euchromatin
EDTA	Ethylenediaminetetraacetic acid
EJ	End joining
EMS	Ethyl methanesulfonate
ER	Endoplasmic reticulum
ERC	Extrachromosomal rDNA circle
EXO	Exonuclease
FEN	Flap structure-specific endonuclease
FKH	Forkhead homolog
FOB	Fork blocking less
GAL	Galactose
Gb	Gigabyte
GFP	Green fluorescent protein
GINS	Go-ichi-ni-san (Sld5, Psf1, Psf2, Psf3)
GLN	Glutamine metabolism
GLU	Glucose
H	Histone
HA	Hemagglutinin
HC	Heterochromatin
HEALTHSPAN	The period of one's life that one is healthy
HGPS	Hutchinson-Gilford progeria syndrome
HIS	Histidine
HML	Homothallic mating left
HMR	Homothallic mating right
HO	Homothallic switching endonuclease
HR	Homologous replication
HRQ	Homologous to RecQ protein
HSC	Hematopoietic stem cells

HU	Hydroxyurea
IGV	Integrative genomics viewer
INM	Inner nuclear membrane
IP	Immunoprecipitation
K	Lysine
Kb	Kilobase
KD	Dissociation constant
KU	Yeast KU protein
LEU	Leucine
LIF	Ligase interacting factor
LOH	Loss of heterozygosity
LSM	Laser scanning microscopy
LYS	Lysine requiring
M	Molar
MAT	Mating type
Mb	Megabyte
MCM	Mini chromosome maintenance
MEP	Mother enrichment programme
MH	Micro homology
MMEJ	Microhomology-mediated end joining
MMS	Methyl methanesulfonate
Mnase-seq	Micrococcal nuclease digestion with sequencing
MPS	Mono polar spindle
MRC1	Mediator of the replication checkpoint
MRE	Meiotic recombination
mRNA	Messenger ribonucleic acid
MRX	Mre11/Rad50/Xrs2 complex
NaCl	Sodium Chloride
NAD	Nicotinamide adenine dinucleotide
NEJ	Non-homologous end joining defective
NER	Nucleotide excision repair
NFR	Nucleosome free region
NHEJ	Non-homologous end-joining
nM	Nanomolar
No	Number
NPC	Nuclear pore complex
NUP	Nuclear Pore
O	Old
OCE	Old cell enrichment

OE	Overexpression
ORC	Origin recognition complex
PBS	Phosphate buffered saline
PCNA	Proliferating cell nuclear antigen
PCR	Polymerase chain reaction
PGK	3-Phosphoglycerate kinase
pH	Potential of hydrogen
PIF	Petite integration frequency
PMSF	Phenylmetylsulfonyl fluoride
POL	Polymerase
POL α	DNA polymerase alpha
POL δ	DNA polymerase delta
POL ε	DNA polymerase epsilon
POL ζ	DNA polymerase zeta
Pre-IC	Pre-initiation complex
Pre-RC	Pre-replication complex
PSF	Partner of Sld Five
RAD	Radiation sensitive
RAP	Repressor/activator site binding protein
rDNA	Ribosomal DNA
RLS	Replicative lifespan
RMI	RecQ-mediated genome instability
RNA	Ribonucleic acid
ROS	Reactive oxygen species
RPA	Replication factor A
RPD	Reduced-potassium dependency
rRNA	Ribosomal RNA
SAE	Sporulation in the absence of spo eleven
SC	Synthetic complete
SDS	Sodium dodecyl sulphate
SDSA	Synthesis dependent strand annealing
SGS	Slow growth suppressor
SIR	Silent information regulator
SLD	Synthetic lethal with Dpb11-1
SMC	Structural maintenance of chromosomes
SSA	Single strand annealing
SSA	Single strand annealing
SSB	Single strand breaks
ssDNA	Single-stranded DNA

STR	Sgs1-Top3-Rmi1 complex
SUMO	Sumoylation
TCA	Tricarboxylic acid
TCA	Tricarboxylic acid cycle
TE	Tris EDTA solution
TOP	Topoisomerase
TOR	Target of rapamycin
T_{Rep}	Time of replication initiation
TRP	Tryptophan
UBC	Ubiquitin-conjugating
URA	Uracil
UV	Ultra-violet
V	Vector
WRN	Werner RecQ-like helicase
WS	Werner Syndrome
WT	Wild type
XRS	X-ray sensitive
Y	Young
YNB	Yeast nitrogen base
YPAD	Yeast peptone adenine dextrose medium
ΔOrigin	Change in the origin of aged cells

Chapter 1 Introduction

1.1 Cellular Aging and Cancer

1.1.1 Aging and Disease

Aging is an inevitable consequence of life that leads to the decline of physiological function and is the predominant risk factor for many diseases. Many easily recognizable phenotypical changes occur in humans during aging, such as wrinkled skin, graying hair and deterioration of eyesight and hearing. Although medical advancements have extended average lifespans, the average health span has not extended as quickly (1). This has led to aging being the most significant contributor to death and disease. Aging researchers have focused on understanding genes that can alter the lifespan of organisms to extend and improve the quality of life (2). Age-related diseases such as Alzheimer's, cancer and heart disease are affecting more people than ever (3,4). Geroscience studies the interactions between natural aging, chronic illness, and health (5). Aging research is often carried out in model organisms such as yeast, worms, flies, and mice. However, much research on animal models such as mice has not considered the aging process, resulting in unsuccessful preclinical trials in cases where age is not accounted for as an experimental variable, particularly for diseases that most often occur in an aged population (6). Therefore, we must understand the cellular and molecular processes that deteriorate during aging. Understanding these fundamental processes will help develop therapies to increase the health span of the population.

As humans age, we are at a higher risk of developing cancer. However, not all mammals have the same cancer risk. For example, mice are often used in research and are very short-lived, with very

high chances of developing cancer (7). By contrast, the naked mole rat, similar in size to a mouse, appears to be cancer resistant and lives much longer (8). The oldest naked mole rat was over 30 years old, ten times longer than a mouse, and there have been very few incidences of cancer (9,10). Studies into the naked mole rat's ability to evade cancer have determined that they have an increase in tumour suppressor mechanisms and do not have replicative senescence. Organisms that are highly efficient at repairing DNA damage have much longer lifespans. Therefore, studies of both short- and long-lived animals can allow us to understand disease progression and its changes during aging.

1.1.2 Cellular Aging in Yeast

Cellular aging is the universal functional deterioration that ultimately results in cellular death. Aging happens at a cellular level, a tissue level, and a whole organism level in humans. However, as yeast is a single-celled eukaryotic organism, we can understand the changes at a cellular level and a whole organismal level during aging. Work in *Saccharomyces cerevisiae* (budding yeast) has been valuable for understanding environmental and genetic modulators of aging. Although a culture of budding yeast can be propagated indefinitely, each cell has a finite lifespan and displays distinct age-related phenotypes (11). Yeast has a fully-sequenced genome and a short lifespan relative to higher eukaryotes. Importantly, yeast has a vast array of powerful genetic tools that allow researchers to easily manipulate the environment to address fundamental questions about yeast aging (12,13).

Yeast aging correlates with an accumulation of cellular damage from both the external environment and internal cellular processes (14). A yeast cell undergoes a limited number of

asymmetric divisions before it becomes sterile and eventually dies (15). When a cell divides, we refer to it as the 'mother' cell. This mother cell continuously ages with each division, while its progeny, the 'daughter' cells, are rejuvenated with full replication potential. However, daughters budding from very old mothers, in the final five replications before death, have a reduced lifespan and divide at a slower rate than daughters of young mothers (16,17). Daughters of aged mothers have a 100-fold increase in mutations (18). Microdissection studies show that the division time increases as the mother cell ages, with the final five divisions before death being the longest (17,19,20). Wild type (WT) yeast of W303 background average 23 divisions during their lifespan. However, the average lifespan of different yeast strains varies depending on their distinct genetic background (21).

Cell size increases with age, which results in a larger volume and smaller surface-to-volume ratio. The most significant increase in size occurs within the final divisions of the mother cell's life (22). Moreover, it has also been shown that up to 20% of WT cells do not undergo more than ten divisions, suggesting that aging can directly impact yeast lifespan (22,23). As cells age, there is an increase in loss of heterozygosity (LOH) and a decrease in the stability of the ribosomal DNA (rDNA) locus. This leads to extrachromosomal rDNA circles (ERCs) accumulating in mother cells and higher levels of genomic instability (24,25). ERCs are external circles of DNA from the rDNA region that occur during HR of nearby double-strand breaks (DSBs).

Cellular senescence is the inability of a cell to progress through the cell cycle in response to a stressor (26). This occurs as the mother cell accumulates damaged cellular material, which is not passed to the daughter cell during asymmetrical division. During yeast cellular division, many

age-induced factors, including ERCs, heat shock proteins and nuclear pore complexes (NPCs), are selectively maintained in the mother cell and not passed to budding daughter cells (27,28).

The age of yeast can be measured in two ways: the replicative lifespan (RLS) and the chronological lifespan (CLS) (29,30). The RLS is the number of cellular replication events a mother cell can undergo and produce a daughter before it undergoes replicative senescence. The CLS is the duration that a population can grow and survive as measured in units of time on a clock. The two forms of yeast aging are suggested to be analogous to different forms of mammalian aging. The RLS is pertinent for the aging of actively dividing cells or stem cell populations. In contrast, CLS is more applicable to non-dividing or postmitotic cells in the tissues of a multicellular organism.

Dietary restriction and inhibition of the TOR pathway extend the lifespan of yeast in the same way it does for other organisms (31–33). Many studies in aging research have involved mutating genes that change the lifespan of yeast. Less research has been performed on natural aging and the mechanisms that result in cellular senescence or apoptosis. Yeast has been critical in developing and researching many anti-aging drugs and will likely be crucial in understanding the mechanism of action (34).

1.1.3 Hallmarks of Cellular Aging

The nine hallmarks of aging have been characterized in eukaryotes and described as a time-dependent decline in function. They include: genomic instability, telomere attrition, epigenetic alterations, loss of proteostasis, deregulated nutrient sensing, mitochondrial dysfunction, cellular senescence, stem cell exhaustion and altered intercellular communication (35). These hallmarks

were identified as occurring during normal aging. They could be exacerbated and alleviated through experimental procedures leading to an increase or decrease in lifespan, and they will be briefly reviewed below.

The use of yeast in aging studies has been monumental in understanding many of these hallmarks and aging processes. Changes have been shown to occur within the yeast organelles and harm cellular survival during aging (Figure 1.1). Mutational studies have expanded the lifespan of yeast by trying to counteract these hallmarks and increase the healthspan of yeast (36).

One heavily studied area within the aging field is genomic stability. DNA is continuously challenged by exogenous and endogenous damage, such as the alkylation of bases and ionizing radiation, and any genetic lesions that occur, which are not repaired, will accumulate with age (37). Although mechanisms exist to prevent and repair DNA damage, DNA repair capacity diminishes over time (38). This leads to an increase in translocations, amplification of chromosomal regions, DNA breaks and retrotransposition in yeast (25). Therefore, aging correlates with a loss of genomic stability and an increase in cellular damage (39). The hypothesis that genomic instability causes aging is supported by the linkage between premature aging syndromes and defects in DNA repair machinery (40). The accumulation of DNA damage can lead to a loss of homeostasis due to the dysfunction of essential proteins, which, if not repaired, can lead to senescence or apoptosis. Defects in the nuclear envelope can also lead to genomic instability (41). The nuclear envelope has an essential role in providing structural support with protein complexes and organizing DNA accessibility in part by tethering certain regions of the genome (42).

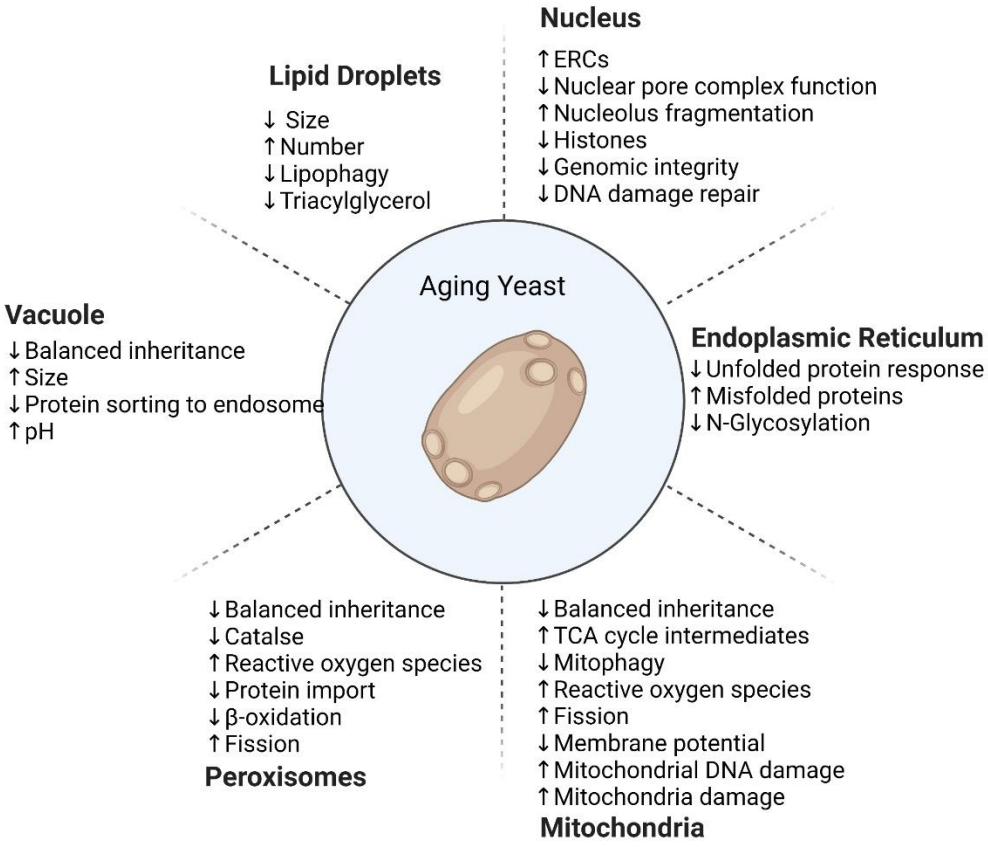

Figure 1.1 Cellular changes that occur in yeast during aging

A schematic of the many cellular changes that occur in the organelles of yeast during aging. These can drastically affect the yeast cell and its overall functionality. A consequence of the interconnectedness of these pathways is that disruption in one system leads to further disruption of others, causing a self-reinforcing cycle of ever-increasing dysregulation. Eventually, the accumulation of damage leads to the death of the cell.

Telomeres are the protective caps at the end of chromosomes that shorten with every round of DNA replication. Telomere shortening occurs during normal aging, which can lead to complete telomere loss and cellular senescence (43). Telomere attrition is a hallmark of aging in many eukaryotes. Telomerase is a reverse transcriptase which can replicate telomeres; however, most mammalian somatic cells do not express telomerase. As telomerase is expressed in yeast cells, they do not experience the same shortening as human cells and therefore have limited relevance regarding changing with age.

There are many changes to the epigenetic landscape as cells age, including posttranslational modifications of histones and chromatin remodelling. During aging, there is a global loss of heterochromatin (HC) and a change in its distribution throughout the genome (44). As cells age, there is a loss of HC at the mating type loci that leads to sterility and at the rDNA locus, which results in genomic instability (21,45). It is thought that this age-related loss of HC leads to adverse changes in DNA repair and changes in transcription (46).

The loss of protein homeostasis (proteostasis) contributes to cellular aging (47). In normal cells, many mechanisms are employed to ensure proteins are folded and maintained within the cell; however, these have been shown to fail as cells age (48). The accumulation of dysfunctional proteins within the cell directly affects cellular function.

Nutrient sensing pathways across many species have also been implicated in the aging process, and dietary restriction increases many eukaryotes' lifespans while decreasing age-related diseases (49). Many studies have been carried out to understand the nutrient signalling pathways, such as the TOR signalling pathway, which senses high amino acid concentrations, the AMPK pathway, which detects AMP levels; and sirturins which detect high NAD levels (50). When

dietary restriction occurs, it reduces the activity in these pathways and can either directly or indirectly lead to reduced growth factors. A yeast deletion collection was used as a high-throughput assay to determine deletions that lead to an enhanced CLS (51). This high throughput study allowed the investigation of 4800 single gene deletions. A decrease in TOR signalling pathway activity increased CLS by deleting 16 genes implicated in the pathway. These included Gln3, Lys12 and Agp1. Although the deletion of genes can increase lifespan, these mutants can be slow growing and have other fitness defects (52).

Mitochondrial function is known to decrease during the aging process (53). Mitochondria create reactive oxygen species (ROS) as a product of respiration; however, as cells age, they cannot detoxify as efficiently, which can further damage the mitochondrial DNA and other organelles in the cell, progressing the aging process (54). It has been shown that oxidative damage drives aging (55). When yeast cells divide, the mother retains mitochondria with a higher oxidative state (56). This leads to an accumulation of damaged mitochondria in mother cells which can result in senescence. During aging in eukaryotes, senescent cells can accumulate in tissues and are deleterious to homeostasis (57). Stem cells regulate tissue homeostasis, and as organisms age, there is a decline in the regenerative capacity of tissue due to the attrition of stem cells. During aging, the telomeres of stem cells become measurably shorter, which can reduce their rejuvenation capacity (58). Hematopoietic stem cells (HSCs) undergo fewer cell divisions as they age and accumulate DNA damage (59).

During human aging, there is a loss of intercellular communication that leads to the dysregulation of inflammatory reactions. This can lead to a loss of immunosurveillance of external and internal threats in mammals. Defects in the inflammatory response have contributed to obesity, type 2

diabetes and atherosclerosis (60). Inflammation is an essential pathway of the adaptive immune system, which declines with age (61). Although this is a critical hallmark in human aging, yeast is an unsuitable model for studying the immune response (62,63).

The hallmarks of aging have been mentioned and described in isolation above. However, the order in which these changes occur is not fully understood. As the hallmarks do not impact natural aging alone, the loss of function of any mechanism severely impacts other cellular processes. Further understanding which hallmarks have the most significant impact on cell survival will allow us to understand the changes during aging.

1.1.4 Premature aging

Progeroid syndromes are rare genetic disorders that have similar symptoms to natural aging. Individuals afflicted with progeroid syndromes have reduced lifespans, high cancer incidence, and, most often, cardiovascular complications or musculoskeletal degeneration leading to premature death (64). These syndromes are heavily studied due to the severity of the disorders, along with the belief that understanding the basis of the disease could lead to a further understanding of aging.

Most premature human aging syndromes are monogenic and caused by defects in a single protein involved in DNA repair or nuclear envelope architecture (65). Examples of progeroid syndromes include Hutchinson-Gilford progeria syndrome (HGPS), Werner syndrome (WS), Bloom syndrome (BS), Rothmund-Thomson syndrome (RTS) and Cockayne syndrome (CS) (65–70). Although progeroid syndromes share common characteristics such as genetic instability,

developmental defects, skin-related problems and cellular senescence, each disorder also has distinct clinical symptoms.

HGPS occurs due to a mutation in *LMNA,* which encodes the scaffold protein Lamin A. Cells are seen to have abnormalities in the nuclear shape, shortening of telomeres and undergo premature senescence due to genomic instability (71). However, progerin accumulates in cells during natural aging, which highlights one reason why investigating premature aging could provide important clues into the molecular changes that occur during the aging process (72). HGPS progeroid cells are susceptible to DNA damage induced by ionizing radiation and have a reduced repair capacity (73). WS, BS and RTS occur due to mutations in different RecQ helicases, which are essential for managing replication stress and telomere stability. Although they have a range of phenotypic characteristics molecularly, the cells are seen to have chromosomal instability, telomere dysfunction and premature senescence (74). CS is a progeroid syndrome caused by mutations in *ERCC6 or ERCC8*, leading to defects in transcription-coupled nucleotide excision repair (NER). The cells fail to repair damage caused by UV light (67). Although the molecular changes in premature and natural aging are not entirely the same, progeria syndromes such as WS and HGPS have been studied as cellular models of human aging (75). By introducing the specific mutations that drive these human disorders into the homologous proteins in model organisms, research labs can address the effects of these diseases at both a cellular and organismal level.

Proteins conserved in yeast have contributed to studying premature aging diseases and mutations affecting the protein's function within the cell. Although yeast does not have a *LMNA* homolog, RecQ is conserved. Sgs1 and Hrq1 are the two RecQ helicases in yeast. Deletion of Sgs1

leads to a dramatically reduced lifespan (76). In comparison, mutation of Hrq1 leads to cells being sensitive to inter-strand cross-links (77).

Both naturally and prematurely aged cells have a reduction in DNA repair, resulting in DNA damage and genomic instability (78). This research has helped lay the groundwork for understanding how the loss of proteins involved in DNA repair and within the nuclear envelope can have a prominent effect on cellular aging and may help identify new therapeutic approaches for progeria and other age-related diseases.

1.1.5 Genome instability model of aging

The DNA damage theory states that genomic instability causes aging. There have been many studies linking the loss of genomic stability with aging. It is well documented that as cells age, there is an increase in the level of damage (79,80). It is estimated that by old age, each cell has thousands of base mutations within its DNA (81). As mentioned above, this has been supported by the discovery that mutations in DNA repair genes cause many progeroid diseases. Furthermore, cancer treatments like radiation and chemotherapy negatively impact non-cancerous cells by causing high levels of DNA damage and accelerating aging (82).

During normal cellular metabolism, DNA is subjected to damage from both endogenous and exogenous sources resulting in single-strand breaks (SSBs), DSBs, and DNA adducts. When DNA damage occurs in cells, the DNA damage response (DDR) is activated to repair the damage and protect the DNA. As yeast cells age, there is an increase in phosphorylated H2A (γH2A) and Rad52 foci, known as a DNA repair center, showing an increase in age-related DNA damage (25,83). Moreover, old mother cells also have an increase in retrotransposon activity, leading to an

increase in genomic instability (25,84). As well as an increase in DNA damage, it has also been shown that as cells age, there is a decrease in repair capacity and increased sensitivity to genotoxic drugs like ethyl methanesulfonate (EMS) (81,85). This increase in DNA damage and decrease in repair results in an age-dependent increase in genomic instability (86).

The asymmetry in cellular division in budding yeast results in very old mother yeast cells accumulating DNA damage. Even though daughters from very old mothers have a shortened replicative lifespan, their granddaughters are born completely rejuvenated, showing that the accumulation of damage is not detrimental to their offspring (16). But also argues that when the mutational burden gets high enough to impact progeny, cellular division stops so that deleterious mutations are not passed on to the next generation. To support the theory that an increase in genomic instability causes aging, researchers have attempted to demonstrate that improving DNA repair and decreasing the mutational burden results in cells aging more slowly. Several studies have used gene mutations that have led to an increased lifespan in the presence of DNA-damaging agents as an example of improving DNA repair (87,88). For example, the deletion of Fob1 has decreased ERC formation, leading to an increase in lifespan (89–91).

1.1.6 Ribosomal DNA and extra ribosomal rDNA circles model of aging

The rDNA is located within the cell's nucleolus, and as cells age, the rDNA fragments into ERCs and the nucleolus becomes enlarged (21). The rDNA is a tandem repeat region of the genome that encodes both genes and intergenic regions with noncoding elements. The rDNA contains two genes, the 35S rRNA (ribosomal RNA) and the 5S rRNA gene, as well as an origin of DNA

replication with three autonomously replicating sequences (ARS) and a replication fork pause site to prevent RNA and DNA polymerase collision.

The loss of genome integrity during aging occurs universally; however, the rDNA is one of the most damaged regions of the genome during aging (92). This is because there is a high demand for ribosomes within the cell. In yeast, there are around 150-200 copies of the multi-copy DNA element, whereas humans have 300-350 (93). The stability of the rDNA and maintenance of the rDNA copy number is correlated with an increase in lifespan (94). As the rDNA is repetitive, with high levels of transcription, it makes the genome region prone to DSB formation. This leads to fluctuations in the copy number of rDNA repeats and the production of ERCs (95). The cell controls recombination within the arrays through transcriptional silencing mediated by Sir2. Sir2 is a histone deacetylase enzyme that silences areas of the genome, including the rDNA, telomeres, and the silent mating-type loci (96,97). When Sir2 is deleted within cells, ERCs accumulate, leading to a shortened replicative lifespan, loss of silencing, increased changes to rDNA copy number and rDNA instability (21,98–100). At the same time, Sir2 overexpression expands lifespan and prevents the accumulation of ERCs (90,101). Fob1 is a replication fork block protein found within the nucleolus. Its role is to prevent the transcription machinery from colliding with the replication fork within the rDNA. The deletion of Fob1 leads to a stabilization of the rDNA array, extension of lifespan and reduced ERCs (89,102). It indicates that Fob1 leads to genomic instability within the rDNA. Cells with *FOB1* deletions live almost twice as long as WT strains (89). ERCs are replicated during the S phase, so their copy number doubles each cellular division, but they are retained in mother cells. Very old mother cells fail at retaining all the accumulated ERCs passing them to daughter cells, which contributes to the daughters of very old

mother cells having a shorter lifespan. Southern blotting experiments show that old cells can accumulate more than 1000 copies of ERCs, which is more DNA than the entire yeast genome (21). There is a correlation between the number of ERCs in a cell and the time it spends in the S phase because it takes longer to replicate the ERCs (21). The accumulation of ERCs during aging causes a burden on replication machinery and compromises the ability of a cell to replicate the DNA leading to a reduction in lifespan (103).

The number of ERCs is inversely correlated with lifespan, and the introduction of ERCs to a virgin cell causes premature aging and a shorter lifespan (21). It is not known how ERCs cause cellular senescence and death, but they likely titrate away necessary transcription and replication factors during DNA replication (103).

1.1.7 Epigenetics and heterochromatin loss model of aging

Epigenetics is the reversible control of gene expression that does not alter the DNA sequence. Chromatin structure and organization are essential for all genomic processes (104). Types of chromatin modifications include phosphorylation, methylation, acetylation, ubiquitination and sumoylation (104). Chromatin modifications can lead to chromatin being in different states. Euchromatin (EC) is considered 'open,' meaning it contains loosely packed chromatin permissive to transcription. In contrast, heterochromatin (HC) is 'closed,' where the chromatin is more compact and transcriptionally silent.

Distinct epigenetic changes occur during aging, and epigenetic alterations can strongly influence lifespan. Some of the changes during aging include a decrease in HC, remodelling and loss of nucleosomes, changes in histones variants, and global DNA hypomethylation, with regions of

hypermethylation and relocalization of chromatin modifying enzymes. During aging, there is a universal loss of HC, leading to changes in global nuclear architecture and gene expression (44). These epigenetic changes result in altered DNA accessibility and, by extension, altered transcription and activation of transposable elements and genomic instability (105). The Sir2/3/4 complex forms HC, and during aging, there is a decline in Sir2 levels, leading to an increase in H4K16 acetylation levels (106,107). Increasing the histone supply of H3 and H4 through an inducible galactose promoter can expand the lifespan of yeast by up to 50% (25,108). DNA methylation within gene promoters represses transcription and compacts the chromatin; however, as metazoans age, there is a decrease in the overall DNA methylation levels (109).

1.1.8 Loss of proteostasis during aging

As cells age, there is a loss of proteostasis, which leads to an accumulation of dysfunctional proteins that directly affect protein and cell function (110). Many studies have been conducted on the proteasome and autophagy systems to understand the changes that occur during aging. Loss of proteostasis is an early event during aging (111–113). For a cell to function successfully, it requires regulated proteostasis, which is the precise balance of protein synthesis and degradation. Protein function relies on translational modifications, folding, and correct subcellular localization. Ribosome profiling shows that translation efficiency and protein synthesis is reduced during aging (114,115).

Following protein synthesis, many proteins require chaperone proteins to fold correctly. Chaperones also help refold unfolded proteins; however, this process becomes less efficient as cells age (116–119). Over-expressing chaperone proteins in flies lead to a 10-12% increase in

lifespan, demonstrating the importance of protein folding (120,121). However, if proteins are not folded correctly in the endoplasmic reticulum (ER), they must be transported to the cytosol for degradation (122). If misfolded proteins are not efficiently degraded, they accumulate and cause ER stress (123). The cell uses two central systems to degrade proteins, the proteasome and autophagy pathways. The proteasome rapidly degrades proteins through ubiquitin conjugation to the protein, which signals the protein for degradation. As cells age, there is a decrease in ATP levels which hampers the cells' ability to degrade proteins and leads to protein accumulation (124). During aging, there is also an increase in the oxidation of proteins, leading to an increase in damaged proteins (125). Oxidized proteins can aggregate in cells due to the loss of cell geometry and the retention of damaged proteins during division (126,127). The loss of proteostasis is part of many human age-related diseases, such as Alzheimer's and Parkinson's. (128). Overall, many processes ensure the correct synthesis, folding and degradation of proteins, and many of these steps are negatively impacted during the aging process.

1.2 DNA Replication

1.2.1 DNA packaging

The DNA within our cells encodes hereditary genetic information. Genomic DNA is composed of two distinct copies in a double helical structure and stored within the cell's nucleus. In all eukaryotes, the genome is duplicated before cellular division by semiconservative replication, which leads to all daughter cells receiving a full complement of chromosomes. Eukaryotic genomes have varying sizes, with *S. cerevisiae* having 12 Mb and humans having 3 Gb (129). The negatively charged DNA is wrapped around positively charged histones to form a nucleosome

complex. Each nucleosome contains 147 base pairs (bp) of DNA wrapped in a histone octamer made up of 2 copies of each core histone protein H2A, H2B, H3, and H4 (130,131). Packaging the DNA into the chromatin structure regulates all genomic processes, such as DNA replication, transcription, recombination, and DNA repair. The accuracy of DNA replication relies on select DNA polymerases, exonucleolytic proofreading and post-replicative mismatch repair.

1.2.2 DNA replication origins

DNA synthesis occurs from specific sites called replication origins and spreads bidirectionally until the whole genome is replicated (132). In budding yeast, the origins of replication are sequence-specific, and replication initiates from the same place in each S phase. However, in humans, these are not sequence-specific but are determined by chromatin structure and transcription (133–135). The location, timing and efficiency of replication origins have been determined, and a database has been compiled (136).

There are over 400 replication origins in the yeast genome (142). Yeast replication origins contain a sequence-specific region called ARS. These are short (100-200bp) sequences that have an 11-17bp ARS consensus sequence (ACS) (137–139). ARS regions contain conserved elements A, B1, B2, and B3. These elements are essential for the origin function (140,141. Replicative helicases are loaded onto more origins than are activated, allowing backup origins in the event of replication stress (137,138). Genomic integrity can be lost if the DNA is under or over-replicated.

1.2.3 Replication initiation

DNA replication is a highly regulated process in which cells produce two identical copies of DNA to allow biological inheritance. Following the recognition and binding of the ORC complex to the sequence-specific ARS, it recruits and loads the replicative helicase Mcm2-7 (MCM) along with Cdt1 and Cdc6 (139–141). This step of loading the MCM is often referred to as origin licensing. The MCM complex is loaded as an inactive helicase during G1 and activated as the cell progresses into the S phase. As the cell goes from G1 to the S phase, Dbf4-dependent kinase (DDK) and Cyclin dependant kinase (CDK) increase, which leads to the phosphorylation and activation of the MCM complex (142–144). This phosphorylation event leads to the recruitment and interaction of Cdc45, Sld3 and Sld7 (Treslin in humans) (140,145–147). The pre-replicative complex is composed of the Mcm2-7 complex, the cell cycle kinases CDK and DDK, Sld2, Sld3, Dpb11, Cdc45, the GINS complex, DNA polymerase epsilon (Pol ε), DNA polymerase alpha (Pol α) /primase and Mcm10 (148). The two strands of DNA are separated, and the polymerases can then continuously synthesize the DNA on the leading strand and in a semi-continuous manner on the lagging strand. This process will be further expanded on in Chapter 3.

1.3 DNA damage repair and genomic instability

1.3.1 DNA damage and genomic instability

Genome instability can include permanent mutations in DNA sequence and chromosomal aberrations (Figure 1.2). These mutations generally affect organismal fitness and can be a significant driver of cancer and other genetic diseases.

The DNA within human cells is damaged thousands of times per day (149). This damage can occur from both endogenous and exogenous sources, such as UV radiation, chemical damage, and

dysfunction during DNA replication. DNA damage encompasses SSBs, mismatch, base lesions, DSBs, bulky DNA protein adducts, interstrand crosslinks, or secondary DNA structures, such as G-quadruplexes. These DNA lesions can affect molecular functions within the cell, such as replication, transcription, and packaging of the DNA, if repair is not carried out quickly and effectively. If the damage is not repaired, it can result in genome instability, telomere dysfunction, epigenetic alterations, proteostatic stress and mitochondrial dysfunction (150). Due to the vast array of damage, cells have evolved multiple repair pathways to maintain genomic integrity (151). The repair pathway depends on the damage type, the cell cycle phase, and the availability of proteins for repair. For example, pyrimidine dimers which can be formed by ultraviolet light, can be repaired by NER, base oxidation, created by metabolic processes in the mitochondria are repaired by base excision repair (BER), and DSBs created by replication fork collapse can be fixed by homologous recombination (HR) and ionizing radiation by non-homologous end-joining (NHEJ) (152).

DSBs within the DNA are the most dangerous types of lesions within a cell. If left unrepaired, they can lead to chromosome discontinuity and genomic deletions, resulting in cell death (153). Therefore, efficient repair of DSBs is essential for genomic stability and cell survival. DSBs are most often repaired by the canonical repair pathways NHEJ and HR. However, there are alternative DSB repair pathways, including single-strand annealing (SSA), synthesis-dependent strand annealing (SDSA), and break induced replication (BIR) which are much more mutagenic than the canonical pathways. Defects in DSB repair pathways can increase the risk of cancer, premature aging, and congenital disorders (154,155).

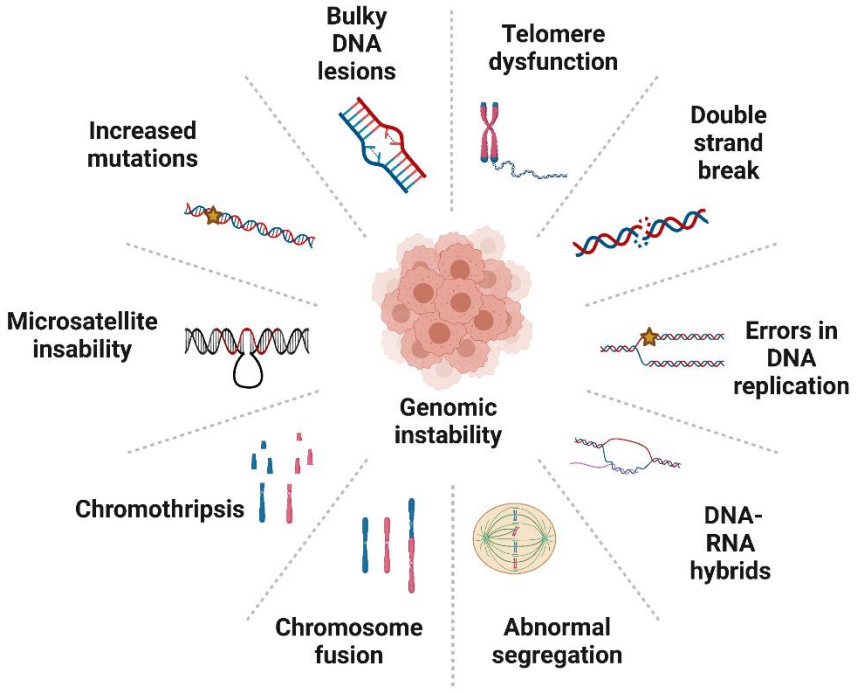

Figure 1.2 Schematic of the overall causes of genomic instability

A schematic of the causes of genomic instability includes telomere dysfunction, DSB, errors in DNA replication, DNA-RNA hybrids, abnormal segregation, chromosomal fusions, chromothripsis, microsatellite instability, and increased mutations and bulky DNA lesions. Any one of these can lead to genomic instability in a cell, a hallmark of cancer and an important area of research.

1.3.2 Non-Homologous End-Joining

NHEJ is the major repair pathway of DSBs in mammals and is still a critical repair method in yeast. NHEJ can repair DSBs through the modification and direct ligation of the two broken ends of DNA. As this does not require a homologous template, NHEJ can often lead to small deletions and insertions or 1-4bp (Figure 1.3) (156–158). NHEJ can occur at any point during the cell cycle but is the most utilized method of DSB repair during G1 phase, as there is no sister chromatid for HR

to use as a template. This is controlled through cell cycle-dependent inhibition of resection and HR. The Ku complex also promotes NHEJ by inhibiting resection (159).

The MRX complex (Mre11-Rad50-Xrs2) is one of the first proteins recruited to DSBs (160), and it is essential to tether the two ends of the DSB and control end resection (161). The MRX complex also recruits and activates Tel1, a protein kinase involved in DSB signalling (162).

The Ku complex is composed of Ku70 and Ku80 and has a very high affinity for double-stranded DNA ends in a sequence-independent way (163). The binding of Ku protects the ends of DNA from exonucleolytic degradation (159,164). The Ku complex binding to the DNA leads to the recruitment of the NHEJ factors Dnl4, Lif1 and Nej1. Dnl4 is the ligase that connects the two ends of the DNA (165). Dnl4 interacts with Lif1, and this interaction is needed for the stability of Dnl4 (166). Dnl4 and Lif1 also stabilize the Ku complex at the DSB and help prevent resection from occurring (167). Nej1 recruits end-processing factors to the DSB. Nej1 and Lif1 interact independently of Dnl4 (168). Nej1 is needed to stabilize Ku at the DSB and also helps to inhibit resection (169,170). Pol4 is an end-processing factor that can help gap-fill during NHEJ (171). Although we have extensive knowledge of NHEJ, large-scale screens continue to identify factors contributing to NHEJ (172,173).

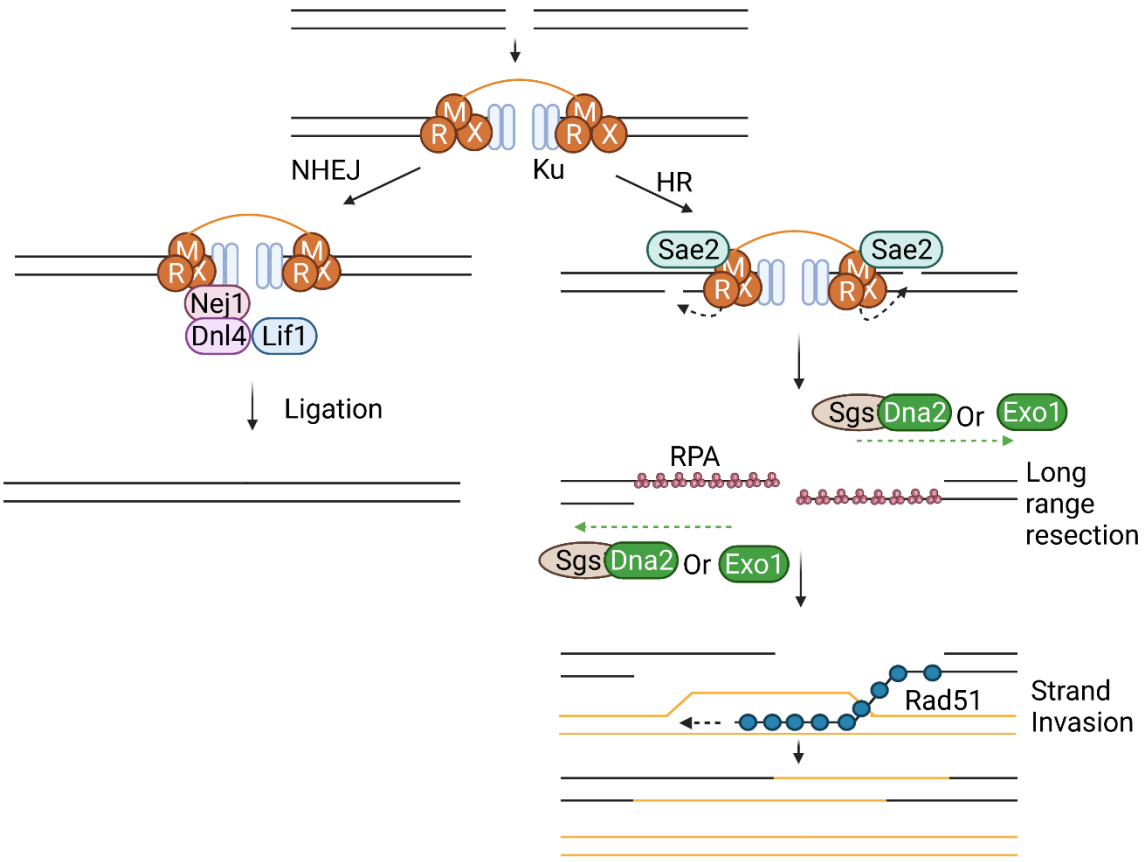

Figure 1.3 Schematic of non-homologous end joining and homologous recombination

A schematic of the two main DSB repair pathways. If a DSB is to occur in a cell, the Ku complex and MRX complex bind to the two ends and tether the ends together. NHEJ can occur any time during the cell cycle; recruitment of Nej1, Lif1 and Dnl4 allows the ends to be processed and directly ligates the two ends back together. HR can only function during S and G2 phases of the cell cycle. When HR is used to repair the DSB, short-range resection is carried out by the MRX complex and Sae2. Long-range resection is then carried out by the Sgs1/Dna2 complex or Exo1 in a 5'-3' direction. RPA coats the ssDNA. Rad51 can then displace the RPA, and the nucleofilament invades a homologous donor to repair the DSB.

1.3.3 Homologous recombination

HR is a highly conserved DSB repair mechanism that uses a homologous DNA sequence from the sister chromatid, a homologous chromosome or an ectopic (non-homologous) sequence (Figure 1.3). The availability of a homologous sequence is generally constrained by the cell cycle; however, other factors, such as chromatin structure and proximity of the donor, can also impact it. HR is the predominant pathway during S and G2 phases of the cell cycle. HR is described as an 'error-free repair pathway' because the sister chromatid is the template for repair, and it is identical in sequence and formed during DNA replication (174). However, mutations can still occur by using the HR pathway, which is believed to occur due to the formation of ssDNA and the use of DNA polymerase zeta (pol ζ) (175–177). Pol ζ is a low-fidelity polymerase responsible for the first DNA synthesis before the recruitment of PCNA and Pol δ (178).

HR repair requires extensive resection of the broken DNA ends. The initiation of resection defines the choice between DSB repair pathways as 5' DNA resection prevents NHEJ (161,179,180). When a DSB is detected within a cell, the MRX binds and bridges the DSB (181). The MRX complex can remove the Ku complex at DNA ends to allow resection to initiate (169,182,183). Mre11 has 3' exonuclease, endonuclease, and DNA unwinding activity, and it is needed for short-range resection and removes about 100 nucleotides (184–186). Initial resection by MRX leads to the recruitment of factors Exo1 and Dna2-Sgs1, which can carry out long-range resection (187,188). RPA then coats the resulting ssDNA. This is then replaced by Rad51 recombinase, which forms a filament on the ssDNA through a process reliant on Rad52. The nucleofilament strand can invade the homologous sequence, and Pol δ or Pol ε can synthesize the new DNA using the invading 3' end as a primer. Rad52 and Rad59 promote the capture of the second DSB end by the D-loop,

and a double Holliday junction (dHJ) is formed. The dHJs are dissolved by Sgs1, Top3, and Rmi (STR complex) in a process called dissolution, which leads to non-crossover products (189). Defects in HR can lead to translocations, LOH, amplifications, and elevated levels of DNA breaks.

1.3.4 Microhomology-mediated end joining (MMEJ)

Alternative EJ (alt-EJ) (also referred to as microhomology-mediated end joining – MMEJ) requires many of the same factors as c-NHEJ (classical-NHEJ); however, MMEJ repairs independently of Dnl4 and Ku (190). Repair by c-NHEJ leads to deletions smaller than five bp, whereas MMEJ is seen to have larger deletions of five-twenty bp (Figure 1.4) (190,191). Resection initiation occurs through MRX-Sae2; however, long-range resection is down-regulated. MMEJ uses small <ten bp microhomologies at both sides of the resected DSB (190,192). End processing and flap removal are then carried out, and repair of the DSB occurs. MMEJ leads to the loss of genetic information due to the microhomologies between chromosomes and the loss of flanking regions. If there is a decrease in DNA repair by the canonical pathways, then the frequency of MMEJ increases to compensate, but this leads to an increase in genomic instability. MMEJ is a vital pathway to repair DSBs with non-compatible ends formed by ionizing radiation in yeast and humans, as unrepaired DSBs can lead to cell death (193). MMEJ occurs at a lower frequency in yeast compared to higher eukaryotes (194).

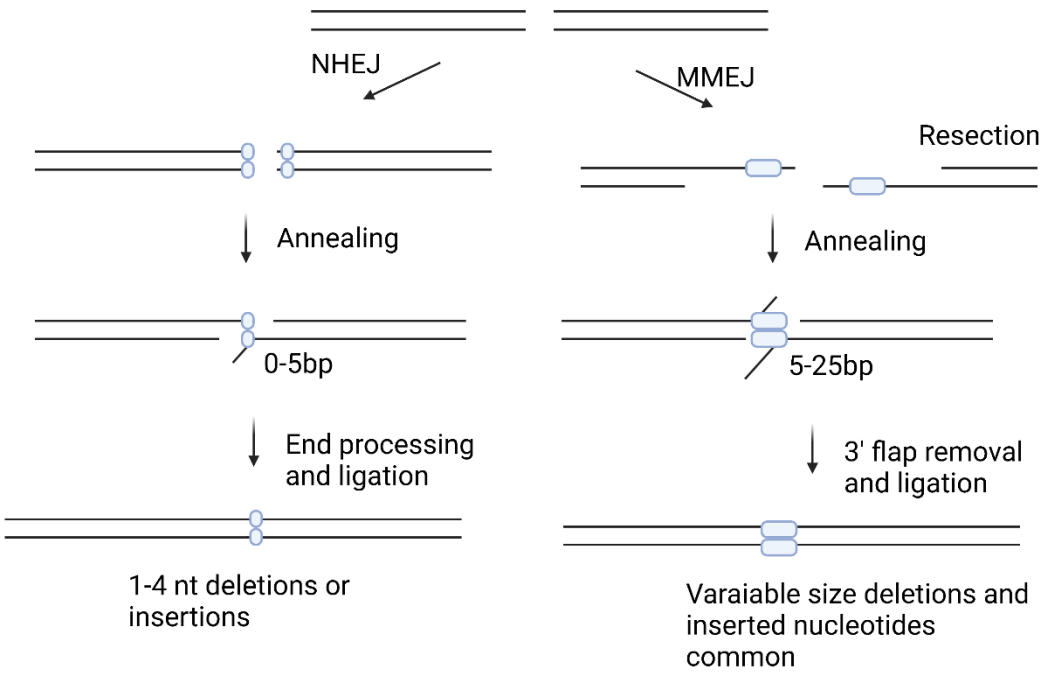

Figure 1.4 Model of NHEJ and MMEJ

A schematic of the NHEJ and MMEJ pathways. NHEJ can occur at any point during the cell cycle and involves the processing and annealing the two ends with small 0-5bp homologies (shown in blue boxes). End processing can result in small insertions of deletions. MMEJ involves the resection of the DSB and the annealing of microhomologies. The 3' flap must be removed, and the DSB annealed, resulting in variable-sized deletions that are always flanked by regions of 5-25bp microhomologies.

1.3.5 Single-strand annealing

Single-strand annealing (SSA) uses homologous repeats at both sides of the DSB that can anneal and lead to a deletion between the sequences. These direct repeats are exposed following resection and are at least 30 nucleotides in length (195,196). However, these homologies are

more extensive than the 5-25bp used in MMEJ. Due to the large deletions, SSA is considered a highly mutagenic repair pathway. In contrast to MMEJ, SSA requires the Rad52 strand annealing activity; however, it does not require Rad51 as there is no strand invasion (197). The size of the microhomologies and the requirement of Rad52 are used to determine whether the repair is occurring through MMEJ or SSA.

1.3.6 Break-induced replication

BIR is critical when (i) only one end of the DSB can detect homology, (ii) two DSB ends find different homologous templates, and (iii) telomere erosion results in a single DNA end (198). BIR has a critical role in telomere maintenance in the absence of telomerase through alternative lengthening of telomeres (ALT) in humans and replication fork restart following replication fork stress (199). The DNA damage context that initiates BIR most likely dictates the particular repair mechanism used (200). When DSBs are not repaired efficiently, the DSB is relocated to the nuclear envelope where BIR occurs (201). Repair by BIR leads to nonreciprocal translocations and extensive LOH if the template used is a homologous chromosome.

There are at least two distinct BIR mechanisms, one that is Rad51-dependent and one that is Rad51-independent (202). The initial steps of the homology search use the same proteins as HR; however, Pol ε, Pol α and Pol δ are needed to synthesize both strands (203–205). Following replication of the first strand (the leading strand), the second strand (the lagging strand) uses the leading strand as a template. As BIR replicates using a D-loop bubble and then replicates from the newly synthesized strand, this leads to frequent mutations, large deletions, and duplications to the chromosome (206). BIR occurs at higher rates in cancer cells with deregulation in origin

firing and over-replication. Over-replication occurs when parts of the genome are replicated more than once during a single cell cycle, which leads to genome instability through chromosomal damage (207). Human cancers often display DNA replication stress and replication fork collapse, making them more dependent on alternative repair pathways such as BIR (208).

1.4 Thesis summary

One main objective of my doctoral work has been to sort young and old cells and compare DNA replication and repair to determine whether age-related changes could lead to genomic instability. My objective in Chapter 2 is to optimize the old cell enrichment process to isolate aged cells from a logarithmically growing culture. Most of our understanding of DNA replication and repair in yeast has been studied in young cells and has never been investigated in aged cells. In Chapter 3, I discuss the need to understand and perform experiments to identify and characterize age-related changes in DNA replication during aging. In Chapter 4, I assess changes in DSB repair in aged cells that could impact genome stability. These include changes in DSB repair pathway choice, the recruitment of repair factors to the damaged site, and the efficiency of relocating the DSB to the nuclear periphery. Altogether, this work identifies mechanisms of DSB repair and DNA replication that are impaired with increasing age.

Chapter 2 Enriching old yeast using old cell enrichment

2.1 Background

To prolong the health span of the population and counteract age-related diseases, it is essential to identify and characterize age-related molecular changes. A breakthrough in the study of aging could delay aging and age-associated diseases and significantly impact the quality of life. Yeast has been at the forefront of many insights into the aging process (49,209). There are many benefits of using yeast as the model system to study aging, including their short generation time, convenient and cost-effective experimental setups, tractable genetic approaches, and high throughput methodologies. As well as many technical benefits, yeast has many highly conserved regulatory homologous and orthologous that allow us to understand how conserved pathways change during aging (210).

Alongside the many benefits of yeast in aging research, a further asset is an ability to determine precisely how many divisions each yeast cell has undergone. When a mother yeast cell gives rise to a daughter cell, a permanent circular chitin ring called a bud scar is left in the cell wall of the mother cell. These bud scars accumulate with every division and can be seen by microscopy upon calcofluor staining. (211). The number of bud scars is a visual indicator of the number of cellular divisions; thus, the stage of a yeast cell's lifespan can be determined.

One of the largest hurdles in studying cellular aging with yeast has been to isolate individual aged cells from a logarithmically growing culture. Within each culture, there is also a range of ages, with the yeast used to initially inoculate the culture being the oldest and the progeny having undergone a varying number of divisions. This leads to an inherently tricky problem of collecting

large quantities of old cells at the same replicative age. Many techniques have been developed to separate young and old yeast cells; however, each has advantages and disadvantages depending on the proposed question. In my studies, it was essential to isolate enough aged cells for biochemical and genetic analysis. During the old cell enrichment (OCE) process, it was necessary to have a reproducible average age after a particular time to allow comparison of young and progressively older cells.

2.1.1 Current techniques to study aging

Advances in the methods to study aging in yeast have allowed researchers to understand how mechanisms change at both a population and a single-cell level. There have also been many advances in the methods being used for sorting young and old yeast cells.

Microdissection involves manually separating the mother and daughter cells using a dissection needle (103,212). The cells are removed from a logarithmically growing liquid culture and transferred to a low-density medium at 30°C. After 3 hours, the daughter cell can be removed from the mother cells and isolated. The average lifespan of W303 yeast is 25 generations, and the average cell cycle is 90 minutes; therefore, this is a timely method to complete (213). Replication of yeast can be paused by storing the assay at 4°C. This method's significant drawbacks include the long time it takes and how few cells are recovered; therefore, no high throughput studies can be carried out. Aged cells are also more fragile than young cells and can unintentionally be damaged by the dissection needle. The agar plates used are often thick and opaque, which impairs the ability to visualize organelles during aging. However, microdissection allows a very sensitive understanding of aging, as the exact number of replications each cell has

undergone is known and can be studied individually. As well as having the daughter cell to study, so it is a great tool to understand the rejuvenation of the daughters compared to mother cells.

Due to the time-consuming process of microdissection, there have been technological advances to automate the separation process and overcome some of the hurdles caused by manual separation. Automated processes using microfluidic devices have been created to remove daughter cells while retaining mother cells (214,215). Microfluidic devices allow researchers to study the entire lifespan of the yeast cell under a microscope (19,20,216). The microfluidic device chemically or mechanically traps the mother yeast cells. The mother cell then begins division and produces a bud which develops into a daughter cell. Once the daughter cell is detached, it is automatically washed away by a continuously flowing medium. To study the changes occurring in the mother cell, time-lapse microscopy can be used to monitor the entire lifespan of the mother under very stable conditions.

These microfluidic devices can also be interfaced with fluorescence microscopy to allow research into the dynamics and interactions of pathways that regulate the lifespan of an individual cell. The ability to observe a cell in real-time has allowed the characterization of cell cycle control, organelle morphology and cellular processes afflicted by aging. Several groups have developed microfluidic devices to study aging for various biological, biomedical and clinical applications (216–222).

One of the significant advantages of using microfluidic devices to investigate aging yeast cells is the ability to track a long-term culture using well-defined environmental conditions. The microfluidic devices can be scaled to allow larger quantities of aged yeast cells, with some

microfluidic systems able to study up to 1000 cells at once (219). Although this is a much larger quantity of aged cells, this is still not enough for larger-scale biochemical and genetic studies where you often need upwards of $1x10^8$ cells. Microfluidic approaches have allowed a complete lifespan study to occur over three days. One of the issues with microfluidic devices is the retention rates of aged cells, with some only having a 15-30% old cell retention rate (223). As the cells must be chemically or mechanically trapped within the device, any modification can complicate the effects on the RLS. Surface modifications can also negatively affect the cell and may alter the results. Lastly, younger, aged cells can not be trapped or used in microfluid devices as they are washed away.

Elutriation is a centrifuge-based method that separates aged cells based on size. This is feasible as mother cells give rise to smaller daughter cells (224). However, as this method separates on size, the fractions significantly overlap, and it isn't easy to separate by exact age (225). Aged cells grow the largest in the final five replications of their lifespan, so the best separation is found when the cells are very old. These cells are very old, leading to difficulty in follow-up biochemical studies. This method can yield around $5x10^8$ cells (226).

Due to previous methods being unable to collect very large quantities of old yeast cells (over $1x10^9$ cells), research was carried out to overcome this barrier. The Mother Enrichment Program (MEP) was a significant development in the yeast aging field as it enriched many old cells with a well-defined replicative age in liquid culture (227). The MEP uses an estradiol-inducible mitotic arrest in only the daughter cells, killing the virgin daughter cells. It uses a Cre-Lox system to disrupt the daughter cells' two essential genes, Ubc9 and Cdc20. These proteins are essential for cell cycle progression. Therefore, following the addition of estradiol, the daughter cells become

arrested in M phase of the cell cycle. This leads to linear population growth instead of exponential growth, which is important in gathering large quantities of old cells.

When a mother cell divides, the formation of the cell wall of the daughter cell is generated *de novo*; therefore, the mother cell wall is not passed to the daughter cell. This property was used to purify mother cells in the culture by labelling a culture of cells with biotin (62). The mother cells can then be separated using streptavidin-coated magnetic beads that bind to the biotin-labelled wall so that the culture only contains old cells.

The apparent advantage of the MEP program, in combination with biotin labelling, was the capability to separate large quantities of old cells at different stages of their lifespan for aging studies. The MEP was also shown not to have any impact on the RLS of the mother cells and was easy to carry out. Although this method was revolutionary, the yeast strains were highly engineered, restricting the availability of markers for genetic studies. Moreover, this protocol also kills new daughter cells, preventing comparing old and young cells from the same cultures. The screening process also prevents changes to environmental conditions. Lastly, one technical challenge the MEP faced was that fast-growing daughter cells developed resistance to estradiol-induced arrest, and these cells quickly divided, saturating the culture. This leads to only being able to get around $5x10^8$ cells that are 7-12 generations old (228). As yeast cells typically undergo an average of ~ 25 divisions, this only allowed work into the first half of their lifespan (21).

For my study, I needed a method which allowed the separation of yeast at specific aged time points, which is highly efficient and capable of separating old cells in quantities large enough

(over $1x10^9$) for biochemical and genetic studies. Furthermore, I also needed a young control sample to compare changes that occur during the yeast aging process.

2.2 Aims

Here, I aimed to develop a method that allows the efficient and effective separation of old mother cells from their young daughter cells. It was imperative to create a technique that reduced the time it had previously taken to separate young and old cells (6-8 hours) and allowed the separation of young and old cells on a much larger scale than had ever been done in our lab. To carry out biochemical analysis, I would need at least $1x10^9$ old cells, and the separation process would need to take less than 4 hours. I also needed to ensure the separation was occurring successfully and to determine, on average, how old the cell population was on each day of separation.

2.3 Methods

Old cell enrichment

Old cell enrichment (OCE) was initially based on (229). For all assays, 20ml of overnight culture was inoculated in YPAD medium at 25°C. Cells were diluted to 100ml of YPAD and grown into log phase. Cells were harvested and washed three times with 1x phosphate-buffered saline (PBS). Cells were then resuspended in 1ml PBS and mixed with 8mg of Sulfo-NHS-LC- Biotin per $1x10^8$ cells for 30 min at 30°C. Cells were washed three times with 1ml PBS and 0.1M Glycine and used to inoculate 500ml SC media overnight at 25°C. Cells were harvested at 5000rpm for 10 minutes

and washed thrice with PBS. Cells were then incubated in 50ml PBS and 20µl of Anti-Biotin Microbeads per 10^7 total cells at four °C for 30 mins.

For separation using the magnetic racks, the 50ml culture was inserted into the BioMag magnetic racks and allowed to separate for 2 minutes at room temperature. The young cells were then removed by a pipette and saved as young cells. The falcon tube was removed from the magnetic rack, washed with 40ml PBS, reinserted into the magnetic rack, and separated for 2 minutes. The PBS was removed and discarded; this process was repeated twice. The old cells could then be resuspended as necessary

For separation using the LS and XS columns, the cells were separated by flowing through an LS or XS column on the SuperMACS II separator at room temperature and washed thoroughly with 15ml (LS) or 150ml (XS) of PBS until no more liquid remained on the column. The column is then removed from the magnetic field, and the old cells are eluted using a syringe, and the old cells can be resuspended as necessary

Bud Scar Microscopy

Following old cell enrichment, 20µl of cells were collected and fixed with 2µl of formaldehyde. Cells were then pelleted and stored at 4°C for imaging. Cells are resuspended in 20µl of PBS and stained with calcofluor. Cells are then placed on coverslips and imaged using Zeiss LSM 880 with Airyscan. Images were analyzed using ZenBlue software. Each cell was analyzed individually, and >50 cells were analyzed per sample. Z-stack images were acquired with 0.35µm along the z plane using a plan-apochromat 63x/1.40 Oil Dic M27 objective.

Flow Cytometry

Samples for flow cytometry were prepared using 500µl of cell suspension with 1 ml of 95% ethanol. The fixed samples were then stored at 4°C for processing. The cells were spun down at 13000 RPM for 1 minute and rinsed with 50 mM sodium citrate (pH 7.0). The cells were spun down again at 13000 RPM for 1 minute and suspended in 50mM sodium citrate, 100µg/mL RNAase A overnight. The next day 400µg/ml of proteinase K was added, and the sample was incubated at 50°C for 1 hour. The cells were then pelleted and resuspended in 50mM sodium citrate and 10µg/ml propidium iodide. Cells were then sonicated for 3 seconds at 10% to break up clumps and analyzed using the Attune Acoustic Focusing Cytometer (Life Technologies).

2.4 Results

2.3.1 Previous techniques using BioMag magnetic tube rack and LS columns vs new XS columns

In the original OCE procedure, I optimized a culture of W303 cells labelled with biotin before it was inoculated into fresh media, where cells could divide and age overnight. After one overnight inoculation, this culture was referred to as O1; however, following the separation process, these aged cells could be reinoculated into fresh media and grown overnight again, creating O2 cells (2 overnight inoculations). The following day, BioMag magnetic tube racks with anti-biotin magnetic beads were used to separate young and old cells. The culture was centrifuged and resuspended into a 50 ml falcon tube. Biotin-labelled old cells remained attached to the tube wall by a magnet, and the young cells could be removed.

However, when I performed this experiment, I observed a lot of heterogeneity with a range of 1-13 bud scars. Therefore, there was a poor separation of young and old cells, resulting in very

mixed cultures (magnetic rack method, Figure 2.1). A large quantity of the 'old' cells failed to be separated from the young cells as it seemed the magnet was not strong enough to hold the cells. The magnetic racks were found inefficient in dividing the young and old cells, with O2 cells only having an average of 6 bud scars. The young cells had an average of 2 bud scars, and the old samples had gone through 2 overnight inoculations. The yield was insufficient for the cell cycle analysis and ChIP, as I only managed to separate $3x10^8$ cells and needed around $1x10^9$ cells. Therefore, I began investigating different separation techniques that would improve the quality and quantity of OCE.

I initially tried separating young and old cells using MACS LS magnetic columns within the SuperMACS II separator magnet (Miltenyi Biotec) (LS columns, Figure 2.1). The LS columns contain para-magnetic that increase the magnetic force of the column to allow the retention of old cells within the column while young cells are eluted out. This column seemed a better option for separating the cells, as it reduced the time to separate them by almost half and was more efficient. Other studies reported using LS columns to separate old yeast cells (230). I managed to separate $5x10^8$ cells, an improvement from the BioMag magnetic tube racks, but more cells would be needed for biochemical studies. The capacity of the column only holds 5mL, and the elution was slow and took around 2 hours per sample; therefore, was not a viable option to upscale this to achieve the yield of old cells required for many experiments.

The MACS XS magnetic column (Miltenyi Biotec) can separate ten times more cells than the LS column and hold up to 60ml of culture, so I considered this a better option for my experiments. The XS columns were larger and allowed efficient separation of cells. They were the most efficient in retaining old cells and separating old cells from young cells within the SuperMACS II separator

(Miltenyi Biotec) (Figure 2.1). The average number of replications the cells recovered from the magnetic racks had undergone was LS and XS columns of 6.16, 7.68, and 10.87, respectively. The LS columns separated, on average $5x10^8$ cells, and the XS column separated $3x10^9$, which was six times more efficient from the same starting volume of cells. The column was not completely saturated, and I believe I could still increase the yield if I required more cells. If a higher quantity of cells is needed, I will tag more cells with biotin; however, during the experiments I carried out, I never needed a larger amount, so I did not push the column to its maximum capacity. For each experiment, I would calculate how many cells I needed and always tagged 10% more to ensure I would have enough cells even if some old cells passed through the column. This always led to slightly more cells than needed; however, when enriching cells to day 3, the culture was passed over the column three times, and around 5% of the initially tagged culture was lost. If this was a concern, the eluted material could be passed over the column a second time. However, I never needed to do this as the enrichment was often above and beyond what I needed for my biochemical studies. Therefore, I used the XS column moving forward to separate young and old cells.

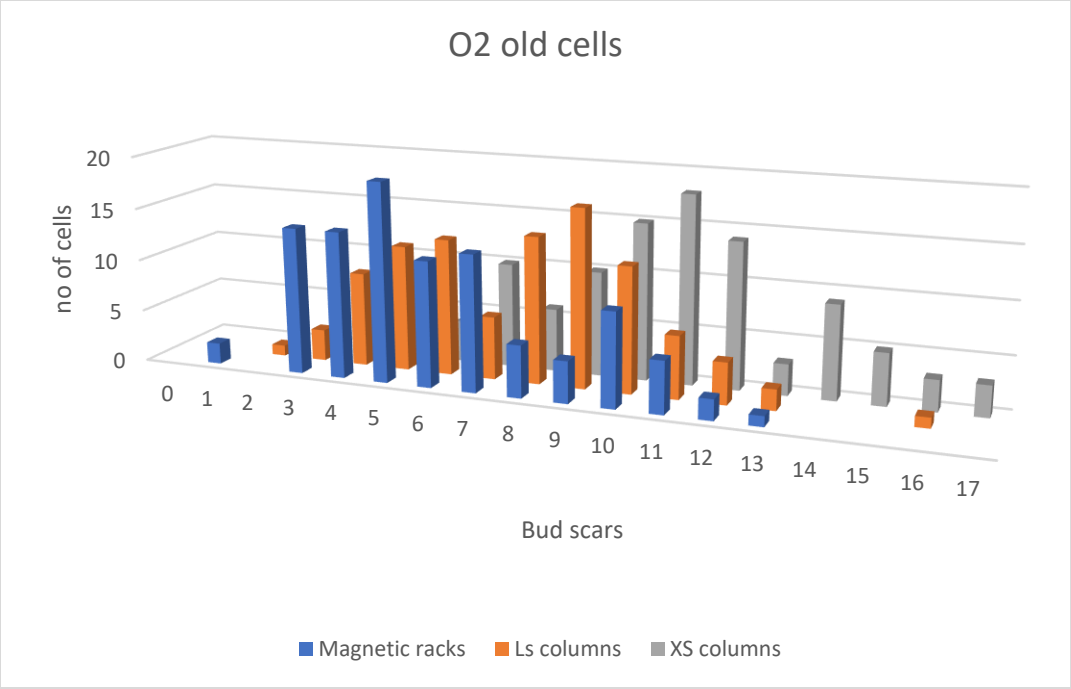

Figure 2.1 Efficiency of Old cell enrichment

Old cell enrichment was carried out using three different separation methods – magnetic racks, Ls columns in a SuperMACS II separator and XS columns in a SuperMACS II separator. Following separation, O2 cells were stained using calcofluor to determine the number of bud scars and the divisions they had undergone. The average number of bud scars the cells had for the magnetic racks, LS columns and XS columns were 6.16, 7.68, and 10.87, respectively. The standard deviation for the magnetic racks, LS, and XS columns were 2.67, 2.67 and 2.72, respectively. N=1

The XS columns were the most efficient and effective way to separate young and old cells (Figure 2.2). I, therefore, adapted the original OCE process and created the following protocol. The initial starting culture was labelled with Sulfo-NHS-LC-Biotin and allowed to expand. The culture was incubated with anti-Biotin microbeads and passed through the magnetic XS column, where the flow through contained only daughter cells, which were collected as the young cell control. After extensive washing (150ml PBS) to remove residual young cells binding non-specifically to the XS

column, the magnetic field was removed, and the old cells were eluted. The mother cells collected from the enrichment process could then be used in an experiment or resuspended in fresh media and aged further. Samples can be collected on a consecutive day to sample the progressively aging population. On O1, the samples were in culture for roughly 18 hours; on O2, they were cultured for 42 hours; on day three, they were cultured for 66 hours. We stained the cells with calcofluor to determine the number of replications the mother cells had undergone. As the yeast gets progressively older, the bud scars on the cell wall increase (Figure 2.3). We determined the average number of bud scars in young, O1 cells, O2 cells and O3 cells (Figure 2.4). Young cells had an average of two bud scars, O1 had six bud scars, O2 had eleven bud scars, and O3 had seventeen bud scars. To ensure the cells were healthy, we checked the cell cycle phase of the aged cells (Figure 2.5). It was seen that the majority of the asynchronous cell samples were in the G1 phase of the cell cycle. This increased as the cells got older, with a smaller proportion of the cells in the S/G2 phase of the cell cycle.

We had shown that the young cells removed from the XS column had, on average, two bud scars (Figure 2.4). However, the young cells had been in culture for 18 hours; therefore, it became apparent that they had entered stationary stage and were no longer logarithmically growing when the culture was being processed. Therefore, the larger proportion of cells in G1 phase could also be accounted for by the growth conditions (Figure 2.5). To keep the cells in stationary phase replacing the media throughout the overnight culture or reducing the time the cells are in culture could allow them to remain in log phase. One limitation of how I cultured these old cells is that these cells may take longer to re-enter the cell cycle following release into new media and may be harder to study in cell cycle-specific studies such as DNA replication and repair.

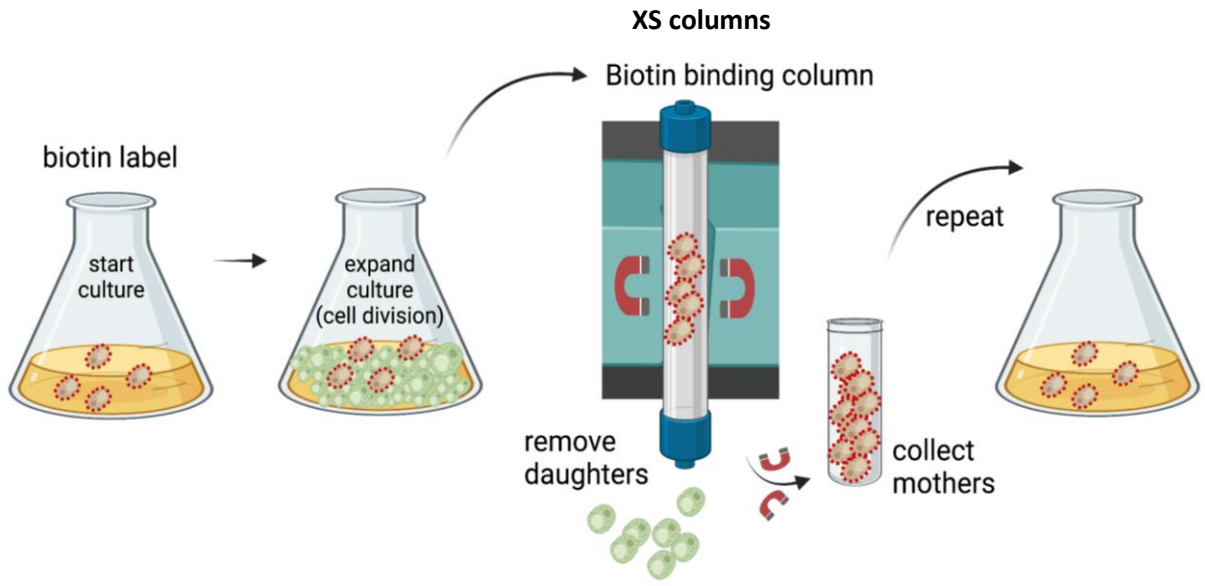

Figure 2.2 Old cell enrichment using XS column

A model showing the separation of young and old cells using the XS column in the SuperMACS II separator. This model demonstrates how the initial yeast culture is biotin-labelled, which will become the old cells. The cells are then cultured overnight to allow expansion. When the mother cell divides, the cell wall is maintained in the mother, and the biotin is not passed to the daughter cells. Anti-biotin microbeads are then added to the culture, which binds to the biotin in the old cells. The culture is then passed through the magnetic XS column, which is in the magnetic field of the SuperMACS II separator, allowing the young daughter cells to pass through the column. In contrast, the old cells are maintained within the column. The XS column is removed from the magnetic field and eluted with a syringe. Old cells can then be cultured and further aged.

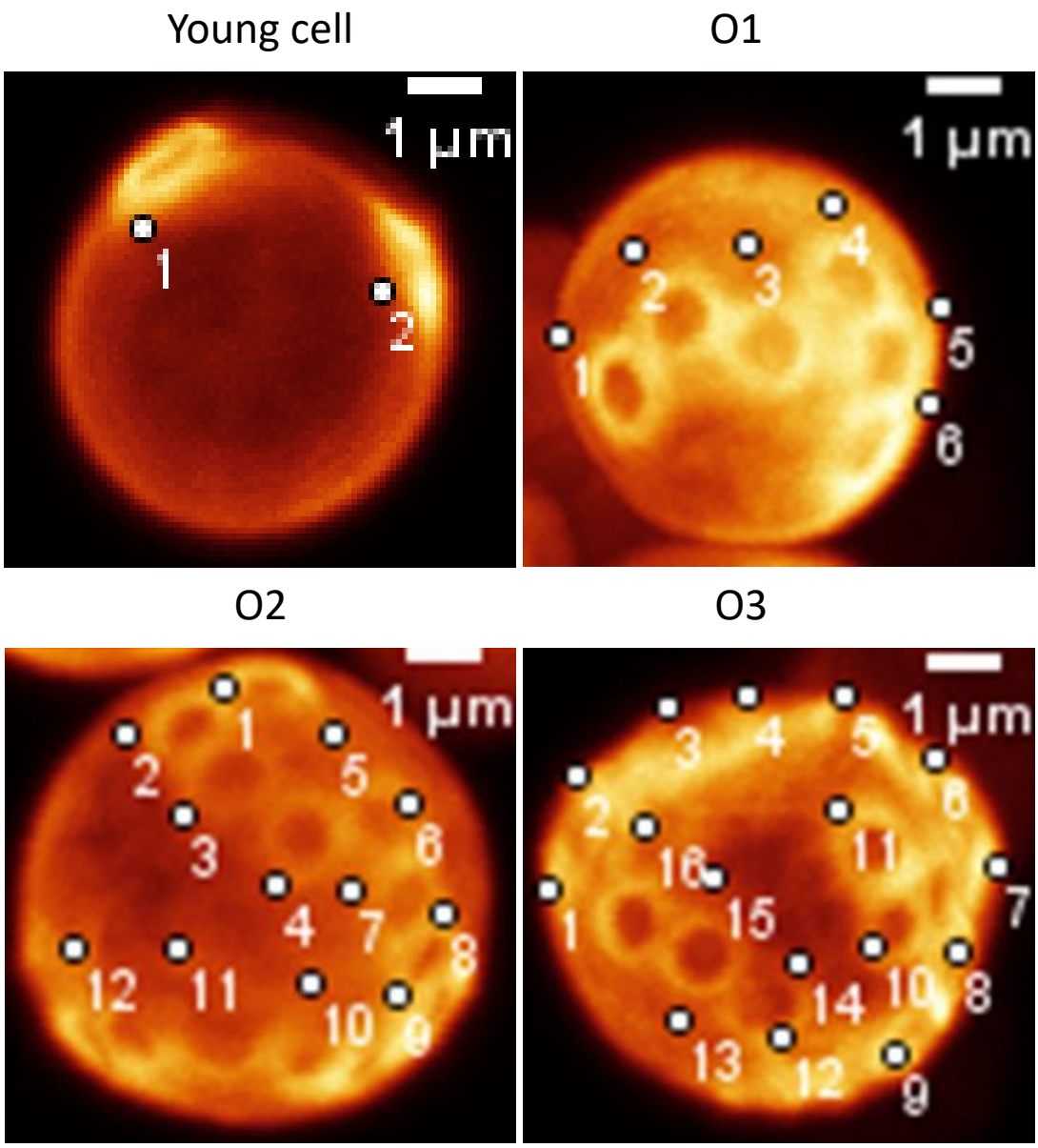

Figure 2.3 Representative images of bud scars on aged cells following enrichment

WT (JC-727) cells were enriched and separated using XS columns. Samples were taken of young O1, O2 and O3 cells. The cells were stained using calcofluor white and imaged using Zeiss LSM 880 with Airyscan. Images were analyzed using ZenBlue software, and bud scars were manually counted. Each cell was analyzed individually, and >50 cells were analyzed per sample.

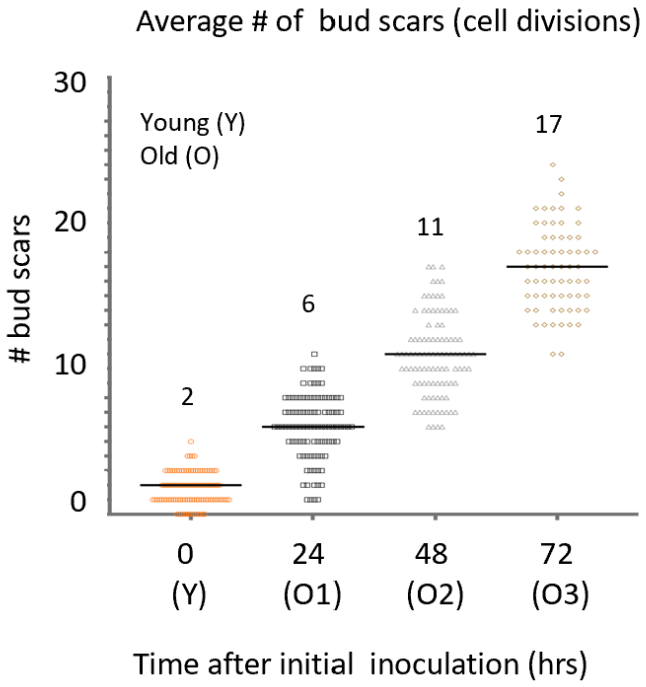

Figure 2.4 Age of cultures that were aged on XS columns

WT (JC-727) cells were enriched and separated using XS columns. Samples were taken of young O1, O2 and O3 cells. The cells were stained using calcofluor white and imaged using Zeiss LSM 880 with Airyscan. Images were analyzed using ZenBlue software, and bud scars were manually counted. Each cell was analyzed individually, one hundred cells were counted, and the average of each population was determined and shown by the solid black line. The average number of bud scars for Y, O1, O2, and O3 cells is 2, 6, 11, and 17, respectively.

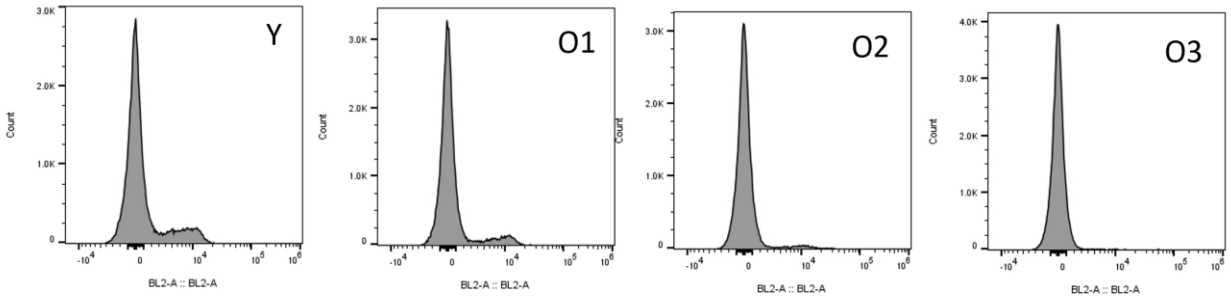

	Y	O1	O2	O3
G1:	67.8%	76.8%	82.6%	84.9%
S/G2:	29.3%	20.4%	13.9%	9.54%

Figure 2.5 Cell cycle analysis of young, O1, O2 and O3 cells

Cell cycle analysis using flow cytometry of WT (JC-727) samples from young, O1, O2 and O3 cells separated using the XS column. Cells were stained with propidium iodide (PI) and analyzed using the Attune Acoustic Focusing Cytometer (Life Technologies). The fraction of each sample in the G1 and S/G2 phases of the cell cycle are shown.

Understanding natural aging is important to help understand age-related disease progression. Many methods were studied to increase the efficiency, reproducibility, and quantity of separation of young and old cells. The method developed allowed the effective and large-scale separation of young and old yeast cells (Over $1x10^9$ cells). Using this method, I can investigate the changes in naturally aged cells using molecular and biochemical tools.

Chapter 3 The changes in DNA replication during aging

This chapter is a version of a manuscript prepared for submission entitled '**Age-related changes in DNA replication timing and location,'** Nicola Mair, Mireille Tittel-Elmer and Jennifer Cobb

I was involved in study design and conceptualization, data collection, data analysis and interpretation. I contributed to the manuscript as the co-first author. Mireille Tittel-Elmer generated the data displayed in 3.5, 3.15, 3.16 and 3.18, and I created all the other figures, performed all the further experimentation, and wrote the manuscript.

3.1 Abstract

DNA replication is a fundamental process in which the DNA within cells is fully replicated so that the cell has two complete copies of the genome. It is highly conserved from *S. cerevisiae* to humans and has been characterized to be both spatially and temporally regulated. Although some work in cells derived from individuals with premature aging syndromes exists, very little is known about replication in natural aging.

I determined that during replicative aging, there is a decrease in the recruitment of replisome components to replication origins, which correlated with replication timing. Using ChIP, we determined a reduction in the recovery of DNA Pol ε, DNA Pol α, Fkh1, Mcm2 and Orc2 to replication origins in older cells. Furthermore, we identified using DNA copy number mapping that there was a decrease in synthesizing new DNA at replication origins in aged cells and that synthesis was initiated from a region distinct from and adjacent to the ACS. Replication was initiated at sites in old cells from 100 to 3100 bps away from the ACS of early firing origins, and replisome components were recovered at these sites too. I termed this new initiation site 'ΔOrigin' for change in origin with aging and this region, which correlated with replication timing and nucleosome occupancy. As cells age, the rate of fork progression increases as measured by DNA combing. This work details the changes in DNA replication in naturally aged yeast cells and shows that age-related changes in DNA replication include an altered start site for initiation, decreased efficiency, and an increase in the speed of fork movement after replication.

3.2 Introduction

DNA replication is the semi-conservative process whereby cells produce two identical copies of DNA before cellular division. If this process is not completed faithfully, genomic integrity is compromised, and mutations, rearrangements and defects in chromosome segregation can occur (231). Many proteins and complexes that form during DNA replication are highly conserved across all species (232). In yeast, replication initiates from multiple sites throughout the genome called replication origins. These origins have three or four 10-15 bp repeat sequences that are spread over 100-150 bp and are capable of being the site where replication begins. The sequences that are required for replication origins are found to vary throughout eukaryotes. There are 16 chromosomes in budding yeast with 500 replication origins spread across the genome. To allow successful replication, there is redundancy, and there are more origins in the genome than needed. Following the initiation of DNA replication, an RNA primer is synthesized at the replication origin, and replication forks progress bidirectionally from both sides of the origin (Figure 3.1) (132). Replication involves the incorporation of nucleotides on the leading and lagging stand by the pol ε and δ. The ligase can seal any DNA nicks created during lagging strand synthesis. Following the complete replication of the DNA, the cell can enter mitosis, resulting in a genetically identical copy of DNA in the daughter cell.

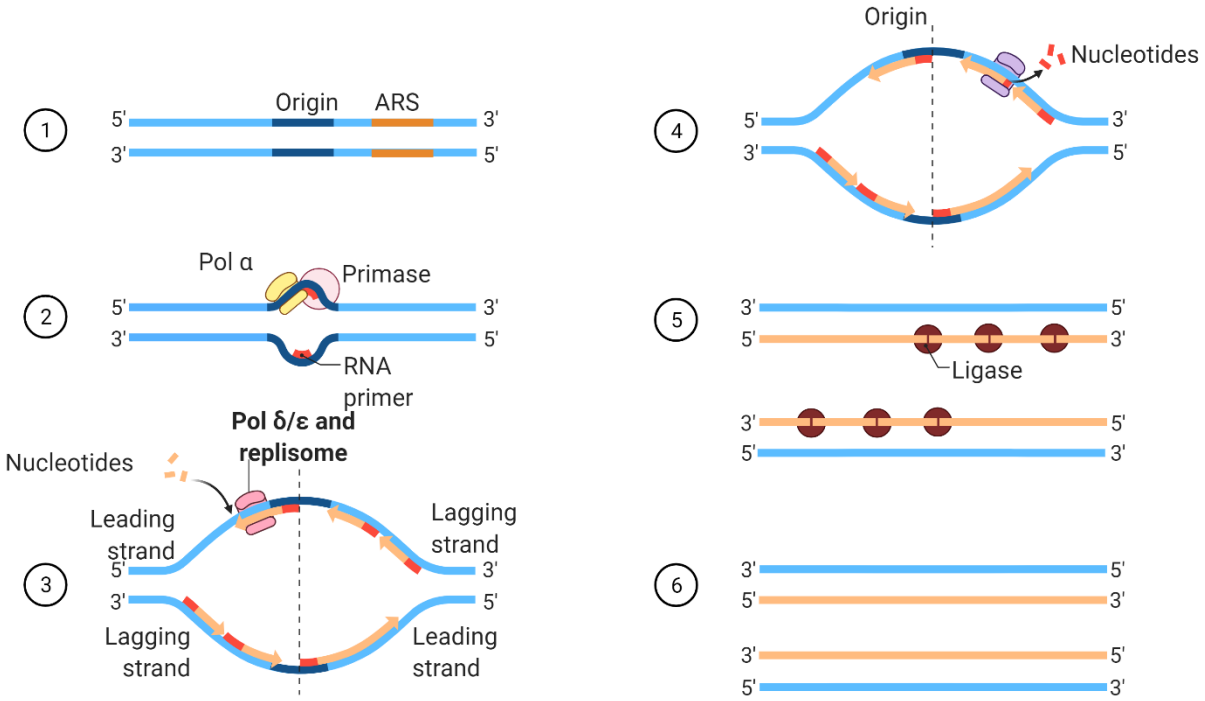

Figure 3.1 Schematic of DNA replication

1. The yeast DNA contains a replication origin that allows replisome binding. The ARS includes the sequence-specific element in yeast.
2. The RNA primer is synthesized through the action of pol α and primase.
3. The replisome is recruited, and the leading and lagging strand is synthesized through pol δ and pol ε.
4. The replisome spreads from the origin, creating a replication bubble.
5. Ligase is recruited to seal up nicks in the DNA.
6. A second copy of the DNA is produced through this semi-conservative process.

3.2.1 DNA Replication origins and timing

The replication program is very complex and involves replicating the genome in small units with orchestrated timing. The replication of the human genome is not defined by DNA sequence but by local DNA structure, chromatin and transcription (133–135). Although the DNA sequence is not specified, replication does occur in discrete areas of the genome and not randomly throughout the genome.

Yeast has been a powerful organism for investigating DNA replication, as there is a large amount of published data, including origin efficiency, replication time, and ORC and MCM binding profiles (233–236). In contrast to humans, yeast replication's origins contain sequence-specific regions called ARS. These short (100-200bp) sequences have an 11-17 bp ACS that allows the binding of the replication machinery to unwind and replicate the DNA (237–239). ARS regions also contain A, B1, B2 and sometimes B3 elements, which are essential for the origin function (240,241).

Within the yeast genome, there are potentially 12000 ACS sites. However, only around 400 replication origins function as sites where replication initiates (242). DNA replication origins are present throughout the whole genome; therefore, they must be able to fire from different chromatin environments. The chromatin structure surrounding replication origins alters the probability of an origin firing (243,244). Therefore, in addition to the DNA sequence, other critical factors are needed to form a replication origin, including chromatin structures (235).

Origins will initiate replication at different times throughout the S phase of the cell cycle, with origins firing early, mid, or late stages of the S phase of the cell cycle. Replication is not initiated from all origins during every cell cycle, but it is critical that if a replication origin fires, this only occurs once per cell cycle (242). Late replication is associated with increased levels of genetic

alterations and chromosome fragility (245). Late-firing origins tend to reside near the nuclear periphery, whereas early origins are within the interior of the nucleus (246). Yeast also contains dormant origins, which tend to fire during replication stress if nearby early origins were unable to initiate replication (247).

Replication timing is established in the cell cycle's G1 phase, and a 'limiting factor' model determines replication timing as factors such as Sld3, Sld7, and Cdc45 are available in limited quantities (248–251). These limiting factors are recruited to early firing origins in G1 in a DDK-dependent manner (249,252). Over-expression of these factors leads to earlier firing of late replication origins (248,249). It has also been shown that repeating elements within the genome that contain replication origins, such as the rDNA array, compete for limiting initiation factors (253). Each origin has a different efficiency; this is measured as the probability of each origin firing during a cell cycle in yeast and can range from 10% to 80% (254).

Replication timing in humans is usually correlated with gene transcription and chromatin structure. Regions of the genome which are euchromatic and transcriptionally active generally replicate early, whereas closed HC regions of the genome replicate late in the cell cycle (251). Staggering replication is essential as there are limited resources, including licencing factors, dNTPs, and histones (248,249). In yeast, replication origins situated near heterochromatic telomeres are shown not to fire until the end of the S phase of the cell cycle (255).

During the G1 phase of the cell cycle, the ORC complex binds to the A and B1 elements of the replication origin in a sequence-specific manner (256–258). ORC binds with the A-rich strand, requiring ATP (259). The B2 region has a similar sequence to the ACS and has been suggested to promote MCM binding (260,261). The B3 region recruits the transcription factor Abf1 (262). ORC

also interacts with nucleosomes and non-histone-associated proteins to help promote the formation of the ORC DNA complex. Therefore the affinity of ORC for an individual origin can vary (263). In yeast and humans, replication origins have a nucleosome-free region (NFR) to allow for helicase loading. Replicative helicases are loaded onto more origins than are activated, allowing backup origins to fire in the event of replication stress (137,138). Early origins have higher MCM levels, allowing their early firing in the S phase (264). Defects in regulating DNA replication can lead to the DNA being over or under-replicated, ultimately leading to genomic instability.

Histone deacetylases such as Sir2 and Rpd3 are also known to have an essential role in replication timing (265–267). Sir2 is associated with nucleosomes adjacent to origins and inhibits MCM loading (268). Rpd3 delays the initiation of late origins and delays more than 100 origins (266,269,270). Rpd3 is a histone deacetylase that can repress late-firing origins locally and through an rDNA mechanism, whereas Sir2 can promote the firing of early origins (266,271). The loss of Sir2 within cells has led to higher levels of Mcm2 at early origins relative to late origins (272). Loss of Sir2 leads to an increase in the firing of rDNA regions which limits initiation factors at other replication origins are prevents their firing (100,253,273). The absence of Sir2, therefore, leads to an increase in genomic instability due to the under-replication of the genome (273).

3.2.2 Replication origin firing

DNA replication is divided into three stages: initiation, elongation, and termination. Replication initiation is divided into two steps – origin licensing and origin firing (274,275).

During the initiation stage, origin licensing involves the recognition and binding of the origin by ORC (Figure 3.2). Although ORC typically binds to the ARS through the ACS and B elements, this

is not required for ORC binding and MCM loading (276–278). It has more recently been shown that ORC searches for and actively remodels nucleosomes within chromatin, which leads to nucleosomes being the determinant for origin recognition and licensing (279). This is followed by loading two inactive replicative helicase rings, Mcm2-7 (MCM), by ORC, Cdt1 and Cdc6 (139–141). The helicase is loaded onto the DNA in a head-to-head double hexamer. This occurs during the G1 phase of the cell cycle; however, the MCM complex remains inactive until the S phase and origin firing (276,280,281).

Origin firing occurs as the cell progresses into the S phase when DDK phosphorylates the N terminal of MCM, leading to the recruitment of the DNA replication firing factors. Following this step, CDK phosphorylates Sld3 and Sld2, which recruits GINS (from the Japanese go-ichi-ni-san meaning 5-1-2-3 after the four subunits Sld5, Psf1, Psf2, Psf3) and Cdc45 which is referred to as the CMG complex (140,145–147). The CMG complex separates strands of the DNA helix at the origin, while the recruitment of Mcm10 triggers bidirectional fork unwinding (282,283), which recruits the polymerases for DNA synthesis (142–144). It has been observed that when the yeast has low levels of two replicative polymerases, Pol α and Pol δ, there are elevated levels of mitotic recombination, chromosomal rearrangements and deletions/duplications (284).

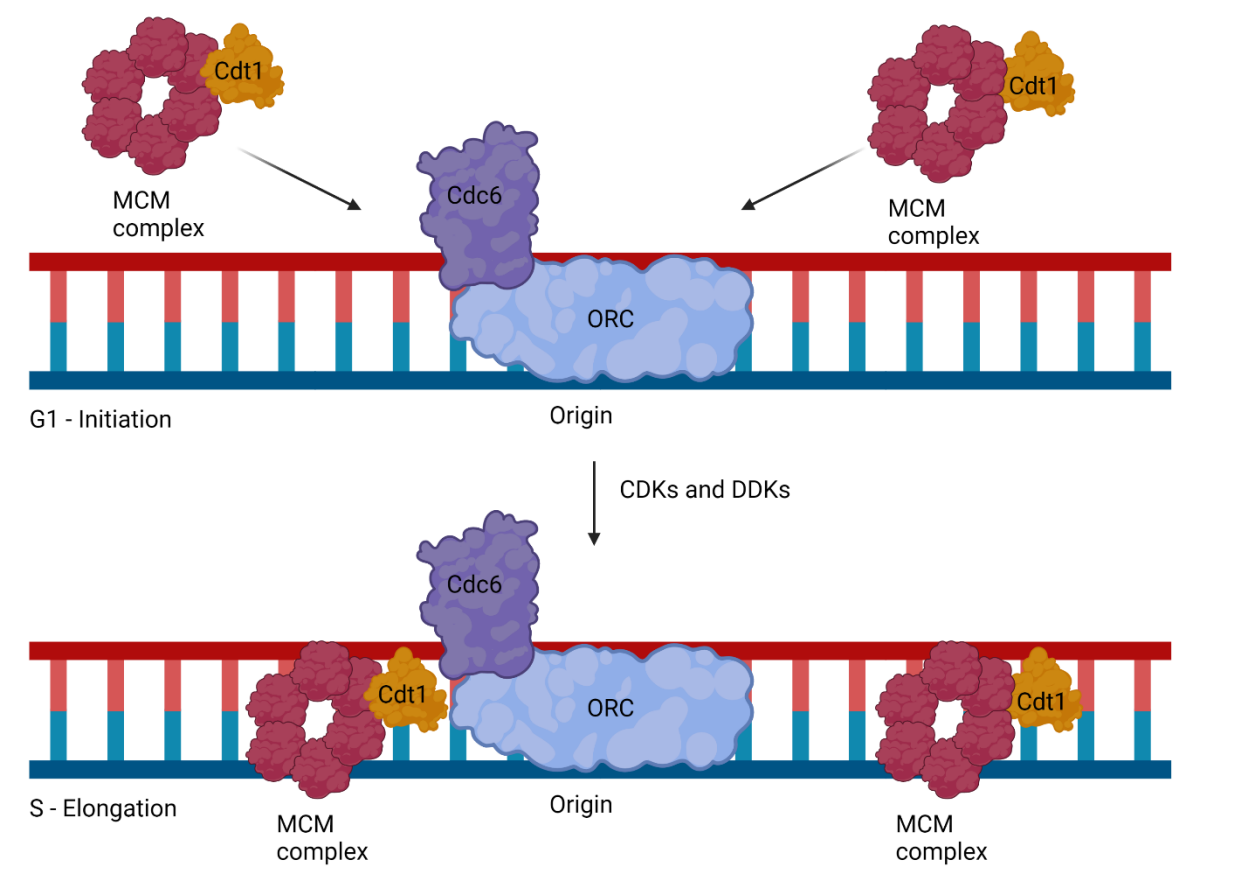

Figure 3.2 DNA replication origin firing

Model of the proteins which bind to DNA replication origins and promote their firing. ORC and Cdc6 bind to the replication origin during the G1 stage of the cell cycle. Then through CDKs and DDKs, recruit the MCM complex and Cdt1.

3.2.3 DNA replication elongation

It is essential for cell viability that DNA replication occurs with a low mutation rate. This accuracy relies on DNA polymerases incorporating the correct nucleotides in a 5'-3' direction (285). DNA replication involves three different polymerases pol α, pol ε and pol δ (286–288).

The DNA is initially primed by the primase subunit of pol α, which synthesizes 7-12 ribonucleotide RNA primers which can be further extended by pol α (289). Pol ε can elongate the mature RNA-DNA primer on the leading strand, and pol δ carries out elongation on the lagging strand with the assistance of PCNA. Replication occurs continuously on the leading strand and discontinuously on the lagging strand. The fragments created during the discontinuous synthesis are called Okazaki fragments, which are between 100-200 bps long in eukaryotic cells. Due to the discontinuous synthesis, the lagging strand constantly requires pol α to synthesize new primers for replication to begin. Lagging strand synthesis occurs slower and is delayed by ~350 nucleotides relative to the leading strand (290).

Following the Okazaki fragment synthesis, the original primer must be removed, and the DNA must be ligated together. The RNA and DNA synthesized by pol α are displaced by pol δ, creating a 5' nucleic acid flap. PCNA binds to pol δ, which helps increase its processivity by acting as a sliding clamp. The flaps are then removed by Rad27/FEN1 alongside Pif1 and Dna2 (291,292). The displacement by Pol δ can lead to up to 30 nucleotide flaps which are coated in RPA (293). Dna2 binds to the end of the flap, and the nuclease activity reduces the flap to 5-6 nucleotides in length. This small flap is too small for RPA to cover; therefore, Rad27 can easily access and cleave it (294). Cdc9 (DNA ligase I in humans) is the ligase that seals the nick created by Rad27, producing a

continuous dsDNA (295). To ensure faithful replication, there are accessory proteins such as Ctf4, which stabilizes Pol α and facilitates replisome progression along with Mrc1 (296,297)

3.2.4 DNA replication termination and the end replication problem

DNA replication terminates when two converging replication fork bubbles meet (298). The replication machinery is then disassembled, and the daughter molecules are resolved. Once replication is complete, specific termination events disassemble the replisome. The locations of termination events have been mapped in yeast, and around 70 of the 300 events occur at specific chromosomal locations (299). It has also been shown that replication termination generally occurs midway between the two origins (236). As the leading strand is known to progress around 350 nucleotides faster than the lagging strand, there is no clashing when the two forks converge, as the leading strand polymerases are on opposite sides (290). The termination of DNA replication is currently still poorly characterized. To disassemble the replisome, Mcm7 is polyubiquitylated, resulting in CMG helicase unloading from the DNA (300,301). This ubiquitination depends on Dia2, which interacts with Mrc1 and Ctf4, factors that travel with the replication fork (302). However, as cells are viable but very sick in the absence of Dia2, other mechanisms may help remove the CMG complex (303). It is then believed that the rest of the replisome complex passively unloads due to CMG disassembly (304). This occurs after the gap between the leading strand and the lagging strands of converging forks have been ligated (304). Another aspect of S phase is the End Replication Problem, a phenomenon whereby the telomeres become progressively shorter following each round of DNA replication (305,306). This occurs due to DNA polymerases synthesizing in a 5’-3’ direction, and following the removal of the final

primer, the length of the RNA primer cannot be turned into DNA. If there were no counter mechanism to this problem, telomeres would continually shorten and become uncapped, which could initiate the DDR and result in chromosome fusions and genomic instability (307,308).

Telomeres are short, repetitive, non-coding TG-rich sequences that end in a 3' overhang (309,310). In vertebrates, this sequence is G_3T_2A, and in yeast, it is TG_{1-3} (311,312). Telomerase is constitutively active in yeast, elongating telomeres and preventing them from becoming critically short and triggering cell cycle arrest. By contrast, telomerase is inactive in most human cells except for in stem cells (313). Therefore, as humans age, the telomeres on their chromosomes become progressively shorter. Human cells, therefore, have a finite replicative capacity referred to as the 'Hayflick limit,' if this is reached, cells initiate replicative senescence or irreversible cell cycle arrest (314,315). Senescence can also occur in cells that are exposed to stresses such as oxidative stress and DNA damage (316).

3.2.5 DNA replication stress

The process of fork progression during DNA replication can be challenged by multiple issues, including DNA lesions, proteins bound to the DNA, secondary structures, and DNA transcription. DNA replication stress is a primary source of DNA damage, and this must be repaired efficiently. Stalled forks can collapse if not properly repaired and can lead to the dissociation of the replisome components and the formation of DSBs (317,318). Replication stress can also include reduced dNTPs and histones needed for DNA synthesis.

The DNA replication checkpoint (DRC) becomes activated if a critical number of forks arrest, resulting in the activation of Rad53 through a mediator Mrc1, which is phosphorylated by Mec1

(319,320). Mrc1 is part of the normal replisome and interacts with DNA pol ε and Mcm6 (321). These kinases lead to multiple changes to bring about the successful restart of the replication fork, including an increase in production of dNTPs, the transcription of DNA repair genes, repression of late-firing replication origins, cell cycle arrest, preservation, then repair and restart of the replication fork. If replication stress is not successfully resolved, this can lead to DNA damage and genomic instability.

Replication stress can result in stalling and uncoupling the polymerases from the CMG complex (322). This uncoupling leads to the activation of the DNA damage checkpoint (DDC) mechanism. First, long stretches of ssDNA are generated, which become bound and protected by RPA. Second, the generation of RPA-ssDNA recruits the obligate heterodimer, Mec1-Ddc2, through Ddc2 interactions with RPA (323,324). Next, Ddc1 as part of the 9-1-1 complex (Ddc1, Mec3, Rad17) is recruited, and together with additional factors including Dpb11, Rad9 and Dna2, activate Mec1 (325). Rad9 is phosphorylated by Mec1, which leads to the autophosphorylation of Mec1 and full activation of Rad53/Chk1 (326). If fork-associated DNA is not properly repaired, this can lead to high levels of genomic instability and result in duplication, deletions, translocations, and aneuploidy.

DNA replication stress often occurs naturally at intrinsically hard-to-replicate areas of the genome that has secondary structures and are difficult to unwind. However, DNA replication fork arrest can be induced in yeast upon the addition of Hydroxyurea (HU) which depletes nucleotides, Camptothecin (CPT) which binds to topoisomerase I resulting in a ternary complex and methyl methanesulfonate (MMS) which is an alkylating agent. These have been used in yeast research to investigate replication fork arrest and repair.

Replication stress is a leading cause of yeast replicative aging and genome instability within the rDNA locus and throughout the genome increase with replicative age (18). During aging, the cells' ability to deal with replication stress is compromised, leading to increased DNA damage. It is, therefore, essential to understanding the changes occurring in the natural aging of yeast.

3.2.6 FKH1 and FKH2 and DNA replication factories

A subset of early replication origins will cluster into foci called replication factories (327). Fkh1 and Fkh2 are highly conserved transcription factors that control global replication timing in yeast (327). Fkh1 and Fkh2 have essential roles in recruiting, limiting replication factors to early origins and promoting the clustering of origins into replication factories. The forkhead transcription factors bind to the DNA through the forkhead DNA binding domain (Fkh-DBD). The domain is a winged helix that binds to the DNA sequence (RYMAAYA) (Figure 3.3). Positive chromatin origins are defined by ORC having low affinity to the ORC binding site, with the Kd being between 30-300nM. The N terminal of Fkh1 is required for the origin activity of 75% of the positive-chromatin origins and promotes the binding of ORC to these origins (328).

In contrast, the positive DNA cohort has a high affinity to the ORC binding site with a Kd between 4-14nM (263,328). Fkh1 and Fkh2 have a critical role in clustering the early origins, and this regulation is independent of local transcription levels. Origin clustering allows the recruitment of limiting initiation factors to one place to allow for sufficient recycling of the factors following successful replication (329). Fkh1 and Fkh2 also have a well-characterized role in regulating the expression of the CLB2 cluster of genes in the G2/M phase of the cell cycle.

4C (chromosome conformation capture on chip) showed that interchromosomal and intrachromosomal interactions between proteins of Fkh-activated origins drive the clustering of these origins. Fkh1 and Fkh2 have been shown to cluster early origins in the G1 phase (327). This clustering helps to establish a high local concentration of DDKs to activate origin firing (328). Replication factories are very dynamic and can be disassembled to allow the following subset of factories to be created (330). This process allows the recycling of rate-limiting proteins during the initiation of replication. During the cell cycle, 30% of origins are Fkh activated, whereas 23% are repressed (327). Loss of Fkh1 and Fkh2 leads to loss of replication origin clustering, and Fkh-activated origins show delayed initiation, whereas Fkh-repressed origins show early initiation (327,331). It is believed that the repressed origins become activated as there is less competition for the rate-limiting initiation factors. During Fkh1 or Fkh2 overexpression, there is earlier firing of many origins through the genome, resulting in a larger quantity of replication origins being fired during the S phase (327).

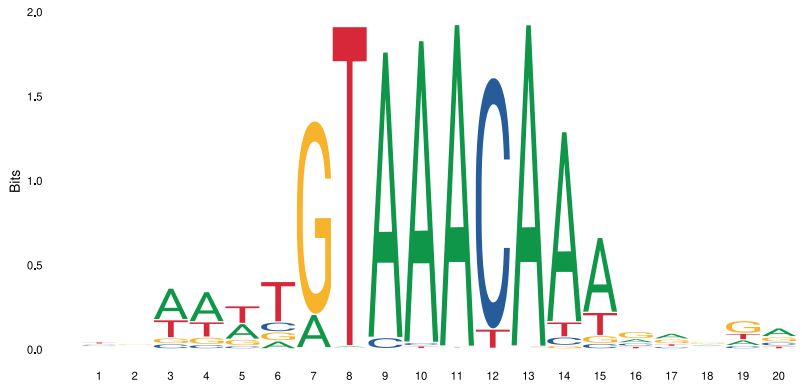

Figure 3.3 Fkh binding motif

The DNA motif bound by Fkh1 in yeast (RYAAAYA). This binding profile was obtained through JASPAR, an open-access database (http://jaspar.genereg.net/)

3.3 Results

3.3.1 Old cell enrichment and DNA replication initiation of early efficient replication origins

Replication was monitored during natural aging to identify age-related changes in progressively older cells. We enriched older yeast using our previously described method of OCE to separate young from old cells (332). In brief, cells were labelled with biotin and old cells were enriched by passage over a SuperMACS™ magnetic column. The method allowed efficient separation of young cells from biotin-labelled older cells.

To study DNA replication, cells were synchronized in G_1 phase of the cell cycle using α-factor before being released into S phase in the presence of 0.2 M HU. HU inhibits ribonucleotide reductase, depletes nucleotide pools and leads to an S-phase cell cycle arrest (333). HU does not affect the timing of early replication origin firing. However, it halts the progression of S phase by dNTP depletion (334,335). Consistent with previous reports, cells of advanced age (>11 divisions) proved difficult to synchronously release from a G1 α-factor block into S phase (336). As this study directly required cell synchronization, we focused on cells aged to O1 and O2. Young cells eluted from the XS column and recovered had undergone an average of 2 cellular divisions. In contrast, cells aged to O1 and O2 had undergone an average of 6 and 11 divisions, respectively. Flow cytometry showed that the α-factor block was successful and confirmed that cells of increased age could enter S phase efficiently after a 2-hour α-factor block and release into S phase and 0.2M HU (Figure 3.4).

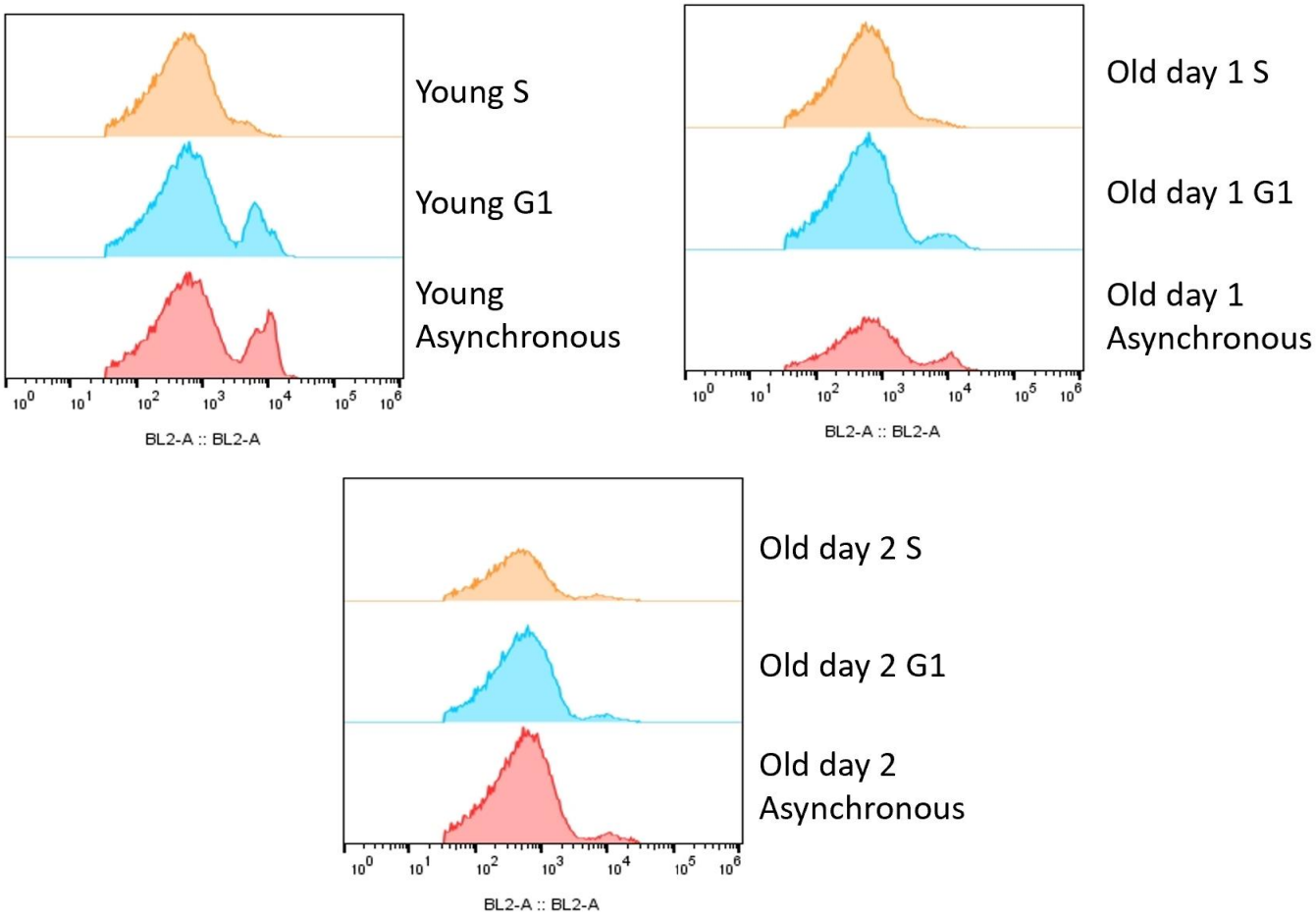

Figure 3.4 Synchronization of young and aged cells

Cell cycle analysis using flow cytometry of WT (JC-727) samples from young, O1 and O2 cells separated using the XS column. Cells were stained with propidium iodide (PI) and analyzed using the Attune Acoustic Focusing Cytometer (Life Technologies). A sample was taken following the separation of young and old cells for an asynchronous control. The cells were then synchronized in G1 using α-factor, and a sample was taken. Cells were then released into HU, and samples were taken at 60 minutes, in which the cells would have entered S phase of the cell cycle.

We performed a genome-wide analysis to map the profile of DNA replication initiation from early origins in young, O1 and O2 cells in the presence of HU (337). Genomic DNA was isolated at 0 and

60 minutes following α-factor release when early replication origins would have successfully fired in young cells. Using the G1:S ratio of DNA copy number between G1 (1N) and S phase (2N), we determined the impact of age on the profile of replication initiation.

A representative region of the genome, including ARS 305, 306 and 307, is shown (Figure 3.5, performed by M. Tittel-Elmer). These origins are all early and efficient, with the replication timing being 19.7, 17.9 and 19.3 minutes, respectively. The DNA copy number ratio of S/G1 is compared to determine replication initiation in young (Y) and progressively older O1-O2-aged cells. There were two copies (2N) of DNA at early-firing replication origins in young cells 60 minutes after entry into S phase, showing replication initiated (dark green, Figure 3.5). In O1 cells, initiation occurred. However, in O2-aged cells, there was a significant defect in origin firing as seen by the decrease in DNA copy number (medium and light green, Figure 3.5). What became apparent while looking at the genome-wide profiles was that the peak representing the site of replication initiation in O1-aged cells at many early firing origins was no longer centred over the ARS. We have termed these regions of initiation adjacent to the ARS sequence as delta origins (ΔOrigins), which will be discussed in further detail below.

To validate the G1:S method, we also performed IP-sequencing in Y and O1-aged cells to determine the signal-to-input ratio of BrdU when cells were released into S phase in the presence of 0.2M HU and BrdU, a thymidine analog that when present is incorporated into newly synthesized DNA. The incorporation of BrdU into O1 cells after 60 minutes decreases compared to young cells, confirming a replication initiation defect in aging cells (Figure 3.5).

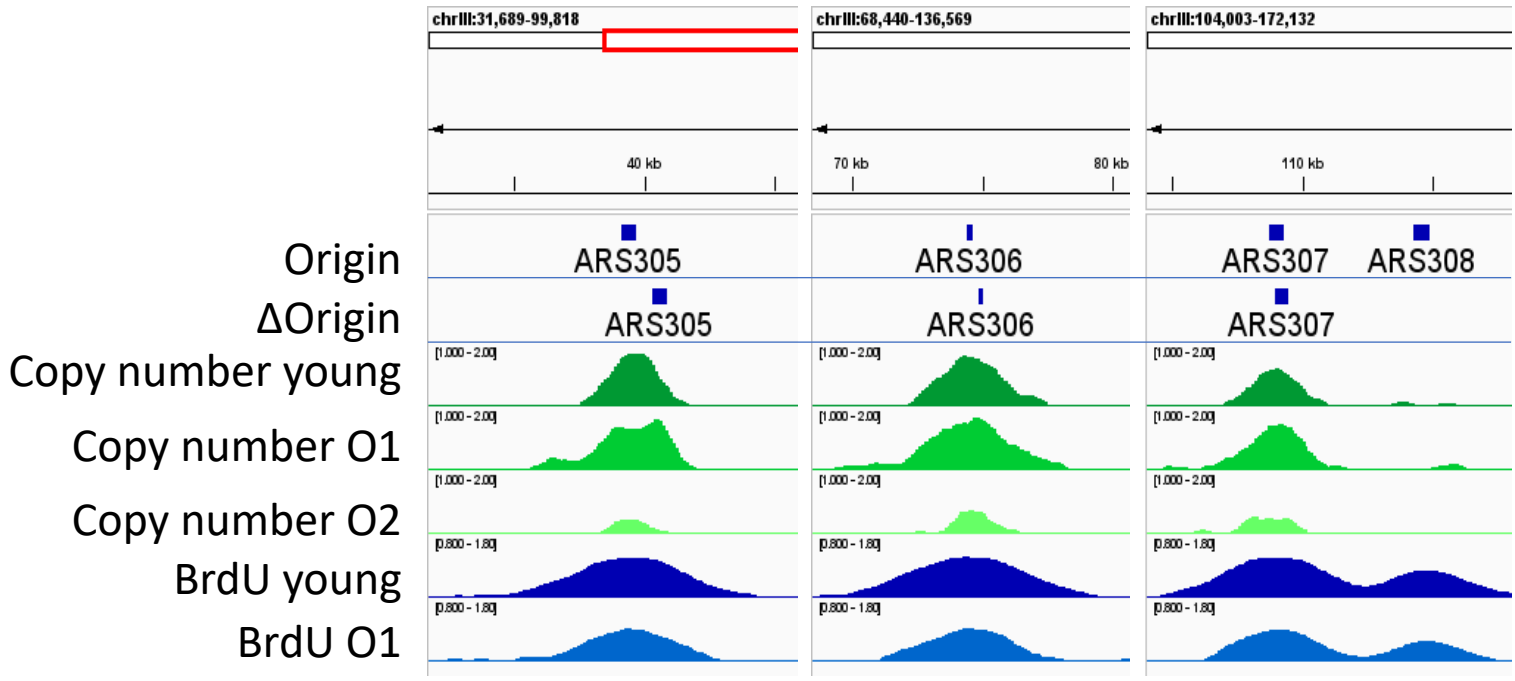

Figure 3.5 Replication origin firing is reduced in O1 cells

WT (JC-727) cells were enriched using the OCE method and synchronized in G1 using α-factor. Cells were then released into HU, and the DNA content was measured after 60 minutes and normalized to 0 minutes. The image represents the DNA copy number at three early and efficient origins from chromosome three – ARS305, ARS306 and ARS307. Dark green shows the copy number in young, medium green is O1, and light green is O2. Dark blue shows the BrdU incorporation in Y and light blue in O1 after 60 minutes.

ChIP at moving replication forks in synchronized aged cells has never been reported, likely because of the previously mentioned issues with enriching and synchronizing large quantities of old cells. Because there was a decrease in the initiation of replication as cells aged, we wanted to determine if this correlated with a failure in the recruitment of the DNA polymerases. We carried out chromatin immunoprecipitation (ChIP) of two polymerases, DNA pol α and pol ε, in young and aged cells that were synchronized in G1 with α-factor and released into the S phase in

the presence of HU. The ΔOrigin at ARS305 was much larger at 1200 bps compared to ARS306 and ARS307, which showed a ΔOrigin of 400 bp and 200 bp, respectively (Figure 3.5). Given the larger change in the initiation position, we used this ARS in ChIP-qPCR experiments as it would allow more precise resolution in factors present at ARS305 vs the ΔOrigin 305.

It has previously been shown that productive firing of replication origins is dependent on pol α concentrations, and firing is reduced when there is a decrease in pol α (338). We, therefore, wanted to determine the recruitment of pol α as cells age as another readout of replication origin efficiency. In this experiment, we normalize ChIP signals at and around ARS 305 to a region 14 Kb away ARS 607. This has been used routinely as a negative control previously in our laboratory and was chosen because ARS 607 has a small ΔOrigin of 100 bp but also because the adjacent replication origin, ARS 608, is highly inefficient and is only activated in less than 10% of cell cycles (339,340). Moreover, our maps indicated that 60 minutes after release into S phase and HU, replication was not detected at the ARS 607 14 Kb region. Lastly, we did not use 14kb away from ARS 305 as this would infringe on ARS 306, which is also an early firing origin.

ARS 305 has a replicating timing of 19.7 minutes after entry into S phase, and consistent with previous reports, peak recruitment of pol α occurs by 20 minutes in young cells (Figure 3.6) (337). However, in O1 cells, less pol α is recruited to the early replicating origin ARS 305 (Figure 3.6). Compared to young cells, there was a significant decrease in the recovery of pol α in old cells at ARS 305 ($P<0.05$), which could help explain the reduction of DNA replication observed at this early firing origin. It is also seen that the recruitment occurs later, which is also seen in a *SIR2* strain; therefore, the known loss of Sir2 in aged cells may be leading to this delay in recruitment

(341). Although there was less recovery, I could successfully perform ChIP on replisome components in aged cells.

Pol ε is the polymerase that is responsible for replicating the leading strand of DNA. We, therefore, also wanted to determine if there was a loss in its recruitment to ARS 305. Like pol α, pol ε recovery was lower in O1-aged compared to young cells at the early replicating origin ARS 305 (Figure 3.7). As cells age, there is a detectable decrease in the recovery of both DNA pol α and pol ε, whose loss impacts replication initiation (338,342). We have shown that aged cells could not initiate replication as efficiently through sequencing showing a loss of DNA content at early firing origins at the time points examined (Figure 3.5) and ChIP showing reduced DNA pol α and ε (Figures 3.6 and 3.7).

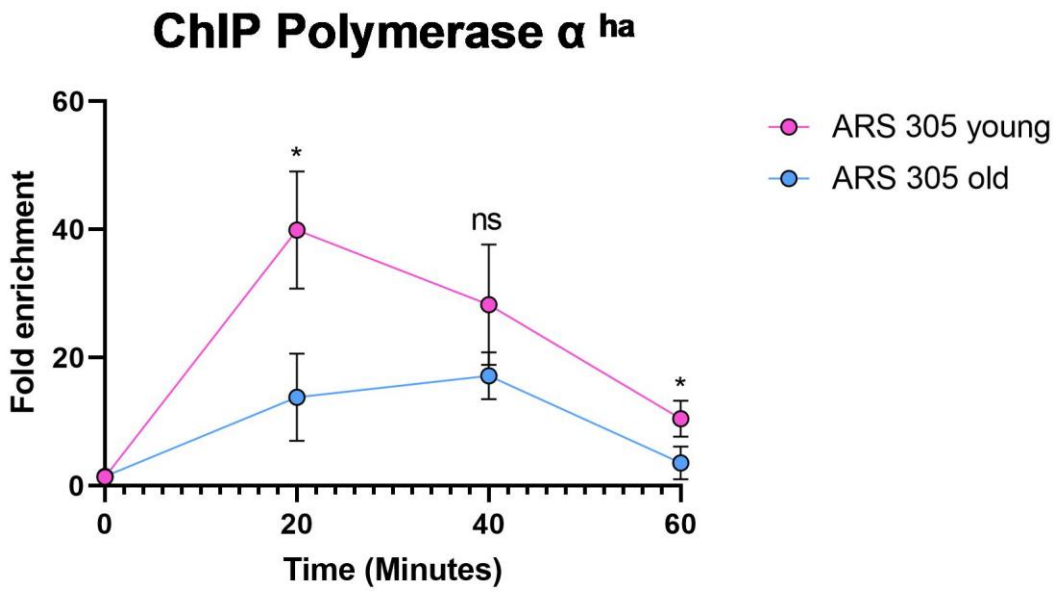

Figure 3.6 Loss of Pol α at ARS 305 in aged cells

ChIP was carried out to determine the enrichment of Pol α ^{HA} (JC - 5264) at ARS 305. Cells were enriched using OCE to O1 and synchronized in G1 using α-factor. Cells were then released into

HU, and time points were taken at 0, 20, 40 and 60 minutes. The fold enrichment was normalized to 14kb away from ARS 607. The error bars represent the standard deviation of three replicates for all the experiments. Significance was determined using a 1-tailed, unpaired Student's t-test. (P>0.05=NS; P<0.05*).

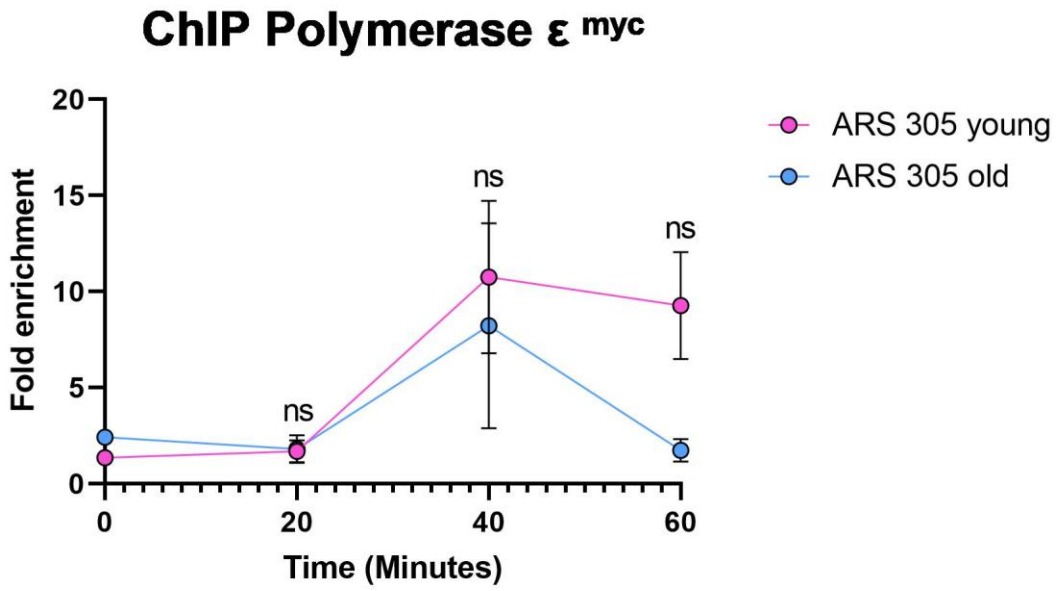

Figure 3.7 Loss of Pol ε at ARS 305 in aged cells

ChIP was carried out to determine the enrichment of Pol ε ^{Myc} (JC- 602) at ARS 305. Cells were enriched using OCE to O1 and synchronized in G1 using α-factor. Cells were then released into HU, and time points were taken at 0, 20, 40 and 60 minutes. The fold enrichment is normalized to 14kb away from ARS 607. The error bars represent the standard deviation of three replicates for all the experiments. Significance was determined using a 1-tailed, unpaired Student's t-test. (P>0.05=NS).

It is known that initiation factors are expressed at limiting levels to regulate replication timing (248,249). Since initiation factors are limiting in young yeast cells, this loss of initiation at early

replication origins could be caused by a decrease in the availability of these factors during aging. We, therefore, hypothesized that overexpression of these limiting factors might resolve the loss of the temporal order of origin firing and restore initiation.

To test this possibility, cells were arrested using α-factor, and Sld3, Sld7 and Cdc45 were induced from an inducible galactose promoter (GALp) by adding galactose (249). To assess overexpression in both young and O1 cells, the RNA content of the cells was measured. The young and O1 cells successfully overexpress Sld3, Sld7 and Cdc45 compared to the empty vector control (Figure 3.8). Although the initiation factors were overexpressed successfully (Figure 3.8), aged cells have a decreased level of protein synthesis; therefore, to confirm that this increase in RNA was leading to an increase in protein production, a western blot should have also been used. This would have allowed us to determine in total protein levels were increased during overexpression, but also allowed us to compare the overall protein levels to the levels of young EV and OE strains.

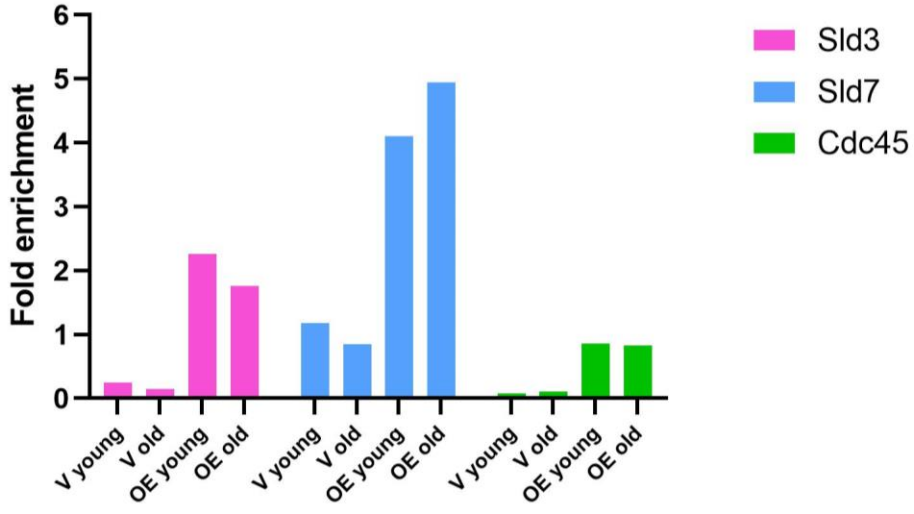

Figure 3.8 Overexpression of replication factors

Cells were collected from the OCE process. The cells were then synchronized in G_1 with α-factor. The cells were then released into media containing galactose and HU, and samples were taken after 60 minutes. RNA was then extracted and quantified using qPCR. RNA expression profile of empty plasmid vector (V) (JC-5606) for Sld3, Sld7, and Cdc45 in young and O1 cells and the overexpression strain (OE) (JC-5607) in young and O1 cells. Normalized to tubulin levels and fold enrichment levels are shown.

After confirming that the galactose inducible plasmid was successfully working in old cells, we wanted to determine the recruitment of pol α when the initiation factors were over-expressed. To express the plasmids successfully, we had to use minimal media. We carried out ChIP in young and O1 cells and synchronized the cells using α-factor before release into S phase and HU. Under these conditions, there was a reduction in the recovery of Pol α in both young and O1 cells. However, we did see a restoration in the relative level of Pol α being recovered at ARS 305 in old cells 60 minutes after cells were released from α-factor into HU when initiation factors were over-expressed. The fold enrichment at 60 minutes without overexpression was 0.6, whereas, with the overexpression, the enrichment was 3.3 (Figure 3.9). Showing that the increased presence of initiation factors was necessary to recruit polymerase in aged cells.

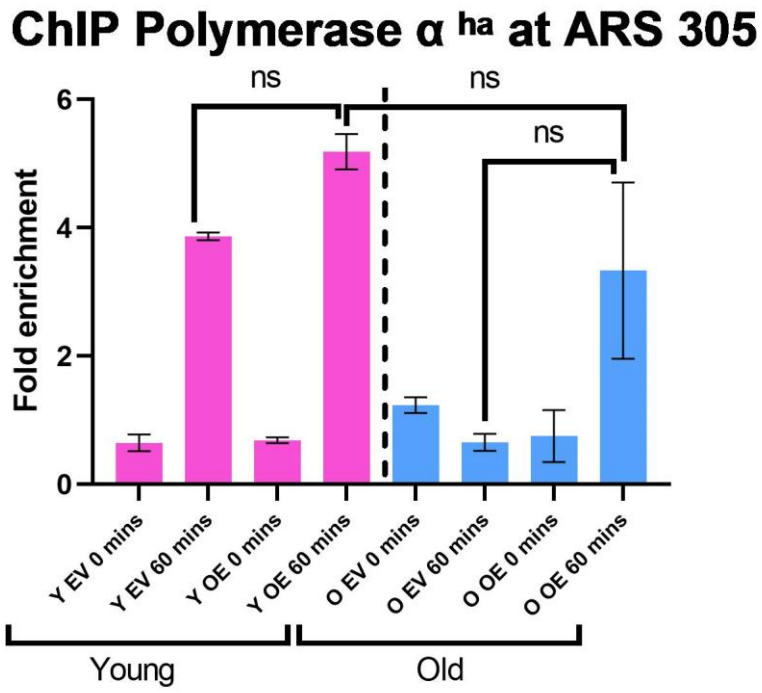

Figure 3.9 Recruitment of Pol α at ARS 305 during initiation factor overexpression

ChIP was carried out to determine the enrichment of Pol α ^{HA} (JC- 5607) in an Sld3, Sld7, Cdc45 overexpression (OE) and empty vector (EV) (JC- 5606) at ARS 305. Cells were enriched using OCE to O1 and synchronized in G1 using α-factor. Cells were then released into HU and galactose, and time points were taken at 0 and 60 minutes. The fold enrichment is normalized to 14kb away from ARS 607. The error bars represent the standard deviation of two replicates. Significance was determined using a 1-tailed, unpaired Student's t-test. (P>0.05=NS).

Encouraged by the recovery of pol α, we next wanted to confirm whether the origin was firing. To this end, we investigated DNA replication from ARS 305 using qPCR to measure DNA copy number when the initiation factors were over-expressed. As was done previously, the cells were synchronized using α-factor and released into HU while in the presence of galactose. As previously seen, there was replication at ARS 305 in young cells (Figure 3.10). When we over-

expressed Sld3, Sld7 and Cdc45, it was also seen that there was inefficient firing of ARS 305 in both the young and old cells. Over-expression of these factors can also advance the timing of replication initiation from late-firing origins (249). Therefore, one explanation is that a more significant number of origins fire at the beginning of the S phase, including ones that would not typically fire, resulting in further nucleotide depletion, replication stress and inefficient firing at some of the early replication origins (249). These results led us to speculate that the over-expression of these factors led to increased recruitment of polymerases at many replication origins rather than restoring the proper temporal pattern of origin firing. Indeed, we also observed a decrease in the DNA copy number at ARS 305 in young cells when Sld3, Sld7 and Cdc45 were induced (Fig 3.10).

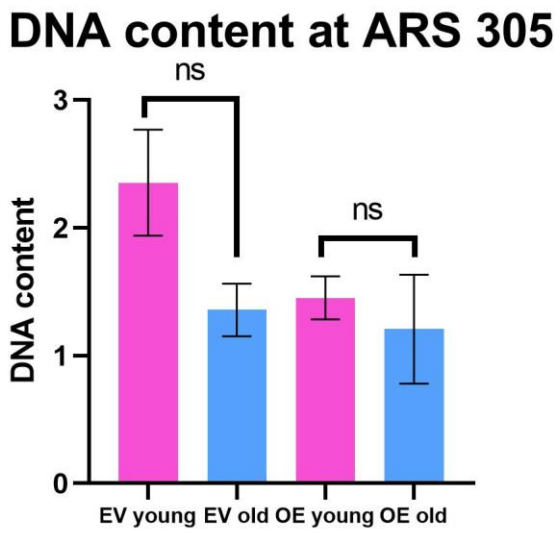

Figure 3.10 DNA content at ARS305 when initiation factors are overexpressed

Sld3, Sld7, Cdc45 overexpression (OE) and empty vector (EV) (JC- 5606) cells were enriched using the OCE method and synchronized in G1 using α-factor, and a sample was collected. Cells were

then released into HU and galactose, and the total DNA content was measured by qPCR at ARS 305 after 60 minutes. DNA content was measured using the ratio of S/G1 (60/0 minutes). Significance was determined using a 1-tailed, unpaired Student's t-test. (P>0.05=NS). The error bars represent the standard error of three replicates for all the experiments.

Functional organization of replication origins is crucial for genome duplication and has also been shown to maintain fork velocity (343). Fkh1 has a crucial role in clustering early origins, allowing their firing to occur in the vicinity of the proteins, nucleotides and histones needed for replication and promoting origin firing. It is known that Fkh1 has a role in replication timing and the loss of these transcription factors leads to reduced lifespan and changes in the replication timing program (344). Fkh2 is known to partially complement the loss of Fkh1 and regulate replication origins (345). Both Fkh1 and Fkh2 have been shown to have reduced protein expression in aged cells (346).

Next, I determined the level of Fkh1 and Fkh2 at ARS 305 in O1-aged cells. ARS 305 is a replication origin in which Fkh1 activates, and its loss leads to less efficient firing of the origin (344). However, the loss of Fkh2 was previously shown not to hamper the firing of ARS 305 (344). I performed ChIP on $Fkh1^{HA}$ and $Fkh2^{Flag,}$ followed by qPCR at ARS305. The levels of Fkh1 were significantly lower in O1-aged cells (P<0.05), whereas there was no difference in the levels of Fkh2 at ARS 305 in aged cells in G1 (Figure 3.11 and Figure 3.12). These data show a decrease in Fkh1 recruitment but no Fkh2 correlation with decreased initiation in O1-aged cells.

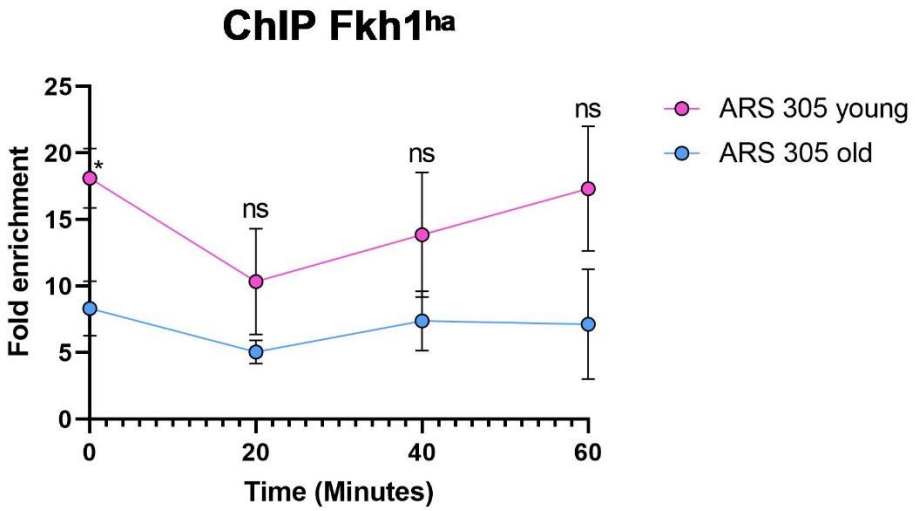

Figure 3.11 Loss of recruitment of Fkh1 at ARS 305 in O1 cells

ChIP was carried out to determine the enrichment of Fkh1 (JC- 5199) at ARS 305. Cells were enriched using the OCE method and synchronized in G1 using α-factor. Cells were then released into HU, and time points were taken at 0, 20, 40 and 60 minutes. The fold enrichment is normalized to 14kb away from ARS 607. Significance was determined using a 1-tailed, unpaired Student's t-test. (P>0.05=NS; P<0.05*).

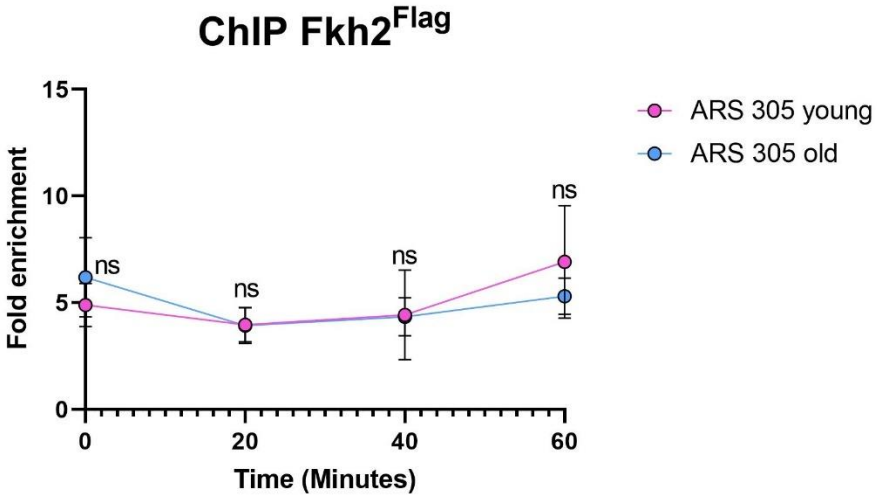

Figure 3.12 Fkh2 recruitment is maintained at ARS 305 in O1 cells

ChIP was carried out to determine the enrichment of $Fkh2^{Flag}$ (JC- 5074) at ARS 305. Cells were enriched using the OCE method and synchronized in G1 using α-factor. Cells were then released into HU, and time points were taken at 0, 20, 40 and 60 minutes. The fold enrichment is normalized to 14kb away from ARS 607. Significance was determined using a 1-tailed, unpaired Student's t-test. ($P>0.05$=NS).

Fkh1 promotes the binding of ORC to replication origins (328). So I hypothesized that if there was less Fkh1 recovery, the downstream impact might include a decrease in ORC recruitment and, by extension, a decrease in MCM recruitment.

To investigate this, ChIP was performed on both $Orc2^{Myc}$ and $Mcm2^{Myc,}$ followed by qPCR with primers to ARS305 in both young and O1-aged cells. Compared to young cells, the recovery of $Orc2^{Myc}$ and $Mcm2^{Myc}$ significantly decreased in O1-aged 60 minutes after release ($P<0.05$) (Figures 3.13 and 3.14). Taken together, these ChIP experiments suggest that in O1-aged cells, a reduction in Fkh1 in G1 could lead to a reduction in the recovery of ORC and MCM protein complexes in S phase that are needed for replication initiation and elongation.

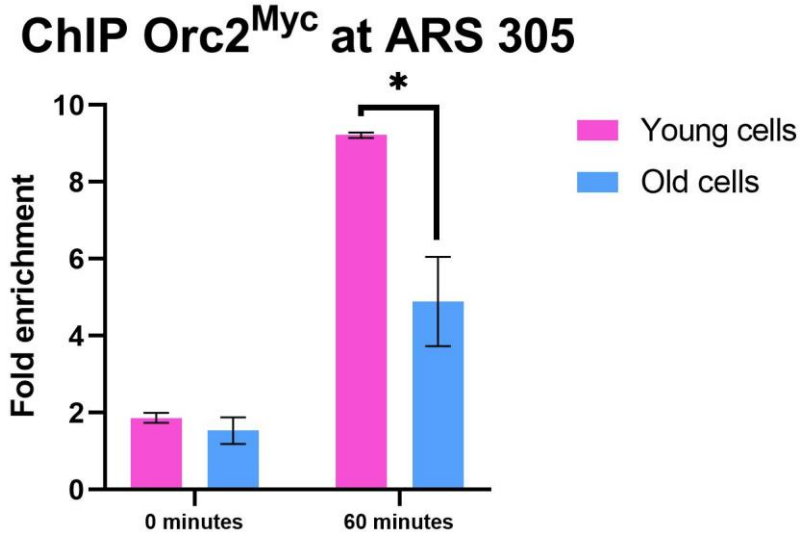

Figure 3.13 Recruitment of Orc2 at ARS 305 is reduced in O1 cells

ChIP was carried out to determine the enrichment of Orc2 ^{Myc} (JC- 764) at ARS 305. Cells were enriched using the OCE method and synchronized in G1 using α-factor. Cells were then released into HU, and time points were taken at 0 and 60 minutes. The fold enrichment is normalized to 14 kb away from ARS 607. Significance was determined using a 1-tailed, unpaired Student's t-test. ($P<0.05$).

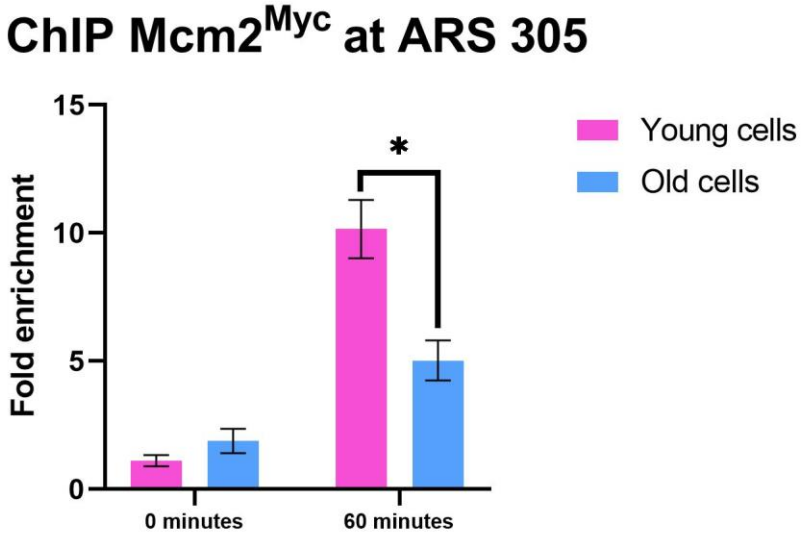

Figure 3.14 Recruitment of Mcm2 at ARS 305 is reduced in O1 cells

ChIP was conducted to determine the enrichment of Mcm2 ^{Myc} (JC- 171) at ARS 305. Cells were enriched using the OCE method and synchronized in G1 using α-factor. Cells were then released into HU, and time points were taken at 60 minutes. The fold enrichment is normalized to 14 kb away from ARS 607. Significance was determined using a 1-tailed, unpaired Student's t-test. ($P<0.05$).

3.3.2 The site of replication initiation changes during aging

ARS 305 is a chromatin-dependent ARS. Therefore, we wanted to look at all origins to determine any global changes occurring in aging cells that could contribute to the loss of Fkh1. Using the genome-wide sequencing data and DNA copy number analysis (Figure 3.5), we analyzed all 146 early-firing replication origins. We sorted them by their T_{Rep} (time of replication initiation) to confirm origin firing (Figure 3.15). There was very little initiation from replication origins that fired 23 minutes after release into S phase in the presence of HU (Figure 3.15). This was most likely due to the depletion of nucleotides. However, it could also be impacted by the cells not being successfully released from G1 phase into S phase. These origins represented 37% of the documented early-firing origins in the absence of HU and were excluded from further analysis (337).

We could see a decrease in initiation from origins firing between 19-23 and those less than 19 minutes also in O1 cells and continued our analysis with the 93 early-firing replication origins that fired < 23 minutes after release into S phase in young and O1 cells (Figure 3.16). What was striking from the analysis was an unusual 'broadening' of the peak in O1-aged cells (red box, figure 3.16). The loss of chromosomal organization at replication origins affects fork velocity (343). As we had shown, there was a decrease in Fkh1 recovery at ARS 305; there is likely a loss of functional

organization. Therefore, we hypothesized that the broadening of these peaks in aged cells might occur because of an increase in the speed of replication forks following initiation.

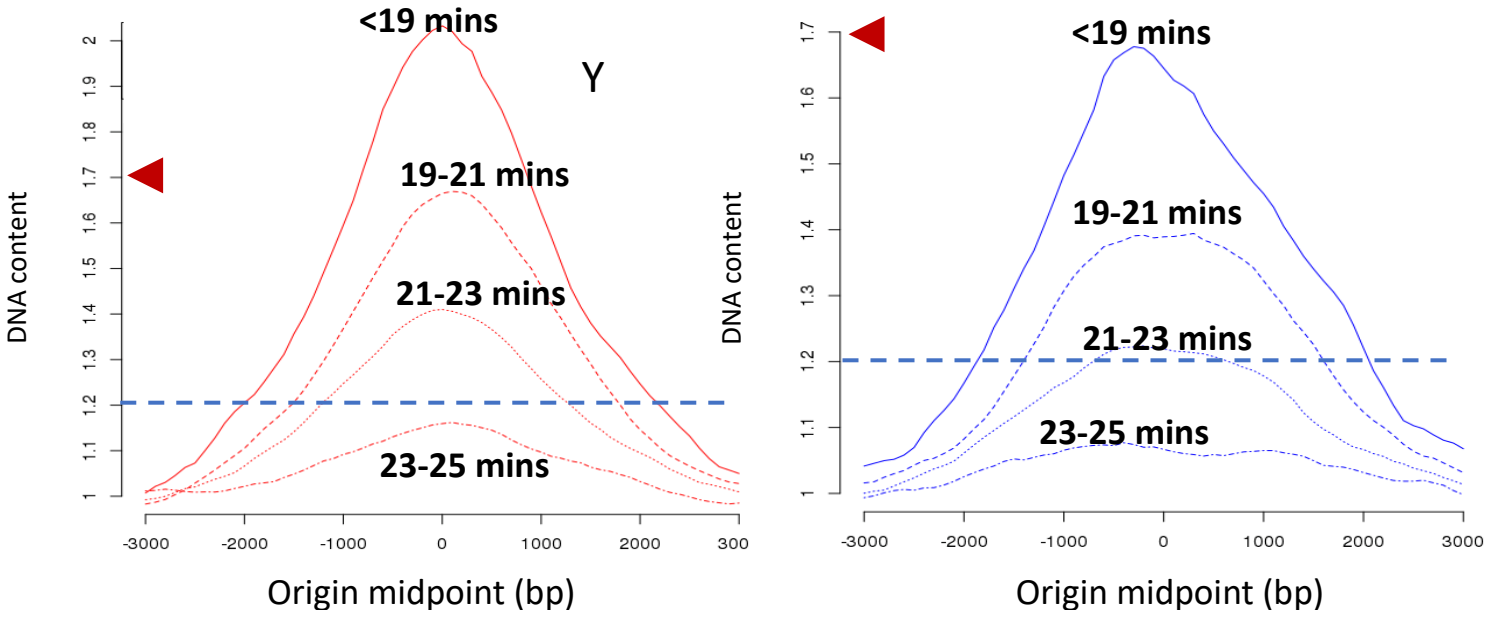

Figure 3.15 The timing of replication in young and old cells

WT (JC-727) cells were enriched using the OCE method and synchronized in G1 using α-factor. Cells were then released into HU, and the DNA content was measured after 60 minutes. The average of 146 early firing origins is shown for young and O1 cells, with the replication origin as 0bp. The origins were sorted into the time they replicate (Trep show in minutes).

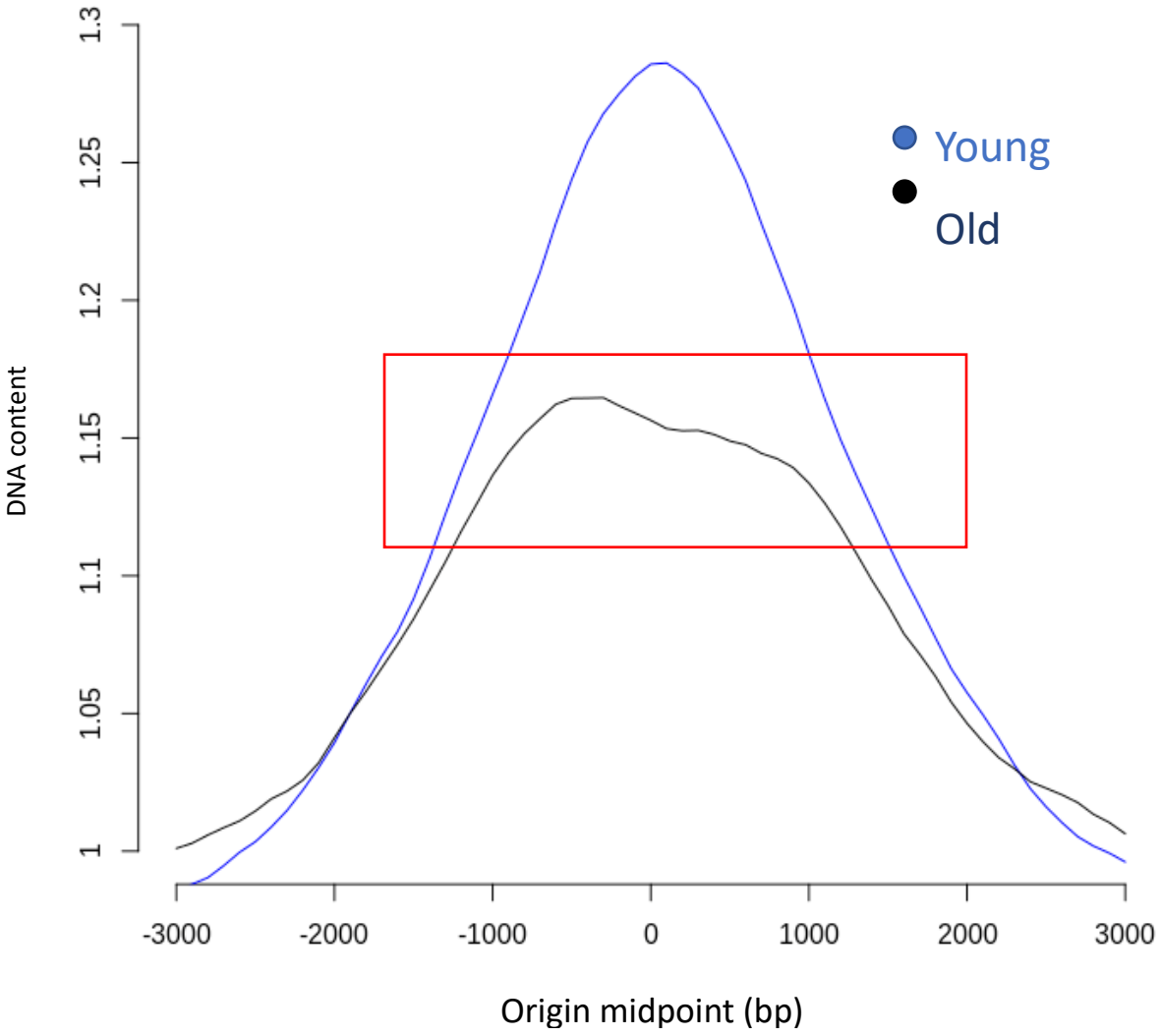

Figure 3.16 The average early replication origin firing is reduced in O1 cells

WT (JC-727) cells were enriched using the OCE method and synchronized in G1 using α-factor. Cells were then released into HU, and the DNA content was measured after 60 minutes. The average of 93 early firing (Trep before 23 minutes) origins is shown for young and O1 cells, with the replication origin as 0bp. The red box highlights the broadening of the peak in old cells.

To this end, we performed DNA combing in collaboration with the Brown Lab (University of Toronto). DNA combing allows the study of DNA replication through the incubation with halogenated thymidine analogs during DNA synthesis in the presence of HU (Figure 3.17A). The DNA tracks can then be visualized by immunofluorescence using antibodies against BrdU and ssDNA (347). The length of the BrdU tracks measures the speed of replication synthesis. We had previously confirmed that old cells successfully incorporate BrdU (as seen in Figure 3.5). Increased BrdU track lengths were observed in O2-aged cells suggesting a faster replication speed than in young cells (Figure 3.17B). We observed a significant increase in the rate of fork progression in O2 cells compared to young ($P<0.05$). However, this was not observed in O1.

As cells age, it is known there is a loss of histone occupancy (108,228). Therefore, the replication fork may be faster as less nucleosome repositioning occurs (25). Cells with faster replication forks also have increased genomic instability (348). However, once replication initiates, forks appear to progress at a faster speed. It was notable that fork progression was similar in O1 and young cells by DNA combing, suggesting fork rate could not account for the broader peak we observed in Figure 3.16.

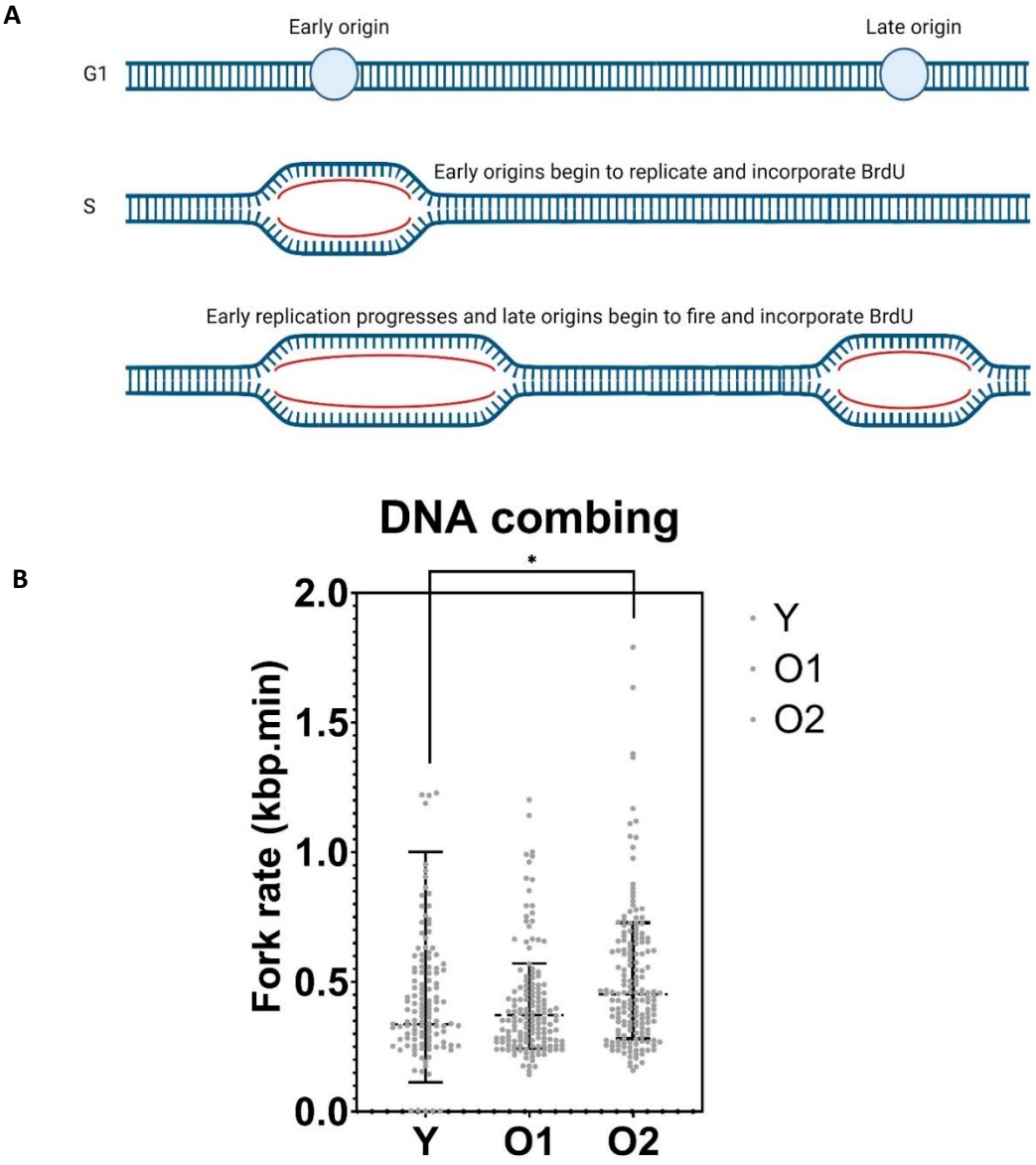

Figure 3.17 A model of DNA combing and increased replication fork rate in O2 cells

(A) Schematic of DNA combing and BrdU incorporation. Cells are synchronized in G1 phase before DNA replication begins. Cells are released into S phase, where DNA replication beings and early replication origins begin to fire, incorporating the BrdU analog into newly synthesized DNA. Replication continues, and the tracks of BrdU become larger. Further origins begin to fire and incorporate BrdU. These BrdU tracks can then be visualized and analyzed to determine replication fork speed.

(B) WT (JC-604) cells were enriched using the OCE method and synchronized in G1 using α-factor. Cells were then released into HU and BrdU, and samples were taken after 60 minutes for DNA

combing. The fork rate was measured in young, O1, and O2. Black lines show the geometric mean with geometric standard deviation. Significance was determined using a 1-tailed, unpaired Student's t-test. N=124,152,172. P=<0.05.

To investigate this further, we viewed the profile of individual origins used in the genome-wide analysis of replication profiles (Figure 3.18). From this, I observed that the peak in DNA content, which marks the start of replication, was not occurring at the ARS midpoint in aged cells. When we looked at the individual profiles of all 96 early firing origins individually, the peak, which represents the location of initiation, was also occurring at a region upstream or downstream of the ACS of the replication origins. We called this the delta origin or (ΔOrigin). In ARS 305, replication was initiated from a region 1200 bp downstream of the ARS midpoint, whereas, at ARS 1529.5, the ΔOrigin was 900 bp downstream of the midpoint. 14 kb from ARS 607 was the negative control for our ChIP experiments, as the ΔOrigin 607 was 100 bp from the ARS. In aged cells, 95% of replication initiation from early origins firing (< 23 minutes) was also occurring from a region separate from the sequence-specific ACS.

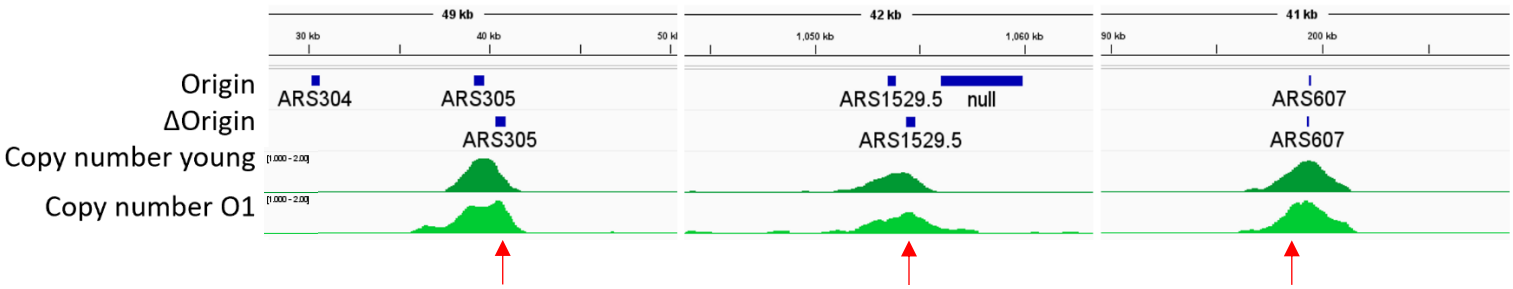

Figure 3.18 The site of DNA replication initiation changes in O1 cells

WT (JC-727) cells were enriched using the OCE method and synchronized in G1 using α-factor. Cells were then released into HU, and the DNA content was measured after 60 minutes. The image represents the DNA copy number at three early and efficient origins ARS305, ARS 1529.5 and ARSS 607. Dark green shows the copy number in young, and medium green is O1. The red arrows show the new initiation site in aged cells defined as the ΔOrigin.

When I looked at all the early firing origins, including the ones that didn't fire very efficiently after 23 minutes, we identified that 143/146 early origins had a ΔOrigin from 100bp to 3100bp of the ARS midpoint (Appendix table 1). Our initial hypothesis was that this could occur due to the transcription of nearby genes. However, we found no correlation between ΔOrigin, and transcription start sites. We determined that 89/143 (62%) of the ΔOrigin regions had a higher GC content on the side flanking the ΔOrigin (p-value <0.01). This correlation was fascinating as it is known that most origins in humans and mice occur in G-rich sequences that contain G4 structures (349). Therefore, early on in aging, in O1-aged cells, DNA replication initiates from regions containing a higher GC content. The alternative site continues to be the origin of replication in even older cells, and by O2, in addition to this, fork progression is occurring at a faster rate (Figure 3.17B).

We identified a correlation between the replication timing and the size of the ΔOrigin ($R^{2=}$ 0.2236 and P=<0.0001). The earliest replication origins fire at around 18 minutes into the S phases. It is seen that these origins have the smallest ΔOrigin (orange), whereas the later the origins fire, there is an increase in the average size of the ΔOrigin occurring (Figure 3.19). We believe this is likely due to the sequential loss of replication factors through S phase as replisomes are still bound at the earliest firing origins, which have stalled due to the presence of HU, and the

replisomes remain bound. This leads to fewer replisome components being available when later origins fire and the ability to replicate the DNA from the ARS midpoint becomes compromised as cells attempt to deal with replication stress.

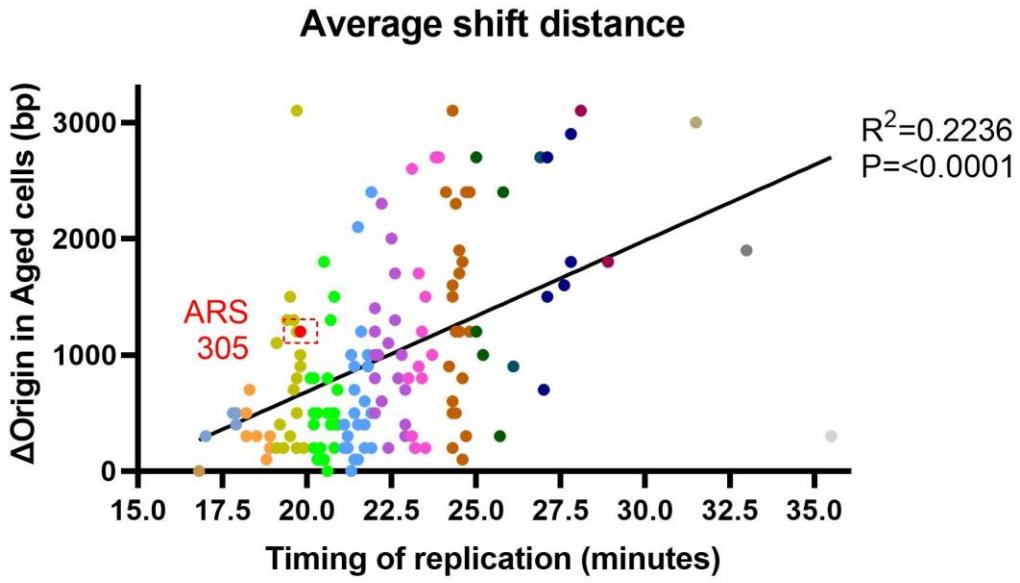

Figure 3.19 The ΔOrigin is seen to increase as the cell progresses through S phase

Analysis of replication ΔOrigin size (bp) and timing of replication origin replication (minutes). Each colour visualizes the replication timing for each minute, e.g., between 16-17 is brown, 17-18 is light blue, and 19-20 minutes is orange etc. The black line shows linear regression.

As mentioned above, the ΔOrigin for ARS 305 resided 1200 upstream of the ARS midpoint (305+1200). As we had seen replication initiate from a ΔOrigin away from the ARS, we wanted to determine if the decrease in polymerase recruitment at the ARS coincided with an increase in

recovery at the ΔOrigin region. Thus, I performed ChIP on Pol α and Pol ε followed by qPCR with primers designed for this region.

For pol α, there was a similar level of recovery at ΔOrigin in both young and old cells at 20 and 40 minutes, with significant loss ($p<0.05$) of pol α at 60 minutes in aged cells (Figure 3.20A). When plotted together with the recovery at ARS 305, as shown previously (Figure 3.6), the notable changes include a reduction in pol α at ARS 305 at 20 minutes ($p<0.05$), which could explain decreased initiation from ARS 305 and an increase in pol α recovery at the ΔOrigin in O1-aged cells, which was statistically different at 60 minutes ($p<0.05$) (Figure 3.20B).

When we carried out ChIP of pol ε, the polymerase recruitment to the ΔOrigin region was higher in aged cells at 40 minutes ($p<0.05$) (Figure 3.21A). However, as previously shown, there is no change in recruitment at ARS 305 at 40 minutes (Figure 3.7 and Figure 3.21B). This shows that as cells age, there is a change in the location of these replisome factors with the loss of recruitment at ARS 305 and the increase in recruitment to ΔOrigin in aging cells.

These data support a model wherein polymerases are recruited to the original ARS and the ΔOrigin region as cells age, with an increasing proportion going to the ΔOrigin region. However, it is seen that replication initiation occurs from the ΔOrigin region (Figure 3.18). The recruitment of polymerases to more than one location might be a mechanism to cope with age-related replication stress and to help improve firing efficiency. However, in young cells, the replication is maintained at the ARS, whereas in aged cells, it fires from the ΔOrigin.

A

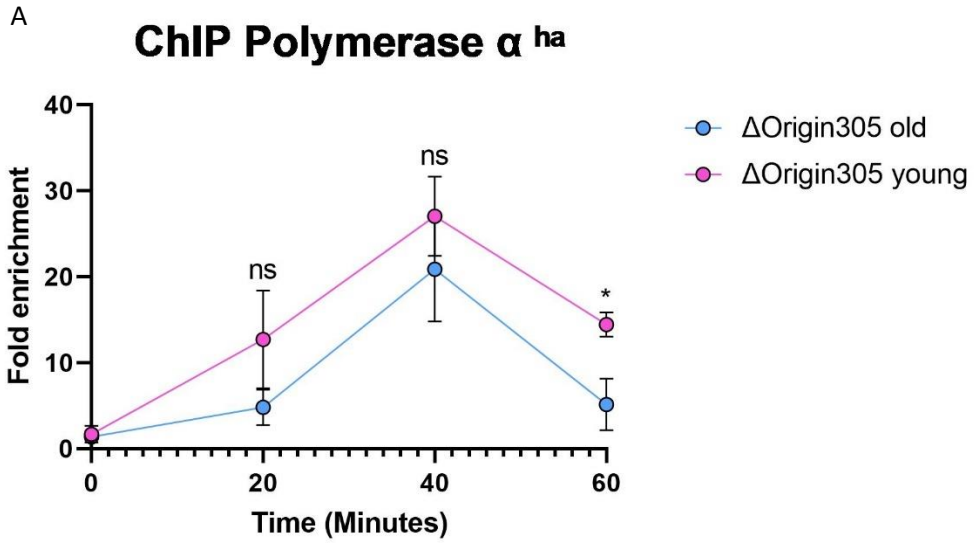

B

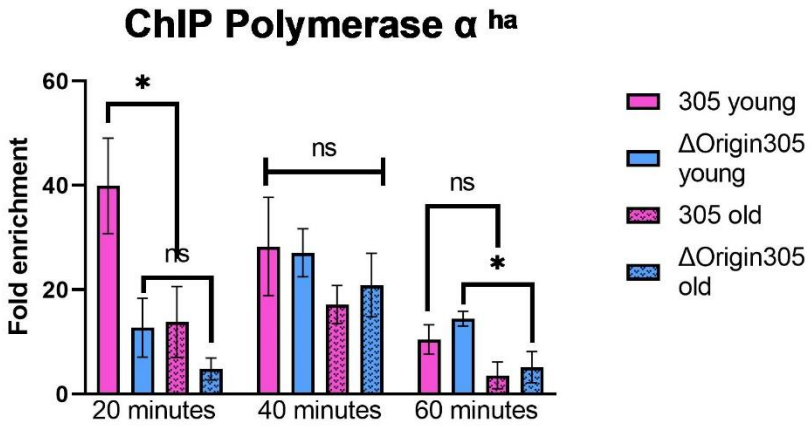

Figure 3.20 Recruitment of Pol α to ΔOrigin increases in O1 cells

ChIP was carried out to determine the enrichment of Pol α^{ha} (JC- 5264) at (A) the ΔOrigin305 region 1200bp downstream of ARS 305 and compared with (B) ARS305 from Figure 3.6 and ΔOrigin305 region. Cells were enriched using the OCE method and synchronized in G1 using α-factor. Cells were then released into HU, and time points were taken at 0, 20, 40 and 60 minutes. The fold enrichment was normalized to 14kb away from ARS 607. The error bars represent the standard deviation of three replicates for all the experiments. Significance was determined using a 1-tailed, unpaired Student's t-test. (P>0.05=NS; P<0.05*) (T-Rep = 20.4 minutes).

A

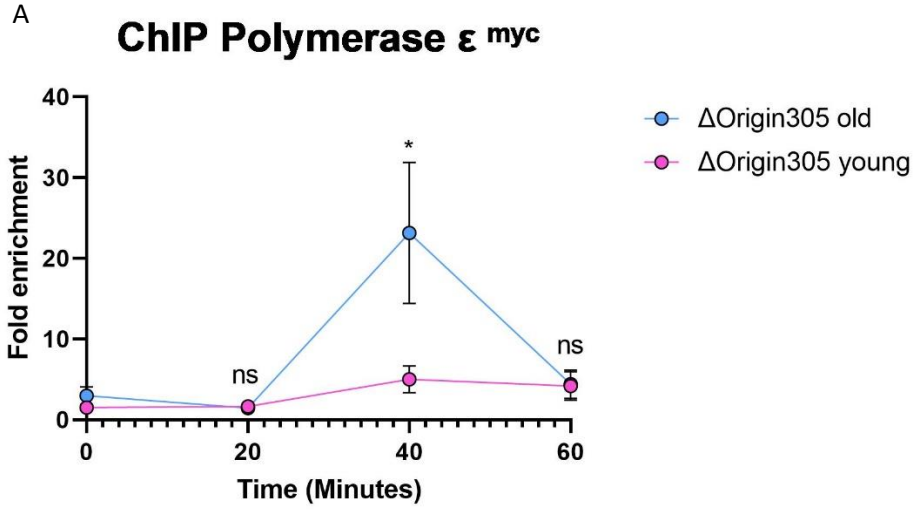

B

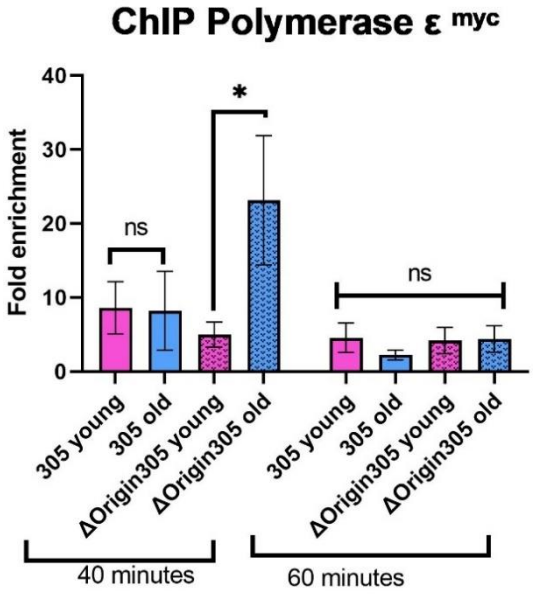

Figure 3.21 Recruitment of Pol ε to the ΔOrigin increases in O1 cells

ChIP was carried out to determine the enrichment of Pol ε ^{Myc} (JC- 602) at (A) the ΔOrigin305 region 1200bp downstream of ARS 305 and compared with (B) ARS305 from Figure 3.7 and ΔOrigin305 region. Cells were enriched using the OCE method and synchronized in G1 using α-factor. Cells were then released into HU, and time points were taken at 0, 20, 40 and 60 minutes. The fold enrichment was normalized to 14kb away from ARS 607. The error bars represent the standard deviation of three replicates for all the experiments. Significance was determined using a 1-tailed, unpaired Student's t-test. (P>0.05=NS; P<0.05*) (T-Rep = 20.4 minutes).

3.4 Discussion

Here we report age-related changes in the initiation of DNA replication and fork progression in yeast. The replication timing program becomes dysfunctional with a decrease in replication initiation. DNA replication occurs at the ARS midpoint less frequently and, instead, is seen to occur at a ΔOrigin. Loss of factors such as Fkh1 may result in changes to replication timing, replication speed and chromosomal organization. All the changes seen during natural yeast aging may impact genome integrity.

3.4.1 Old cell enrichment

The ability to collect cells at different time points throughout the cell cycle has allowed us to understand how the progression of age impacted DNA replication. As discussed in chapter two, our adapted process using a SuperMACS II separator with the XS column led to a faster and more efficient separation of aged and young cells. This allowed us to synchronize many old cells in G1 with α-factor for release into S-phase and HU, where the replication profile of aged cells could be determined. However, as the cells were cultured into stationary phase, the difficulty in releasing into the S phase likely increased as the culture was primarily in the G1 phase. This makes it hard to interpret cell cycle-based experiments, as the decrease in initiation may be due to fewer cells entering S phase and beginning replication. Therefore, OCE must be carried out whilst the cells are in the exponential phase to determine if this was a compounding factor. This could be done by replacing the media before the cells enter stationary phase or by decreasing the incubation time so the cells do not enter stationary phase. As the cells were in stationary phase, they also experienced cell stress brought on by the lack of nutrients in the culture. However, as

both young and old cells would be experiencing the same cellular stress and we still see changes in DNA replication, we account for this as changes related to age, not how they are cultured.

Supported by preliminary results, we anticipate that as cells age further to O3, there will be more pronounced defects in replication initiation and the inefficient recruitment of the replisome to replication origins. This would also correlate with the longer cell cycle in very old yeast cells (16). We also anticipate greater levels of replication stress which are less efficiently repaired through the DRC and DDC. However, this is difficult to determine experimentally due to the difficulty of synchronizing very old cells.

3.4.2 Age-related changes to the replication timing program

DNA replication has been extensively studied in yeast. However, all the monumental studies have always been performed in cultures containing predominantly young cells. Many studies have utilized cells harbouring deletions in proteins that result in a shortened lifespan (that age prematurely) to infer age-related changes in DNA replication. However, we wanted to investigate age-related changes in DNA replication in WT cells.

Replication during natural aging differed from replication in young and mutant cells that age prematurely. Compared to young WT cells, we show that following the enrichment of old cells, there is a decrease in the firing of early replication origins as cells enter the S phase of the cell cycle (Figure 3.5). After 60 minutes in HU, O2 cells were seen to be unable to initiate replication from early-firing replication origins efficiently. In follow-up ChIP qPCR experiments, I determined that there was significantly less recruitment of replisome factors, including DNA pol ε, DNA pol

α, MCM and ORC to ARS 305 ($p<0.05$) (Figures 3.6, 3.7, 3.13, 3.14). When there is less recruitment of Pol α to the replication fork, it is known that there is an increase in cells stalling during the S phase of the cell cycle (338). This increase in stalling will lead to higher levels of replication stress, which is a significant driver of genomic instability (350).

When there is a loss of Sir2, there is an increase in origin licensing of early euchromatic and telomeric origins. In contrast, late replicating EC failed to duplicate completely (272,351). Sir2 deletion also leads to a favoured loading of MCM at early origins over late origins. However, an alternative initiation, ΔOrigin, has not been observed. As cells age naturally, there is a decrease in Sir2 levels, likely leading to increased MCM levels at early origins. Therefore, premature aging mutants like Sir2 may not be a good model to determine the changes that occur during natural aging, as they cannot fully replicate the changes we observe. The MCM paradox has shown that the number of MCM complexes loaded on the genome far exceeds the number of origins that fire (352). It has been hypothesized that any NFR may enable double hexamer MCM loading by ORC in the G1 phase (353). These replication sites can be licensed during an S phase in replicative stress (354). It has been proposed that MCM is present on un-replicated chromatin as a way in which the cell can monitor and control that the whole genome has been replicated (352). Late origins are less efficiently activated in cells with low Sir2 levels, leading to replication gaps at the end of the S phase (272). As aged cells have low Sir2, they are likely to have increased gaps in genome replication.

Fkh1 has an essential role in replication timing, and its loss leads to premature aging (344). When *FKH1* is deleted, there is a decrease in the firing of 35 origins and an increase in 16 origins (344). Fkh1 has a role in the timing of the earliest firing origins. However, the loss of Fkh1 has also never

been shown to result in new initiation sites (such as ΔOrigins). In naturally aged cells, we find a significant decrease in Fkh1 localization to ARS 305 in G1 ($p<0.05$) (Figure 3.11) (329). Functional organization of the origins is crucial for genome duplication when there are varying inter-origin distances and for maintaining fork velocity (343). The loss of Fkh1 recruitment will lead to a loss of functional organization of the replication origins. Previous studies have used an Fkh1 and Fkh2 deletion strain with an Fkh1 overexpression plasmid and demonstrated that the Fkh1 overexpression could restore origin firing and yield a similar temporal replication programme to WT cells (331). It has been shown that there are fewer Fkh1 proteins in old cells (346); therefore, I would anticipate that if we over-expressed Fkh1 in aged cells, we might be able to restore origin firing and clustering as has previously been seen, resulting in fewer cells using the ΔOrigin to initiate replication (329).

Sld3, Sld7 and Cdc45 are rate-limiting initiation factors for origin activation (249). As aged cells had a defect in early origin firing, we hypothesized that overexpression of these factors might facilitate the firing of early origins in aged cells. The overexpression of these factors did facilitate the recruitment of Pol α to ARS. However, in aged cells, there was still a failure in the initiation of DNA replication (Figures 3.9 and 3.10). DDK phosphorylation of MCM is necessary for interaction with Sld3, Sld7 and Cdc45, which leads to DNA replication initiation (252); therefore, although we overexpressed the initiation factors in aged cells, the phosphorylation by DDK in aged cells is likely not occurring at all the origins, which are now able to recruit Pol α in the presence of increased initiation factors. Furthermore, replication initiation was not occurring. *BOB1* encodes for the Mcm5 subunit of the MCM replicative helicase. A *bob1-1* mutant bypasses

the requirement for DDK, and similar experiments performed in this genetic background might lead to an increase in replication initiation in both young and old cells (249).

Here, we find that once replication initiates, the rate of fork progression is significantly faster in O2 cells than in younger cells ($p<0.05$) (Figure 3.17). When replication forks progress at high speed, there is an increase in replication stress and genomic instability (348,355). It is known that when fewer origins fire, there is an increase in replication speed (343). This, together with reduced Fkh1 recovery at early-firing origins (like ARS 305), suggests that reduced initiation likely contributes to increased replication fork speed in aged cells. To confirm this hypothesis, it would be essential to determine if the loss of Fkh1 in young cells also increases replication fork speed. To do this, I would carry out DNA combing in an Fkh1 deletion strain.

3.4.3 Early firing origins of replication in aging cells do not initiate replication from the ACS midpoint

While identifying a decrease in replication initiation from early firing origins, it became apparent that firing no longer occurred from the midpoint of the ARS as it did in young cells. Replication initiation occurred at an adjacent alternative region located 100-3100 bps away from the mapped ARS in 98% of the early firing origins. Previous studies in replication timing and efficiency in premature aging mutants such as Sir2 and Fkh1 have never detected alternative initiation sites. However, a recent study by Lee et al., identified a change in the location of ORC complex binding when the ACS sequence-specific binding motif in Orc2 was removed (278). In humans, ORC does not bind DNA through sequence-specificity but binds to open chromatin with a high GC content (356). This may have been how human ORC evolved. This mutation was defined as a ‘humanized

ORC' as human ORC does not contain a sequence-specific region. They identified that this mutant binds the genome more promiscuously and preferentially to nucleosome-free regions (NFR), but what was interesting to us was that 54% of our ΔOrigins overlapped with where the mutant ORC binds and, to highlight this observation, we show Orc2 binding at ARS 305 (Figure 3.22; data from (278)). Although they never identified replication initiation from ΔOrigins, as we had seen, they were using young cells in the early S phase. This shows that the natural affinity for the ΔOrigin NFR is not the only driving force for replication in this region. Further features may be necessary, such as histone variants and post-translational modifications. It would be interesting in the future to determine what features of the ΔOrigin are driving replication occurring at these new sites.

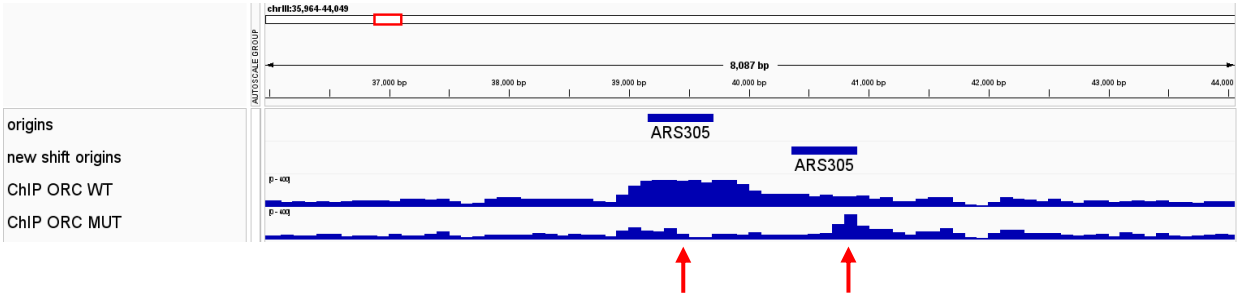

Figure 3.22 Mutations that prevent ORC binding to the ACS sequence bind to the ARS 305 ΔOrigin

Chip-seq was carried out by (278) to identify the binding of ORC and ORC-humanized (MUT). The published maps were reanalyzed to determine if the binding of ORC humanized bound to the ΔOrigin. The red arrows show the binding of the WT ORC to ARS 305 and the binding of ORC MUT to the ΔOrigin at ARS 305.

To study DNA replication, we used HU to deplete the nucleotides and slow down replication. As replication begins, the nucleotide pools are depleted, pausing fork progression, and causing

replication stress. Interestingly, as cells enter S phase, we see a distance increase in adjacent ΔOrigins from ARSs as a function of their TRep. This might be a consequence of decreased nucleotide levels and increased replication stress. In old cells, it is possible that replication is occurring from the ΔOrigin to cope with the replication stress and is utilizing sites where MCMs are loaded that are not typically utilized in young cells to complete replication. The decrease in Sir2 levels leads to increased MCM loading at early replication origins and is likely driving the ability of the cell to fire from the ΔOrigin (267).

RPA and Rad51 are the first proteins recruited during replication stress, and as cells age, there is a decrease in the expression of these proteins (99,332,357–359). Therefore, as cells age, there is likely to be less recruitment of these ssDNA binding factors necessary to carry out DDR. This could be investigated by performing ChIP on these factors to determine if this further contributes to increased genomic instability during aging. Loss of these factors would likely fail to restart the replication fork, and the replication fork collapse leading to genomic instability within the cell.

Replication origins are situated in an NFR, with well-situated nucleosomes surrounding the NFR. It was previously shown that ORC could bind to genome regions without an ACS but contain a nucleosome-NRF junction (354). However, not all NFR serve as replication origins, as there are 4000-5000 NFR in yeast. Previous studies have looked at changes in nucleosome occupancy during aging, showing a 50% loss of nucleosome occupancy genome-wide (25). I, therefore, wanted to identify if the ΔOrigin areas were also seen to be occurring in an NFR (25). I reanalyzed the MNAse-seq published maps in aging cells from the Tyler lab, and I identified that the ARS 305 ΔOrigin region was seen to be in a low nucleosome region in young cells, and this was further exacerbated in aged cells where there is reduced nucleosome occupancy (Figure 3.23) (25). An

increase in histones, through overexpression of H3 and H4, increases lifespan in yeast; this may occur in part due to the cells' ability to maintain the location of replication initiation and binding of ORC to the ARS instead of other accessible nucleosomes (25). It would be interesting to determine whether overexpressing histones in aged cells restores the replication initiation from the ARS. This suggests that the ΔOrigin regions are occurring in low nucleosome regions that were highly accessible for aged cells to start replication, with high GC content and further away from the origin midpoint as the cell progresses through the S phase. Immediate-early firing origins contain sequence-specific motifs that lead to their firing even if they are relocated to late-firing regions of the genome (360). When ARS 305, 607 and 731.5 are relocated to a late-firing VPS13 locus in chromosome XII (which has no other replication origins within 60 kb), they maintain their firing timing even though they are in a late-firing chromatin environment. It is, therefore, plausible that the T_{Rep} is being maintained through adjacent GC content in immediate early firing origins.

Our study identifies that, as cells age, ORC no longer binds to the ACS and instead binds to a ΔOrigin region upstream or downstream, compared to young cells where all replication studies have been determined. Aged cells have an altered profile of DNA replication. The dysfunctional replication timing program leads to an increased replication fork speed and misregulation of replication origin firing. All these combined increase replication stress, replication fork collapse and genomic instability during aging.

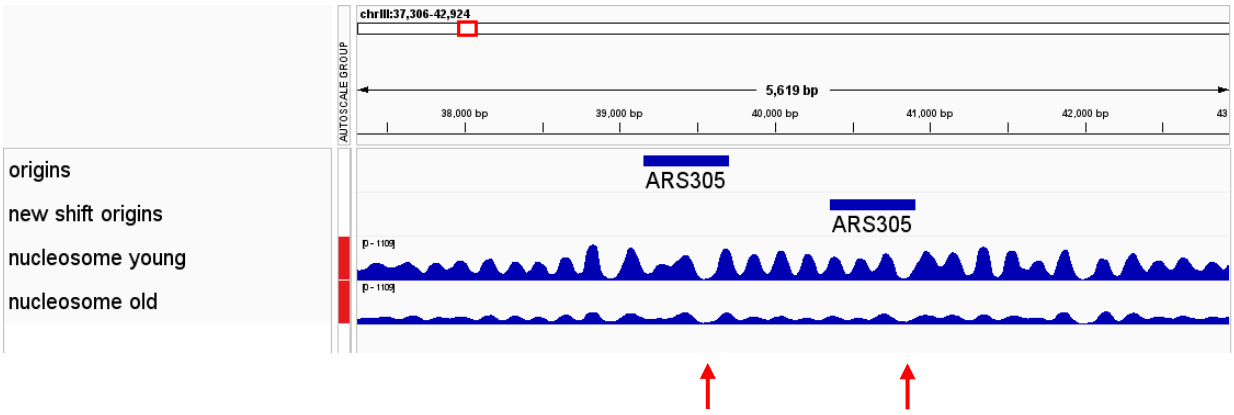

Figure 3.23 Nucleosome maps identify a NFR at ARS 305

Nucleosome mapping was carried out by (25) to identify nucleosome occupancy in young and old cells. The published maps were reanalyzed to determine if there was an NFR at the ΔOrigin. The red arrows show an NFR at ARS 305 and an NFR at ΔOrigin.

3.5 Materials and methods

Table 3.1 Key resource table

REAGENT or RESOURCE	SOURCE	IDENTIFIER
Antibodies		
HA-probe mouse monoclonal antibody	Santa Cruz Biotechnology	F-7
FLAG-Probe mouse monoclonal antibody	Santa Cruz Biotechnology	M2F12
Myc-Probe mouse monoclonal antibody	Abcam	ab32
Chemicals		
α – factor	EZBiolab	CP7206
Adenine	Sigma	A8626
Albumin, Bovine Serum, Fraction V, low heavy metals	Calbiochem	12659
Ammonium sulfate	VWR	BDH9216
Anti-Biotin MicroBeads	Miltenyi Biotec	130-090-485
Bacto™ Peptone	BD Biosciences	211677
Bacto™ Yeast extract	BD Biosciences	212750
5-Bromo-2'-deoxyuridine (BRDU)	Sigma	B5002
Calcofluor white stain	Sigma	18909
Complete EDTA-free protease inhibitor cocktail	Roche	04693159001
Dextrose	Sigma	D1912
Difco™ Agar	BD Biosciences	214530
Difco™ Yeast Nitrogen Base without Amino Acids and Ammonium Sulfate	BD Biosciences	233520
Dynabeads Sheep anti-Mouse IgG	Invitrogen	20230531
EDTA	VWR	0322
Ethanol	Commercial alcohols	P006EAAN
Ez-Link™ Sulfo-NHS-LC-Biotin Sulfosuccinimidyl-6-(biotinamido) hexanoate	Thermoscientific	21335
Formaldehyde	Sigma	F8775
Galactose	Sigma	G0750
Glycine	VWR	CA93291
Glycogen	Roche	10901393001
HU	US Biological	H9120
L-Arginine monohydrochloride	Sigma	A5131
L-Aspartic Acid	Sigma	A9256
L-Glutamic Acid	Sigma	G1626
L-Histidine	Sigma	H8000
L-Isoleucine	Sigma	I2752

L-leucine	Sigma	L8000
L-Lysine	Sigma	L5501
L-Methionine	Sigma	M9625
L-Phenylalanine	Sigma	P2126
L-Serine	Sigma	S4500
L-Threonine	Sigma	T8625
L-Tryptophan	Sigma	T0254
L-Tyrosine	Sigma	T3754
L-Valine	Sigma	V0500
Lactic acid	Sigma	69785
2-Mercaptoethanol	Sigma	M6250
Paraformaldehyde	Sigma	158127
Phenol-Chloroform-Isoamylalcohol	Invitrogen	15593049
PMSF	Sigma	78830
Potassium Chloride	EMD Chemicals	1049360500
Potassium phosphate monobasic	Sigma	P9791
Raffinose	US Biological	R1030
RNase A	Thermoscientific	EN0531
SDS	Avantor	409502
Sodium Acetate	VWR	BDH9278
Sodium citrate dihydrate	Sigma	W302600
Sodium Chloride	Fisher Chemical	S64212
Sodium hydroxide	EMD Millipore	1310-73-2
Sodium phosphate, dibasic, anhydrous	VWR	84486-300
Sorbitol	Sigma	S1876
SuperMACS^{TM} II Separator	Miltenyi Biotec	130-044-104
Tris base	Fisher Chemical	BP1525
Triton	Sigma	9002931
Uracil Minimum 99%	Sigma	U0750
XS Columns	Miltenyi Biotec	130-041-202
Zirconia Silica beads	BioSpec Products	11079105z
Zymolyase	US Biological	Z1000
Enzymes		
Proteinase K	Invitrogen	25530031
RNase A	Sigma	R6513
RsaI	New England Biolabs	R0167S
Kits		
DNeasy Blood and tissue kit	Qiagen	69504
PowerUp SYBR Green Master Mix	Applied Biosystems	A25743
RNeasy mini kit	Qiagen	74104
Western Lightning Plus-ECL	PerkinElmer	NEL105001EA
Primers		

Primers used in this study	Table 3.2	
Yeast strains		
Yeast strains used in this study	Table 3.3	

3.5.1 Method details

Old Cell Enrichment

Old cell enrichment (OCE) was based on (229). For all assays, 20ml of overnight culture was inoculated in YPAD medium at 25°C. Cells were diluted to 100ml of YPAD and grown into log phase. Cells were harvested and washed three times with 1x phosphate-buffered saline (PBS). Cells were then resuspended in 1ml PBS and mixed with 8mg of Sulfo-NHS-LC- Biotin per $1x10^8$ cells for 30 min at 30°C. Cells were washed three times with 1ml PBS and 0.1M Glycine and used to inoculate 500ml SC media overnight at 25°C. Cells were harvested at 5000rpm for 10 minutes and washed thrice with PBS. Cells were then incubated in 50ml PBS and 20µl of Anti-Biotin Microbeads per 10^7 total cells at 4°C for 30 mins. Young and old cells were then separated by flowing through an XS column on the SuperMACS II separator at room temperature and washed thoroughly with 150ml of PBS until no more liquid remained on the column. The XS column is removed from the magnetic field, and the old cells are eluted using a syringe.

Bud Scar Microscopy

Following old cell enrichment, 20µl of cells were collected and fixed with 2µl of formaldehyde. Cells were then pelleted and stored at 4°C for imaging. Cells are resuspended in 20µl of PBS and stained with calcofluor. Cells are then placed on coverslips and imaged using Zeiss LSM 880 with Airyscan. Images were analyzed using ZenBlue software. Each cell was analyzed individually, and

>50 cells were analyzed per sample. Z-stack images were acquired with 0.35µm along the z plane using a plan-apochromat 63x/1.40 Oil Dic M27 objective.

Flow Cytometry

Samples for flow cytometry were prepared using 500µl of cell suspension with 1 ml of 95% ethanol. The fixed samples were then stored at 4°C for processing. The cells were spun down at 13000 RPM for 1 minute and rinsed with 50 mM sodium citrate (pH 7.0). The cells were spun down again at 13000 RPM for 1 minute and suspended in 50mM sodium citrate, 100µg/mL RNAase A overnight. The next day 400µg/ml of proteinase K was added, and the sample was incubated at 50°C for 1 hour. The cells were then pelleted and resuspended in 50mM sodium citrate and 10µg/ml propidium iodide. Cells were then sonicated for 3 seconds at 10% to break up clumps and analyzed using the Attune Acoustic Focusing Cytometer (Life Technologies).

Western Blot

Cells were lysed by re-suspending them in lysis buffer (with PMSF and protease inhibitor cocktail tablets) followed by bead beating. The protein concentration of the whole-cell extract was determined using the Nanodrop. Equal amounts of whole-cell extract were added to wells of 10% polyacrylamide SDS gel. After the run, the protein was transferred to a Nitrocellulose membrane at 100V for 80mins. The membrane was Ponceau stained (which served as a loading control), followed by blocking in 10% milk-PBST for 1 hour at room temperature. Respective primary antibody solution (1:1000 dilution) was added and left for overnight incubation at 4°C. The membranes were washed with PBST and left for 1 hour with a secondary antibody. Followed by washing the membranes, adding the ECL substrates and imaging them.

Chromatin Immunoprecipitation

ChIP assay was performed as described previously (361). Cells were collected from the OCE process. The cells were then synchronized in G_1 by resuspending in YPAD ph5 containing α-factor for 2 hours at 30°C. The cells were washed three times with water and released into YPAD ph7 media containing 0.2M HU. Cells were harvested and cross-linked at various time points using a 1% formaldehyde solution. After cross-linking, the cells were washed with ice-cold PBS, and the pellet was stored at -80°C. The pellet was re-suspended in lysis buffer (50mM Hepes pH 7.5, 1mM EDTA, 140mM NaCl, 1% Triton, 1mM PMSF and protease inhibitor cocktail), and cells were lysed using Zirconia beads and a bead beater. Chromatin fractionation was performed to enhance the chromatin-bound nuclear fraction by spinning the cell lysate at 13,200rpm for 15 minutes and discarding the supernatant. The pellet was re-suspended in lysis buffer and sonicated to yield DNA fragments (~500bps in length). The sonicated lysate was then incubated in beads + anti-HA/Myc Antibody or unconjugated beads (control) for 2 hrs at 4°C. The beads were washed using wash buffer (100mM Tris pH 8, 500mM NaCl, 0.5% NP-40, 1mM EDTA, 1mM PMSF and protease inhibitor cocktail) and the protein-DNA complex was eluted by reverse crosslinking using 1% SDS in TE buffer, followed by proteinase K treatment and DNA isolation via phenol-chloroform-isoamyl alcohol extraction. Quantitative PCR was performed using the Applied Biosystem QuantStudio 6 Flex machine. Primer sequences are listed in Table 3.2.

RNA expression

Cells were collected from the OCE process. The cells were then synchronized in G_1 by resuspending in YPAGalactose pH5 containing α-factor for 2 hours at 30°C. The cells were washed three times with water and released into YPAGalactose ph7 media containing 0.2M HU. Cells per

collected for 60 minutes and stored at -80°C. RNA was extracted following a Qiagen RNeasy mini kit. Reverse transcription was carried out using a Quantitect reverse transcription kit. Quantitative PCR was performed using the Applied Biosystem QuantStudio 6 Flex machine. Primer sequences are listed in Table 3.2.

DNA Combing

DNA combing was performed as previously described (361). Cells were collected from the OCE process. The cells were then synchronized in G_1 by resuspending in YPAD pH5 containing α-factor for 2 hours at 30°C. 400µg/ml of BrdU was added to the culture after 1 hour. The cells were washed three times with water and released into YPAD ph7 media containing 0.2M HU and 400µg/ml BrdU. Cells were harvested at 60 minutes in 0.1% sodium azide. Agarose plug preparation and digestion, and DNA combing were then carried out following the (362) protocol.

DNA content

Cells were collected from the OCE process. The cells were then synchronized in G_1 by resuspending in YPAGalactose ph5 containing α-factor for 2 hours at 30°C. The cells were washed three times with water and released into YPAGalactose ph7 media containing 0.2M HU. Cells were harvested at various time points and in 0.1% sodium azide, and pellets were stored at -80°C. Preparation of genomic DNA in SCE buffer (1M sorbitol, 0.1M sodium citrate pH7.0, 60mM EDTA pH 8, 0.125% (v/v) β-mercaptoethanol, 10 U/ml zymolyase). DNA was extracted using Qiagen DNeasy Blood and tissue kit and diluted to 0.3ηg/µl. Quantitative PCR was performed using the Applied Biosystem QuantStudio 6 Flex machine. Primer sequences are listed in Table 3.2.

Table 3.2 Primers

Primer name	**Sequence**
ARS607 14kb FW	CAG GAT ATG CGG CCA AAT TT
ARS607 14kb RV	GCA TGA CAG CCG AAT CGA T
ARS305 FW	TGGATTGAGGCCACAGCAA
ARS305 RV	TCACACCGGACAGTACATGAAAC
ARS305+1200 FW	CCATGTGTCTCTTGTCGGATTC
ARS305+1200 RV	TGACCCCAACCGATTTATTGA
ARS305-1200 FW	TCGGGTATCCCAGCTTTGC
ARS305-1200 RV	CGCATTAGCTGATCGTAGGAAA
SLD3 OE FW	AGCTTGAGAAGGACAAAGACC
SLD3 OE RV	ACTTGGTTCGGCAGGTATTT
SLD7 OE FW	TCTCAACAAAGGAAGATCGGAAC
SLD7 OE RV	TCCCTGTGCGTAAATTCAGC
CDC45 OE FW	TGCTCATAGACCGTGGAATCT
CDC45 OE RV	GTCTGTGACTTCATCGGCAT

Table 3.3 Yeast strains used in this study

Strain	**Genotype**	**Reference**
JC-171	MATa, *ade2*-1*, trp1*-1*, his3*-11, -15*, ura3*-1*, leu2*-3,-112*, can1*-100, *pep4*::*LEU2,* CDC54- 13Myc::*KanMX6*	(340)
JC- 602	MATa, ade2-1 trp1-1 his3-11 his3-15 ura3-1 leu2-3 leu2-112	This study
JC-604	MATa, *ade2-1,trp1-1, can1-100, leu2-3, 112, his3-11, 15, ura3-1, GAL, psi+,RAD5,URA3*::*GPD-TK*	(363)
JC-727	MAT α; *hml*::*ADE1 hmr*::*ADE1 ade3*::GAL-HO *ade1*-100 *leu*2-3, 112 *lys*5 *trp*1::*hisG ura3*-52	JKM179, (364)
JC-764	MATa, *RAD50-3HA*::*TRP1*, *ORC2-9Myc*::*LEU2*, *ade2*-1*, trp1*-1*, his3*-11, -15*, ura3*-1*, leu2*-3,-112	(340)
JC-5074	MATa, ade2-1 trp1-1 his3-11 his3-15 ura3-1 leu2-3 leu2-112, can1-100 fkh2-FLAG::KAN	This study
JC-5199	MATa, ade2-1 trp1-1 his3-11 his3-15 ura3-1 leu2-3 leu2-112, can1-100 HA-Fkh1::TRP	This study
JC-5264	ade2-1 trp1-1 his3-11 his3-15 ura3-1 leu2-3 leu2-112, HA-pola::TRP	This study
JC-5265	MATa, ade2-1 trp1-1 his3-11 his3-15 ura3-1 leu2-3 leu2-112, Myc-MCM7::URA	This study
JC-5606	JC5264 with his3-11,15::GALp-MycHis9::HIS3	This study (249)
JC5607	JC5264 with cdc7-4 his3-11,15::GALp-SLD3/SLD7/CDC45::HIS3	This study (249)

Table 3.4 Plasmids

Plasmid	**Description**
1845 GALp vector (YST1019)	**Empty plasmid as used for overexpression**
1846 GALp-SLD3/SLD7/CDC45 (YST1053)	**Plasmid for overexpression of Sld3/Sld7/Cdc45**

Chapter 4 The changes in DNA repair during aging

This chapter contains published work in the Journal of Molecular Biology titled '**Changes in DNA double-strand break repair during aging correlate with an increase in genomic mutations.'** by Aditya Mojumdar[†], Nicola Mair[†], Nancy Adam, and Jennifer Cobb.

I contributed to the manuscript as the co-first author. I was involved in study design and conceptualization, data collection, data analysis and interpretation and writing the original draft. I contributed to all the experiments in this paper in conjunction with Aditya Mojumdar. Nancy Adam imaged the aged yeast samples I had prepared for Figures 4.8, 4.22 and 4.23.

4.1 Abstract

A DSB is one of the most harmful forms of DNA damage. In eukaryotic cells, two main repair pathways have evolved to repair DSBs, HR and NHEJ. HR is the predominant repair pathway in the unicellular eukaryotic organism *S. cerevisiae*. However, during replicative aging, the relative use of HR and NHEJ shifts in favour of end-joining repair. By monitoring repair events in the HO-DSB system, we find that early in replicative aging; there is a decrease in the association of long-range resection factors, Dna2-Sgs1 and Exo1 at the break site and a decrease in DNA resection. Subsequently, as aging progressed, the recovery of Ku70 at DSBs decreased and the break site associated with the nuclear pore complex at the nuclear periphery, which is the location where DSB repair occurs through alternative pathways that are more mutagenic. End-bridging remained intact as HR and NHEJ declined, but eventually, it became disrupted in cells at advanced replicative age. Our work provides insight into the molecular changes in the DSB repair pathway during replicative aging. HR first declined, resulting in a transient increase in the NHEJ. However, Ku70 recovery at DSBs and NHEJ declined with increased cellular divisions. In WT cells of advanced replicative age, there was a high frequency of repair products with genomic deletions and microhomologies at the break junction. These events were not observed in young cells, which were repaired primarily by HR.

4.2 Introduction

Age is the most significant risk factor for developing cells with genome instability and most types of cancer (365). There are strong links between aging and genome instability diseases. For example, DNA damage is a driver of aging and most diseases with accelerated or premature aging

phenotypes are caused by mutations in DNA repair factors. The overall accumulation of DNA damage is governed by the relative rate of damage formation balanced with the rate of repair, and both are impacted by age. In older cells, DNA damage formation increases and correlates with changes in genome organization and compaction (228). At the same time, however, the rate of DNA repair decreases. Indeed, cells from older individuals show a lower rate of DSB repair compared to cells from younger individuals (366,367). However, identifying the molecular underpinnings that drive age-related increases in genome instability has remained challenging (81).

Genomic rearrangements are the types of mutations that accumulate with increased age and arise from defects in DSB repair (368). The phosphorylation of histone H2AX (gH2AX) in humans, which corresponds to H2A (gH2A) in budding yeast, is an indirect measure of DSB formation. The level of gH2AX increases with age, yet a unified model for understanding why this occurs is proving complex because there are multiple pathways for repairing DSBs. There are two canonical pathways, NHEJ and HR, and multiple alternative pathways. The alt repair pathways are highly mutagenic compared to the canonical pathways and are used when the rates of NHEJ and HR decrease. HR is considered error-free as it uses the sister chromatid as a repair template and can faithfully repair a DSB without losing genetic material. By contrast, NHEJ is error-prone and often incorporates small DNA insertions or deletions at the break site. The relative use of these DSB repair pathways is not uniform across eukaryotes or in different cell types or developmental stages of the same organism, even under optimal conditions. Yeast cells repair DSBs primarily by HR, whereas human cells rely on NHEJ to a greater extent. However, HR and NHEJ are functional in both.

Insights about how DSB repair proceeds during aging have been gained, although working with aging tissue in multicellular organisms remains challenging (81,368). Altered intracellular distribution of Ku70/80 (Ku) and decreased protein levels for Ku and Mre11 have been reported in aging human cells (369–372). However, changes in protein expression do not necessarily specify which pathway will be used to repair a DSB. Highlighting this case in point, the rate of HR repair decreased in the germline of old flies compared to young flies, yet the expression of HR components increased rather than decreased (373).

Cell cycle properties and genome maintenance factors are widely conserved in all eukaryotes, and budding yeast has proven to be a robust system for identifying many steps in DSB repair. Moreover, recent work has shown a reduction in the levels of HR proteins in older yeast cells and a reduction in the use of SSA. This alternative repair pathway relies on DNA resection and sequence homology (99,374). However, little is known about the integrity of DSB repair mechanisms over the RLS of yeast. Much seminal work monitoring physical events in DSB repair has used the galactose-inducible HO endonuclease system, which synchronizes one site-specific DSB in the yeast genome (375). Here, we use this well-characterized system to evaluate key steps in DSB repair in different stages of replicative aging. We measured the recruitment of HR and NHEJ repair factors to the HO-induced DSB during aging, determined that DSBs accumulate at the nuclear pore complex in older cells, and measured repair products as replicative age increased by sequencing across the break junction.

4.3 Results

4.3.1 Old cell enrichment and DSB repair pathway choice

Due to difficulties obtaining old yeast cells, knowledge about age-related changes in DSB repair is only starting to emerge (99,374,376,377). We have optimized an old cell enrichment (OCE) approach with cells containing the HO-DSB where one site-specific DSB can be created by galactose-induction of the HO endonuclease (229,375). This enhanced OCE method transformed our ability to rapidly collect many progressively older cells without needing specialized microfluidics or a specific genetic background used for the MEP (227). Our method involved biotin cell labelling but differed from previous approaches by the technology used to enrich old cells. Biotin-labelled cells bind to anti-biotin antibody-coupled microbeads in an XS column (Miltenyi), amplifying the magnetic field 10,000-fold when combined with the SuperMACS^{TM} II separator system. Young cells pass through the column, and old biotinylated cells are retained. After washing to remove young cell contaminants, old cells can be eluted from the XS column by withdrawing the magnetic field.

We sorted young (Y) from progressively older (O) cells at the following times 18 hrs (O1), 42 hrs (O2) and 66 hrs (O3) after the initial biotin labelling (Figure 4.1A). The Y cells were the daughters from the first night of old cell enrichment that did not bind to the XS column when O1 cells were recovered. O1 cells were either used for experiments or re-inoculated into fresh media and grown 24 hrs more (O2 cells). The exact process was repeated with O2-aged cells to yield O3 cells. Haploid W303 yeast average ~25 divisions during their lifespan (15), and the number of cellular divisions was determined by counting the number of bud scars on the surface of the mother cell visualized by calcofluor white, which labels chitin encircling the site of budding (Figure 4.1B) (378). O3-aged cells were propagated for 66 hours and had an average of ~ 17 bud scars (Figure

4.1B). The level of Sir2, a histone deacetylase, is known to decrease with replicative age. The target of Sir2 is histone H4K16, and older cells obtained from this OCE method showed increased H4K16 acetylation (Figure 4.2). Therefore, in addition to bud scar count, we verified that old cells displayed other known markers of replicative aging.

A B

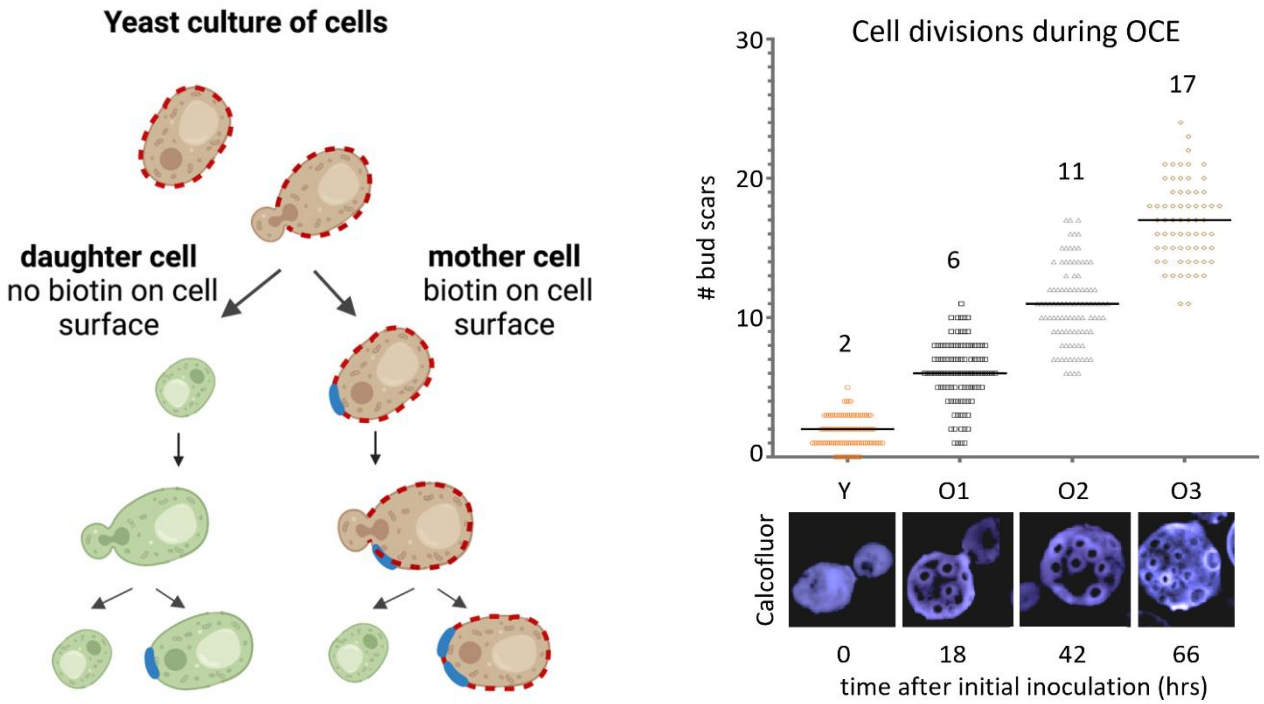

Figure 4.1 The replicative age of yeast following OCE

(A) Schematic depicting the biotin labelling (red dashed outline) of mother cells. The initial culture is incubated with biotin, and the biotin labelling remains within the cell wall of only the mother because the cell wall of daughter cells has new cell wall material. This allows the selective separation of old and young cells.

(B) Representative images of aging yeast cells at the different stages of old cell enrichment (OCE). WT (JC-727) cells were enriched and separated using XS columns. Samples were taken of young O1, O2 and O3 cells. Bud scars are visualized after cell staining with

calcofluor. The number of bud scars is a readout for the number of cell divisions during replicative aging, with images shown for young (Y) to increasingly older (O1-O3) cells. Scatter plot of the average number of bud scars over three days of OCE in Y, O1 (18 hrs), O2 (42 hrs), and O3 (66 hours), the average of each population was determined and is shown by the solid black line.

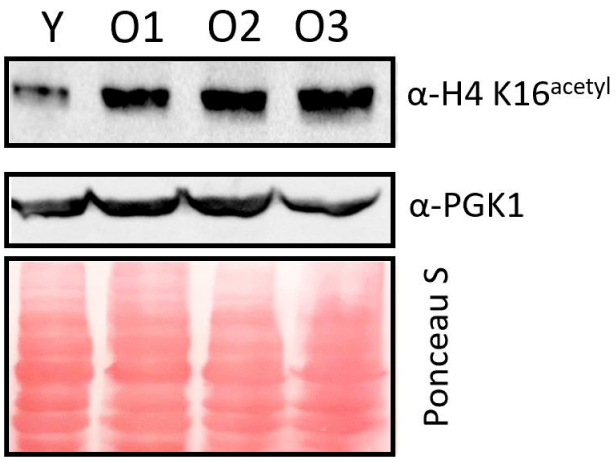

Figure 4.2 H4K16 increases with age

Western blot of WT cells (JC-727) that were separated using the XS column. The WB show the expression of H4K16 acetylation in Y and O1-O3 cells. PGK1 and ponceau S were used as loading control.

We first assessed two important events at a DSB: DNA resection and end-bridging (Figure 4.3). Resection is necessary for HR, but if 5' resection initiates, then NHEJ is prevented. DNA end-bridging holds the broken ends in proximity and provides structural support during end processing. To determine resection at the HO-DSB, we used a quantitative PCR-based approach after galactose induction of the HO endonuclease. HO is a yeast enzyme that initiates mating type switching by creating a DSB at the MAT mating type locus that removes the donor sequence.

Genomic DNA was prepared at the indicated time points and digested with the *Rsa*I restriction enzyme, followed by quantitative PCR. This method relies on a *Rsa*I cut site, with two located at 0.15 and 4.8 Kb from the HO-DSB (Figure 4.4). If resection progresses past the *Rsa*I recognition site, then the single-stranded DNA generated from resection would not be cleaved by *Rsa*I and amplified by PCR (379–382).

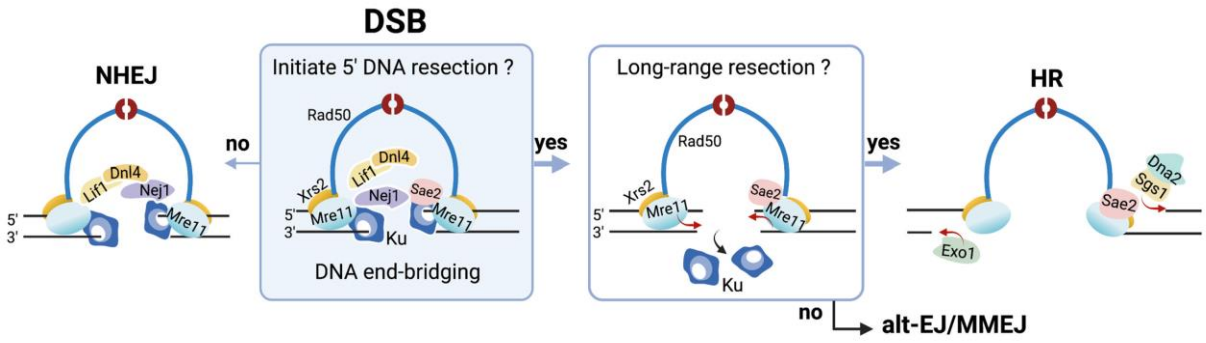

Figure 4.3 DSB repair pathways

Schematic representation of DSB repair pathway choice, where repair factors play critical roles in DNA end-bridging, end-resection, and end-joining. If end-resection initiates, then NHEJ is no longer an option, and the cell will initiate long-range resection and repair the DSB by HR. If long-range resection can not occur, MMEJ can repair the resected DSB.

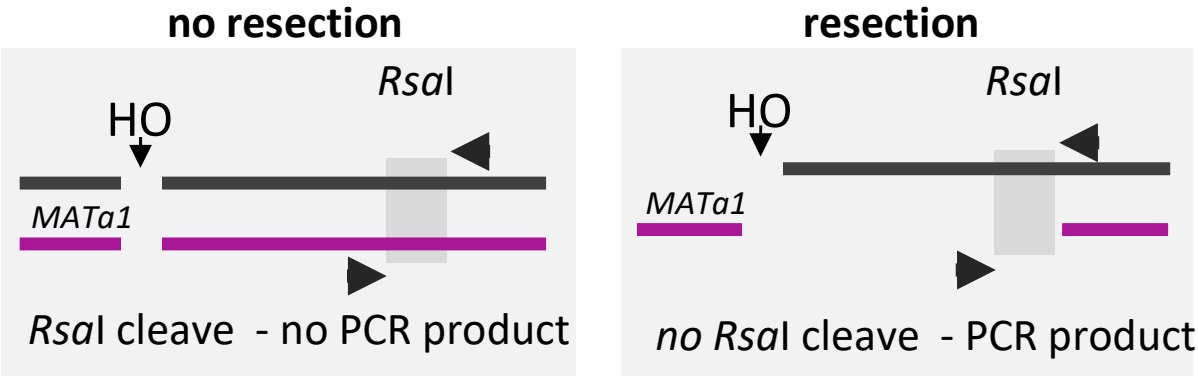

Figure 4.4 Model of resection assay

Schematic of the HO cut site on chromosome III showing the method used to measure the frequency of resection using the *RsaI* recognition site. The HO cuts the site-specific MATα1 creating a DSB. The only *RsaI* sites are 0.15 kb and 4.8 Kb away from the HO cut site allowing us to determine if resection has occurred.

Resection in Y cells proceeds similarly to standard overnight cultures, not passed over the XS column (Figure 4.5). We were encouraged that there were no off-target effects to resection arising during the OCE process. As cellular age increased from Y to O3, resection decreased at 0.15 Kb from the break and decreased further 4.8 Kb from the break (Figure 4.6). In O2 and O3 samples, this might be partly due to a decrease in DSB formation that was most pronounced 40 minutes after induction of the HO endonuclease (Figure 4.7). Loss of DSB formation is likely due to the decrease in expression of the HO endonuclease as the cells age. However, compared to the low level of resection 0.15kb from the DSB, resection was abrogated 4.8 Kb in O2 and O3 - aged cells (Figure 4.6). O1-aged cells averaged ~ 6 divisions showed a marked decrease in resection, yet the cell has > 75% of its lifespan remaining (15). We ruled out significant cell-cycle differences between Y and O1-aged cells that might account for the marked decrease in resection, which occurs in S/G2 when a sister chromatid is available. Flow cytometry before galactose induction showed that Y cells had ~9% more cells in S/G2 than O1 (Figure 2.5), a minor difference that likely could not account for the 2-3-fold decrease in resection (Figure 4.6).

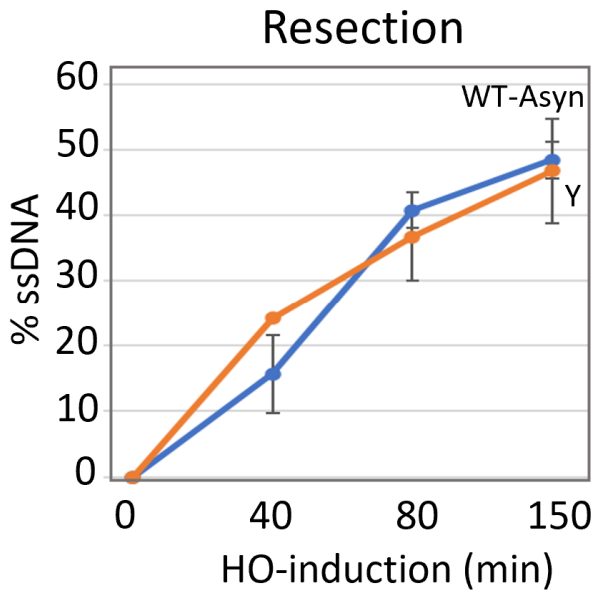

Figure 4.5 Resection assay in control and young cells

Resection of DNA 0.15 Kb away from the HO cut site is measured as the percent of ssDNA at 0, 40, 80 and 150 minutes following the induction of the DSB in WT (JC-727) overnight cultures (blue) or Y cells obtained from the OCE process (orange).

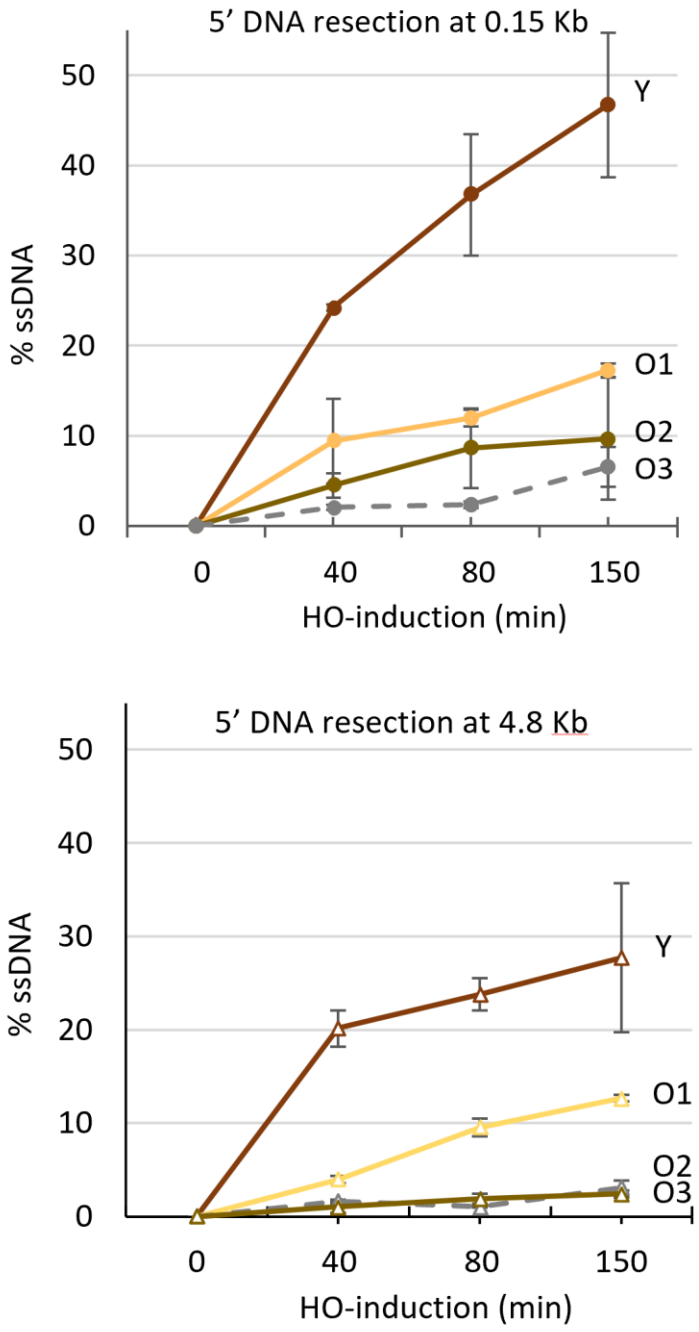

Figure 4.6 Resection of DSB in age cells

Resection of DNA 0.15 Kb and 4.8 Kb away from the HO cut site was reported as the percent of ssDNA at the indicated time points (0, 40, 80 and 150 mins) after induction of the DSB in WT (JC-727) in Y and O1-O3 aged enriched cells. Analysis was performed in triplicate from at least three biological replicate experiments.

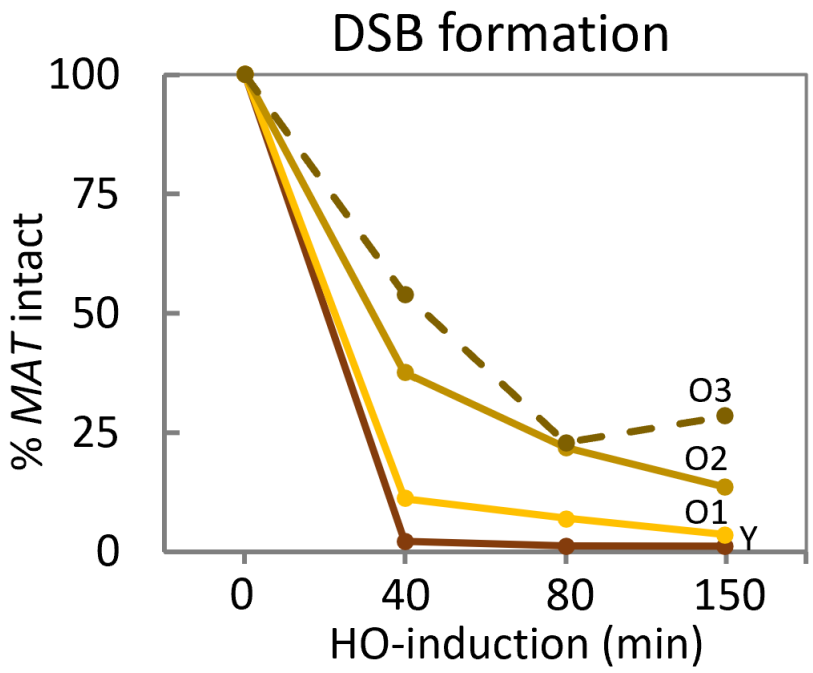

Figure 4.7 Efficiency of HO cutting in aged cells

WT cells (JC-727) aged using the OCE process to sort Y and O1-O3. The efficiency of the HO cut was determined by measuring the percentage of MAT that remains uncut (intact) at 0, 40, 80 and 150 minutes after induction with galactose.

End bridging was next measured in cells where both sides of the DSB were tagged with fluorescent markers. The TetO array and the LacO array were integrated 5.2 Kb upstream and 3.2 Kb downstream, respectively, from the DSB in cells expressing $TetR^{GFP}$ and $LacO^{mCherry}$ fusions, enabling us to visualize both sides of the break by fluorescence microscopy (Figure 4.8). 2 hours after HO-induction the distance between the GFP and mCherry foci was similar for Y and O1-aged cells at 0.30 µm and 0.27 µm respectively and increased slightly in O2 cells (0.39 µm). In O3-aged cells, there was a significant increase in the mean distance (0.58 µm) ($P<0.001$***). and a wide

distribution of inter-foci distance, which at the population level, was potentially a reflection of the HO cutting defects we observed in older cells (Figure 4.8 and 4.7). If the cutting is less efficient in older cells, the DSB will be less efficiently formed, and therefore you will see some cells where bridging is perceived to be intact when there was no DSB in the first place. Taken together, early in the aging process, DNA resection decreased. However, end-bridging remained intact, although it deteriorated later in replicative aging. HR is the main DSB repair pathway in yeast. However, most, if not all, studies investigating pathway choice have been performed with cultures containing mostly young cells. Thus, one possibility is that the preference for HR repair is a 'young' cell phenomenon that declines with age. To explore this, we were prompted to investigate the recruitment of the nucleases that mediate resection and other repair factors to the DSB during aging.

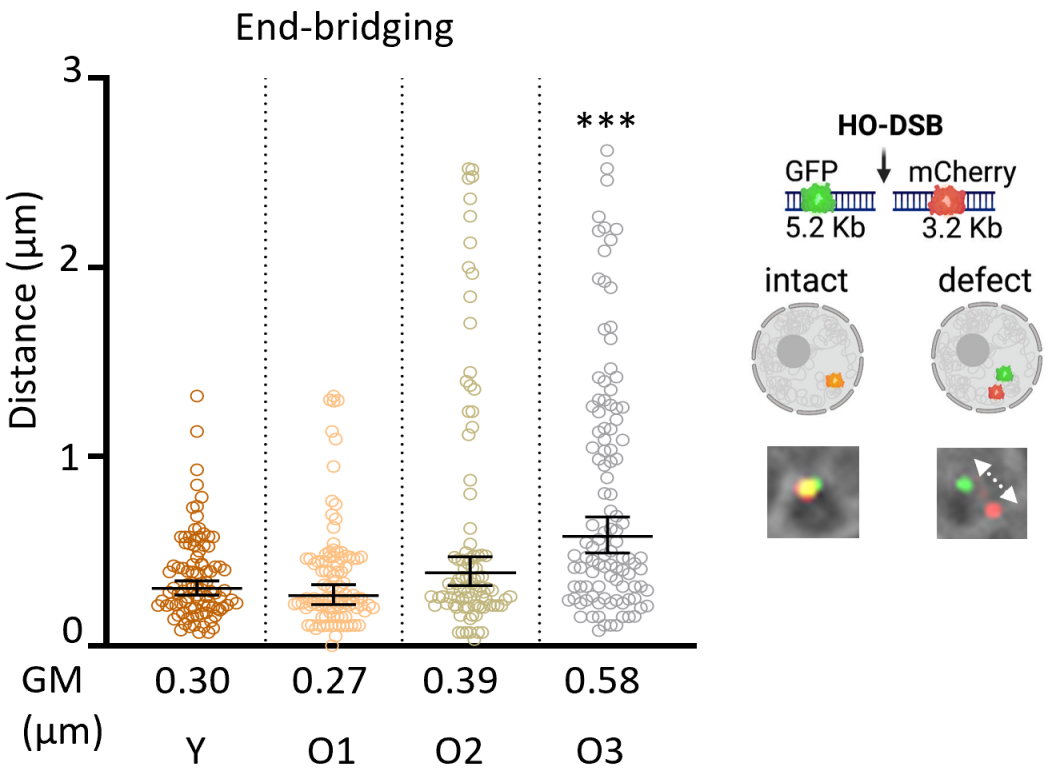

Figure 4.8 Aged cells fail to bridge DSBs

Representative image of yeast cells with tethered (co-localized GFP and mCherry) and untethered (distant GFP and mCherry) ends of the DSB. Scatter plot showing the tethering of DSB ends, as measured by the distance between the GFP and mCherry foci in Y and O1-O3 aged cells 2 hours after DSB induction. The Geometric mean (GM) distance for each sample was specified under the respective sample data plot. Significance was determined using Kruskal-Wallis and Dunn's multiple comparison test. All ages are compared to Y cells ($P<0.05$*; $P<0.01$**; $P<0.001$***).

4.3.2 Reduced recruitment of resection factors during aging

MRX and KU are the first complexes recruited to a DSB (Figure 4.9) (169). DNA resection occurs through a two-step process (383). In the first step, Sae2, the yeast homologue of human CtIP, activates Mre11 endonuclease to cleave ~ 100 bp away from the DSB and initiate 3'-5 DNA resection towards the break. This causes Ku to dissociate, and when that happens, NHEJ is prevented. In the second step of resection, two functionally redundant 5' to 3' nucleases, Dna2 in complex with Sgs1 and Exo1, catalyze long-range resection (187,384). The physical presence of the MRX complex is critical for all stages of resection because both long-range nucleases require MRX for their localization. (184,187). We performed ChIP on Mre11 and Rad50, two members of the MRX complex, with primers located 0.6 kb from the DSB (Figure 4.10). The recovery of both increased 2 to 4-fold in O1 and O2 cells. Unfortunately, ChIP with O3 was precluded due to inefficient HO-cutting (Figure 4.7). O3 cells also showed a significant reduction in survival with continuous galactose induction (Figure 4.11). Cells that survive continuous HO cutting arise from imprecise repair where the HO recognition site becomes disrupted, and no DSB can be formed. Survival was determined by normalizing the number of surviving colonies in the GAL plates to the number of colonies in the GLU plates. The increased recovery of Mre11 and Rad50 was surprising as previous work showed that older cells have a decreased level of HR proteins (99). Consistent with Pal et al., we also observed a decrease in the overall expression of proteins, including MRX components (Figure 4.12). Changes in expression levels have been used as readouts for a cell's proficiency in a particular repair pathway (372,373,385). However, these results show that there is not necessarily a direct correlation between protein and recruitment levels.

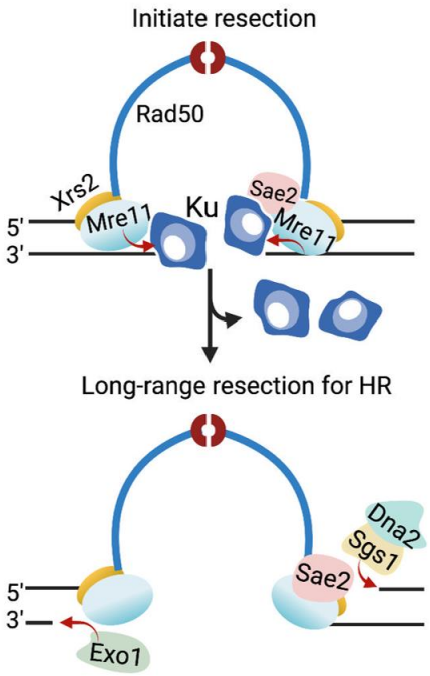

Figure 4.9 Model of the resection steps of HR

Schematic model showing the resection steps of homologous recombination. MRX and Ku are recruited first to the DSB. MRX helps bridge the ends of the DSB, and Sae2 then binds Mre11 endonuclease, which initiates short-range resection and leads to the removal of Ku. Long-range resection is then carried out by either Exo1 or Dna2-Sgs1.

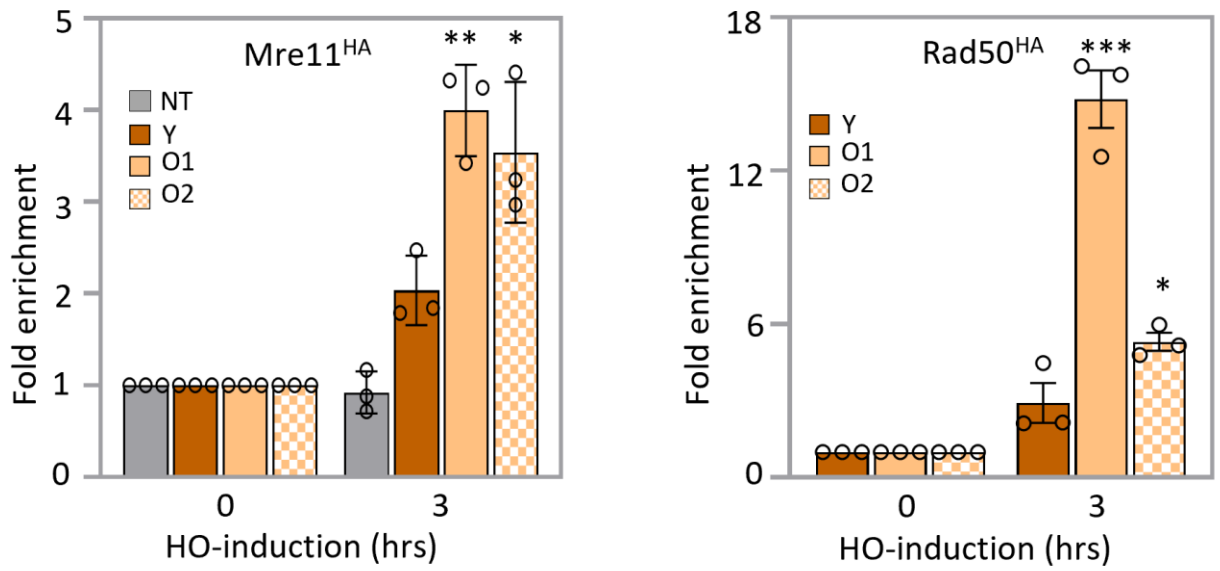

Figure 4.10 Recruitment of Mre11 and Rad50 during aging

ChIP showed enrichment of no tag control (JC-727), Mre11^{HA} (JC-3802) or Rad50^{HA} (JC-3306) 0.6kb away from the DSB at 0- and 3-hour time points in Y and O1-O2 aged cells. The fold enrichment at the break was normalized to enrichment at the *SMC2* locus and then to time point 0. The error bars represent the standard error of three replicates for all the experiments. Significance was determined using a 1-tailed, unpaired Student's t-test. All comparisons are to Y cells and marked (P<0.05*; P<0.01**; P<0.001***).

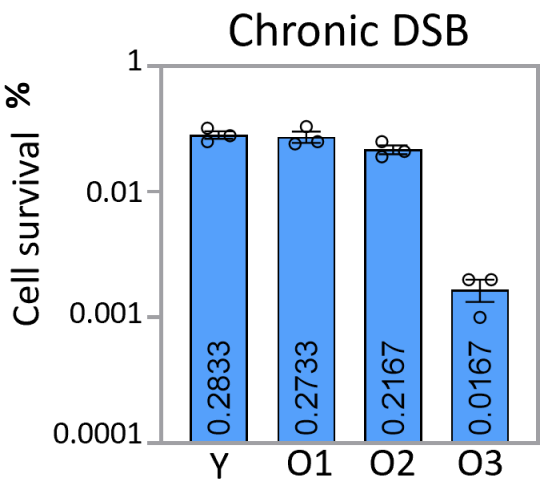

Figure 4.11 Cell survival in aged cells

Percentage cell survival upon chronic HO induction on galactose plates in WT (JC-727) Y and O1, O2, O3 aged cells following continuous induction of the HO endonuclease. The survival is normalized to the number of colonies on glucose (uninduced plates). Analysis was performed in triplicate from at least three biological replicate experiments, and error bars represent standard deviation.

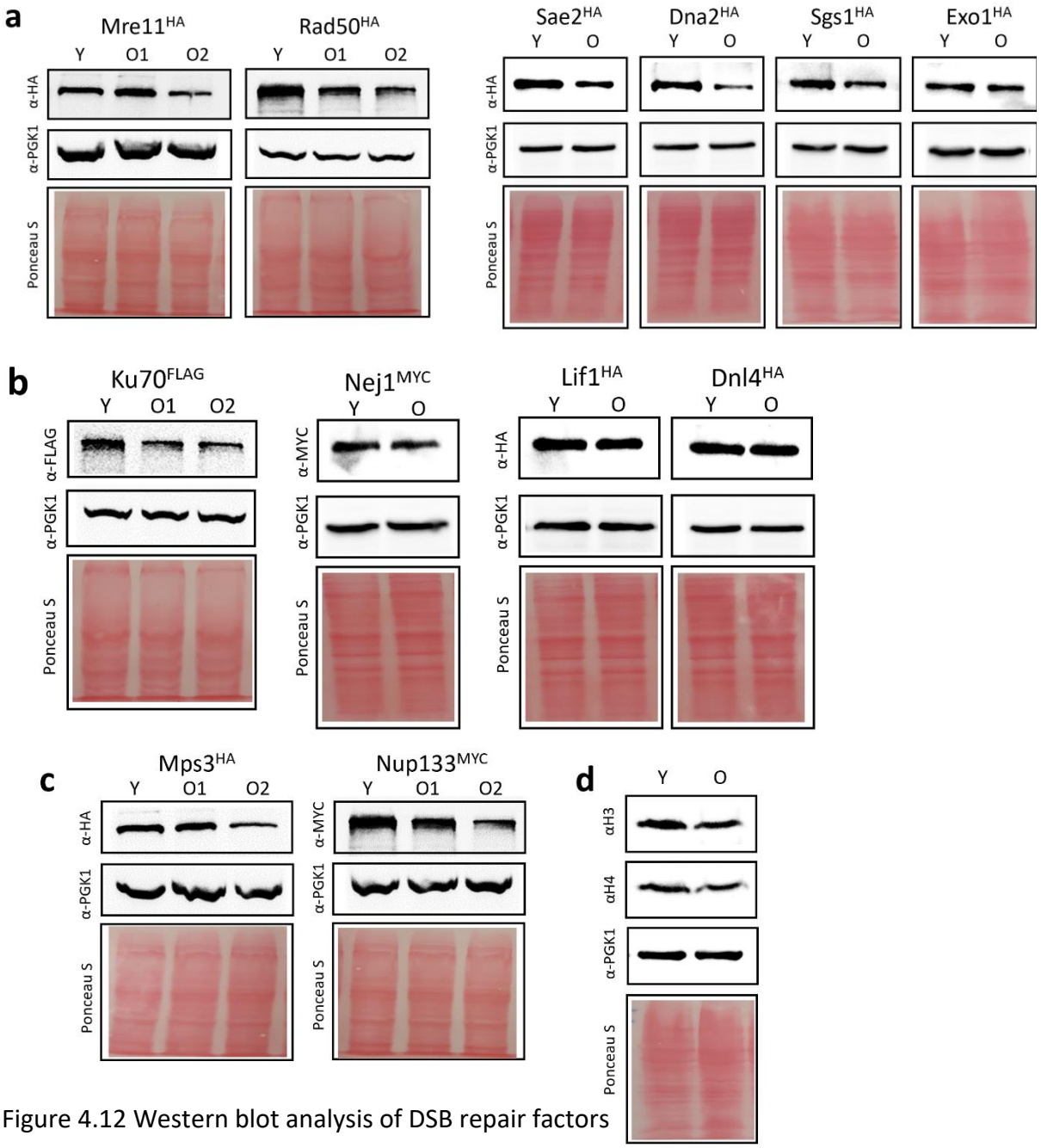

Figure 4.12 Western blot analysis of DSB repair factors

(a-c) Western blots determine the expression of DSB repair proteins in young and old cells with either aMyc (ab32), aHA (F-7) or aFLAG (M2F12). The strains used were Mre11^{HA} (JC-3802), Rad50^{HA} (JC-3306), Sae2^{HA} (JC-5116), Dna2^{HA} (JC-4117), Sgs1^{HA} (JC-4135), Exo1^{HA} (JC-4869), Ku70^{FLAG} (JC-3964), Nej1^{MYC} (JC-1687), Lif1^{HA} (JC-3319), Dnl4^{HA} (JC-5672), Mps3^{HA} (JC-3167), Nup133^{MYC} (JC-1510), and (**d)** WT (JC-727) was used for histone H3 and H4. PGK1 and Ponceau staining were used as loading controls.

In contrast to MRX, the recruitment of Sae2 was reduced in O1 cells ($P<0.05$) (Figure 4.13), as was the recruitment of the long-range resection components, Dna2-Sgs1 and Exo1 ($P<0.05$) (Figure 4.14). In all, O1-aged cells, which have undergone ~ 6 divisions, showed a decrease in the recruitment of critical factors driving DNA resection, although MRX showed increased retention. Our observations underscore the value of performing molecular and biochemical work in old cells as we gained mechanistic information about age-related changes in DSB repair. We did not perform ChIP with these factors aged to the O2 stage as we found it unlikely that their recruitment, which decreased in O1, would increase in older cells with an even more significant resection defect.

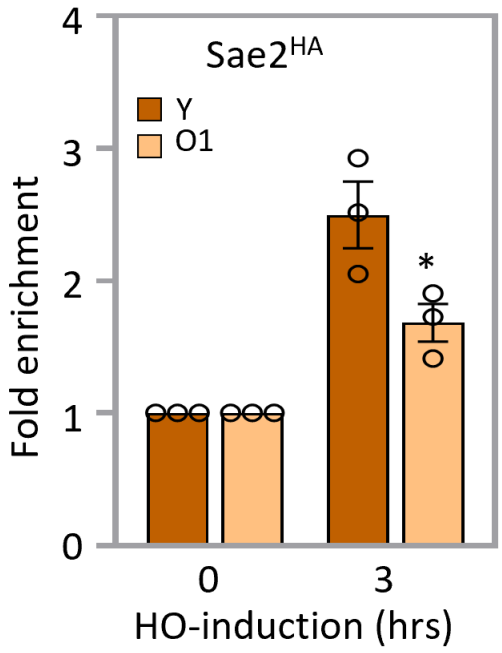

Figure 4.13 Recruitment of Sae2 during aging

ChIP showed Sae2 ^{HA} (JC-5116) enrichment 0.6kb away from the DSB at 0- and 3-hour time points in Y and O1-aged cells. The fold enrichment was normalized to enrichment at the *SMC2* locus and then to time point 0. The error bars represent the standard error of three replicates for all the

experiments. Significance was determined using a 1-tailed, unpaired Student's t-test. All comparisons are to Y cells and marked (P<0.05*; P<0.01**; P<0.001***).

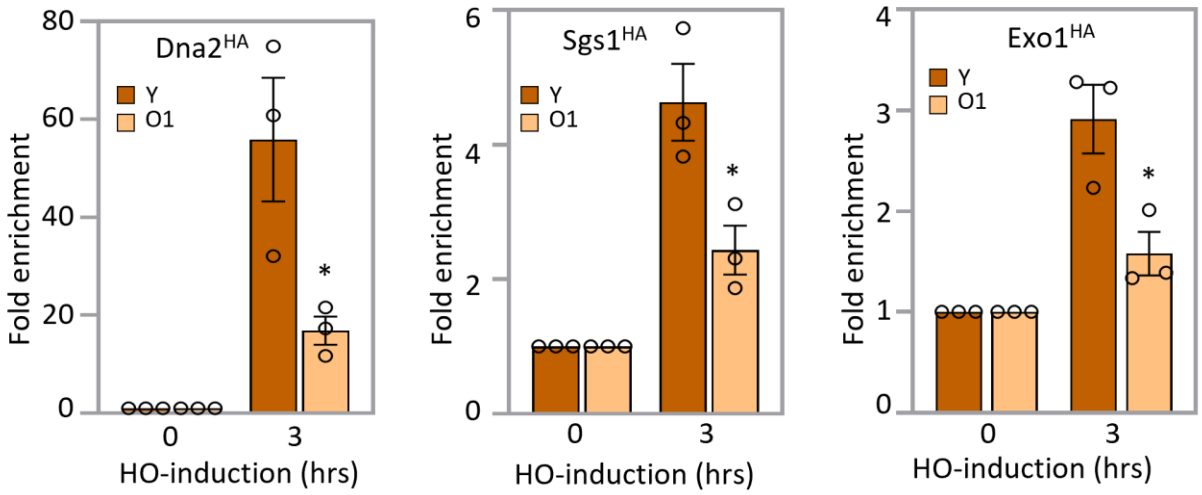

Figure 4.14 Recruitment of Dna2, Sgs1 and Exo1 during aging

ChIP showed enrichment of Dna2^{HA} (JC-4117), Sgs1^{HA}(JC-4135), or Exo1^{HA} (JC-4869) 0.6kb away from the DSB at 0- and 3-hour time point in Y and O1 aged cells. The fold enrichment was normalized to enrichment at the *SMC2* locus and then to time point 0. The error bars represent the standard error of three replicates for all the experiments. Significance was determined using a 1-tailed, unpaired Student's t-test. All comparisons are to Y cells and marked (P<0.05*; P<0.01**; P<0.001***).

4.3.3 Increase in error-prone DSB repair with aging

We were curious how DSB repair proceeded when resection, the main event driving HR, declined early in the aging process. Thus, we were next prompted to investigate the usage of NHEJ as end-joining reactions are supported structurally by DNA end-bridging (380,386), and this remained intact from Y to O2-aged cells. We measured the recruitment levels of the core NHEJ factors by

ChIP. All the factors showed a similar level of recruitment to the DSB in Y and O1 cells, except for Ku70, which showed increased recovery in O1 cells (Figures 4.15 and 4.16). As mentioned, Ku is one of the first responders to a DSB, and it plays a crucial role in recruiting the other NHEJ factors, such as Nej1 and Lif1-Dnl4 (387).

We next determined the level of end-ligation repair in old cells. For this, a DSB was induced by galactose for 3 hours. Then cells were washed and released into glucose to prevent further re-cutting (Figure 4.17). Genomic DNA was prepared at the indicated time points, followed by qPCR using primers flanking the break site. Amplification across the DSB after release into glucose would occur if the broken DNA ends were joined (388). Ligation in O1-aged cells increased 2-fold above Y cells and correlated with the increased recovery of Ku70 ($P<0.05$) (Figure 4.15 and 4.18). This increase in end-joining was dependent on NHEJ as deletion of *KU70* in O1 cells resulted in a complete disruption of end-joining (Figure 4.18). As aging progressed to O2, there was a reduction in the rate of end-joining (Figure 4.18), which correlated with a marked decrease in Ku70 recovery at DSBs in O2-aged cells (Figure 4.15). By contrast, the recovery of Nej1 at DSBs was not statistically different in Y-O2-aged cells (Figure 4.15). Notably, the recovery of Nej1 and MRX did not decrease as cells progressed from Y to O2 as both factors function to maintain end-bridging, which remained intact at these stages of replicative aging (Figure 4.8) (380,386).

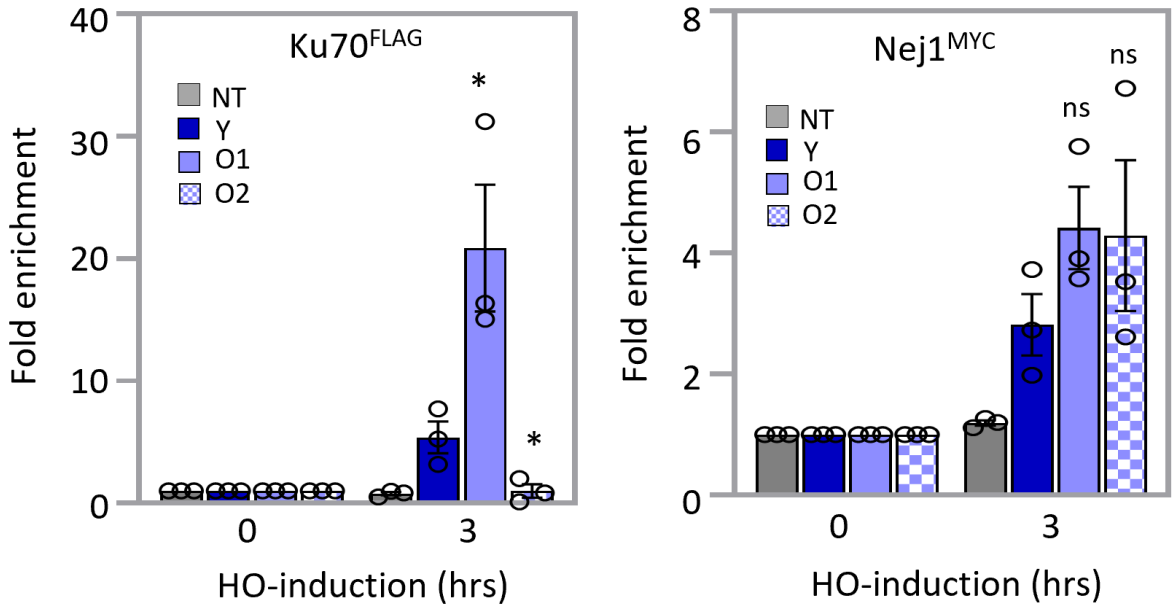

Figure 4.15 Recruitment of Ku70 in aged cells

ChIP showed enrichment of Ku70^{Flag} (JC-3964) and Nej1^{Myc} (JC-1687) 0.6kb away from the DSB at 0- and 3-hour time point in Y and O1-O2 aged cells. The fold enrichment was normalized to enrichment at the *SMC2* locus and then to time point 0. The error bars represent the standard error of three replicates for all the experiments. Significance was determined using a 1-tailed, unpaired Student's t-test. All comparisons are to Y cells and marked ($P<0.05$*; $P<0.01$**; $P<0.001$***).

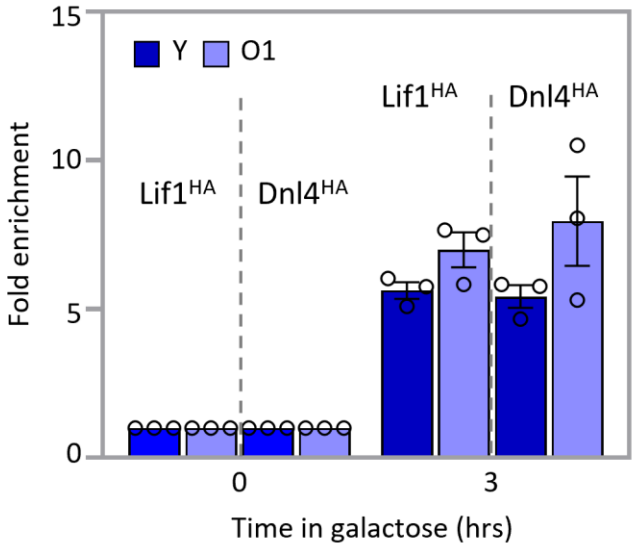

Figure 4.16 Recruitment of Lif1 and Dnl4 in aged cells

Enrichment of Lif1^{HA} and Dnl4^{HA} (JC-3319 and JC-5672) 0.6kb away from the DSB at 0- and 3-hour time points in Y and O1-aged cells. T The fold enrichment was normalized to enrichment at the *SMC2* locus and then to time point 0. The error bars represent the standard error of three replicates for all the experiments.

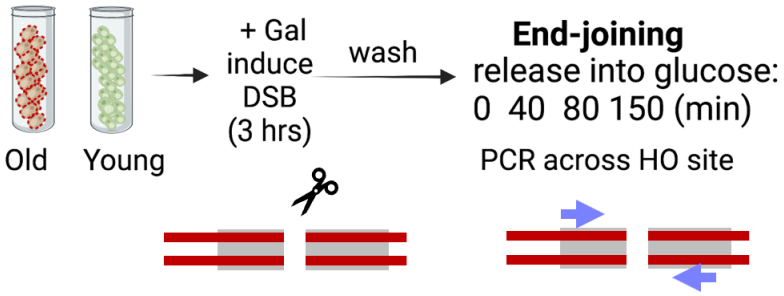

Figure 4.17 Model of ligation assay

Schematic of qPCR ligation assay of the HO cut site on chromosome III. Following DSB induction for 3 hours, cells were released into glucose. This allows the DSB to be repaired. The end-joining repair was determined with qPCR amplification with primers flanking the cut site.

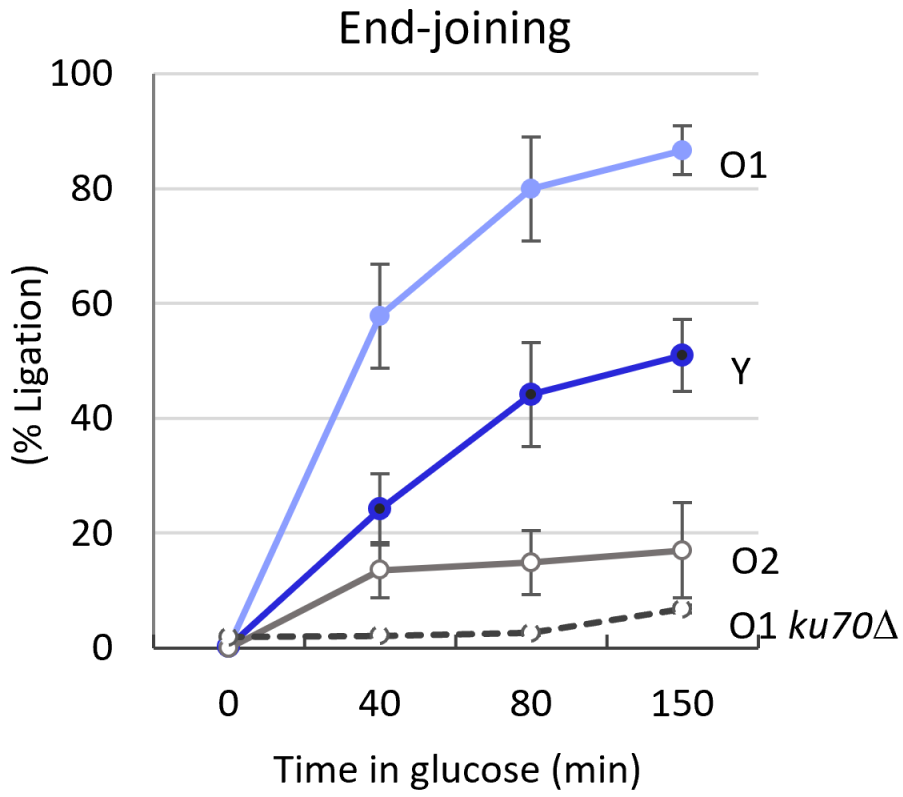

Figure 4.18 NHEJ frequency in aging cells

Ligation of DNA at the HO cut site is measured as the percent signal amplified 0, 40, 80 and 150 minutes following the release into glucose. Ligation was determined in WT (JC-727) and ku70Δ (JC-1904) in Y and O1-O2 aged cells. The error bars represent the standard error of three replicates for all the experiments.

The relative change in 5' resection at DSBs highlights the fluid nature of HR and end-joining repair pathway choice early in replicative aging. In O1 cells, resection decreased (Figure 4.6), and end-joining increased, suggesting that an almost equivalent rise in NHEJ can compensate for age-related declines in HR. We tried to increase HR by disrupting NHEJ in O1 because, in Y cells,

resection increased when core NHEJ factors were deleted (Figure 4.19). However, unlike in Y cells, preventing NHEJ with *dnl4*Δ in O1-aged cells did not give rise to a compensatory increase in resection (Figure 4.20), suggesting changes in NHEJ per se at this stage cannot restore HR repair. Notably, deletions of KU70 or NEJ1 increased resection (Figure 4.20). However, this is attributed to their additional roles of inhibiting Exo1 and Dna2, respectively, rather than their essential NHEJ function shared with *DNL4* (159,380,381,388). It is striking that the increase in resection by NHEJ disruption wanes in older cells, suggesting that genotype-phenotype readouts can change with age and that age can have a more penetrant impact than genetic manipulations.

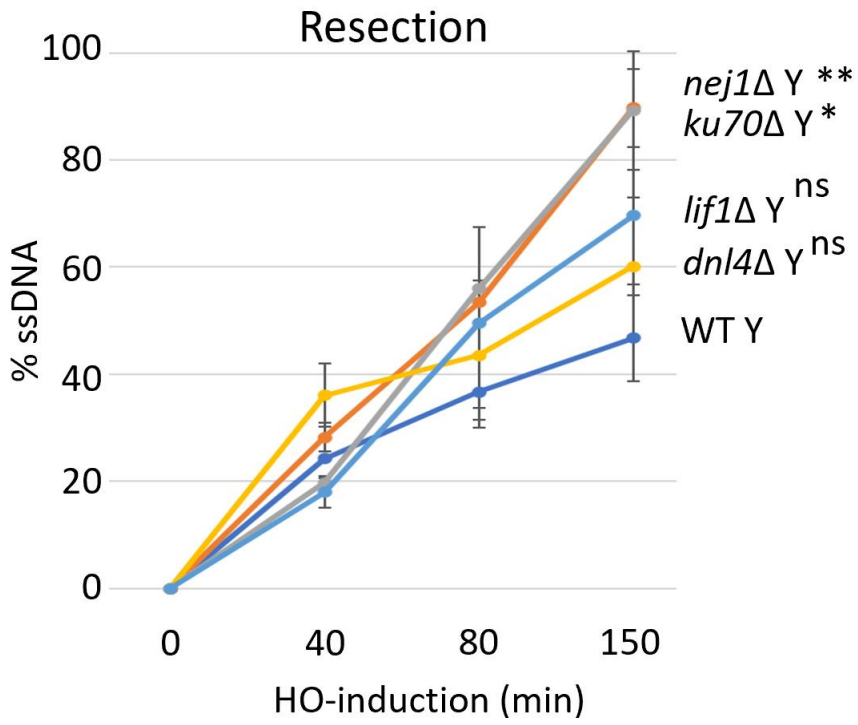

Figure 4.19 Resection of DSB in a mutant background

Resection of DNA 0.15kb away from the HO cut site was reported as the percent of single-stranded DNA (ssDNA) at the indicated time points (0, 40, 80 and 150 mins) after induction of the

DSB in Y cells for WT (JC-727), *nej1*Δ (JC-1342), *ku70*Δ (JC-1904) and *dnl4*Δ (JC-3290). Analysis was performed in triplicate from at least three biological replicate experiments. For all the experiments - error bars represent the standard error of three replicates. Significance was determined using a 1-tailed, unpaired Student's t-test. All strains were compared to Y cells and marked (P<0.05*; P<0.01**; P<0.001***).

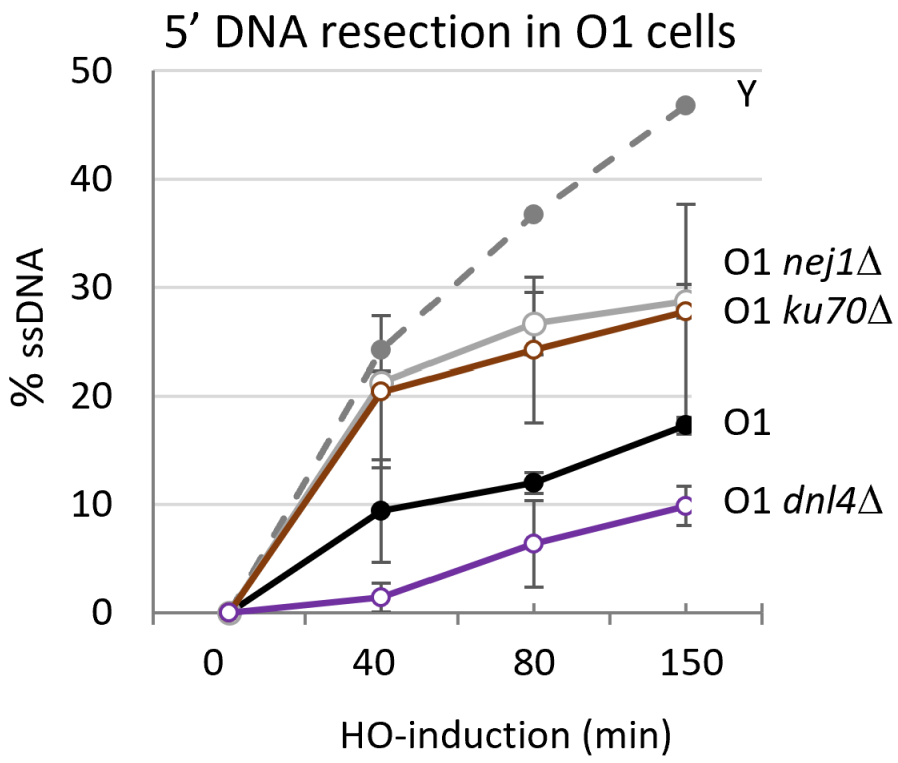

Figure 4.20 Resection in mutant backgrounds in aged cells

Resection of DNA 0.15kb away from the HO cut site was reported as the percent of single-stranded DNA (ssDNA) at the indicated time points (0, 40, 80 and 150 mins) after induction of the DSB in Y and O1 aged cells for WT (JC-727), *nej1*Δ (JC-1342), *ku70*Δ (JC-1904) and *dnl4*Δ (JC-3290). Cut efficiency for all strains and time points was determined and reported in table 4.4. Analysis was performed in triplicate from at least three biological replicate experiments. For all the experiments - error bars represent the standard error of three replicates.

4.3.4 During aging, imprecise DSB repair increases the mutational burden on cells

Recent work in mammals, flies and yeast have shown that difficult-to-repair DNA damage relocates to specific 'repair sites' at the nuclear periphery (389–395). Previous work showed that DSBs relocate to the periphery within 1 hour of HO-cutting and can be detected for up to 4 hours after induction. In WT cells after galactose induction, the level of DSBs increase in the outermost zone 1 (Figure 4.21) (389,395,396).

Given the age-related changes in repair pathway usage, we next investigated whether there were changes in DSB localization to the periphery. To do this, we performed high-resolution microscopy and monitored the repositioning of the HO-DSB after induction of the HO endonuclease. The DSB was visualized by expression of $LacI^{GFP}$ in cells where an array *lacO* sites were integrated 4.4 kb from the HO site at the *MAT* locus. A focal stack of images through a field of cells allowed us to determine the position of the DSB relative to the nuclear periphery, visualized by $Nup49^{CFP}$. The nuclear position of the DSB was determined in Y and O1 after OCE. O1 cells showed altered nuclear morphology as visualized by $Nup49^{CFP}$ in 2D and 3D reconstructed images (cyan; Figure 4.22). This prevented quantitative zoning analysis, which relies on three concentric circles representing equal areas within the nucleus. However, the overlap of GFP-CFP signals indicated that 52% and 50% of DSBs touched the nuclear periphery in Y and O1-aged cells, respectively (Figure 4.23), which was above the 33% level if the distribution was random. These results demonstrate that 2 hours after HO induction, irreparable DSBs in O1-aged cells were enriched at repair centers located at the nuclear envelope, similarly to Y cells.

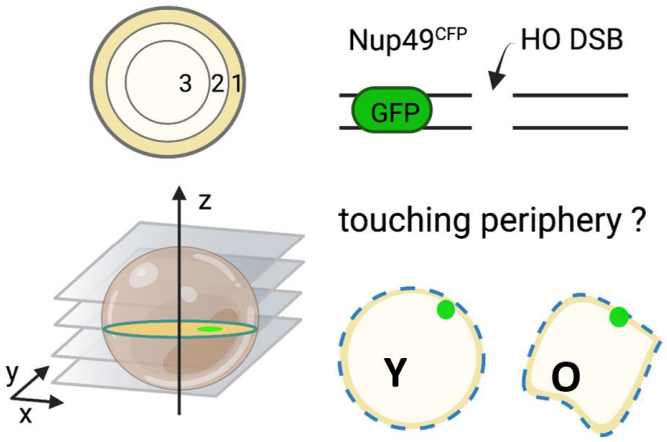

Figure 4.21 Schematic for determining the location of the DSB at the nuclear periphery

Schematic for measuring the position of the DSB at the nuclear periphery by microscopy for a GFP-tagged DSB and CFP-tagged Nup49. Z stacks were used to determine if the DSB was in contact with the nuclear periphery.

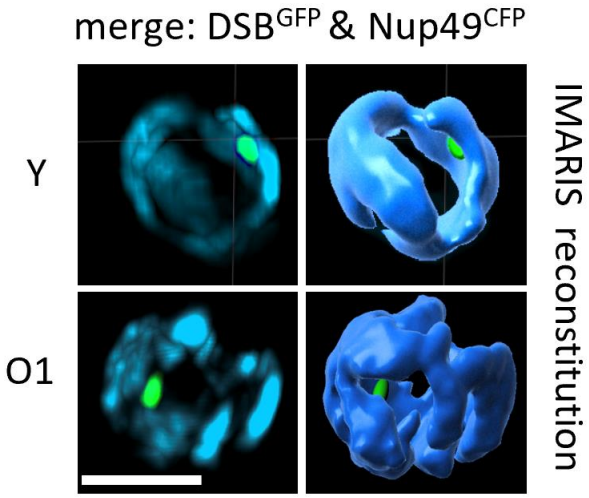

Figure 4.22 Reconstruction of the DSB location

2D and 3D Reconstruction of the nuclear periphery using IMARIS showing the DSB^{GFP} and $Nup49^{CFP}$.

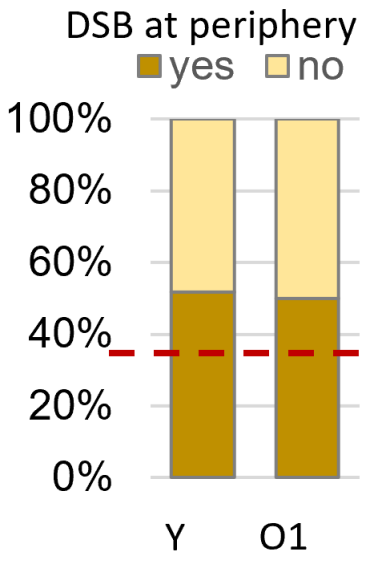

Figure 4.23 DSBs at the nuclear periphery in aged cells

The location of the DSB within the nucleus was measured in Y and O1-aged cells. The percentage of DSBs at the nuclear periphery was measured. The red line would show 33% if the distribution were random.

In yeast, the nuclear periphery has two independent sites where yeast damage accumulates, the nuclear pore complex (NPC) and the SUN domain protein, Mps3 (397,398). These sites have different requirements for damage localization, leading to different repair outcomes. The nuclear pore is associated with NHEJ and non-canonical alternative repair pathways (399). DNA intermediates with extensive resection at DSBs are targeted to Mps3, a protective environment that promotes canonical HR and reduces promiscuous recombination events in S/G2. By contrast, DSBs without extensive resection becomes enriched at the NPC in all cell cycle phases (Figure 4.24). ChIP with NPC components and Mps3 have verified microscopy-based methods and can also quantitatively distinguish between these specific locations at the periphery. We followed up

with ChIP in O2-aged cells because we felt microscopy-based approaches posed a challenge given the age-related morphological changes and because ChIP had worked well for measuring the recruitment of repair factors to DSBs in Y to O2 cells (Figures 4.10, 4.13, 4.14 and 4.15).

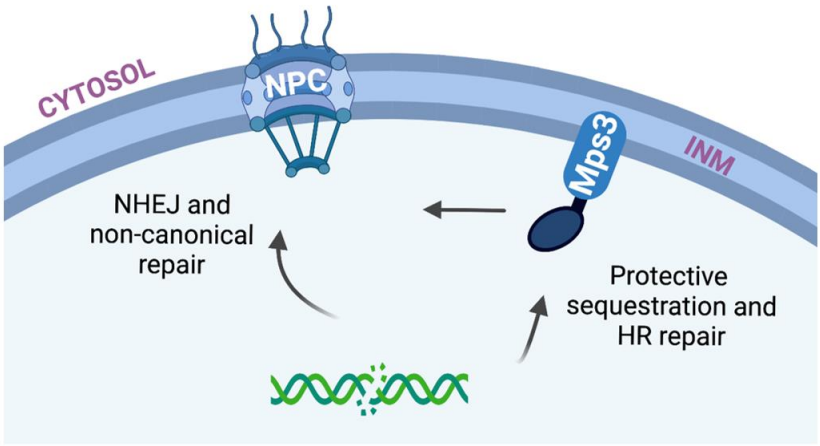

Figure 4.24 Model for DSB relocation to the nuclear envelope

Model for DSB re-localization to Mps3, located in the inner nuclear membrane (INM) of the nuclear envelope for repair via HR or to the NPC, the site of NHEJ and non-canonical /alternative repair pathways.

We performed ChIP with Nup133^{Myc}, a component of the NPC, and Mps3^{HA}. Consistent with previous work, DSBs in Y cells are associated robustly with Mps3 and to a lower level with the NPC after galactose induction (Figure 4.25 and 4.26)(396). DSB association with Mps3 significantly declined in O1 and O2 cells, and in O2-aged cells, recovery levels were indistinguishable from the background (Figure 4.25). By contrast, the association of DSBs with the NPC showed a progressive two and three-fold increase in O1- and O2-aged cells, respectively

(Figure 4.26). These changes were different than predicted when considering only age-related cell cycle alterations and the percentage of cells in G1 and S/G2 in young and old cells (Table 4.1).

Continuous HO endonuclease induction survivors arise when the repair is mutagenic, as the recognition site is mutated, preventing re-cleavage. As mentioned, the NPC is associated with NHEJ and other mutagenic alt-repair pathways (389,393,395,399,400). To determine whether age-related changes in end-joining and nuclear periphery location reflected a physiological change in how DSBs were being processed, we induced a break in young and old cells and then sequenced across the repaired break junction. Consistent with previous work, the most common mutations in Y and O1 survivors were a 2-bp (+CA) insertion and a 3-bp (-ACA) deletion, and other small 1-3 bp indels (Table 4.2) (380,401). By contrast, mutations in O2 survivors were primarily 4-6 bp deletions with 1-2 bp of microhomology (MH) (Table 4.2) (190). Taken together, these data are consistent with a model whereby older cells use an end-joining mechanism to repair DSBs other than NHEJ, one correlated with decreased Ku and increased NPC association, and one infrequently used in young cells.

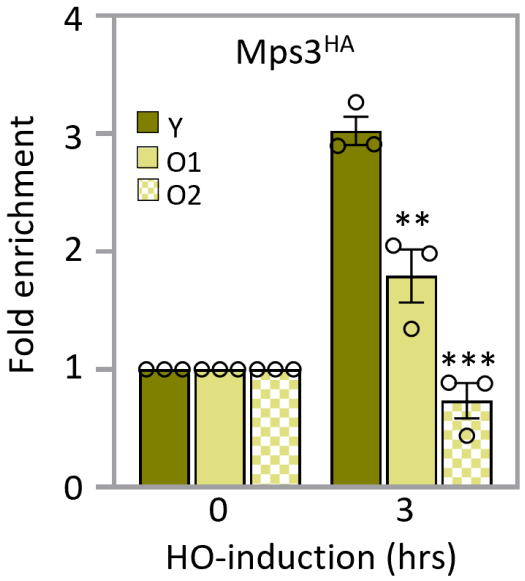

Figure 4.25 Relocalisation of DSB to Mps3 in aged cells

ChIP showed enrichment of Mps3^{HA} (JC-3167) 0.6kb away from the DSB at 0- and 3-hour time point in Y and O1-O2 aged cells. The fold enrichment was normalized to enrichment at the *SMC2* locus and then to time point 0. The error bars represent the standard error of three replicates for all the experiments. Significance was determined using a 1-tailed, unpaired Student's t-test. All comparisons are to Y cells and marked ($P<0.05$*; $P<0.01$**; $P<0.001$***).

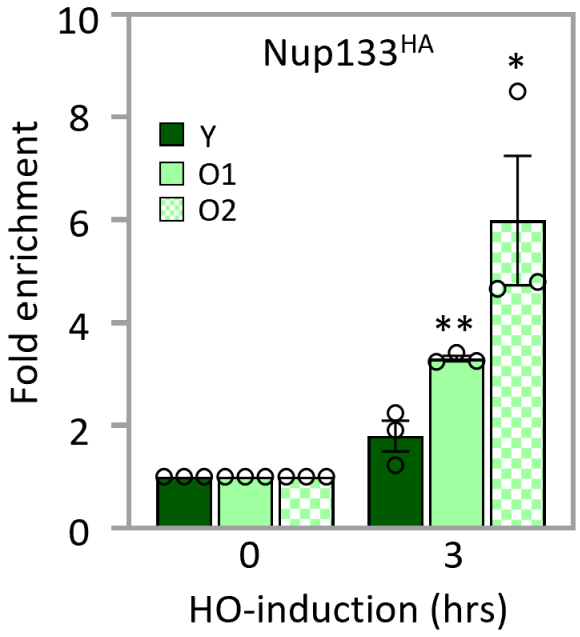

Figure 4.26 Relocation of DSB to Nup133 in aged cells

ChIP showed enrichment of Nup133^{Myc} (JC-1510) 0.6kb away from the DSB at 0- and 3-hour time point in Y and O1-O2 aged cells. The fold enrichment was normalized to enrichment at the *SMC2* locus and then to time point 0. The error bars represent the standard error of three replicates for all the experiments. Significance was determined using a 1-tailed, unpaired Student's t-test. All comparisons are to Y cells and marked (P<0.05*; P<0.01**; P<0.001***).

Table 4.1 Resection efficiency

5’ resection and ChIP at the DSB in Young and Old cells; **Actual** and **Predicted** (from values with young cells and normalized for changes in cell cycle and cut efficiency)

Cell cycle (from Supplementary Fig 1f)

		G1	%	G1 (rel. to Y)	S/G2	%	S/G2 (rel. to Y)			%
	Y	67.8	69.82492276	1.00	29.3	30.1750772	1.000000001		97.1	100
	O1	76.8	79.01234568	1.13	20.4	20.9876543	0.695529433		97.2	100
	O2	82.6	85.59585492	1.23	13.9	14.4041451	0.477352385		96.5	100
	O3	84.9	89.89834816	1.29	9.54	10.1016518	0.334768053		94.44	100

Actual (measured) values | **Normalized to cut efficiency** | **Predicted based on young (Y) and only cell cycle**

Resection 150 min (0.15 KB)

	actual	Supplementary Table 2 cut efficiency (150 min)		norm to cut efficiency
Y	**46.73**	98.69	0.9869	**47.35**
O1	**17.27**	96.35	0.9635	**17.92**
O2	**9.66**	86.48	0.8648	**11.17**
O3	**6.54**	77.1	0.771	**8.48**

predicted	Resect	S/G2 cell cycle norm.	predicted
Y	46.7	1.000000001	**46.70**
O1	46.7	0.695529433	**32.48**
O2	46.7	0.477352385	**22.29**
O3	46.7	0.334768053	**15.63**

ChIP Nup133 (3hr)

	actual	Supplementary Table 3 cut efficiency (3hr)		norm to cut efficiency
Y	**1.80**	99.75	0.9975	**1.80**
O1	**3.31**	99.72	0.9972	**3.32**
O2	**5.99**	82.37	0.8237	**7.27**

predicted	enrichment	G1 cell cycle norm	predicted
Y	1.797	1.000000011	**1.80**
O1	1.797	1.131578001	**2.03**
O2	1.797	1.225863953	**2.20**

ChIP Mps3 (3hr)

	actual	Supplementary Table 3 cut efficiency (3hr)		norm to cut efficiency
Y	**3.02**	99.75	0.9975	**3.03**
O1	**1.79**	99.72	0.9972	**1.80**
O2	**0.74**	82.37	0.8237	**0.89**

predicted	hment	S/G2 (rel. to Y)	predicted
Y	3.025	1.000000001	**3.02**
O1	3.025	0.695529433	**2.10**
O2	3.025	0.477352385	**1.44**

SUMMARY

Resection 150 min (0.15 KB)

	actual	norm. (cut efficiency)	predicted
Y	**46.70**	47.35	**46.70**
O1	**17.27**	17.92	32.48
O2	**9.66**	11.17	22.29
O3	**6.54**	8.48	15.63

ChIP Nup133 (3hr)

	actual	norm. (cut efficiency)	predicted
Y	**1.80**	1.80	**1.80**
O1	**3.31**	3.32	2.03
O2	**5.99**	7.27	2.20

ChIP Nup133 (3hr)

	actual	norm. (cut efficiency)	predicted
Y	**3.02**	3.03	**3.02**
O1	**1.79**	1.80	2.10
O2	**0.74**	0.89	1.44

Events	Young	# (total)
+CA	...GCGCAACACAGTATAA...	5 (15)
-ACA	...GCGCA(ACA)GTATAA...	5 (15)
+C	...GCGCAACCAGTATAA...	2 (15)
-A	...GCGC(A)ACAGTATAA...	3 (15)
Old 1 (6 divisions)		
+CA	...GCGCAACACAGTATAA...	5 (25)
-ACA	...GCGCA(ACA)GTATAA...	13 (25)
+C	...GCGCAACCAGTATAA...	5 (25)
-A	...GCGC(A)ACAGTATAA...	1 (25)
-GCA	...GC(GCA)ACAGTATAA...	1 (25)
Old 2 (11 divisions)		
-ACA	...GCGCA(ACA)GTATAA...	4 (25)
-ACAGT	...GCGCA(ACAGT)ATAA...	10 (25)
-GCAA	...CTTCGC(GCAA)CAGTATAA...	5 (25)
-CAGTAT	...GCGCAA(CAGTAT)AATTTT...	2 (25)
-GT	...GCGCAACA(GT)ATAATTTT...	2 (25)
-GCGCAA	...CTTC(GCGCAA)CAGTATAA...	1 (25)
-GTATA	...GCGCAACA(GTATA)ATTTT...	1 (25)

Table 4.2 Sequencing of survivors

Cells were plated on chronic HO induction on galactose plates in WT (JC-727) Y and O1, O2, and O3 aged cells. Survivors were sequenced to determine mutations of the DSB cut site. Green shows insertions, red shows deletions, and blue shows microhomologies. The total number of survivors harbouring the mutation is shown.

4.4 Discussion

Here we report age-dependent mechanistic changes in DSB repair in the unicellular eukaryotic organism *S. cerevisiae*. Early in replicative aging, resection and the recruitment of HR factors decreased. As HR declined, there was a shift towards end-joining mechanisms and a progressive increase in the frequency of repair products with larger deletions and MHs at break junctions. For this work to be possible, we optimized an old cell enrichment protocol that allowed us to isolate enough old cells at various stages of aging for molecular and biochemical studies.

The old cell enrichment method used was an adapted biotin labelling method made possible by enhanced biotin binding technology that was commercially available (Figure 2.2) (Sinclair 2013). Our approach was surprisingly uncomplicated and allowed large quantities of biotin-labelled mother cells to be isolated with minimal young cell contamination. Many yeast aging studies have combined biotin labelling with the 'Mother enrichment program' (MEP), based on a Cre-Lox system that needs to be integrated into the yeast genome (227). Our approach was not combined with the MEP. It did not require estradiol treatment to kill off daughter cells but permitted their recovery. It might be valuable for future large-scale studies comparing daughter cells from young and old mothers.

Our work catalogued molecular changes in DSB repair in yeast cells at different stages of the replicative lifespan, providing insight into how mechanisms that preserve genome maintenance in eukaryotic cells evolve with age. While the relative use and efficiency of repair pathways are known to be impacted by cell type, cell cycle phase, and ploidy, very little is known about how cellular age impacts the molecular events driving DSB repair pathway choice (402,403).

DSBs are dangerous lesions and can lead to an increased mutational burden or cell death when not correctly repaired. We have measured age-dependent mechanistic changes in DSB repair and see that cellular age accentuates unfortunate repair outcomes.

In yeast, the relative use of the two canonical DSB pathways, HR and NHEJ, is 10 to 1 in favour of HR (404). Our data suggest that this ratio is specific to young cells. We find that early in the cell's replicative lifespan, by ~6 divisions, DNA resection at an induced DSB markedly decreased to a level that could not be attributed to slight changes in the cell cycle or DSB cut efficiency (Figures 4.6, 4.7 and 2.5) (Tables 4.1, 4.3, 4.4). Another possibility for the decrease in DSB formation could be accounted to mutagenic repair of the DSB. This would lead to altering the cut site and, therefore, no induction of the DSB. In cultures of the same replicative age, the end-joining frequency increased to serve as a backup when HR declined rather than competing with HR (Figure 4.18 and 4.20). Deletion of *DNL4* in O1 cells did not restore resection at the HO-DSB (Figure 4.20), indicating that there are intrinsic age-related decreases in HR efficiency, independent of NHEJ usage, that decline with age. These results align with previous work that showed single-strand annealing (SSA), an alternative DSB repair pathway dependent on resection, declined with increased replicative age and was not restored by *dnl4*D (374). Decreased resection likely stems from a reduction in HR factors because their overexpression in older cells restores DSB repair following MMS treatment and extends lifespan (99). First shown by others and reproduced here by us, the expression of HR proteins decreased with age (Figure 4.12) (99). In addition to reduced protein levels, we observed a significant decrease in the recruitment of specific HR factors to the DSB (Figures 4.13 and 4.14). The largest relative decrease

we observed between Y and O1 cells was the 3-fold decrease in Dna2 recruitment to the DSB (Figure 4.14 and Figure 4.12).

Our work also showed that changes in the stoichiometry of repair proteins at DSBs impacted repair pathway choice and corresponded with the shift from HR to end-joining early in replicative aging. There was a significant increase in the retention of Ku at DSBs in O1-aged cells, as well as Mre11 and Rad50, even though protein levels decreased (Figure 4.10, Figure 4.15, and 4.12). However, in O2-aged cells, Ku was a significant loss. Although the levels of Ku protein were reduced compared to the high levels seen in young cells, it was surprising to see such a lack of recruitment. This may result from the loss of nuclear import of the protein, which is known to decrease during aging. To determine if this was occurring, Ku could be fluorescently tagged, and then microscopy could be used to determine the location of Ku during aging. Furthermore, when most HR factors in resection recovery decreased, the core NHEJ factors remained constant, including Nej1 and Lif1-Dnl4. In O2-aged cells, resection and end-joining decreased, correlated with a marked decrease in Ku. However, other end-joining factors, such as Nej1, remained constant (Figure 4.15). This is likely due to their importance in end bridging and MMEJ. One further caveat to this approach is that we only studied one-time points at 3 hours following the induction of the DSB, which provided a snapshot of the proteins at the DSB. However, there is the possibility that these proteins are successfully recruited to the DSB initially; however, there is a loss of retention. Therefore it may be imperative that we take samples at different times following the DSB induction as cells age to determine if this may be the case. This may also explain why there are large differences in the recruitment of repair factors with factors of the same

complex, such as Mre11 and Rad50, having such different enrichments. Taking time points may allow us to see repair proteins' recruitment and retention kinetics more clearly.

DNA sequencing across the breakpoint junction showed that repair events in survivors of continuous HO induction shifted from 1-3 bp indel events when the break was induced in Y cells to larger deletions with 1-2 bp MHs at the junction when the break was induced in O2 cells (Table 4.1) (190). It is thought-provoking to consider whether repair products in O2 cells result from NHEJ or whether these repair events can be categorized as microhomology end-joining (MMEJ). NHEJ products can have MH, and one litmus test for MMEJ is whether the end-joining event occurs in the absence of Ku. MMEJ products in yeast typically have 4-6 bp MHs and occur in the absence of Ku when the thermodynamics of NHEJ is not favoured. However, most MMEJ work has been performed in young cells with reporter systems where MH length and location relative to the break have been regulated (405–407).

Naturally occurring MMEJ in cells late in their RLS has never been reported. In O2-aged cells, which is ~44% of the lifespan, Ku70 recovery at the DSB was reduced to background levels (Figure 4.15). Thus, the local environment might be a site where end-joining events are coordinated independently of Ku. Alternatively, Ku70 might be present below the level of detection. Either way, the repair products in O2 are rarely seen in young cells of the same genotype.

Interestingly, factors identified by using reporter systems to be critical for MMEJ, such as MRX and Nej1, were present at the DSB in O2 cells (405,406). In yeast, MRX is an integral component of most repair mechanisms, including HR, NHEJ and MMEJ. MRX may help regulate repair pathway usage by controlling the extent of resection at the break. While HR requires extensive

resection, MMEJ requires minimal resection. The 3'-5'exonuclease activity of MRX is essential to initiate resection as it removes nucleotides at the DSB in ~100 bp increments in a 3' to 5' direction (405,406). If Ku dissociates, then NHEJ cannot occur, and if resection is reduced, then HR will not proceed. However, if other end-joining factors like Nej1 and Lif1-Dnl4 or Cdc9 ligase, the break can be sealed through MMEJ, but with larger deletions. This represents the culmination of events in O2-aged cells.

Work performed in human and yeast have linked nuclear architecture with aging and genome stability pathways (408,409). The stability of the genome relies on the sequestration and compartmentalization of irreparable DSBs at the nuclear periphery to environments conducive to repair. In humans, breaks at the nuclear lamina are repaired through MMEJ. In yeast, the NPC is where end-joining repair occurs, both NHEJ and MMEJ. Naturally aged yeast showed increased nuclear envelope herniations associated with NPC regions and a decline in NPC assembly (376,410). In O2-aged cells, there was a 3-fold increase in DSBs associated with the NPC (Figure 4.26). Indeed, disruptions in nuclear pore components result in reduced survival after DNA damage exposure (389,411), and single cells that maintain NPC components live longer (376,410). Thus, declined NPC function in older cells might impact not only shuttling in and out of the nucleus but also the repair efficiency of DSBs, which accumulate more at nuclear pores in older cells (Figure 4.25 and 4.26).

Aging research has also focused on the rDNA repeat region (98). The accumulation of ERCs, produced by recombination within the repeat region, is retained in old cells through a mechanism involving their localization to the NPC (412). Given that this is where we see irreparable DSBs targeted for repair in older cells, our observations may be related to why rDNA instability and

ERC formation impact global genome stability in old cells (98,99). Increased ERCs at nuclear pores could impact the efficiency of end-joining repair in old cells, resulting in increased rates of genomic gH2AX and translocations in old cells (228). Understanding events in the NPC compartments at the nuclear periphery might be vital to understanding the relationship between aging and genome stability.

Many pathways controlling replicative yeast aging appear to be fundamentally conserved, including pathways critical in DSB repair and genome stability (413). Thus, the work presented here, which involved determining DSB repair using the HO system in yeast at different stages of replicative aging, will bring insight into the connection between cellular aging and genome maintenance in higher eukaryotes.

Table 4.3 *DSB cut efficiency at time points used in resection experiments*

Strain	**Genotype**	**HO cutting:**		
		40 min	80 min	150 min
JC-727 -Y	*Wild type*	97.66	98.76	98.69
JC-727 -O1	*Wild type*	88.90	92.92	96.35
JC-727 -O2	*Wild type*	62.54	77.16	86.48
JC-727 -O3	*Wild type*	45.94	71.48	77.10
JC-1342 -Y	*nej1Δ*	98.51	98.33	98.88
JC-1342 -O1	*nej1Δ*	97.17	98.19	98.57
JC-1343 -Y	*lif1Δ*	94.90	95.63	97.13
JC-1343 -O1	*lif1Δ*	93.45	97.16	98.54
JC-1904 -Y	*ku70Δ*	89.22	87.03	93.88
JC-1904 -O1	*ku70Δ*	91.95	91.41	93.92
JC-3290 -Y	*dnl4Δ*	96.12	97.36	99.20
JC-3290 -O1	*dnl4Δ*	89.05	95.08	94.00

Table 4.4 *DSB cut efficiency used in ChIP experiments*

Strain	Genotype	DSB cut (%) 3hrs		Strain	Genotype	DSB cut (%) #hrs
JC-727 -Y	Wild type	99.75		JC-3306 -Y	*RAD50-6HA*	98.93
JC-727 -O1	Wild type	99.72		JC-3306 -O1	*RAD50-6HA*	98.61
JC-727 -O2	Wild type	82.37		JC-3306 -O2	*RAD50-6HA*	99.13
JC-727 -O3	Wild type	73.73		JC-3319 -Y	*LIF1-6HA*	99.51
JC-1342 -Y	*nej1*Δ	97.96		JC-3319 -O1	*LIF1-6HA*	99.48
JC-1342 -O1	*nej1*Δ	99.99		JC-3802 -Y	*MRE11-6HA*	98.97
JC-1343 -Y	*lif1*Δ	99.68		JC-3802 -O1	*MRE11-6HA*	99.32
JC-1343 -O1	*lif1*Δ	99.66		JC-3802 -O2	*MRE11-6HA*	98.85
JC-1510 -Y	*NUP133-13MYC*	99.16		JC-3964 -Y	*KU70-FLAG*	98.83
JC-1510 -O1	*NUP133-13MYC*	99.05		JC-3964 -O1	*KU70-FLAG*	99.46
JC-1510 -O2	*NUP133-13MYC*	99.22		JC-3964 -O2	*KU70-FLAG*	99.04
JC-1687 -Y	*NEJ1-13MYC*	99.29		JC-4117 -Y	*DNA2-6HA*	99.25
JC-1687 -O1	*NEJ1-13MYC*	99.08		JC-4117 -O1	*DNA2-6HA*	99.04
JC-1687 -O2	*NEJ1-13MYC*	99.01		JC-4135 -Y	*SGS1-6HA*	99.11
JC-1904 -Y	*ku70*Δ	99.66		JC-4135 -O1	*SGS1-6HA*	99.22
JC-1904 -O1	*ku70*Δ	97.06		JC-4869 -Y	*EXO1-6HA*	99.57
JC-3167 -Y	*MPS3-6HA*	99.52		JC-4869 -O1	*EXO1-6HA*	99.44
JC-3167 -O1	*MPS3-6HA*	98.99		JC-5116 -Y	*SAE2-6HA*	98.86
JC-3167 -O2	*MPS3-6HA*	99.12		JC-5116 -O1	*SAE2-6HA*	99.14
JC-3290 -Y	*dnl4*Δ	98.56		JC-5672 -Y	*DNL4-6HA*	99.19
JC-3290 -O1	*dnl4*Δ	98.24		JC-5672 -O1	*DNL4-6HA*	99.22

4.5 Materials and Methods

Table 4.5 *Yeast strains used in this study.*

Strain	Genotype	Reference
JC-727	MAT α; *hml*::*ADE1 hmr*::*ADE1 ade3*::GAL-HO *ade1*-100 *leu*2-3, 112 *lys*5 *trp*1::*hisG ura3*-52	JKM179, [Lee et al. 1998]
JC-1342	JC-727 with *nej1*Δ::*KanMX6*	MAV015, [Valencia et al. 2001]
JC-1343	JC-727 with *lif1*Δ::*KanMX6*	Sorenson et al. 2017
JC-1510	JC-727 with *NUP133-13MYC::TRP1*	This study
JC-1687	JC-727 with *NEJ1-13MYC*::*TRP1*	Sorenson et al. 2017
JC-1904	JC-727 with *ku70*Δ::*KanMX6*	Sorenson et al. 2017
JC-3013	JC-727 with *NUP49-CFP; LacI-GFP::LEU2; MAT-LacO::TRP1*	Horigome et al. 2016
JC-3167	JC-727 with *MPS3-6HA::TRP1*	This study
JC-3290	JC-727 with *dnl4*Δ::*KanMX6*	Sorenson et al. 2017
JC-3306	JC-727 with *RAD50-6HA::TRP1*	Mojumdar er al. 2022b
JC-3319	JC-727 with *LIF1-6HA::TRP1*	Sorenson et al. 2017
JC-3802	JC-727 with *MRE11-6HA::TRP1*	Mojumdar et al. 2022b
JC-3964	JC-727 with *KU70-FLAG::TRP1*	Mojumdar et al. 2022a
JC-4066	JC-3585 with *ura3::LacI-mCherry-URA3; leu2::TetR-GFP-LEU2; TAF2-LacOpFx-TRP1; 4.4kb MAT-TetO-Leu2*	Mojumdar et al., 2019
JC-4117	JC-727 with *DNA2-6HA::TRP1*	Mojumdar et al., 2019
JC-4135	JC-727 with *SGS1-6HA::TRP1*	Mojumdar et al. 2022b
JC-4869	JC-727 with *EXO1-6HA::TRP1*	Mojumdar et al. 2022b
JC-5116	JC-727 with *SAE2-6HA::TRP1*	Mojumdar et al. 2022b
JC-5672	JC-727 with *DNL4-6HA::TRP1*	Mojumdar et al. 2022a

Table 4.6 Primers and Probes

Primer Name	**Primer Sequence (5’-3’)**
HO2 Forward Primer	TTGCCCACTTCTAAGCTGATTTC
HO2 Reverse Primer	GTACTTTTCTACATTGGGAAGCAATAAA
HO2 Probe	FAM-ATGATGTCTGGGTTTTGTTTGGGATGCA-TAMRA
SMC2 Forward Primer	AATTGGATTTGGCTAAGCGTAATC
SMC2 Reverse Primer	CTCCAATGTCCCTCAAAATTTCTT
SMC2 Probe	FAM-CGACGCGAATCCATCTTCCCAAATAATT-TAMRA
MAT1 Forward Primer	CCTGGTTTTGGTTTTGTAGAGTGG
MAT1 Reverse Primer	GAGCAAGACGATGGGGAGTTTC
HO6 Forward Primer	AATATGGGACTACTTCGCGCAACA
HO6 Reverse Primer	CGTCACCACGTACTTCAGCATAA
Pre1 Forward Primer	CCCACAAGTCCTCTGATTTACATTCG
Pre1 Reverse Primer	ATTCGATTGACAGGTGCTCCCTTTTC
S1	TCTTGCCCACTTCTAAGCTG
S2	TCGAAAGATAAACAACCTCC

Table 4.7 *List of Key Resources*

REAGENT or RESOURCE	SOURCE	IDENTIFIER
Antibodies		
αHA mouse monoclonal antibody	Santa Cruz Biotechnology	F-7
αFLAG mouse monoclonal antibody	Santa Cruz Biotechnology	M2F12
αMyc mouse monoclonal antibody	Abcam	ab32
αH3 rabbit polyclonal	Abcam	ab1791
αH4 rabbit polyclonal	Invitrogen	AB_10977843
αH4 acetyl mouse monoclonal antibody	Millipore	3HH4-4C10
Peroxidase conjugated AffiniPure Goat anti-Mouse antibody	Jackson ImmunoResearch	115035174
Chemicals		
α – factor	EZBiolab	CP7206
Adenine	Sigma	A8626
Albumin, Bovine Serum, Fraction V, low heavy metals	Calbiochem	12659
Ammonium sulfate	VWR	BDH9216
Anti-Biotin MicroBeads	Miltenyi Biotec	130-090-485
Bacto™ Peptone	BD Biosciences	211677
Bacto™ Yeast extract	BD Biosciences	212750
Calcofluor white stain	Sigma	18909
Complete EDTA-free protease inhibitor cocktail	Roche	04693159001
Dextrose	Sigma	D1912
Difco™ Agar	BD Biosciences	214530
Difco™ Yeast Nitrogen Base without Amino Acids and Ammonium Sulfate	BD Biosciences	233520
Dynabeads Sheep anti-Mouse IgG	Invitrogen	20230531
EDTA	VWR	0322
Ethanol	Commercial alcohols	P006EAAN
Ez-Link™ Sulfo-NHS-LC-Biotin Sulfosuccinimidyl-6-(biotinamido) hexanoate	Thermoscientific	21335
Formaldehyde	Sigma	F8775
Galactose	Sigma	G0750
Glycine	VWR	CA93291
Glycogen	Roche	10901393001
L-Arginine monohydrochloride	Sigma	A5131
L-Aspartic Acid	Sigma	A9256
L-Glutamic Acid	Sigma	G1626
L-Histidine	Sigma	H8000
L-Isoleucine	Sigma	I2752
L-leucine	Sigma	L8000
L-Lysine	Sigma	L5501
L-Methionine	Sigma	M9625
L-Phenylalanine	Sigma	P2126

L-Serine	Sigma	S4500
L-Threonine	Sigma	T8625
L-Tryptophan	Sigma	T0254
L-Tyrosine	Sigma	T3754
L-Valine	Sigma	V0500
Lactic acid	Sigma	69785
Lithium Chloride	EMD Millipore	LX03311
Paraformaldehyde	Sigma	158127
Phenol-Chloroform-Isoamylalcohol	Invitrogen	15593049
PMSF	Sigma	78830
Potassium Chloride	EMD Chemicals	1049360500
Potassium phosphate monobasic	Sigma	P9791
Raffinose	US Biological	R1030
SDS	Avantor	409502
Sodium Acetate	VWR	BDH9278
Sodium Chloride	Fisher Chemical	S64212
Sodium hydroxide	EMD Millipore	1310-73-2
Sodium phosphate, dibasic, anhydrous	VWR	84486-300
SuperMACS^{TM} II Separator	Miltenyi Biotec	130-044-104
Tris base	Fisher Chemical	BP1525
Triton	Sigma	9002931
Uracil Minimum 99%	Sigma	U0750
XS Columns	Miltenyi Biotec	130-041-202
Zirconia Silica beads	BioSpec Products	11079105z
Enzymes		
Proteinase K	Invitrogen	25530031
RNase A	Sigma	R6513
RsaI	New England Biolabs	R0167S
Kits		
PerfeCTa qPCR SuperMix, ROX	Quanta BioSciences Inc.	89168-786
PowerUp SYBR Green Master Mix	Applied Biosystems	A25743
Western Lightning Plus-ECL	PerkinElmer	NEL105001EA

Old Cell Enrichment

Old cell enrichment (OCE) was based on (229). For all assays, 20ml of overnight culture was inoculated in YPAD medium at 25 degrees. Cells were diluted to 100ml of YPAD and grown into log phase. Cells were harvested and washed three times with 1x phosphate-buffered saline (PBS). Cells were then resuspended in 1ml PBS and mixed with 8mg of Sulfo-NHS-LC- Biotin per $1x10^8$ cells for 30 min at 30°C. Cells were washed three times with 1ml PBS and 0.1M Glycine and used to inoculate 500ml SC media overnight at 25°C. Cells were harvested at 5000rpm for 10 minutes and washed thrice with PBS. Cells were then incubated in 50ml PBS and 20µl of Anti-Biotin Microbeads per 10^7 total cells at four °C for 30 mins. Young and old cells were then separated by flowing through an XS column on the SuperMACS II separator at room temperature and washed thoroughly with 150ml of PBS until no more liquid remained on the column. The XS column is removed from the magnetic field, and the old cells are eluted using a syringe.

Chromatin Immunoprecipitation

ChIP assay was performed as described previously (380). Cells were collected from the OCE process and resuspended in 200ml of 1% yeast extract, 2% peptone, 2% lactate, and 2% galactose (YPLG) at 30°C cells were harvested and cross-linked at various time points using 3.7% formaldehyde solution. Following crosslinking, the cells were washed with ice-cold PBS, and the pellet was stored at -80°C. Pellets were re-suspended in lysis buffer (50mM Hepes pH 7.5, 1mM EDTA, 80mM NaCl, 1% Triton, 1mM PMSF and protease inhibitor cocktail) and then lysed using Zirconia beads and a bead beater. Chromatin fractionation was performed to enhance the chromatin-bound nuclear fraction by spinning the cell lysate at 13,200 RPM for 15 minutes and

discarding the supernatant. The pellet was re-suspended in lysis buffer and sonicated to yield DNA fragments (~500 bps in length). The sonicated lysate was then incubated in beads + anti-HA, or Myc conjugated dynabeads or unconjugated beads (control) for 2 hrs at 4°C. The beads were washed using wash buffer (100 mM Tris pH 8, 250 mM LiCl, 0.5% NP-40, 1mM EDTA, 1mM PMSF, protease inhibitor cocktail, and either 150 mM NaCl (for HA-epitope tagged samples) or 500mM NaCl (for Myc-epitope tagged samples). DNA bound by proteins was recovered by reverse crosslinking using 1% SDS in TE buffer, followed by proteinase K treatment and DNA isolation via phenol-chloroform-isoamyl alcohol extraction. Quantitative PCR was performed using the Applied Biosystem QuantStudio 6 Flex machine. PerfeCTa qPCR SuperMix, ROX was used to visualize enrichment at HO2 (0.5 kb from DSB) and HO1 (1.6 kb from DSB) and SMC2 was used as an internal control.

Continuous DSB assay and identification of mutations in survivors

Cells from each strain were collected from the OCE process by centrifugation at 2500 RPM for 3 minutes, and pellets were washed 1x in ddH_2O and re-suspended in ddH_2O. Cells were counted and spread on 1% yeast extract, 2% peptone, and 0.004% adenine sulphate dihydrate (YPA) plates supplemented with either 2% GLU or 2% GAL. On the Glucose plates, $1x10^3$ total cells were added, and on the galactose plates, $1x10^5$ total cells were added. The cells were incubated for 3-4 days at room temperature, and colonies were counted on each plate. Survival was determined by normalizing the number of surviving colonies in the GAL plates to the number of colonies in the GLU plates. As previously described, one hundred survivors from each strain were scored for the mating type assay (414). The genomic DNA of sterile-type survivors was amplified with

primers S1-S2, followed by DNA sequencing. All primer sequences are listed in Supplementary Table 5.

Western Blot

Cells were lysed by re-suspending them in lysis buffer (with PMSF and protease inhibitor cocktail tablets) followed by bead beating. The protein concentration of the whole cell extract was determined using the NanoDrop. Equal amounts of whole-cell extracts were added to wells of 10% polyacrylamide SDS gel. After the run, the protein was transferred to Nitrocellulose membrane at 100 V for 80 mins. The membrane was Ponceau stained (which served as a loading control), followed by blocking in 10% milk-PBST for 1 hour at room temperature. The respective primary antibody solution (1:1000 dilution) was added for incubation overnight at 4°C. The membranes were washed with PBST and left for 1 hour with a secondary antibody. Followed by washing the membranes, adding the ECL substrates and imaging them.

Resection Assay

Cells from each strain were collected from the OCE process and resuspended in 15ml YPLG. 2.5mL of the cells were pelleted as timepoint 0 sample, and 2% GAL was added to the remaining cells to induce a DSB. Following that, respective timepoint samples were collected. Genomic DNA was purified using the standard genomic preparation method by isopropanol precipitation and ethanol washing, and DNA was re-suspended in 100 mL ddH_2O. Genomic DNA was treated with 0.005µg/µL RNase A for 45min at 37°C. 2 µL of DNA was added to tubes containing CutSmart buffer with or without the *Rsa*I restriction enzyme and incubated at 37°C for 2hrs. Quantitative PCR was performed using the Applied Biosystem QuantStudio 6 Flex machine. PowerUp SYBR

Green Master Mix was used to quantify resection at *MAT*1 (0.15 kb from DSB) locus. Resection at *PRE1* was used as a negative control. *Rsa*I cut DNA was normalized to uncut DNA as previously described to quantify the % ssDNA / total DNA (379).

Ligation Assay

Cells from each strain were collected from the OCE process and resuspended in 15ml YPLG. Next, 2.5mL of the cells were pelleted as a 'No break' sample, and 2% GAL was added to the remaining cells to induce a DSB. 2.5ml of cells were pelleted after 3hr incubation as timepoint 0 sample. After that, GAL was washed off, the cells were released in YPAD, and respective timepoint samples were collected. Genomic DNA was purified using the standard genomic preparation method by isopropanol precipitation and ethanol washing, and DNA was re-suspended in 100mL ddH_2O. Quantitative PCR was performed using the Applied Biosystem QuantStudio 6 Flex machine. PowerUp SYBR Green Master Mix was used to quantify resection at the HO6 (at DSB) locus. *PRE1* was used as a negative control. Signals from the HO6 timepoints were normalized to 'No break' signals, and % Ligation was determined.

Bud Scar Microscopy

Following old cell enrichment, 20 µl of cells were collected and fixed with 2 µl of formaldehyde. Cells were then pelleted and stored at 4°C before imaging. Cells are resuspended in 20 µl of PBS and stained with Calcofluor White. Cells are then placed on coverslips and imaged using Zeiss LSM 880 with Airyscan. Z-stack images were acquired with 0.35 µm along the z plane using a plan-apochromat 63x/1.40 Oil Dic M27 objective. Images were analyzed using ZenBlue software. Each cell was analyzed individually, and >50 cells were analyzed per sample.

End-bridging Microscopy

Cells derived from the parent strain JC-4066 were collected following the OCE process. Cells were resuspended in SC with 2% lactate, 0.05% Glucose and 2% glycerol (SCLGg) media and then treated with 2% GAL for 2 hours. Cells were washed 2 times with PBS, placed on coverslips, and imaged using a fully motorized Nikon Ti Eclipse inverted epi-fluorescence microscope. Z-stack images were acquired with 200 nm increments along the z plane, using a 60 X oil immersion 1.4 N.A. objective. Images were captured with a Hamamatsu Orca flash 4.0 v2 sCMOS 16-bit camera, and the system was controlled by Nikon NIS-Element Imaging Software (Version 5.00). All images were deconvolved with Huygens Essential version 18.10 (Scientific Volume Imaging, The Netherlands, http://svi.nl), using the Classic Maximum Likelihood Estimation (CMLE) algorithm, with SNR:40 and 50 iterations. To measure the distance between the GFP and mCherry foci, the ImageJ plug-in Distance Analysis (DiAna) was used (415). Distance measurements represent the shortest distance between the brightest pixel in the mCherry channel and the GFP channel. Each cell was measured individually, and > 50 cells were analyzed per condition per biological replicate.

Nuclear Pore Localization Microscopy

Cells derived from the parent strain JC-3013 were collected following the OCE process. Cells were resuspended in SCLGg media and then treated with 2% GAL for 2 hours. Cells were collected and washed 2 times with PBS, placed on coverslips, and imaged using a fully motorized Nikon Ti Eclipse inverted epi-fluorescence microscope. Z-stack images were acquired with 200 nm increments along the z plane, using a 60X oil immersion 1.4 N.A. objective. Images were captured

with a Hamamatsu Orca flash 4.0 v2 sCMOS 16-bit camera, and the system was controlled by Nikon NIS-Element Imaging Software (Version 5.00). All images were deconvolved with Huygens Essential version 18.10 (Scientific Volume Imaging, The Netherlands, http://svi.nl), using the Classic Maximum Likelihood Estimation (CMLE) algorithm, with SNR:40 and 50 iterations. The 2D and 3D image reconstruction was done using IMARIS microscopy image analysis software (https://imaris.oxinst.com/). When the objects assigned to CFP and GFP intensities were touching, the cell was scored as DSB located at the nuclear envelope. To measure the distance between the GFP and CFP foci, the ImageJ plug-in Distance Analysis (DiAna) was used (415).

Data Availability Statement

This study did not generate/analyze any code. Original data supporting the figures in the paper is available from the corresponding author upon request.

Acknowledgements

We acknowledge the resources provided by the Live Cell Imaging Laboratory. Operating grants from CIHR MOP-82736 supported this work; MOP-137062 and NSERC 418122 were awarded to J.A.C. The Nikon Ti Eclipse inverted epi-fluorescence microscope system was purchased with funds from the International Microbiome Centre, which is supported by the Cumming School of Medicine at the University of Calgary, Western Economic Diversification (WED) and Alberta Economic Development and Trade (AEDT), Canada.

Declaration of Competing Interest

The authors declare that they have no real or perceived conflicts of interest, financially or otherwise.

Authors Contributions

Aditya Mojumdar: Methodology, Investigation, Supervision, Formal analysis, Writing-original draft and revisions, **Nicola Mair:** Methodology, Investigation, Writing-original draft and revisions, **Nancy Adam:** Investigation, **Jennifer A Cobb:** Supervision, Conceptualization, Funding acquisition, Writing- original draft and revisions,

Chapter 5 General discussion and future directions

5.1 The integrative biology of yeast aging

Aging is a significant risk factor associated with many human diseases, and these cellular pathways are highly conserved from yeast to humans. There are multiple ways in which yeast is crucial to understand aging. This includes direct studies on old yeast, how genetic modifications affect aging, and the identification of molecules and drugs that alter the aging process. Previous studies have used premature aging mutations to understand changes in aging further. These genetic modifications can alter how cells age and provide insight into the importance of specific proteins and their role during aging. Screens have been carried out to identify genes that change how yeast cells age using knock-out collections containing deletions of non-essential genes (51,416,417). Studies have also used yeast as a biological screening platform to understand conserved genes and aging mechanisms between yeast and humans (418). Following the knockout screens, identifying the pathways involved in the proteins can allow us to understand a single protein's impact on aging. Galactose inducible overexpression libraries can inform target proteins that can improve aging phenotypes (419,420). Although this is useful for studying aging, it does not represent how average cells age and the molecular changes that occur during natural aging. It is known that a single mutation does not cause aging; therefore, studying young mutant cells may not give us a complete understanding of aging. Therefore, studying natural aging in WT cells is crucial and the biggest strength of this work. One of the biggest challenges of aging research in yeast has been the isolation of a large enough quantity of aged cells to carry out biochemical studies that haven’t involved multiple genetic modifications to the yeast. Through

the adaption of the old cell enrichment method, I have overcome this barrier. The ease of this technique will facilitate future aging studies in yeast, as it is highly reproducible and is optimized for larger-scale recovery as the separation methodology is much shorter than with previously published approaches. However, as previously noted, this technique should be adapted to maintain yeast in logarithmic phase. This will be important to allow better synchronization of the yeast in S phase to study DNA replication and to prevent a study bias by having a larger population of the cells in G1 phase.

As our population is living to a much older age than any previous generation, it is also succumbing to more age-related diseases than ever before, such as heart disease, neurodegeneration, and cancer. Yeast has also been utilized to study molecular defects found in human-specific diseases and has been used to study anti-cancer agents (34). Therefore, this work allows an increased understanding of how crucial processes change during natural aging. It is known that there are many age-related changes to other major pathways in yeast, including the DNA damage pathway and the stress response, and this work expands on this knowledge (99,332,421). It is also known that cancerous cells are known to duplicate their genome at faster rates than normal cells, which may be correlated with an increase in age (422). By understanding cellular aging, future work can study slowing down the aging process and preventing the development of chronic diseases, leading to better health outcomes and quality of life.

5.2 Old yeast has replication ΔOrigin

Until now, DNA replication has only been studied in young cells. I, therefore, endeavoured to show how this process changed during aging. DNA replication is an important mechanism to understand, as errors can lead to increased mutations and loss of cellular viability. The misregulation of origin timing is shown to have profound effects on genomic integrity (423). Protein coding regions of the genome replicate early in the cell cycle to maintain genomic integrity, and I show a loss in the initiation of early replication origins during aging (424). This will lead to higher incorporation of mutations and a loss of genomic integrity, likely occurring during cellular aging.

I have shown that replication of DNA no longer occurs at sequence-specific ACSs in old yeast, and it tends to occur from an NFR nearby that we call the ΔOrigin. It is thought that the sequence-specific replication origins have evolved to increase fitness in yeast, as yeast have a high gene density in relation to its genome size, which helps avoid replication-transcription collisions. However, during aging, it likely becomes more critical that the entire genome is replicated and the importance of replication initiating from the sequence-specific region likely decreases. A third of yeast replication origins do not contain an ACS, and only 20% show ORC binding to the ACS through ChIP studies, but replication initiation can still occur at these sites (354). ORC can bind to nucleosomes independent of the ACS consensus sequence, which likely plays a more prominent role in replication during aging (354). Nucleosomes are the primary determinant of origin recognition, and ORC can bind to nucleosomes nearby the ACS even if the ACS has a strong ORC binding sequence (354). When ORCs bind to replication origins, they have nucleosome

repositioning capabilities to increase the size of the NFR (425). ORC can also reposition nucleosomes of non-ARS sites to increase the NFR. This increases accessibility; therefore, when ORC binds to the NFR of the ΔOrigin, this likely increases the accessibility to allow replisome recruitment. Cells with an *ORC2* have a smaller NFR at DNA replication origins (426). Highlighting the importance of ORC binding in maintaining a large NFR to allow replisome binding. *FKH1* leads to a change in the recruitment of ORC at replication origins, with 42% of all origins being dependent on Fkh1 for ORC binding (328). Likely, the decrease in Fkh1 during aging and loss of recruitment to replication origins destabilizes ORC binding and origin firing (346). This loss of ORC binding due to a loss of Fkh1 during aging likely decreases the NFR and promotes replication at the ΔOrigin. This highlights the importance of nucleosomes at an NFR and supports my data which shows ORC can bind to a nearby NFR and initiate DNA replication from these sites in aged cells.

Fkh1 is needed for DDK recruitment; the loss of DDK results in less Cdc45 loading in G1 (329,427). Reduced levels of DDK are known to lead to less MCM phosphorylation and decreased CMG formation, leading to less efficient replication origin firing (427). When Fkh1 binds to DNA replication origins, it creates a bend in the DNA (428); this bending has been proposed to increase initiation rates by increasing accessibility to the DNA. The loss of Fkh1 in aging and, therefore, loss of this bend may restrict access to replisome factors, resulting in replication occurring at the ΔOrigin, which is seen to have an NFR and therefore increased access for replisome factors to initiate replication.

Cohesion is essential for forming replication loops at replication foci, and there is less cohesion within cells during aging (99,429). It is, therefore, likely that as cells age, there are fewer and

longer replication loops at replication foci leading to a reduced frequency of origin firing leading to an extended S phase. It would be interesting to visualise DNA replication foci in aged cells. I would hypothesise that there are fewer foci due to less Fkh1 in G1 and the foci formed are less intense due to fewer loops due to loss of cohesion.

During aging, there is an increase in the number of ERCs. ERCs contain an origin of replication and must be replicated during the S phase of the cell cycle. This dilutes the efficiency and fidelity of the DNA replication machinery. I have shown that the recruitment of replisome proteins to replication origins decreases during aging, which will significantly impact genomic instability. It would be interesting to determine if ORC can bind to the replication origins in the ERCs, or if this also becomes increased, decreased, or unspecific during aging. In strains where Fob1 is deleted, there is increased rDNA stability and a decrease in ERC formation. It would be interesting to investigate if there are any changes to the site of replication in aged cells in a *FOB1* deletion to help determine the leading cause of the change in the initiation site.

Dna2 was studied in chapter 4 in the process of DNA repair; however, Dna2 is also known to have a role in DNA replication through Okazaki fragment processing. I have shown that the levels of Dna2 protein are reduced in aging cells (Figure 4.12). Therefore, this protein reduction is likely less efficient in processing Okazaki fragments. Dna2 is important to counteract fork reversal and promote fork restart (430). Therefore, there is likely an increase in lethal DNA structures as cells age due to the loss of Dna2. Transmission electron microscopy can be used to determine replication intermediates. I hypothesize that there is an increase in unprocessed replication forks and aberrant replication structures as cells age.

Although this thesis did not cover replication-coupled repair, I would hypothesize that as such major changes are seen in DSB repair, there would also be age-related changes to replication-coupled repair that decrease efficiency and increase genomic instability. This thesis has highlighted the importance of understanding fundamental cellular processes in the context of aging, as there are significant differences in DNA maintenance as cells age.

5.3 Old yeast repair by MMEJ

Understanding the molecular changes of aging will allow future interventions to delay age-related disorders (431). As cells age from yeast to flies to human fibroblasts, there is a decline in DNA repair capacity. I show that DSBs are repaired less by HR, which NHEJ can initially compensate for; however, further aging results in a decreased repair through NHEJ. This change to a more error-prone pathway leads to age-related genomic instability and increased cancer incidence as we age.

HR is the first DSB repair pathway to fail in aged cells; cells that have gone through an average of 6 replication cycles reduce utilization of this pathway. Although HR is considered error-free, mutations can still occur by using the HR pathway, which is believed to occur due to the formation of ssDNA and the use of pol ζ. It would be interesting to sequence the complete repair products to determine if there is a higher increase in mutational burden in cells that carry out HR but incorporate mutations during the invasion of a homologous sequence. It would also be interesting to determine if there is a higher usage of pol ζ in aging cells through ChIP. As yeast cells age, there are changes to transcription and a loss of overall protein synthesis (25). We see this in our study with the loss of total repair proteins and loss of recruitment to DSBs. The loss of

these proteins may impact the ability to form stoichiometry dependant complexes and allow their function. Although some studies have shown that overexpression of some proteins restores repair function, as many of these proteins work in a complex, simply overexpressing one of the factors that decrease during aging does not always restore HR function (372). Perhaps a further understanding of how we could supplement the repair factors in the ideal ratios to restore HR may restore DSB repair capacity and prevent cancer development.

Future studies need to be carried out to address what causes aged cells to repair DSBs inefficiently and look at chromatin and nuclear envelope changes. It is possible that DSB signalling is no longer occurring as efficiently or that loss of chromatin organization is occurring due to an increase in progerin as cells age. It would also be interesting to study protein function and whether the protein still available in the cells can maintain genomic stability. Single-cell protein sequencing is one of the most exciting new fields that will lead to fascinating developments in the future as it can determine mutations that occur during translation (432). Sequencing proteins of individual young and old cells to determine mutations that occur during translation as cells age and would help understand protein functionality. I hypothesize there is an increase in mutations within the proteins that are not seen in the DNA, as well as changes in post-translational modifications of individual proteins that lead to defects in protein function during aging. Using mass spectrometry in young and old cells, you could identify changes in post-translational modifications in both young and old cells. As I have shown, DSB in aged cells are being relocated to the NPC; however, these are known to accumulate during aging (433,434). The nuclear periphery also shows protein aggregation and clustered and altered stoichiometry of the NPCs

(435–438). ERCs are bound to the NPC; this is important to maintain ERCs within mother cells as yeast undergo closed mitosis, which results in NPCs being retained in mother cells (439).

When cells age, there is an increase in ERCs and a corresponding 10-fold increase in NPCs in aging cells (439). Therefore, the increase in recruitment of the DSB to NPCs that we observe may be influenced by the large increase in NPCs during aging. However, it is interesting to note that when ERCs bind to NPC, the NPC basket is lost (440). Nup84 is a nuclear basket component required for DNA replication and repair (441). It would be fascinating to determine how this change is structure of the NPC due to ERC binding affects DSB recruitment and if this change promotes MMEJ over NHEJ in aged cells. As well as to determine how much NPCs still maintain the NPC basket or if the majority becomes lost and bound by ERCs. Using *FOB1* would allow insight into how fewer ERCs would impact the NPCs during aging.

Many chromatin modulators affect pathway choice in yeast, such as NuA4, Chd1, INO80 and the saga complex (442,443). Determining how these proteins change during aging could help understand their role in DSB repair during aging. I hypothesize that these chromatin-remodelling proteins become less functional during aging as many are large protein complexes. Even the loss of one of the proteins will affect the overall complex function. This would lead to the cell being unable to modulate nucleosomes to allow efficient repair and may be one of the important reasons why cells resort to an MMEJ repair pathway that requires less chromatin remodelling.

MMEJ anneals ends that contain short microhomologies in a Ku and Rad52 independent process (194) lead to DNA mutations, telomere fusions and chromosomal rearrangements (196,444). Mre11 and Sae2 are needed to reveal the microhomology for repair (191). RPA inhibits MMEJ

(445), and loss of RPA has been shown to lead to an increase in MMEJ (446). It has previously been shown that there is a decrease in RPA protein levels in aging cells, likely leading to an increase in MMEJ (99). Therefore, the loss of RPA during aging helps drive the increase in MMEJ during aging. MMEJ has been an exciting field for cancer drug targets in NHEJ and HR-deficient cancers (447,448). Many yeast studies have used reporters to understand the position length and types of homologies used in the repair. The understanding that aged cells use MMEJ as they age may allow us to understand how cells naturally use MMEJ to repair DSBs.

It is very exciting to think about future 'anti-aging' interventions and what they may involve. Understanding the basic aging processes will allow us to develop interventions that target the molecular mechanisms of aging. This could include stem cell therapies to target age-associated diseases, dietary restriction drugs such as rapamycin to increase lifespan, and CRISPR to target known mutations in DNA damage repair that could effectively alter susceptibility to cancer and increase lifespan. Any intervention that may delay or prevent aging mechanisms, such as restoring DSB repair protein stoichiometry, may increase individuals' health span. Recent studies have developed small molecules that can alter the rate of aging, and it seems we are on the brink of developing interventions that can promote healthspan (449,450). Therefore, understanding how genetic and environmental factors affect aging is critical for research.

There are still significant questions in the aging field, such as how cells sense aging. What cellular change occurs first? What feedback systems are involved in aging, and could these be targeted to counteract age-related phenotypes? The advanced new methods being developed to study aging in yeast at both the high throughput and single-cell levels will be instrumental in identifying the molecular changes that occur during aging.

5.4 Conclusions

The field of geroscience is one of the most complicated yet essential research areas. Aging is a multi-component process and is incredibly complex and hard to study. The need to study aging stems from the desire to improve the quality of life of our aging population and decrease the burden on global healthcare.

Here, I focussed on the changes that occur to DNA maintenance during yeast aging and its impact on genomic stability. I describe an adapted method which allows a high-throughput approach to study differently aged yeast cells and processes which change during aging. In this thesis, I have explored two highly conserved molecular pathways in the context of aging. First, I demonstrated the changes in the well-defined DNA replication during aging. I determine that DNA replication initiation is significantly decreased, and that replication no longer occurs from sequence-specific genome regions; instead, origin firing occurs from low nucleosome-occupied regions adjacent to origins. These new sites of replication correspond with the recruitment of replisome factors.

Next, I focus on how cells repair DSBs as they age. Again, DSB repair has been extensively studied in young cells and has never been characterized in an aged yeast population. I show that young yeast predominantly repairs DSBs through HR; however, as cells age, there is a loss of repair by HR and cell repair through NHEJ. When cells are very old, they cannot repair DBS by HR or NHEJ and repair DSBs using MMEJ, as shown by the sequencing of the survivors resulting in mutagenic repair as cells age. My work highlights that well-documented mechanisms such as DNA replication and repair are fundamentally different in aging cells. I have highlighted that both processes have age-related changes that lead to genomic instability.

My work adds to the field of yeast aging and challenges how we understand well-studied mechanisms. It is very likely that other processes which have been well defined in young cells may be characteristic of only young cells and are inherently different during the aging process. Overall, this thesis provides evidence that molecular DNA replication and repair changes occur during aging, negatively impacting genomic stability. This thesis has added to our understanding of aging and hopefully will prime future research to account for aging going forward.

Chapter 6 References

1. Garmany A, Yamada S, Terzic A. Longevity leap: mind the healthspan gap. Npj Regen Med. 2021 Sep 23;6(1):1–7.

2. Miller RA. Extending Life: Scientific Prospects and Political Obstacles. Milbank Q. 2002;80(1):155–74.

3. Pal S, Tyler JK. Epigenetics and aging. Sci Adv. 2016 Jul;2(7):e1600584.

4. Jaul E, Barron J. Age-Related Diseases and Clinical and Public Health Implications for the 85 Years Old and Over Population. Front Public Health. 2017 Dec 11;5:335.

5. Sierra F, Kohanski R. Geroscience and the trans-NIH Geroscience Interest Group, GSIG. GeroScience. 2017 Feb 1;39(1):1–5.

6. Kennedy BK, Berger SL, Brunet A, Campisi J, Cuervo AM, Epel ES, et al. Geroscience: Linking Aging to Chronic Disease. Cell. 2014 Nov 6;159(4):709–13.

7. Seluanov A, Gladyshev VN, Vijg J, Gorbunova V. Mechanisms of cancer resistance in long-lived mammals. Nat Rev Cancer. 2018 Jul;18(7):433–41.

8. Liang S, Mele J, Wu Y, Buffenstein R, Hornsby PJ. Resistance to experimental tumorigenesis in cells of a long-lived mammal, the naked mole-rat (Heterocephalus glaber). Aging Cell. 2010;9(4):626–35.

9. Buffenstein R, Jarvis JUM. The Naked Mole Rat--A New Record for the Oldest Living Rodent. Sci Aging Knowl Environ. 2002 May 29;2002(21):pe7–pe7.

10. Delaney MA, Ward JM, Walsh TF, Chinnadurai SK, Kerns K, Kinsel MJ, et al. Initial Case Reports of Cancer in Naked Mole-rats (Heterocephalus glaber). Vet Pathol. 2016 May;53(3):691–6.

11. Barton AA. Some aspects of cell division in saccharomyces cerevisiae. J Gen Microbiol. 1950 Jan;4(1):84–6.

12. Bitterman KJ, Medvedik O, Sinclair DA. Longevity regulation in Saccharomyces cerevisiae: linking metabolism, genome stability, and heterochromatin. Microbiol Mol Biol Rev MMBR. 2003 Sep;67(3):376–99, table of contents.

13. Steinkraus KA, Kaeberlein M, Kennedy BK. Replicative aging in yeast: the means to the end. Annu Rev Cell Dev Biol. 2008;24:29–54.

14. Kaeberlein M. Lessons on longevity from budding yeast. Nature. 2010 Mar 25;464(7288):513–9.

15. Mortimer RK, Johnston JR. Life Span of Individual Yeast Cells. Nature. 1959 Jun;183(4677):1751–2.

16. Kennedy BK, Austriaco NR, Guarente L. Daughter cells of Saccharomyces cerevisiae from old mothers display a reduced life span. J Cell Biol. 1994 Dec;127(6 Pt 2):1985–93.

17. Egilmez NK, Jazwinski SM. Evidence for the involvement of a cytoplasmic factor in the aging of the yeast Saccharomyces cerevisiae. J Bacteriol. 1989 Jan;171(1):37–42.

18. McMurray MA. An Age-Induced Switch to a Hyper-Recombinational State. Science. 2003 Sep 26;301(5641):1908–11.

19. Lee SS, Avalos Vizcarra I, Huberts DHEW, Lee LP, Heinemann M. Whole lifespan microscopic observation of budding yeast aging through a microfluidic dissection platform. Proc Natl Acad Sci U S A. 2012 Mar 27;109(13):4916–20.

20. Xie Z, Zhang Y, Zou K, Brandman O, Luo C, Ouyang Q, et al. Molecular phenotyping of aging in single yeast cells using a novel microfluidic device. Aging Cell. 2012 Aug;11(4):599–606.

21. Sinclair DA, Guarente L. Extrachromosomal rDNA Circles— A Cause of Aging in Yeast. Cell. 1997 Dec 26;91(7):1033–42.

22. Barros MH, Bandy B, Tahara EB, Kowaltowski AJ. Higher Respiratory Activity Decreases Mitochondrial Reactive Oxygen Release and Increases Life Span in Saccharomyces cerevisiae*. J Biol Chem. 2004 Nov 26;279(48):49883–8.

23. Qin H, Lu M. Natural variation in replicative and chronological life spans of Saccharomyces cerevisiae. Exp Gerontol. 2006 Apr 1;41(4):448–56.

24. Lindstrom DL, Leverich CK, Henderson KA, Gottschling DE. Replicative Age Induces Mitotic Recombination in the Ribosomal RNA Gene Cluster of Saccharomyces cerevisiae. PLOS Genet. 2011 Mar 17;7(3):e1002015.

25. Hu Z, Chen K, Xia Z, Chavez M, Pal S, Seol JH, et al. Nucleosome loss leads to global transcriptional up-regulation and genomic instability during yeast aging. Genes Dev. 2014 Feb 15;28(4):396–408.

26. Herbig U, Jobling WA, Chen BPC, Chen DJ, Sedivy JM. Telomere Shortening Triggers Senescence of Human Cells through a Pathway Involving ATM, p53, and p21CIP1, but Not p16INK4a. Mol Cell. 2004 May 21;14(4):501–13.

27. King GA, Goodman JS, Schick JG, Chetlapalli K, Jorgens DM, McDonald KL, et al. Meiotic cellular rejuvenation is coupled to nuclear remodeling in budding yeast. Mizushima N, Malhotra V, Mizushima N, Haraguchi T, Lusk CP, editors. eLife. 2019 Aug 9;8:e47156.

28. Koch BA, Staley E, Jin H, Yu HG. The ESCRT-III complex is required for nuclear pore complex sequestration and regulates gamete replicative lifespan in budding yeast meiosis. Nucleus. 2020 Jan 1;11(1):219–36.

29. Carmona-Gutierrez D, Büttner S. The many ways to age for a single yeast cell: Ageing paradigms in yeast. Yeast. 2014 Aug;31(8):289–98.

30. Mirisola MG, Braun RJ, Petranovic D. Approaches to study yeast cell aging and death. FEMS Yeast Res. 2014 Feb;14(1):109–18.

31. Bishop NA, Guarente L. Genetic links between diet and lifespan: shared mechanisms from yeast to humans. Nat Rev Genet. 2007 Nov;8(11):835–44.

32. Wasko BM, Kaeberlein M. Yeast replicative aging: a paradigm for defining conserved longevity interventions. FEMS Yeast Res. 2014 Feb 1;14(1):148–59.

33. Spadaro O, Youm Y, Shchukina I, Ryu S, Sidorov S, Ravussin A, et al. Caloric restriction in humans reveals immunometabolic regulators of health span. Science. 2022 Feb 11;375(6581):671–7.

34. Simon JA, Bedalov A. Yeast as a model system for anticancer drug discovery. Nat Rev Cancer. 2004 Jun;4(6):481–92.

35. López-Otín C, Blasco MA, Partridge L, Serrano M, Kroemer G. The Hallmarks of Aging. Cell. 2013 Jun 6;153(6):1194–217.

36. Dahiya R, Mohammad T, Alajmi MF, Rehman MdT, Hasan GM, Hussain A, et al. Insights into the Conserved Regulatory Mechanisms of Human and Yeast Aging. Biomolecules. 2020 Jun 9;10(6):882.

37. Moskalev AA, Shaposhnikov MV, Plyusnina EN, Zhavoronkov A, Budovsky A, Yanai H, et al. The role of DNA damage and repair in aging through the prism of Koch-like criteria. Ageing Res Rev. 2013 Mar;12(2):661–84.

38. Young TZ, Liu P, Urbonaite G, Acar M. Quantitative Insights into Age-Associated DNA-Repair Inefficiency in Single Cells. Cell Rep. 2019 Aug 20;28(8):2220-2230.e7.

39. Kirkwood TBL. Understanding the Odd Science of Aging. Cell. 2005 Feb 25;120(4):437–47.

40. Burtner CR, Kennedy BK. Progeria syndromes and ageing: what is the connection? Nat Rev Mol Cell Biol. 2010 Aug;11(8):567–78.

41. Dechat T, Pfleghaar K, Sengupta K, Shimi T, Shumaker DK, Solimando L, et al. Nuclear lamins: major factors in the structural organization and function of the nucleus and chromatin. Genes Dev. 2008 Apr 1;22(7):832–53.

42. Liu B, Wang J, Chan KM, Tjia WM, Deng W, Guan X, et al. Genomic instability in laminopathy-based premature aging. Nat Med. 2005 Jul;11(7):780–5.

43. Armanios M, Alder JK, Parry EM, Karim B, Strong MA, Greider CW. Short Telomeres are Sufficient to Cause the Degenerative Defects Associated with Aging. Am J Hum Genet. 2009 Dec 11;85(6):823–32.

44. Tsurumi A, Li WX. Global heterochromatin loss: a unifying theory of aging? Epigenetics. 2012 Jul;7(7):680–8.

45. Kennedy BK, Gotta M, Sinclair DA, Mills K, McNabb DS, Murthy M, et al. Redistribution of Silencing Proteins from Telomeres to the Nucleolus Is Associated with Extension of Life Span in S. cerevisiae. Cell. 1997 May;89(3):381–91.

46. Harries LW, Hernandez D, Henley W, Wood AR, Holly AC, Bradley-Smith RM, et al. Human aging is characterized by focused changes in gene expression and deregulation of alternative splicing. Aging Cell. 2011;10(5):868–78.

47. Powers ET, Morimoto RI, Dillin A, Kelly JW, Balch WE. Biological and Chemical Approaches to Diseases of Proteostasis Deficiency. Annu Rev Biochem. 2009 Jun 1;78(1):959–91.

48. Koga H, Kaushik S, Cuervo AM. Protein homeostasis and aging: The importance of exquisite quality control. Ageing Res Rev. 2011 Apr 1;10(2):205–15.

49. Fontana L, Partridge L, Longo VD. Extending healthy life span--from yeast to humans. Science. 2010 Apr 16;328(5976):321–6.

50. Johnson SC, Rabinovitch PS, Kaeberlein M. mTOR is a key modulator of ageing and age-related disease. Nature. 2013 Jan;493(7432):338–45.

51. Powers RW, Kaeberlein M, Caldwell SD, Kennedy BK, Fields S. Extension of chronological life span in yeast by decreased TOR pathway signaling. Genes Dev. 2006 Jan 15;20(2):174–84.

52. Delaney JR, Murakami CJ, Olsen B, Kennedy BK, Kaeberlein M. Quantitative evidence for early life fitness defects from 32 longevity-associated alleles in yeast. Cell Cycle. 2011 Jan;10(1):156–65.

53. Green DR, Galluzzi L, Kroemer G. Mitochondria and the Autophagy–Inflammation–Cell Death Axis in Organismal Aging. Science. 2011 Aug 26;333(6046):1109–12.

54. Wallace DC, Fan W, Procaccio V. Mitochondrial Energetics and Therapeutics. Annu Rev Pathol. 2010;5:297–348.

55. Liguori I, Russo G, Curcio F, Bulli G, Aran L, Della-Morte D, et al. Oxidative stress, aging, and diseases. Clin Interv Aging. 2018 Apr 26;13:757–72.

56. Pernice WM, Vevea JD, Pon LA. A role for Mfb1p in region-specific anchorage of high-functioning mitochondria and lifespan in Saccharomyces cerevisiae. Nat Commun. 2016 Feb 3;7(1):10595.

57. Wang C, Jurk D, Maddick M, Nelson G, Martin-Ruiz C, Von Zglinicki T. DNA damage response and cellular senescence in tissues of aging mice. Aging Cell. 2009;8(3):311–23.

58. Flores I, Cayuela ML, Blasco MA. Effects of Telomerase and Telomere Length on Epidermal Stem Cell Behavior. Science. 2005 Aug 19;309(5738):1253–6.

59. Rossi DJ, Bryder D, Seita J, Nussenzweig A, Hoeijmakers J, Weissman IL. Deficiencies in DNA damage repair limit the function of haematopoietic stem cells with age. Nature. 2007 Jun;447(7145):725–9.

60. Barzilai N, Huffman DM, Muzumdar RH, Bartke A. The Critical Role of Metabolic Pathways in Aging. Diabetes. 2012 May 14;61(6):1315–22.

61. Deeks SG. HIV Infection, Inflammation, Immunosenescence, and Aging. Annu Rev Med. 2011;62:141–55.

62. Smeal T, Claus J, Kennedy B, Cole F, Guarente L. Loss of Transcriptional Silencing Causes Sterility in Old Mother Cells of S. cerevisiae. Cell. 1996 Feb;84(4):633–42.

63. Mei SC, Brenner C. Calorie Restriction-Mediated Replicative Lifespan Extension in Yeast Is Non-Cell Autonomous. PLoS Biol. 2015 Jan 29;13(1):e1002048.

64. Garinis GA, van der Horst GTJ, Vijg J, Hoeijmakers JHJ. DNA damage and ageing: new-age ideas for an age-old problem. Nat Cell Biol. 2008 Nov;10(11):1241–7.

65. Gordon LB, Rothman FG, López-Otín C, Misteli T. Progeria: A Paradigm for Translational Medicine. Cell. 2014 Jan;156(3):400–7.

66. Puzianowska-Kuznicka M, Kuznicki J. Genetic alterations in accelerated ageing syndromes: Do they play a role in natural ageing? Int J Biochem Cell Biol. 2005 May 1;37(5):947–60.

67. Tan WH, Baris H, Robson CD, Kimonis VE. Cockayne syndrome: The developing phenotype. Am J Med Genet A. 2005;135A(2):214–6.

68. Huang S, Lee L, Hanson NB, Lenaerts C, Hoehn H, Poot M, et al. The spectrum of WRN mutations in Werner syndrome patients. Hum Mutat. 2006;27(6):558–67.

69. Ellis NA, Sander M, Harris CC, Bohr VA. Bloom's syndrome workshop focuses on the functional specificities of RecQ helicases. Mech Ageing Dev. 2008 Nov 1;129(11):681–91.

70. Sahin E, DePinho RA. Linking functional decline of telomeres, mitochondria and stem cells during ageing. Nature. 2010 Mar;464(7288):520–8.

71. Gonzalo S, Kreienkamp R. DNA repair defects and genome instability in Hutchinson–Gilford Progeria Syndrome. Curr Opin Cell Biol. 2015 Jun;34:75–83.

72. Scaffidi P, Misteli T. Reversal of the cellular phenotype in the premature aging disease Hutchinson-Gilford progeria syndrome. Nat Med. 2005 Apr;11(4):440–5.

73. Camozzi D, Capanni C, Cenni V, Mattioli E, Columbaro M, Squarzoni S, et al. Diverse lamin-dependent mechanisms interact to control chromatin dynamics. Nucleus. 2014 Sep 1;5(5):427–40.

74. Carrero D, Soria-Valles C, López-Otín C. Hallmarks of progeroid syndromes: lessons from mice and reprogrammed cells. Dis Model Mech. 2016 Jul 1;9(7):719–35.

75. Navarro CL, Cau P, Lévy N. Molecular bases of progeroid syndromes. Hum Mol Genet. 2006 Oct 15;15(suppl_2):R151–61.

76. McVey M, Kaeberlein M, Tissenbaum HA, Guarente L. The short life span of Saccharomyces cerevisiae sgs1 and srs2 mutants is a composite of normal aging processes and mitotic arrest due to defective recombination. Genetics. 2001 Apr;157(4):1531–42.

77. Bochman ML, Paeschke K, Chan A, Zakian VA. Hrq1, a homolog of the human RecQ4 helicase, acts catalytically and structurally to promote genome integrity. Cell Rep. 2014 Jan 30;6(2):346–56.

78. Gorbunova V, Seluanov A, Mao Z, Hine C. Changes in DNA repair during aging. Nucleic Acids Res. 2007;35(22):7466–74.

79. Sedelnikova OA, Horikawa I, Zimonjic DB, Popescu NC, Bonner WM, Barrett JC. Senescing human cells and ageing mice accumulate DNA lesions with unrepairable double-strand breaks. Nat Cell Biol. 2004 Feb;6(2):168–70.

80. Wang J, Clauson CL, Robbins PD, Niedernhofer LJ, Wang Y. The oxidative DNA lesions 8,5'-cyclopurines accumulate with aging in a tissue-specific manner. Aging Cell. 2012 Aug;11(4):714–6.

81. Niedernhofer LJ, Gurkar AU, Wang Y, Vijg J, Hoeijmakers JHJ, Robbins PD. Nuclear Genomic Instability and Aging. Annu Rev Biochem. 2018;87(1):295–322.

82. Armstrong GT, Kawashima T, Leisenring W, Stratton K, Stovall M, Hudson MM, et al. Aging and Risk of Severe, Disabling, Life-Threatening, and Fatal Events in the Childhood Cancer Survivor Study. J Clin Oncol. 2014 Apr 20;32(12):1218–27.

83. Novarina D, Mavrova SN, Janssens GE, Rempel IL, Veenhoff LM, Chang M. Increased genome instability is not accompanied by sensitivity to DNA damaging agents in aged yeast cells. DNA Repair. 2017 Jun 1;54:1–7.

84. Patterson MN, Scannapieco AE, Au PH, Dorsey S, Royer CA, Maxwell PH. Preferential retrotransposition in aging yeast mother cells is correlated with increased genome instability. DNA Repair. 2015 Oct 1;34:18–27.

85. Kale SP, Jazwinski SM. Differential response to UV stress and DNA damage during the yeast replicative life span. Dev Genet. 1996;18(2):154–60.

86. Ramsey MJ, Moore DH, Briner JF, Lee DA, Olsen LA, Senft JR, et al. The effects of age and lifestyle factors on the accumulation of cytogenetic damage as measured by chromosome painting. Mutat Res. 1995 Oct;338(1–6):95–106.

87. Johnson TE, Henderson S, Murakami S, de Castro E, de Castro SH, Cypser J, et al. Longevity genes in the nematode Caenorhabditis elegans also mediate increased resistance to stress and prevent disease. J Inherit Metab Dis. 2002 May;25(3):197–206.

88. Kaeberlein M, Kirkland KT, Fields S, Kennedy BK. Genes determining yeast replicative life span in a long-lived genetic background. Mech Ageing Dev. 2005 Apr;126(4):491–504.

89. Defossez PA, Prusty R, Kaeberlein M, Lin SJ, Ferrigno P, Silver PA, et al. Elimination of Replication Block Protein Fob1 Extends the Life Span of Yeast Mother Cells. Mol Cell. 1999 Apr 1;3(4):447–55.

90. Kaeberlein M, McVey M, Guarente L. The SIR2/3/4 complex and SIR2 alone promote longevity in Saccharomyces cerevisiae by two different mechanisms. Genes Dev. 1999 Oct 1;13(19):2570–80.

91. Lin SJ, Defossez PA, Guarente L. Requirement of NAD and SIR2 for life-span extension by calorie restriction in Saccharomyces cerevisiae. Science. 2000 Sep 22;289(5487):2126–8.

92. Warmerdam DO, Wolthuis RMF. Keeping ribosomal DNA intact: a repeating challenge. Chromosome Res Int J Mol Supramol Evol Asp Chromosome Biol. 2019 Mar;27(1–2):57–72.

93. Kasselimi E, Pefani DE, Taraviras S, Lygerou Z. Ribosomal DNA and the nucleolus at the heart of aging. Trends Biochem Sci. 2022 Apr;47(4):328–41.

94. Hein N, Sanij E, Quin J, M. K, Ganley A, D. R. The Nucleolus and Ribosomal Genes in Aging and Senescence. In: Nagata T, editor. Senescence [Internet]. InTech; 2012 [cited 2022 Nov 22]. Available from: http://www.intechopen.com/books/senescence/the-nucleolus-in-aging-and-senescence-

95. Kobayashi T. A new role of the rDNA and nucleolus in the nucleus--rDNA instability maintains genome integrity. BioEssays News Rev Mol Cell Dev Biol. 2008 Mar;30(3):267–72.

96. Klar AJS, Fogel S, Macleod K. MAR1—A REGULATOR OF THE HM a AND HMα LOCI IN SACCHAROMYCES CEREVISIAE. Genetics. 1979 Sep 1;93(1):37–50.

97. Gottschling DE, Aparicio OM, Billington BL, Zakian VA. Position effect at S. cerevisiae telomeres: reversible repression of Pol II transcription. Cell. 1990 Nov 16;63(4):751–62.

98. Ganley ARD, Kobayashi T. Ribosomal DNA and cellular senescence: new evidence supporting the connection between rDNA and aging. FEMS Yeast Res. 2014 Feb;14(1):49–59.

99. Pal S, Postnikoff SD, Chavez M, Tyler JK. Impaired cohesion and homologous recombination during replicative aging in budding yeast. Sci Adv. 2018 Feb;4(2):eaaq0236.

100. Foss EJ, Gatbonton-Schwager T, Thiesen AH, Taylor E, Soriano R, Lao U, et al. Sir2 suppresses transcription-mediated displacement of Mcm2-7 replicative helicases at the ribosomal DNA repeats. PLoS Genet [Internet]. 2019 May 13 [cited 2020 Dec 3];15(5). Available from: https://www.ncbi.nlm.nih.gov/pmc/articles/PMC6532929/

101. Kennedy BK, Austriaco NR, Zhang J, Guarente L. Mutation in the silencing gene S/R4 can delay aging in S. cerevisiae. Cell. 1995 Feb 10;80(3):485–96.

102. Kobayashi T, Heck DJ, Nomura M, Horiuchi T. Expansion and contraction of ribosomal DNA repeats in Saccharomyces cerevisiae: requirement of replication fork blocking (Fob1) protein and the role of RNA polymerase I. Genes Dev. 1998 Dec 15;12(24):3821–30.

103. Sinclair DA, Mills K, Guarente L. Molecular mechanisms of yeast aging. Trends Biochem Sci. 1998 Apr;23(4):131–4.

104. Hauer MH, Gasser SM. Chromatin and nucleosome dynamics in DNA damage and repair. Genes Dev. 2017 Nov 15;31(22):2204–21.

105. Feser J, Tyler J. Chromatin structure as a mediator of aging. FEBS Lett. 2011 Jul 7;585(13):2041–8.

106. Suka N, Luo K, Grunstein M. Sir2p and Sas2p opposingly regulate acetylation of yeast histone H4 lysine16 and spreading of heterochromatin. Nat Genet. 2002 Nov;32(3):378–83.

107. Dang W, Steffen KK, Perry R, Dorsey JA, Johnson FB, Shilatifard A, et al. Histone H4 lysine 16 acetylation regulates cellular lifespan. Nature. 2009 Jun;459(7248):802–7.

108. Feser J, Truong D, Das C, Carson JJ, Kieft J, Harkness T, et al. Elevated Histone Expression Promotes Life Span Extension. Mol Cell. 2010 Sep;39(5):724–35.

109. Bormann F, Rodríguez-Paredes M, Hagemann S, Manchanda H, Kristof B, Gutekunst J, et al. Reduced DNA methylation patterning and transcriptional connectivity define human skin aging. Aging Cell. 2016 Jun;15(3):563–71.

110. Kaushik S, Cuervo AM. Proteostasis and aging. Nat Med. 2015 Dec;21(12):1406–15.

111. Ben-Zvi A, Miller EA, Morimoto RI. Collapse of proteostasis represents an early molecular event in Caenorhabditis elegans aging. Proc Natl Acad Sci. 2009 Sep;106(35):14914–9.

112. Hipp MS, Kasturi P, Hartl FU. The proteostasis network and its decline in ageing. Nat Rev Mol Cell Biol. 2019 Jul;20(7):421–35.

113. Yang L, Cao Y, Zhao J, Fang Y, Liu N, Zhang Y. Multidimensional Proteomics Identifies Declines in Protein Homeostasis and Mitochondria as Early Signals for Normal Aging and Age-associated Disease in Drosophila*, [S]. Mol Cell Proteomics. 2019 Oct 1;18(10):2078–88.

114. Hu Z, Xia B, Postnikoff SD, Shen ZJ, Tomoiaga AS, Harkness TA, et al. Ssd1 and Gcn2 suppress global translation efficiency in replicatively aged yeast while their activation extends lifespan. eLife. 2018;7:e35551.

115. Anisimova AS, Alexandrov AI, Makarova NE, Gladyshev VN, Dmitriev SE. Protein synthesis and quality control in aging. Aging. 2018 Dec 18;10(12):4269–88.

116. Söti C, Csermely P. Chaperones and aging: role in neurodegeneration and in other civilizational diseases. Neurochem Int. 2002 Dec;41(6):383–9.

117. Sőti C, Csermely P. Aging and molecular chaperones. Exp Gerontol. 2003 Oct 1;38(10):1037–40.

118. Walther DM, Kasturi P, Zheng M, Pinkert S, Vecchi G, Ciryam P, et al. Widespread Proteome Remodeling and Aggregation in Aging C. elegans. Cell. 2015 May 7;161(4):919–32.

119. Basisty N, Meyer JG, Schilling B. Protein Turnover in Aging and Longevity. Proteomics. 2018 Mar;18(5–6):e1700108.

120. Tatar M, Khazaeli AA, Curtsinger JW. Chaperoning extended life. Nature. 1997 Nov;390(6655):30–30.

121. Postnikoff SDL, Johnson JE, Tyler JK. The integrated stress response in budding yeast lifespan extension. Microb Cell. 2017;4(11):368–75.

122. Berner N, Reutter KR, Wolf DH. Protein Quality Control of the Endoplasmic Reticulum and Ubiquitin-Proteasome-Triggered Degradation of Aberrant Proteins: Yeast Pioneers the Path. Annu Rev Biochem. 2018 Jun 20;87:751–82.

123. Walter P, Ron D. The unfolded protein response: from stress pathway to homeostatic regulation. Science. 2011 Nov 25;334(6059):1081–6.

124. Calderwood SK, Murshid A, Prince T. The shock of aging: molecular chaperones and the heat shock response in longevity and aging--a mini-review. Gerontology. 2009;55(5):550–8.

125. Farrugia G, Balzan R. Oxidative Stress and Programmed Cell Death in Yeast. Front Oncol. 2012 Jun 21;2:64.

126. Zhou C, Slaughter BD, Unruh JR, Eldakak A, Rubinstein B, Li R. Motility and Segregation of Hsp104-Associated Protein Aggregates in Budding Yeast. Cell. 2011 Nov 23;147(5):1186–96.

127. Zhou C, Slaughter BD, Unruh JR, Guo F, Yu Z, Mickey K, et al. Organelle-Based Aggregation and Retention of Damaged Proteins in Asymmetrically Dividing Cells. Cell. 2014 Oct 23;159(3):530–42.

128. Morimoto RI, Cuervo AM. Proteostasis and the aging proteome in health and disease. J Gerontol A Biol Sci Med Sci. 2014 Jun;69 Suppl 1:S33-38.

129. Marks AB, Fu H, Aladjem MI. Regulation of Replication Origins. Adv Exp Med Biol. 2017;1042:43–59.

130. Kornberg RD. Chromatin structure: a repeating unit of histones and DNA. Science. 1974 May 24;184(4139):868–71.

131. Luger K, Mäder AW, Richmond RK, Sargent DF, Richmond TJ. Crystal structure of the nucleosome core particle at 2.8 A resolution. Nature. 1997 Sep 18;389(6648):251–60.

132. Ekundayo B, Bleichert F. Origins of DNA replication. PLoS Genet. 2019 Sep 12;15(9):e1008320.

133. Vashee S, Cvetic C, Lu W, Simancek P, Kelly TJ, Walter JC. Sequence-independent DNA binding and replication initiation by the human origin recognition complex. Genes Dev. 2003 Aug 1;17(15):1894–908.

134. Aladjem MI, Redon CE. Order from clutter: selective interactions at mammalian replication origins. Nat Rev Genet. 2017 Feb;18(2):101–16.

135. Kelly T, Callegari AJ. Dynamics of DNA replication in a eukaryotic cell. Proc Natl Acad Sci U S A. 2019 Mar 12;116(11):4973–82.

136. Nieduszynski CA, Hiraga S ichiro, Ak P, Benham CJ, Donaldson AD. OriDB: a DNA replication origin database. Nucleic Acids Res. 2007 Jan;35(suppl_1):D40–6.

137. Ge XQ, Jackson DA, Blow JJ. Dormant origins licensed by excess Mcm2-7 are required for human cells to survive replicative stress. Genes Dev. 2007 Dec 15;21(24):3331–41.

138. Ibarra A, Schwob E, Méndez J. Excess MCM proteins protect human cells from replicative stress by licensing backup origins of replication. Proc Natl Acad Sci U S A. 2008 Jul 1;105(26):8956–61.

139. Diffley JFX. Regulation of early events in chromosome replication. Curr Biol CB. 2004 Sep 21;14(18):R778-786.

140. Remus D, Diffley JFX. Eukaryotic DNA replication control: lock and load, then fire. Curr Opin Cell Biol. 2009 Dec;21(6):771–7.

141. Bleichert F, Botchan MR, Berger JM. Mechanisms for initiating cellular DNA replication. Science. 2017 Feb 24;355(6327):eaah6317.

142. Sheu YJ, Stillman B. Cdc7-Dbf4 phosphorylates MCM proteins via a docking site-mediated mechanism to promote S phase progression. Mol Cell. 2006 Oct 6;24(1):101–13.

143. Francis LI, Randell JCW, Takara TJ, Uchima L, Bell SP. Incorporation into the prereplicative complex activates the Mcm2-7 helicase for Cdc7-Dbf4 phosphorylation. Genes Dev. 2009 Mar 1;23(5):643–54.

144. Sun J, Fernandez-Cid A, Riera A, Tognetti S, Yuan Z, Stillman B, et al. Structural and mechanistic insights into Mcm2-7 double-hexamer assembly and function. Genes Dev. 2014 Oct 15;28(20):2291–303.

145. Zegerman P, Diffley JFX. Phosphorylation of Sld2 and Sld3 by cyclin-dependent kinases promotes DNA replication in budding yeast. Nature. 2007 Jan 18;445(7125):281–5.

146. Deegan TD, Yeeles JT, Diffley JF. Phosphopeptide binding by Sld3 links Dbf4-dependent kinase to MCM replicative helicase activation. EMBO J. 2016 May 2;35(9):961–73.

147. Fang D, Cao Q, Lou H. Sld3-MCM Interaction Facilitated by Dbf4-Dependent Kinase Defines an Essential Step in Eukaryotic DNA Replication Initiation. Front Microbiol. 2016;7:885.

148. Abid Ali F, Costa A. The MCM Helicase Motor of the Eukaryotic Replisome. J Mol Biol. 2016 May 8;428(9 Pt B):1822–32.

149. Lindahl T, Barnes DE. Repair of endogenous DNA damage. Cold Spring Harb Symp Quant Biol. 2000;65:127–33.

150. Malkova A, Haber JE. Mutations Arising During Repair of Chromosome Breaks. Annu Rev Genet. 2012 Dec 15;46(1):455–73.

151. Hoeijmakers JHJ. DNA repair mechanisms. Maturitas. 2001 Feb 28;38(1):17–22.

152. Chatterjee N, Walker GC. Mechanisms of DNA damage, repair and mutagenesis. Environ Mol Mutagen. 2017 Jun;58(5):235–63.

153. Jackson SP. Sensing and repairing DNA double-strand breaks. Carcinogenesis. 2002 May 1;23(5):687–96.

154. Pierce AJ, Stark JM, Araujo FD, Moynahan ME, Berwick M, Jasin M. Double-strand breaks and tumorigenesis. Trends Cell Biol. 2001 Nov;11(11):S52-59.

155. McKinnon PJ, Caldecott KW. DNA Strand Break Repair and Human Genetic Disease. Annu Rev Genomics Hum Genet. 2007 Sep 1;8(1):37–55.

156. Lieber MR. The mechanism of double-strand DNA break repair by the nonhomologous DNA end-joining pathway. Annu Rev Biochem. 2010;79:181–211.

157. Wang C, Lees-Miller SP. Detection and repair of ionizing radiation-induced DNA double strand breaks: new developments in nonhomologous end joining. Int J Radiat Oncol Biol Phys. 2013 Jul 1;86(3):440–9.

158. Zhao X, Wei C, Li J, Xing P, Li J, Zheng S, et al. Cell cycle-dependent control of homologous recombination. Acta Biochim Biophys Sin. 2017 Aug 1;49(8):655–68.

159. Mimitou EP, Symington LS. Ku prevents Exo1 and Sgs1-dependent resection of DNA ends in the absence of a functional MRX complex or Sae2. EMBO J. 2010 Oct 6;29(19):3358–69.

160. Lisby M, Barlow JH, Burgess RC, Rothstein R. Choreography of the DNA Damage Response: Spatiotemporal Relationships among Checkpoint and Repair Proteins. Cell. 2004 Sep 17;118(6):699–713.

161. Symington LS. End resection at double-strand breaks: mechanism and regulation. Cold Spring Harb Perspect Biol. 2014 Aug 1;6(8):a016436.

162. Gobbini E, Cesena D, Galbiati A, Lockhart A, Longhese MP. Interplays between ATM/Tel1 and ATR/Mec1 in sensing and signaling DNA double-strand breaks. DNA Repair. 2013 Oct 1;12(10):791–9.

163. Walker JR, Corpina RA, Goldberg J. Structure of the Ku heterodimer bound to DNA and its implications for double-strand break repair. Nature. 2001 Aug;412(6847):607–14.

164. Clerici M, Mantiero D, Guerini I, Lucchini G, Longhese MP. The Yku70-Yku80 complex contributes to regulate double-strand break processing and checkpoint activation during the cell cycle. EMBO Rep. 2008 Aug;9(8):810–8.

165. Wilson TE, Grawunder U, Lieber MR. Yeast DNA ligase IV mediates non-homologous DNA end joining. Nature. 1997 Jul 31;388(6641):495–8.

166. Herrmann G, Lindahl T, Schär P. Saccharomyces cerevisiae LIF1: a function involved in DNA double-strand break repair related to mammalian XRCC4. EMBO J. 1998 Jul 15;17(14):4188–98.

167. Zhang Y, Hefferin ML, Chen L, Shim EY, Tseng HM, Kwon Y, et al. Role of Dnl4-Lif1 in nonhomologous end-joining repair complex assembly and suppression of homologous recombination. Nat Struct Mol Biol. 2007 Jul;14(7):639–46.

168. Ooi SL, Shoemaker DD, Boeke JD. A DNA microarray-based genetic screen for nonhomologous end-joining mutants in Saccharomyces cerevisiae. Science. 2001 Dec 21;294(5551):2552–6.

169. Wu D, Topper LM, Wilson TE. Recruitment and Dissociation of Nonhomologous End Joining Proteins at a DNA Double-Strand Break in Saccharomyces cerevisiae. Genetics. 2008 Mar;178(3):1237–49.

170. Chen X, Tomkinson AE. Yeast Nej1 is a key participant in the initial end binding and final ligation steps of nonhomologous end joining. J Biol Chem. 2011 Feb 11;286(6):4931–40.

171. Bebenek K, Garcia-Diaz M, Patishall SR, Kunkel TA. Biochemical properties of Saccharomyces cerevisiae DNA polymerase IV. J Biol Chem. 2005 May 20;280(20):20051–8.

172. McKinney JS, Sethi S, Tripp JD, Nguyen TN, Sanderson BA, Westmoreland JW, et al. A multistep genomic screen identifies new genes required for repair of DNA double-strand breaks in Saccharomyces cerevisiae. BMC Genomics. 2013 Apr 15;14:251.

173. Jessulat M, Malty RH, Nguyen-Tran DH, Deineko V, Aoki H, Vlasblom J, et al. Spindle Checkpoint Factors Bub1 and Bub2 Promote DNA Double-Strand Break Repair by Nonhomologous End Joining. Mol Cell Biol. 2015 Jul;35(14):2448–63.

174. Guirouilh-Barbat J, Lambert S, Bertrand P, Lopez BS. Is homologous recombination really an error-free process? Front Genet. 2014;5:175.

175. Hicks WM, Kim M, Haber JE. Increased mutagenesis and unique mutation signature associated with mitotic gene conversion. Science. 2010 Jul 2;329(5987):82–5.

176. Rodgers K, McVey M. Error-Prone Repair of DNA Double-Strand Breaks. J Cell Physiol. 2016 Jan;231(1):15–24.

177. Her J, Bunting SF. How cells ensure correct repair of DNA double-strand breaks. J Biol Chem. 2018 Jul 6;293(27):10502–11.

178. McVey M, Khodaverdian VY, Meyer D, Cerqueira PG, Heyer WD. Eukaryotic DNA Polymerases in Homologous Recombination. Annu Rev Genet. 2016 Nov 23;50:393–421.

179. Symington LS, Gautier J. Double-strand break end resection and repair pathway choice. Annu Rev Genet. 2011;45:247–71.

180. Daley JM, Niu H, Miller AS, Sung P. Biochemical mechanism of DSB end resection and its regulation. DNA Repair. 2015 Aug;32:66–74.

181. Gobbini E, Cassani C, Villa M, Bonetti D, Longhese MP. Functions and regulation of the MRX complex at DNA double-strand breaks. Microb Cell. 3(8):329–37.

182. Wasko BM, Holland CL, Resnick MA, Lewis LK. Inhibition of DNA double-strand break repair by the Ku heterodimer in mrx mutants of Saccharomyces cerevisiae. DNA Repair. 2009 Feb 1;8(2):162–9.

183. Balestrini A, Ristic D, Dionne I, Liu XZ, Wyman C, Wellinger RJ, et al. The Ku heterodimer and the metabolism of single-ended DNA double-strand breaks. Cell Rep. 2013 Jun 27;3(6):2033–45.

184. Mimitou EP, Symington LS. Sae2, Exo1 and Sgs1 collaborate in DNA double-strand break processing. Nature. 2008 Oct 9;455(7214):10.1038/nature07312.

185. Ghodke I, Muniyappa K. Processing of DNA double-stranded breaks and intermediates of recombination and repair by Saccharomyces cerevisiae Mre11 and its stimulation by Rad50, Xrs2, and Sae2 proteins. J Biol Chem. 2013 Apr 19;288(16):11273–86.

186. Trujillo KM, Sung P. DNA structure-specific nuclease activities in the Saccharomyces cerevisiae Rad50*Mre11 complex. J Biol Chem. 2001 Sep 21;276(38):35458–64.

187. Zhu Z, Chung WH, Shim EY, Lee SE, Ira G. Sgs1 helicase and two nucleases Dna2 and Exo1 resect DNA double strand break ends. Cell. 2008 Sep 19;134(6):981–94.

188. Shim EY, Chung WH, Nicolette ML, Zhang Y, Davis M, Zhu Z, et al. Saccharomyces cerevisiae Mre11/Rad50/Xrs2 and Ku proteins regulate association of Exo1 and Dna2 with DNA breaks. EMBO J. 2010 Oct 6;29(19):3370–80.

189. Cejka P, Cannavo E, Polaczek P, Masuda-Sasa T, Pokharel S, Campbell JL, et al. DNA end resection by Dna2-Sgs1-RPA and its stimulation by Top3-Rmi1 and Mre11-Rad50-Xrs2. Nature. 2010 Sep 2;467(7311):112–6.

190. Ma JL, Kim EM, Haber JE, Lee SE. Yeast Mre11 and Rad1 Proteins Define a Ku-Independent Mechanism To Repair Double-Strand Breaks Lacking Overlapping End Sequences. Mol Cell Biol. 2003 Dec;23(23):8820–8.

191. Lee K, Lee SE. Saccharomyces cerevisiae Sae2- and Tel1-dependent single-strand DNA formation at DNA break promotes microhomology-mediated end joining. Genetics. 2007 Aug;176(4):2003–14.

192. Bennardo N, Cheng A, Huang N, Stark JM. Alternative-NHEJ is a mechanistically distinct pathway of mammalian chromosome break repair. PLoS Genet. 2008 Jun 27;4(6):e1000110.

193. Scuric Z, Chan CY, Hafer K, Schiestl RH. Ionizing radiation induces microhomology-mediated end joining in trans in yeast and mammalian cells. Radiat Res. 2009 Apr;171(4):454–63.

194. Lee K, Ji JH, Yoon K, Che J, Seol JH, Lee SE, et al. Microhomology Selection for Microhomology Mediated End Joining in Saccharomyces cerevisiae. Genes. 2019 Apr 8;10(4):284.

195. Sugawara N, Ira G, Haber JE. DNA length dependence of the single-strand annealing pathway and the role of Saccharomyces cerevisiae RAD59 in double-strand break repair. Mol Cell Biol. 2000 Jul;20(14):5300–9.

196. Villarreal DD, Lee K, Deem A, Shim EY, Malkova A, Lee SE. Microhomology directs diverse DNA break repair pathways and chromosomal translocations. PLoS Genet. 2012;8(11):e1003026.

197. Ivanov EL, Sugawara N, Fishman-Lobell J, Haber JE. Genetic requirements for the single-strand annealing pathway of double-strand break repair in Saccharomyces cerevisiae. Genetics. 1996 Mar;142(3):693–704.

198. Sakofsky CJ, Malkova A. Break induced replication in eukaryotes: mechanisms, functions, and consequences. Crit Rev Biochem Mol Biol. 2017 Jul 4;52(4):395–413.

199. McEachern MJ, Haber JE. Break-induced replication and recombinational telomere elongation in yeast. Annu Rev Biochem. 2006;75:111–35.

200. Malkova A, Ivanov EL, Haber JE. Double-strand break repair in the absence of RAD51 in yeast: a possible role for break-induced DNA replication. Proc Natl Acad Sci U S A. 1996 Jul 9;93(14):7131–6.

201. Freudenreich CH, Su XA. Relocalization of DNA lesions to the nuclear pore complex. FEMS Yeast Res [Internet]. 2016 Dec 1 [cited 2021 May 3];16(fow095). Available from: https://doi.org/10.1093/femsyr/fow095

202. Ira G, Haber JE. Characterization of RAD51-independent break-induced replication that acts preferentially with short homologous sequences. Mol Cell Biol. 2002 Sep;22(18):6384–92.

203. Lydeard JR, Jain S, Yamaguchi M, Haber JE. Break-induced replication and telomerase-independent telomere maintenance require Pol32. Nature. 2007 Aug 16;448(7155):820–3.

204. Lydeard JR, Lipkin-Moore Z, Sheu YJ, Stillman B, Burgers PM, Haber JE. Break-induced replication requires all essential DNA replication factors except those specific for pre-RC assembly. Genes Dev. 2010 Jun 1;24(11):1133–44.

205. Jain S, Sugawara N, Lydeard J, Vaze M, Tanguy Le Gac N, Haber JE. A recombination execution checkpoint regulates the choice of homologous recombination pathway during DNA double-strand break repair. Genes Dev. 2009 Feb 1;23(3):291–303.

206. Deem A, Keszthelyi A, Blackgrove T, Vayl A, Coffey B, Mathur R, et al. Break-Induced Replication Is Highly Inaccurate. Lichten M, editor. PLoS Biol. 2011 Feb 15;9(2):e1000594.

207. Green BM, Finn KJ, Li JJ. Loss of DNA Replication Control Is a Potent Inducer of Gene Amplification. Science. 2010 Aug 20;329(5994):943–6.

208. Kramara J, Osia B, Malkova A. Break-Induced Replication: The Where, The Why, and The How. Trends Genet. 2018 Jul;34(7):518–31.

209. Shcheprova Z, Baldi S, Frei SB, Gonnet G, Barral Y. A mechanism for asymmetric segregation of age during yeast budding. Nature. 2008 Aug;454(7205):728–34.

210. Karathia H, Vilaprinyo E, Sorribas A, Alves R. Saccharomyces cerevisiae as a Model Organism: A Comparative Study. de Polavieja G, editor. PLoS ONE. 2011 Feb 2;6(2):e16015.

211. Powell CD, Quain DE, Smart KA. Chitin scar breaks in aged Saccharomyces cerevisiae. Microbiol Read Engl. 2003 Nov;149(Pt 11):3129–37.

212. Kaeberlein M, Kennedy BK. Large-scale identification in yeast of conserved ageing genes. Mech Ageing Dev. 2005 Jan;126(1):17–21.

213. Yu R, Jo MC, Dang W. Measuring the replicative lifespan of Saccharomyces cerevisiae using the HYAA microfluidic platform. Methods Mol Biol Clifton NJ. 2020;2144:1–6.

214. Ryley J, Pereira-Smith OM. Microfluidics device for single cell gene expression analysis in Saccharomyces cerevisiae. Yeast Chichester Engl. 2006 Nov;23(14–15):1065–73.

215. Zhang Y, Luo C, Zou K, Xie Z, Brandman O, Ouyang Q, et al. Single Cell Analysis of Yeast Replicative Aging Using a New Generation of Microfluidic Device. PLoS ONE. 2012 Nov 8;7(11):e48275.

216. Liu P, Young TZ, Acar M. Yeast Replicator: A High-Throughput Multiplexed Microfluidics Platform for Automated Measurements of Single-Cell Aging. Cell Rep. 2015 Oct 20;13(3):634–44.

217. Bennett MR, Hasty J. Microfluidic devices for measuring gene network dynamics in single cells. Nat Rev Genet. 2009 Sep;10(9):628–38.

218. Fehrmann S, Paoletti C, Goulev Y, Ungureanu A, Aguilaniu H, Charvin G. Aging Yeast Cells Undergo a Sharp Entry into Senescence Unrelated to the Loss of Mitochondrial Membrane Potential. Cell Rep. 2013 Dec 26;5(6):1589–99.

219. Crane MM, Clark IBN, Bakker E, Smith S, Swain PS. A microfluidic system for studying ageing and dynamic single-cell responses in budding yeast. PloS One. 2014;9(6):e100042.

220. Mehling M, Tay S. Microfluidic cell culture. Curr Opin Biotechnol. 2014 Feb 1;25:95–102.

221. Duncombe TA, Tentori AM, Herr AE. Microfluidics: reframing biological enquiry. Nat Rev Mol Cell Biol. 2015 Sep;16(9):554–67.

222. Jo MC, Liu W, Gu L, Dang W, Qin L. High-throughput analysis of yeast replicative aging using a microfluidic system. Proc Natl Acad Sci U S A. 2015 Jul 28;112(30):9364–9.

223. Jo MC, Qin L. Microfluidic Platforms for Yeast-Based Aging Studies. Small Weinh Bergstr Ger. 2016 Nov;12(42):5787–801.

224. Woldringh CL, Fluiter K, Huls PG. Production of senescent cells of Saccharomyces cerevisiae by centrifugal elutriation. Yeast Chichester Engl. 1995 Apr 15;11(4):361–9.

225. Svenkrtova A, Belicova L, Volejnikova A, Sigler K, Jazwinski SM, Pichova A. Stratification of Yeast Cells during Chronological Aging by Size Points to the Role of Trehalose in Cell Vitality. Biogerontology. 2016 Apr;17(2):395–408.

226. Lesur I, Campbell JL. The Transcriptome of Prematurely Aging Yeast Cells Is Similar to That of Telomerase-deficient Cells. Mol Biol Cell. 2004 Mar;15(3):1297–312.

227. Lindstrom DL, Gottschling DE. The Mother Enrichment Program: A Genetic System for Facile Replicative Life Span Analysis in *Saccharomyces cerevisiae*. Genetics. 2009 Oct;183(2):413–22.

228. Hu Z, Chen K, Xia Z, Chavez M, Pal S, Seol JH, et al. Nucleosome loss leads to global transcriptional up-regulation and genomic instability during yeast aging. Genes Dev. 2014 Feb 15;28(4):396–408.

229. Sinclair DA. Studying the Replicative Life Span of Yeast Cells. In: Tollefsbol TO, editor. Biological Aging [Internet]. Totowa, NJ: Humana Press; 2013 [cited 2020 May 5]. p. 49–63. (Methods in Molecular Biology; vol. 1048). Available from: http://link.springer.com/10.1007/978-1-62703-556-9_5

230. Beas AO, Gordon PB, Prentiss CL, Olsen CP, Kukurugya MA, Bennett BD, et al. Independent regulation of age associated fat accumulation and longevity. Nat Commun. 2020 Jun 3;11(1):2790.

231. Cortez D. Replication-Coupled DNA Repair. Mol Cell. 2019 Jun;74(5):866–76.

232. Siddiqui K, On KF, Diffley JFX. Regulating DNA replication in eukarya. Cold Spring Harb Perspect Biol. 2013 Sep 1;5(9):a012930.

233. Wyrick JJ. Genome-Wide Distribution of ORC and MCM Proteins in S. cerevisiae: High-Resolution Mapping of Replication Origins. Science. 2001 Dec 14;294(5550):2357–60.

234. Shor E, Warren CL, Tietjen J, Hou Z, Müller U, Alborelli I, et al. The Origin Recognition Complex Interacts with a Subset of Metabolic Genes Tightly Linked to Origins of Replication. PLoS Genet. 2009 Dec 4;5(12):e1000755.

235. Eaton ML, Galani K, Kang S, Bell SP, MacAlpine DM. Conserved nucleosome positioning defines replication origins. Genes Dev. 2010 Apr 15;24(8):748–53.

236. McGuffee SR, Smith DJ, Whitehouse I. Quantitative, Genome-Wide Analysis of Eukaryotic Replication Initiation and Termination. Mol Cell. 2013 Apr;50(1):123–35.

237. Stinchcomb DT, Struhl K, Davis RW. Isolation and characterisation of a yeast chromosomal replicator. Nature. 1979 Nov 1;282(5734):39–43.

238. Brewer BJ, Fangman WL. The localization of replication origins on ARS plasmids in S. cerevisiae. Cell. 1987 Nov 6;51(3):463–71.

239. Huberman JA, Spotila LD, Nawotka KA, el-Assouli SM, Davis LR. The in vivo replication origin of the yeast 2 microns plasmid. Cell. 1987 Nov 6;51(3):473–81.

240. Marahrens Y, Stillman B. A yeast chromosomal origin of DNA replication defined by multiple functional elements. Science. 1992 Feb 14;255(5046):817–23.

241. Rao H, Marahrens Y, Stillman B. Functional conservation of multiple elements in yeast chromosomal replicators. Mol Cell Biol. 1994 Nov;14(11):7643–51.

242. Nieduszynski CA, Knox Y, Donaldson AD. Genome-wide identification of replication origins in yeast by comparative genomics. Genes Dev. 2006 Jul 15;20(14):1874–9.

243. Shen Z, Sathyan KM, Geng Y, Zheng R, Chakraborty A, Freeman B, et al. A WD-Repeat Protein Stabilizes ORC Binding to Chromatin. Mol Cell. 2010 Oct;40(1):99–111.

244. Hayashi MT, Masukata H. Regulation of DNA replication by chromatin structures: accessibility and recruitment. Chromosoma. 2011 Feb 1;120(1):39–46.

245. Stamatoyannopoulos JA, Adzhubei I, Thurman RE, Kryukov GV, Mirkin SM, Sunyaev SR. Human mutation rate associated with DNA replication timing. Nat Genet. 2009 Apr;41(4):393–5.

246. Heun P, Laroche T, Raghuraman MK, Gasser SM. The Positioning and Dynamics of Origins of Replication in the Budding Yeast Nucleus. J Cell Biol. 2001 Jan 22;152(2):385–400.

247. Pardo B, Crabbé L, Pasero P. Signaling Pathways of Replication Stress in Yeast. FEMS Yeast Res. 2016 Dec 2;fow101.

248. Mantiero D, Mackenzie A, Donaldson A, Zegerman P. Limiting replication initiation factors execute the temporal programme of origin firing in budding yeast. EMBO J. 2011 Nov 11;30(23):4805–14.

249. Tanaka S, Nakato R, Katou Y, Shirahige K, Araki H. Origin Association of Sld3, Sld7, and Cdc45 Proteins Is a Key Step for Determination of Origin-Firing Timing. Curr Biol. 2011 Dec;21(24):2055–63.

250. Wong PG, Winter SL, Zaika E, Cao TV, Oguz U, Koomen JM, et al. Cdc45 limits replicon usage from a low density of preRCs in mammalian cells. PloS One. 2011 Mar 1;6(3):e17533.

251. Rhind N, Gilbert DM. DNA Replication Timing. Cold Spring Harb Perspect Biol [Internet]. 2013 Aug [cited 2020 Jun 5];5(8). Available from: https://www.ncbi.nlm.nih.gov/pmc/articles/PMC3721284/

252. Heller RC, Kang S, Lam WM, Chen S, Chan CS, Bell SP. Eukaryotic Origin-Dependent DNA Replication In Vitro Reveals Sequential Action of DDK and S-CDK Kinases. Cell. 2011 Jul 8;146(1):80–91.

253. Yoshida K, Bacal J, Desmarais D, Padioleau I, Tsaponina O, Chabes A, et al. The Histone Deacetylases Sir2 and Rpd3 Act on Ribosomal DNA to Control the Replication Program in Budding Yeast. Mol Cell. 2014 May;54(4):691–7.

254. Friedman KL, Brewer BJ, Fangman WL. Replication profile of Saccharomyces cerevisiae chromosome VI. Genes Cells. 1997;2(11):667–78.

255. Ferguson BM, Fangman WL. A position effect on the time of replication origin activation in yeast. Cell. 1992 Jan 24;68(2):333–9.

256. Rowley A, Cocker JH, Harwood J, Diffley JF. Initiation complex assembly at budding yeast replication origins begins with the recognition of a bipartite sequence by limiting amounts of the initiator, ORC. EMBO J. 1995 Jun 1;14(11):2631–41.

257. Chang F, May CD, Hoggard T, Miller J, Fox CA, Weinreich M. High-resolution analysis of four efficient yeast replication origins reveals new insights into the ORC and putative MCM binding elements. Nucleic Acids Res. 2011 Aug 1;39(15):6523–35.

258. Li N, Lam WH, Zhai Y, Cheng J, Cheng E, Zhao Y, et al. Structure of the origin recognition complex bound to DNA replication origin. Nature. 2018 Jul;559(7713):217–22.

259. Lee DG, Bell SP. Architecture of the yeast origin recognition complex bound to origins of DNA replication. Mol Cell Biol. 1997 Dec;17(12):7159–68.

260. Wilmes GM, Bell SP. The B2 element of the Saccharomyces cerevisiae ARS1 origin of replication requires specific sequences to facilitate pre-RC formation. Proc Natl Acad Sci U S A. 2002 Jan 8;99(1):101–6.

261. Coster G, Diffley JFX. Bidirectional eukaryotic DNA replication is established by quasi-symmetrical helicase loading. Science. 2017 Jul 21;357(6348):314–8.

262. Diffley JF, Cocker JH. Protein-DNA interactions at a yeast replication origin. Nature. 1992 May 14;357(6374):169–72.

263. Hoggard T, Shor E, Müller CA, Nieduszynski CA, Fox CA. A Link between ORC-origin binding mechanisms and origin activation time revealed in budding yeast. PLoS Genet. 2013;9(9):e1003798.

264. Das SP, Borrman T, Liu VWT, Yang SCH, Bechhoefer J, Rhind N. Replication timing is regulated by the number of MCMs loaded at origins. Genome Res. 2015 Dec 1;25(12):1886–92.

265. Pasero P, Bensimon A, Schwob E. Single-molecule analysis reveals clustering and epigenetic regulation of replication origins at the yeast rDNA locus. Genes Dev. 2002 Oct 1;16(19):2479–84.

266. Knott SRV, Viggiani CJ, Tavaré S, Aparicio OM. Genome-wide replication profiles indicate an expansive role for Rpd3L in regulating replication initiation timing or efficiency, and reveal genomic loci of Rpd3 function in Saccharomyces cerevisiae. Genes Dev. 2009 May 1;23(9):1077–90.

267. Lengronne A, Pasero P. Sir2 takes affirmative action to ensure equal opportunity in replication origin licensing. Proc Natl Acad Sci. 2020 Jun 30;202010001.

268. Hoggard TA, Chang F, Perry KR, Subramanian S, Kenworthy J, Chueng J, et al. Yeast heterochromatin regulators Sir2 and Sir3 act directly at euchromatic DNA replication origins. PLoS Genet [Internet]. 2018 May 24 [cited 2020 Jun 5];14(5). Available from: https://www.ncbi.nlm.nih.gov/pmc/articles/PMC5991416/

269. Vogelauer M, Rubbi L, Lucas I, Brewer BJ, Grunstein M. Histone Acetylation Regulates the Time of Replication Origin Firing. Mol Cell. 2002 Nov 1;10(5):1223–33.

270. Aparicio JG, Viggiani CJ, Gibson DG, Aparicio OM. The Rpd3-Sin3 Histone Deacetylase Regulates Replication Timing and Enables Intra-S Origin Control in Saccharomyces cerevisiae. Mol Cell Biol. 2004 Jun;24(11):4769–80.

271. Collart C, Allen GE, Bradshaw CR, Smith JC, Zegerman P. Titration of Four Replication Factors Is Essential for the Xenopus laevis Midblastula Transition. Science. 2013 Aug 23;341(6148):893–6.

272. Hoggard T, Müller CA, Nieduszynski CA, Weinreich M, Fox CA. Sir2 mitigates an intrinsic imbalance in origin licensing efficiency between early- and late-replicating euchromatin. Proc Natl Acad Sci U S A. 2020 Jun 23;117(25):14314–21.

273. Foss EJ, Lao U, Dalrymple E, Adrianse RL, Loe T, Bedalov A. SIR2 suppresses replication gaps and genome instability by balancing replication between repetitive and unique sequences. Proc Natl Acad Sci. 2017 Jan 17;114(3):552–7.

274. Natsume T, Müller CA, Katou Y, Retkute R, Gierliński M, Araki H, et al. Kinetochores coordinate pericentromeric cohesion and early DNA replication by Cdc7-Dbf4 kinase recruitment. Mol Cell. 2013 Jun 6;50(5):661–74.

275. Deegan TD, Diffley JF. MCM: one ring to rule them all. Curr Opin Struct Biol. 2016 Apr 1;37:145–51.

276. Remus D, Beuron F, Tolun G, Griffith JD, Morris EP, Diffley JFX. Concerted loading of Mcm2-7 double hexamers around DNA during DNA replication origin licensing. Cell. 2009 Nov 13;139(4):719–30.

277. Yeeles JTP, Deegan TD, Janska A, Early A, Diffley JFX. Regulated eukaryotic DNA replication origin firing with purified proteins. Nature. 2015 Mar 26;519(7544):431–5.

278. Lee CSK, Cheung MF, Li J, Zhao Y, Lam WH, Ho V, et al. Humanizing the yeast origin recognition complex. Nat Commun. 2021 Jan 4;12(1):33.

279. Li S, Wasserman MR, Yurieva O, Bai L, O'Donnell ME, Liu S. ORC binds and remodels nucleosomes to specify MCM loading onto DNA [Internet]. bioRxiv; 2021 [cited 2022 Oct 11]. p. 2021.08.17.456647. Available from: https://www.biorxiv.org/content/10.1101/2021.08.17.456647v1

280. Evrin C, Clarke P, Zech J, Lurz R, Sun J, Uhle S, et al. A double-hexameric MCM2-7 complex is loaded onto origin DNA during licensing of eukaryotic DNA replication. Proc Natl Acad Sci U S A. 2009 Dec 1;106(48):20240–5.

281. Riera A, Barbon M, Noguchi Y, Reuter LM, Schneider S, Speck C. From structure to mechanism-understanding initiation of DNA replication. Genes Dev. 2017 Jun 1;31(11):1073–88.

282. Lõoke M, Maloney MF, Bell SP. Mcm10 regulates DNA replication elongation by stimulating the CMG replicative helicase. Genes Dev. 2017 Feb 1;31(3):291–305.

283. Douglas ME, Ali FA, Costa A, Diffley JFX. The mechanism of eukaryotic CMG helicase activation. Nature. 2018 Mar 8;555(7695):265–8.

284. Zheng DQ, Petes TD. Genome Instability Induced by Low Levels of Replicative DNA Polymerases in Yeast. Genes. 2018 Nov 7;9(11):E539.

285. Steitz TA. DNA Polymerases: Structural Diversity and Common Mechanisms*. J Biol Chem. 1999 Jun 18;274(25):17395–8.

286. Pursell ZF, Isoz I, Lundström EB, Johansson E, Kunkel TA. Yeast DNA polymerase epsilon participates in leading-strand DNA replication. Science. 2007 Jul 6;317(5834):127–30.

287. Nick McElhinny SA, Gordenin DA, Stith CM, Burgers PMJ, Kunkel TA. Division of labor at the eukaryotic replication fork. Mol Cell. 2008 Apr 25;30(2):137–44.

288. Burgers PMJ. Polymerase dynamics at the eukaryotic DNA replication fork. J Biol Chem. 2009 Feb 13;284(7):4041–5.

289. Doublié S, Zahn KE. Structural insights into eukaryotic DNA replication. Front Microbiol [Internet]. 2014 [cited 2022 Mar 4];5. Available from: https://www.frontiersin.org/article/10.3389/fmicb.2014.00444

290. Claussin C, Vazquez J, Whitehouse I. Single-molecule mapping of replisome progression. Mol Cell [Internet]. 2022 Mar 2 [cited 2022 Mar 2];0(0). Available from: https://www.cell.com/molecular-cell/abstract/S1097-2765(22)00115-0

291. Harrington JJ, Lieber MR. Functional domains within FEN-1 and RAD2 define a family of structure-specific endonucleases: implications for nucleotide excision repair. Genes Dev. 1994 Jun 1;8(11):1344–55.

292. Budd ME, Reis CC, Smith S, Myung K, Campbell JL. Evidence suggesting that Pif1 helicase functions in DNA replication with the Dna2 helicase/nuclease and DNA polymerase delta. Mol Cell Biol. 2006 Apr;26(7):2490–500.

293. Kang YH, Lee CH, Seo YS. Dna2 on the road to Okazaki fragment processing and genome stability in eukaryotes. Crit Rev Biochem Mol Biol. 2010 Apr;45(2):71–96.

294. Bae SH, Bae KH, Kim JA, Seo YS. RPA governs endonuclease switching during processing of Okazaki fragments in eukaryotes. Nature. 2001 Jul 26;412(6845):456–61.

295. Bambara RA, Murante RS, Henricksen LA. Enzymes and reactions at the eukaryotic DNA replication fork. J Biol Chem. 1997 Feb 21;272(8):4647–50.

296. Simon AC, Zhou JC, Perera RL, van Deursen F, Evrin C, Ivanova ME, et al. A Ctf4 trimer couples the CMG helicase to DNA polymerase α in the eukaryotic replisome. Nature. 2014 Jun;510(7504):293–7.

297. Baretić D, Jenkyn-Bedford M, Aria V, Cannone G, Skehel M, Yeeles JTP. Cryo-EM Structure of the Fork Protection Complex Bound to CMG at a Replication Fork. Mol Cell. 2020 Jun 4;78(5):926-940.e13.

298. Dewar JM, Walter JC. Mechanisms of DNA replication termination. Nat Rev Mol Cell Biol. 2017 Aug;18(8):507–16.

299. Fachinetti D, Bermejo R, Cocito A, Minardi S, Katou Y, Kanoh Y, et al. Replication termination at eukaryotic chromosomes is mediated by Top2 and occurs at genomic loci containing pausing elements. Mol Cell. 2010 Aug 27;39(4):595–605.

300. Maric M, Maculins T, De Piccoli G, Labib K. Cdc48 and a ubiquitin ligase drive disassembly of the CMG helicase at the end of DNA replication. Science. 2014 Oct 24;346(6208):1253596.

301. Moreno SP, Bailey R, Campion N, Herron S, Gambus A. Polyubiquitylation drives replisome disassembly at the termination of DNA replication. Science. 2014 Oct 24;346(6208):477–81.

302. Morohashi H, Maculins T, Labib K. The amino-terminal TPR domain of Dia2 tethers SCF(Dia2) to the replisome progression complex. Curr Biol CB. 2009 Dec 1;19(22):1943–9.

303. Lengronne A, Pasero P. Closing the MCM cycle at replication termination sites. EMBO Rep. 2014 Dec;15(12):1226–7.

304. Dewar JM, Budzowska M, Walter JC. The mechanism of DNA replication termination in vertebrates. Nature. 2015 Sep 17;525(7569):345–50.

305. Watson JD. Origin of Concatemeric T7DNA. Nature New Biol. 1972 Oct;239(94):197–201.

306. Olovnikov AM. A theory of marginotomy. The incomplete copying of template margin in enzymic synthesis of polynucleotides and biological significance of the phenomenon. J Theor Biol. 1973 Sep 14;41(1):181–90.

307. Aylon Y, Kupiec M. The checkpoint protein Rad24 of Saccharomyces cerevisiae is involved in processing double-strand break ends and in recombination partner choice. Mol Cell Biol. 2003 Sep;23(18):6585–96.

308. de Lange T. Shelterin-Mediated Telomere Protection. Annu Rev Genet. 2018 Nov 23;52:223–47.

309. Soudet J, Jolivet P, Teixeira MT. Elucidation of the DNA End-Replication Problem in Saccharomyces cerevisiae. Mol Cell. 2014 Mar 20;53(6):954–64.

310. Wellinger RJ. In the End, What's the Problem? Mol Cell. 2014 Mar 20;53(6):855–6.

311. Tran PLT, Mergny JL, Alberti P. Stability of telomeric G-quadruplexes. Nucleic Acids Res. 2011 Apr;39(8):3282–94.

312. Wellinger RJ, Zakian VA. Everything you ever wanted to know about Saccharomyces cerevisiae telomeres: beginning to end. Genetics. 2012 Aug;191(4):1073–105.

313. Shay JW, Wright WE. Telomeres and telomerase in normal and cancer stem cells. FEBS Lett. 2010 Sep 10;584(17):3819–25.

314. Hayflick L, Moorhead PS. The serial cultivation of human diploid cell strains. Exp Cell Res. 1961 Dec;25:585–621.

315. Demidenko ZN, Blagosklonny MV. Growth stimulation leads to cellular senescence when the cell cycle is blocked. Cell Cycle Georget Tex. 2008 Nov 1;7(21):3355–61.

316. Debacq-Chainiaux F, Ben Ameur R, Bauwens E, Dumortier E, Toutfaire M, Toussaint O. Stress-Induced (Premature) Senescence. In: Rattan SIS, Hayflick L, editors. Cellular Ageing and Replicative Senescence [Internet]. Cham: Springer International Publishing; 2016 [cited 2022 Mar 30]. p. 243–62. Available from: https://doi.org/10.1007/978-3-319-26239-0_13

317. Carr AM, Paek AL, Weinert T. DNA replication: Failures and inverted fusions. Semin Cell Dev Biol. 2011 Oct 1;22(8):866–74.

318. Zeman MK, Cimprich KA. Causes and Consequences of Replication Stress. Nat Cell Biol. 2014 Jan;16(1):2–9.

319. Alcasabas AA, Osborn AJ, Bachant J, Hu F, Werler PJH, Bousset K, et al. Mrc1 transduces signals of DNA replication stress to activate Rad53. Nat Cell Biol. 2001 Nov;3(11):958–65.

320. Tourrière H, Pasero P. Maintenance of fork integrity at damaged DNA and natural pause sites. DNA Repair. 2007 Jul 1;6(7):900–13.

321. Komata M, Bando M, Araki H, Shirahige K. The direct binding of Mrc1, a checkpoint mediator, to Mcm6, a replication helicase, is essential for the replication checkpoint against methyl methanesulfonate-induced stress. Mol Cell Biol. 2009 Sep;29(18):5008–19.

322. Devbhandari S, Remus D. Rad53 limits CMG helicase uncoupling from DNA synthesis at replication forks. Nat Struct Mol Biol. 2020 May;27(5):461–71.

323. Rouse J, Jackson SP. Lcd1p Recruits Mec1p to DNA Lesions In Vitro and In Vivo. Mol Cell. 2002 Apr 1;9(4):857–69.

324. Zou L, Elledge SJ. Sensing DNA damage through ATRIP recognition of RPA-ssDNA complexes. Science. 2003 Jun 6;300(5625):1542–8.

325. Pardo B, Crabbé L, Pasero P. Signaling pathways of replication stress in yeast. FEMS Yeast Res. 2017 Mar 1;17(2):fow101.

326. Ma JL, Lee SJ, Duong JK, Stern DF. Activation of the Checkpoint Kinase Rad53 by the Phosphatidyl Inositol Kinase-like Kinase Mec1 *. J Biol Chem. 2006 Feb 17;281(7):3954–63.

327. Knott SRV, Peace JM, Ostrow AZ, Gan Y, Rex AE, Viggiani CJ, et al. Forkhead Transcription Factors Establish Origin Timing and Long-Range Clustering in S. cerevisiae. Cell. 2012 Jan;148(1–2):99–111.

328. Hoggard T, Hollatz AJ, Cherney RE, Seman MR, Fox CA. The Fkh1 Forkhead associated domain promotes ORC binding to a subset of DNA replication origins in budding yeast. Nucleic Acids Res [Internet]. 2021 Jun 7 [cited 2021 Jul 6];(gkab450). Available from: https://doi.org/10.1093/nar/gkab450

329. Zhang H, Petrie MV, He Y, Peace JM, Chiolo IE, Aparicio OM. Dynamic relocalization of replication origins by Fkh1 requires execution of DDK function and Cdc45 loading at origins. eLife. 2019 May 14;8:e45512.

330. Sporbert A, Gahl A, Ankerhold R, Leonhardt H, Cardoso MC. DNA Polymerase Clamp Shows Little Turnover at Established Replication Sites but Sequential De Novo Assembly at Adjacent Origin Clusters. Mol Cell. 2002 Dec 1;10(6):1355–65.

331. Peace JM, Villwock SK, Zeytounian JL, Gan Y, Aparicio OM. Quantitative BrdU immunoprecipitation method demonstrates that Fkh1 and Fkh2 are rate-limiting activators of replication origins that reprogram replication timing in G1 phase. Genome Res. 2016 Mar;26(3):365–75.

332. Mojumdar A, Mair N, Adam N, Cobb J. During replicative aging, changes in DNA double-strand break repair correlate with an increased rate of mutation [Internet]. bioRxiv; 2022 [cited 2022 Apr 20]. p. 2022.02.04.479125. Available from: https://www.biorxiv.org/content/10.1101/2022.02.04.479125v1

333. Singh A, Xu YJ. The Cell Killing Mechanisms of Hydroxyurea. Genes. 2016 Nov 17;7(11):99.

334. Alvino GM, Collingwood D, Murphy JM, Delrow J, Brewer BJ, Raghuraman MK. Replication in hydroxyurea: it's a matter of time. Mol Cell Biol. 2007 Sep;27(18):6396–406.

335. Poli J, Tsaponina O, Crabbé L, Keszthelyi A, Pantesco V, Chabes A, et al. dNTP pools determine fork progression and origin usage under replication stress. EMBO J. 2012 Feb 15;31(4):883–94.

336. Schlissel G, Krzyzanowski MK, Caudron F, Barral Y, Rine J. Aggregation of an RNA-binding protein, not loss of heterochromatin, causes sterility of aging yeast cells. Science. 2017 Mar 17;355(6330):1184–7.

337. Yabuki N, Terashima H, Kitada K. Mapping of early firing origins on a replication profile of budding yeast. Genes Cells Devoted Mol Cell Mech. 2002 Aug;7(8):781–9.

338. Porcella SY, Koussa NC, Tang CP, Kramer DN, Srivastava P, Smith DJ. Separable, Ctf4-mediated recruitment of DNA Polymerase α for initiation of DNA synthesis at replication origins and lagging-strand priming during replication elongation. PLOS Genet. 2020 May 7;16(5):e1008755.

339. Cobb JA, Bjergbaek L, Shimada K, Frei C, Gasser SM. DNA polymerase stabilization at stalled replication forks requires Mec1 and the RecQ helicase Sgs1. EMBO J. 2003 Aug 15;22(16):4325–36.

340. Tittel-Elmer M, Alabert C, Pasero P, Cobb JA. The MRX complex stabilizes the replisome independently of the S phase checkpoint during replication stress. EMBO J. 2009 Apr 22;28(8):1142–56.

341. Pappas DL, Frisch R, Weinreich M. The NAD+-dependent Sir2p histone deacetylase is a negative regulator of chromosomal DNA replication. Genes Dev. 2004 Apr 1;18(7):769–81.

342. Meng X, Wei L, Devbhandari S, Zhang T, Xiang J, Remus D, et al. DNA polymerase ε relies on a unique domain for efficient replisome assembly and strand synthesis. Nat Commun. 2020 May 15;11(1):2437.

343. Conti C, Saccà B, Herrick J, Lalou C, Pommier Y, Bensimon A. Replication fork velocities at adjacent replication origins are coordinately modified during DNA replication in human cells. Mol Biol Cell. 2007 Aug;18(8):3059–67.

344. Knott SRV, Peace JM, Ostrow AZ, Gan Y, Rex AE, Viggiani CJ, et al. Forkhead transcription factors establish origin timing and long-range clustering in S. cerevisiae. Cell. 2012 Jan 20;148(1–2):99–111.

345. Ostrow AZ, Nellimoottil T, Knott SRV, Fox CA, Tavaré S, Aparicio OM. Fkh1 and Fkh2 Bind Multiple Chromosomal Elements in the S. cerevisiae Genome with Distinct Specificities and Cell Cycle Dynamics. Wang Y, editor. PLoS ONE. 2014 Feb 4;9(2):e87647.

346. Ghavidel A, Baxi K, Prusinkiewicz M, Swan C, Belak ZR, Eskiw CH, et al. Rapid Nuclear Exclusion of Hcm1 in Aging Saccharomyces cerevisiae Leads to Vacuolar Alkalization and Replicative Senescence. G3 GenesGenomesGenetics. 2018 Mar 8;8(5):1579–92.

347. Tourrière H, Saksouk J, Lengronne A, Pasero P. Single-molecule Analysis of DNA Replication Dynamics in Budding Yeast and Human Cells by DNA Combing. Bio-Protoc. 2017 Jun 5;7(11):e2305.

348. Maya-Mendoza A, Moudry P, Merchut-Maya JM, Lee M, Strauss R, Bartek J. High speed of fork progression induces DNA replication stress and genomic instability. Nature. 2018 Jul;559(7713):279–84.

349. Akerman I, Kasaai B, Bazarova A, Sang PB, Peiffer I, Artufel M, et al. A predictable conserved DNA base composition signature defines human core DNA replication origins. Nat Commun. 2020 Sep 21;11(1):4826.

350. Lukášová E, Řezáčová M, Bačíková A, Šebejová L, Vávrová J, Kozubek S. Distinct cellular responses to replication stress leading to apoptosis or senescence. FEBS Open Bio. 2019 Apr 13;9(5):870–90.

351. Stevenson JB, Gottschling DE. Telomeric chromatin modulates replication timing near chromosome ends. Genes Dev. 1999 Jan 15;13(2):146–51.

352. Das M, Singh S, Pradhan S, Narayan G. MCM Paradox: Abundance of Eukaryotic Replicative Helicases and Genomic Integrity. Mol Biol Int. 2014 Oct 19;2014:1–11.

353. Das SP, Rhind N. How and why multiple MCMs are loaded at origins of DNA replication. BioEssays. 2016;38(7):613–7.

354. Li S, Wasserman MR, Yurieva O, Bai L, O'Donnell ME, Liu S. Nucleosome-directed replication origin licensing independent of a consensus DNA sequence. Nat Commun. 2022 Aug 23;13(1):4947.

355. Singh G. Mechanistic Model of Replication Fork Progression in Yeast [Internet]. Systems Biology; 2021 Oct [cited 2022 Feb 2]. Available from: http://biorxiv.org/lookup/doi/10.1101/2021.10.03.462908

356. Petryk N, Kahli M, d'Aubenton-Carafa Y, Jaszczyszyn Y, Shen Y, Silvain M, et al. Replication landscape of the human genome. Nat Commun. 2016 Jan 11;7(1):10208.

357. Byun TS, Pacek M, Yee M ching, Walter JC, Cimprich KA. Functional uncoupling of MCM helicase and DNA polymerase activities activates the ATR-dependent checkpoint. Genes Dev. 2005 May 1;19(9):1040–52.

358. Hashimoto Y, Ray Chaudhuri A, Lopes M, Costanzo V. Rad51 protects nascent DNA from Mre11-dependent degradation and promotes continuous DNA synthesis. Nat Struct Mol Biol. 2010 Nov;17(11):1305–11.

359. Bhat KP, Cortez D. RPA and RAD51: fork reversal, fork protection, and genome stability. Nat Struct Mol Biol. 2018 Jun;25(6):446–53.

360. Lõoke M, Kristjuhan K, Värv S, Kristjuhan A. Chromatin-dependent and -independent regulation of DNA replication origin activation in budding yeast. EMBO Rep. 2013 Feb;14(2):191–8.

361. Tittel-Elmer M, Lengronne A, Davidson MB, Bacal J, François P, Hohl M, et al. Cohesin association to replication sites depends on Rad50 and promotes fork restart. Mol Cell. 2012 Oct 12;48(1):98–108.

362. Gallo D, Wang G, Yip CM, Brown GW. Analysis of Replicating Yeast Chromosomes by DNA Combing. Cold Spring Harb Protoc. 2016 Feb 1;2016(2):pdb.prot085118.

363. Tourrière H, Versini G, Cordón-Preciado V, Alabert C, Pasero P. Mrc1 and Tof1 promote replication fork progression and recovery independently of Rad53. Mol Cell. 2005 Sep 2;19(5):699–706.

364. Lee SE, Moore JK, Holmes A, Umezu K, Kolodner RD, Haber JE. Saccharomyces Ku70, Mre11/Rad50, and RPA Proteins Regulate Adaptation to G2/M Arrest after DNA Damage. Cell. 1998 Aug 7;94(3):399–409.

365. Hoeijmakers JHJ. DNA Damage, Aging, and Cancer. N Engl J Med. 2009 Oct 8;361(15):1475–85.

366. Mayer PJ, Lange CS, Bradley MO, Nichols WW. Age-dependent decline in rejoining of X-ray-induced DNA double-strand breaks in normal human lymphocytes. Mutat Res. 1989 Mar;219(2):95–100.

367. Singh NP, Danner DB, Tice RR, Brant L, Schneider EL. DNA damage and repair with age in individual human lymphocytes. Mutat Res. 1990 Jul;237(3–4):123–30.

368. Gorbunova V, Seluanov A. DNA double strand break repair, aging and the chromatin connection. Mutat Res Mol Mech Mutagen. 2016 Jun;788:2–6.

369. Um JH, Kim SJ, Kim DW, Ha MY, Jang JH, Kim DW, et al. Tissue-specific changes of DNA repair protein Ku and mtHSP70 in aging rats and their retardation by caloric restriction. Mech Ageing Dev. 2003 Sep;124(8–9):967–75.

370. Ju YJ, Lee KH, Park JE, Yi YS, Yun MY, Ham YH, et al. Decreased expression of DNA repair proteins Ku70 and Mre11 is associated with aging and may contribute to the cellular senescence. Exp Mol Med. 2006 Dec 31;38(6):686–93.

371. Seluanov A, Danek J, Hause N, Gorbunova V. Changes in the level and distribution of Ku proteins during cellular senescence. DNA Repair. 2007 Dec 1;6(12):1740–8.

372. Mao Z, Tian X, Van Meter M, Ke Z, Gorbunova V, Seluanov A. Sirtuin 6 (SIRT6) rescues the decline of homologous recombination repair during replicative senescence. Proc Natl Acad Sci U S A. 2012 Jul 17;109(29):11800–5.

373. Delabaere L, Ertl HA, Massey DJ, Hofley CM, Sohail F, Bienenstock EJ, et al. Aging impairs double-strand break repair by homologous recombination in Drosophila germ cells. Aging Cell. 2017;16(2):320–8.

374. Young TZ, Liu P, Urbonaite G, Acar M. Quantitative Insights into Age-Associated DNA-Repair Inefficiency in Single Cells. Cell Rep. 2019 Aug 20;28(8):2220-2230.e7.

375. Connolly B, White CI, Haber JE. Physical monitoring of mating type switching in Saccharomyces cerevisiae. Mol Cell Biol. 1988 Jun;8(6):2342–9.

376. Janssens G, Veenhoff L. Evidence for the hallmarks of human aging in replicatively aging yeast. Microb Cell. 2016 Jul 4;3(7):263–74.

377. He C, Zhou C, Kennedy BK. The yeast replicative aging model. Biochim Biophys Acta BBA - Mol Basis Dis. 2018 Sep;1864(9):2690–6.

378. Vrsanská M, Krátký Z, Biely P, Machala S. Chitin structures of the cell walls of synchronously grown virgin cells of Saccharomyces cerevisiae. Z Allg Mikrobiol. 1979;19(5):357–62.

379. Ferrari M, Dibitetto D, De Gregorio G, Eapen VV, Rawal CC, Lazzaro F, et al. Functional Interplay between the 53BP1-Ortholog Rad9 and the Mre11 Complex Regulates Resection, End-Tethering and Repair of a Double-Strand Break. PLoS Genet. 2015 Jan 8;11(1):e1004928.

380. Mojumdar A, Sorenson K, Hohl M, Toulouze M, Lees-Miller SP, Dubrana K, et al. Nej1 Interacts with Mre11 to Regulate Tethering and Dna2 Binding at DNA Double-Strand Breaks. Cell Rep. 2019 06;28(6):1564-1573.e3.

381. Mojumdar A, Adam N, Cobb JA. Nej1XLF interacts with Sae2CTIP to inhibit Dna2 mediated resection at DNA double strand break [Internet]. bioRxiv; 2022 [cited 2022 Jan 30]. p. 2021.04.10.439283. Available from: https://www.biorxiv.org/content/10.1101/2021.04.10.439283v4

382. Hohl M, Mojumdar A, Hailemariam S, Kuryavyi V, Ghisays F, Sorenson K, et al. Modeling cancer genomic data in yeast reveals selection against ATM function during tumorigenesis. PLoS Genet. 2020 Mar;16(3):e1008422.

383. Ciccia A, Symington LS. Stressing Out About RAD52. Mol Cell. 2016 Dec;64(6):1017–9.

384. Cejka P. DNA End Resection: Nucleases Team Up with the Right Partners to Initiate Homologous Recombination. J Biol Chem. 2015 Sep 18;290(38):22931–8.

385. Titus S, Li F, Stobezki R, Akula K, Unsal E, Jeong K, et al. Impairment of BRCA1-related DNA double-strand break repair leads to ovarian aging in mice and humans. Sci Transl Med. 2013 Feb 13;5(172):172ra21.

386. Hohl M, Kochańczyk T, Tous C, Aguilera A, Krężel A, Petrini JHJ. Interdependence of the Rad50 hook and globular domain functions. Mol Cell. 2015 Feb 5;57(3):479–91.

387. Zahid S, Seif El Dahan M, Iehl F, Fernandez-Varela P, Le Du MH, Ropars V, et al. The Multifaceted Roles of Ku70/80. Int J Mol Sci. 2021 Jan;22(8):4134.

388. Mojumdar A, Adam N, Cobb J. Multifunctional properties of Nej1XLF C-terminus promote end-joining and impact DNA double-strand break repair pathway choice [Internet]. bioRxiv; 2022 [cited 2022 Jan 30]. p. 2022.01.13.476264. Available from: https://www.biorxiv.org/content/10.1101/2022.01.13.476264v1

389. Nagai S, Dubrana K, Tsai-Pflugfelder M, Davidson MB, Roberts TM, Brown GW, et al. Functional Targeting of DNA Damage to a Nuclear Pore–Associated SUMO-Dependent Ubiquitin Ligase. Science. 2008 Oct 24;322(5901):597–602.

390. Chiolo I, Minoda A, Colmenares SU, Polyzos A, Costes SV, Karpen GH. Double-Strand Breaks in Heterochromatin Move Outside of a Dynamic HP1a Domain to Complete Recombinational Repair. Cell. 2011 Mar 4;144(5):732–44.

391. Chung I, Zhao X. DNA break-induced sumoylation is enabled by collaboration between a SUMO ligase and the ssDNA-binding complex RPA. Genes Dev. 2015 Aug 1;29(15):1593–8.

392. Ryu T, Spatola B, Delabaere L, Bowlin K, Hopp H, Kunitake R, et al. Heterochromatic breaks move to the nuclear periphery to continue recombinational repair. Nat Cell Biol. 2015 Nov;17(11):1401–11.

393. Su XA, Dion V, Gasser SM, Freudenreich CH. Regulation of recombination at yeast nuclear pores controls repair and triplet repeat stability. Genes Dev. 2015 May 15;29(10):1006–17.

394. Churikov D, Charifi F, Eckert-Boulet N, Silva S, Simon MN, Lisby M, et al. SUMO-Dependent Relocalization of Eroded Telomeres to Nuclear Pore Complexes Controls Telomere Recombination. Cell Rep. 2016 May;15(6):1242–53.

395. Horigome C, Bustard DE, Marcomini I, Delgoshaie N, Tsai-Pflugfelder M, Cobb JA, et al. PolySUMOylation by Siz2 and Mms21 triggers relocation of DNA breaks to nuclear pores through the Slx5/Slx8 STUbL. Genes Dev. 2016 Apr 15;30(8):931–45.

396. Horigome C, Oma Y, Konishi T, Schmid R, Marcomini I, Hauer MH, et al. SWR1 and INO80 Chromatin Remodelers Contribute to DNA Double-Strand Break Perinuclear Anchorage Site Choice. Mol Cell. 2014 Aug 21;55(4):626–39.

397. Kalocsay M, Hiller NJ, Jentsch S. Chromosome-wide Rad51 Spreading and SUMO-H2A.Z-Dependent Chromosome Fixation in Response to a Persistent DNA Double-Strand Break. Mol Cell. 2009 Feb 13;33(3):335–43.

398. Oza P, Jaspersen SL, Miele A, Dekker J, Peterson CL. Mechanisms that regulate localization of a DNA double-strand break to the nuclear periphery. Genes Dev. 2009 Apr 15;23(8):912–27.

399. Khadaroo B, Teixeira MT, Luciano P, Eckert-Boulet N, Germann SM, Simon MN, et al. The DNA damage response at eroded telomeres and tethering to the nuclear pore complex. Nat Cell Biol. 2009 Aug;11(8):980–7.

400. Therizols P, Fairhead C, Cabal GG, Genovesio A, Olivo-Marin JC, Dujon B, et al. Telomere tethering at the nuclear periphery is essential for efficient DNA double strand break repair in subtelomeric region. J Cell Biol. 2006 Jan 16;172(2):189–99.

401. Moore JK, Haber JE. Capture of retrotransposon DNA at the sites of chromosomal double-strand breaks. Nature. 1996 Oct 17;383(6601):644–6.

402. Kadyk LC, Hartwell LH. Sister chromatids are preferred over homologs as substrates for recombinational repair in Saccharomyces cerevisiae. Genetics. 1992 Oct;132(2):387–402.

403. Trovesi C, Falcettoni M, Lucchini G, Clerici M, Longhese MP. Distinct Cdk1 requirements during single-strand annealing, noncrossover, and crossover recombination. PLoS Genet. 2011 Aug;7(8):e1002263.

404. Valencia-Burton M, Oki M, Johnson J, Seier TA, Kamakaka R, Haber JE. Different mating-type-regulated genes affect the DNA repair defects of Saccharomyces RAD51, RAD52 and RAD55 mutants. Genetics. 2006 Sep;174(1):41–55.

405. McVey M, Lee SE. MMEJ repair of double-strand breaks (director's cut): deleted sequences and alternative endings. Trends Genet TIG. 2008 Nov;24(11):529–38.

406. Sinha S, Villarreal D, Shim EY, Lee SE. Risky Business: Microhomology-Mediated End Joining. Mutat Res. 2016 Jun;788:17–24.

407. Pannunzio NR, Li S, Watanabe G, Lieber MR. Non-homologous end joining often uses microhomology: implications for alternative end joining. DNA Repair. 2014 May;17:74–80.

408. Lans H, Hoeijmakers JHJ. Cell biology: ageing nucleus gets out of shape. Nature. 2006 Mar 2;440(7080):32–4.

409. Kubben N, Misteli T. Shared molecular and cellular mechanisms of premature ageing and ageing-associated diseases. Nat Rev Mol Cell Biol. 2017 Oct;18(10):595–609.

410. Rempel IL, Steen A, Veenhoff LM. Poor old pores—The challenge of making and maintaining nuclear pore complexes in aging. FEBS J. 2020;287(6):1058–75.

411. Loeillet S, Palancade B, Cartron M, Thierry A, Richard GF, Dujon B, et al. Genetic network interactions among replication, repair and nuclear pore deficiencies in yeast. DNA Repair. 2005 Apr 4;4(4):459–68.

412. Denoth Lippuner A, Julou T, Barral Y. Budding yeast as a model organism to study the effects of age. FEMS Microbiol Rev. 2014 Mar;38(2):300–25.

413. Jasin M, Haber JE. The Democratization of Gene Editing: Insights from site-specific cleavage and double-strand break repair. DNA Repair. 2016 Aug;44:6–16.

414. Sorenson KS, Mahaney BL, Lees-Miller SP, Cobb JA. The non-homologous end-joining factor Nej1 inhibits resection mediated by Dna2-Sgs1 nuclease-helicase at DNA double strand breaks. J Biol Chem. 2017 Sep 1;292(35):14576–86.

415. Gilles JF, Dos Santos M, Boudier T, Bolte S, Heck N. DiAna, an ImageJ tool for object-based 3D co-localization and distance analysis. Methods. 2017 Feb 15;115:55–64.

416. Murakami CJ, Burtner CR, Kennedy BK, Kaeberlein M. A method for high-throughput quantitative analysis of yeast chronological life span. J Gerontol A Biol Sci Med Sci. 2008 Feb;63(2):113–21.

417. Matecic M, Jr DLS, Pan X, Maqani N, Bekiranov S, Boeke JD, et al. A Microarray-Based Genetic Screen for Yeast Chronological Aging Factors. PLOS Genet. 2010 Apr 22;6(4):e1000921.

418. Zimmermann A, Hofer S, Pendl T, Kainz K, Madeo F, Carmona-Gutierrez D. Yeast as a tool to identify anti-aging compounds. FEMS Yeast Res. 2018 Mar 4;18(6):foy020.

419. Giaever G, Flaherty P, Kumm J, Proctor M, Nislow C, Jaramillo DF, et al. Chemogenomic profiling: identifying the functional interactions of small molecules in yeast. Proc Natl Acad Sci U S A. 2004 Jan 20;101(3):793–8.

420. Hoon S, Smith AM, Wallace IM, Suresh S, Miranda M, Fung E, et al. An integrated platform of genomic assays reveals small-molecule bioactivities. Nat Chem Biol. 2008 Aug;4(8):498–506.

421. Chen K, Shen W, Zhang Z, Xiong F, Ouyang Q, Luo C. Age-dependent decline in stress response capacity revealed by proteins dynamics analysis. Sci Rep. 2020 Sep 16;10(1):15211.

422. Somyajit K, Gupta R, Sedlackova H, Neelsen KJ, Ochs F, Rask MB, et al. Redox-sensitive alteration of replisome architecture safeguards genome integrity. Science. 2017 Nov 10;358(6364):797–802.

423. Donley N, Thayer MJ. DNA Replication Timing, Genome Stability and Cancer. Semin Cancer Biol. 2013 Apr;23(2):80–9.

424. Fu H, Baris A, Aladjem MI. Replication timing and nuclear structure. Curr Opin Cell Biol. 2018 Jun;52:43–50.

425. Li S, Wasserman MR, Yurieva O, Bai L, O'Donnell ME, Liu S. Origin recognition complex harbors an intrinsic nucleosome remodeling activity. Proc Natl Acad Sci. 2022 Oct 18;119(42):e2211568119.

426. Berbenetz NM, Nislow C, Brown GW. Diversity of Eukaryotic DNA Replication Origins Revealed by Genome-Wide Analysis of Chromatin Structure. PLoS Genet. 2010 Sep 2;6(9):e1001092.

427. De Jesús-Kim L, Friedman LJ, Lõoke M, Ramsoomair CK, Gelles J, Bell SP. DDK regulates replication initiation by controlling the multiplicity of Cdc45-GINS binding to Mcm2-7. Botchan MR, Struhl K, Botchan MR, Remus D, editors. eLife. 2021 Feb 22;10:e65471.

428. Ostrow AZ, Aparicio OM. Identification of Fkh1 and Fkh2 binding site variants associated with dynamically bound DNA elements including replication origins. Nucleus. 2017 Nov 13;8(6):600–4.

429. Guillou E, Ibarra A, Coulon V, Casado-Vela J, Rico D, Casal I, et al. Cohesin organizes chromatin loops at DNA replication factories. Genes Dev. 2010 Dec 15;24(24):2812–22.

430. Rossi SE, Foiani M, Giannattasio M. Dna2 processes behind the fork long ssDNA flaps generated by Pif1 and replication-dependent strand displacement. Nat Commun [Internet]. 2018 Nov 16 [cited 2020 Jun 5];9. Available from: https://www.ncbi.nlm.nih.gov/pmc/articles/PMC6240037/

431. de Magalhães JP, Wuttke D, Wood SH, Plank M, Vora C. Genome-environment interactions that modulate aging: powerful targets for drug discovery. Pharmacol Rev. 2012 Jan;64(1):88–101.

432. Alfaro JA, Bohländer P, Dai M, Filius M, Howard CJ, van Kooten XF, et al. The emerging landscape of single-molecule protein sequencing technologies. Nat Methods. 2021 Jun;18(6):604–17.

433. D'Angelo MA, Raices M, Panowski SH, Hetzer MW. Age-dependent deterioration of nuclear pore complexes causes a loss of nuclear integrity in postmitotic cells. Cell. 2009 Jan 23;136(2):284–95.

434. Toyama BH, Savas JN, Park SK, Harris MS, Ingolia NT, Yates JR, et al. Identification of long-lived proteins reveals exceptional stability of essential cellular structures. Cell. 2013 Aug 29;154(5):971–82.

435. Lord CL, Timney BL, Rout MP, Wente SR. Altering nuclear pore complex function impacts longevity and mitochondrial function in S. cerevisiae. J Cell Biol. 2015 Mar 16;208(6):729–44.

436. Cabrera M, Novarina D, Rempel IL, Veenhoff LM, Chang M. A simple microfluidic platform to study age-dependent protein abundance and localization changes in Saccharomyces cerevisiae. Microb Cell Graz Austria. 2017 Apr 13;4(5):169–74.

437. Saarikangas J, Caudron F, Prasad R, Moreno DF, Bolognesi A, Aldea M, et al. Compartmentalization of ER-Bound Chaperone Confines Protein Deposit Formation to the Aging Yeast Cell. Curr Biol CB. 2017 Mar 20;27(6):773–83.

438. Rempel IL, Crane MM, Thaller DJ, Mishra A, Jansen DP, Janssens G, et al. Age-dependent deterioration of nuclear pore assembly in mitotic cells decreases transport dynamics. eLife. 2019 Jun 3;8:e48186.

439. Denoth-Lippuner A, Krzyzanowski MK, Stober C, Barral Y. Role of SAGA in the asymmetric segregation of DNA circles during yeast ageing. Gottschling DE, editor. eLife. 2014 Nov 17;3:e03790.

440. Meinema AC, Marzelliusardottir A, Mirkovic M, Aspert T, Lee SS, Charvin G, et al. DNA circles promote yeast ageing in part through stimulating the reorganization of nuclear pore complexes. Dang W, Tyler JK, Schmidt HB, editors. eLife. 2022 Apr 4;11:e71196.

441. Gaillard H, Santos-Pereira JM, Aguilera A. The Nup84 complex coordinates the DNA damage response to warrant genome integrity. Nucleic Acids Res. 2019 May 7;47(8):4054–67.

442. Cheng X, Côté V, Côté J. NuA4 and SAGA acetyltransferase complexes cooperate for repair of DNA breaks by homologous recombination. PLoS Genet. 2021 Jul;17(7):e1009459.

443. Gnugnoli M, Casari E, Longhese MP. The chromatin remodeler Chd1 supports MRX and Exo1 functions in resection of DNA double-strand breaks. PLoS Genet. 2021 Sep;17(9):e1009807.

444. Simsek D, Brunet E, Wong SYW, Katyal S, Gao Y, McKinnon PJ, et al. DNA ligase III promotes alternative nonhomologous end-joining during chromosomal translocation formation. PLoS Genet. 2011 Jun;7(6):e1002080.

445. Deng SK, Gibb B, de Almeida MJ, Greene EC, Symington LS. RPA antagonizes microhomology-mediated repair of DNA double-strand breaks. Nat Struct Mol Biol. 2014 Apr;21(4):405–12.

446. Wang H, Xu X. Microhomology-mediated end joining: new players join the team. Cell Biosci. 2017 Jan 13;7(1):6.

447. Ledermann JA, Drew Y, Kristeleit RS. Homologous recombination deficiency and ovarian cancer. Eur J Cancer Oxf Engl 1990. 2016 Jun;60:49–58.

448. Liu FW, Tewari KS. New Targeted Agents in Gynecologic Cancers: Synthetic Lethality, Homologous Recombination Deficiency, and PARP Inhibitors. Curr Treat Options Oncol. 2016 Mar;17(3):12.

449. Kennedy BK, Pennypacker JK. Drugs that modulate aging: the promising yet difficult path ahead. Transl Res. 2014 May 1;163(5):456–65.

450. Barzilai N, Crandall JP, Kritchevsky SB, Espeland MA. Metformin as a Tool to Target Aging. Cell Metab. 2016 Jun 14;23(6):1060–5.

Chapter 7 Appendix

Origin of replication	Range of ΔOrigin
ARS315 ARS1104.5 ARS417 ARS1513.5 ARS1619 ARS1605 ARS211 ARS820 ARS1614 ARS1223 ARS152 ARS110 ARS418 ARS516 ARS807 ARS1106 ARS1213 ARS1211 ARS1206 ARS1424 ARS1510 ARS922 111kb null ARS1103 ARS432 ARS430 ARS920 ARS719 269kb null ARS1116 ARS1207 ARS1422 ARS1426 ARS1623 ARS913 ARS510 ARS720 ARS1013 ARS1019 ARS1217 ARS1209 ARS1312 ARS1303 464kb null ARS607 ARS806 ARS1114ARS416 ARS518 ARS731.5 ARS415 ARS517 302kb null ARS1220 ARS208 ARS307 ARS919 ARS605 ARS710 ARS718 ARS1528 ARS1621 ARS1511 ARS108 ARS306 ARS606 ARS1018 ARS1310 ARS1309 ARS428 ARS728 ARS1513 ARS214 ARS202 ARS508 ARS1021 ARS507 ARS731 ARS727 ARS1215 ARS1407 ARS414 ARS1015 ARS1113 1054kb null ARS511 ARS1509 ARS1626.5 ARS1627	0 - 1000
ARS309 ARS1014 ARS305 ARS413 ARS909 ARS805 ARS1109 ARS1320 ARS1307 ARS1323 ARS1008 ARS1106.7 ARS914 ARS1009 ARS1232 459kb null ARS1305 ARS1120 483kb null ARS1506.5 ARS106 ARS437 ARS714ARS514 ARS1526 ARS1512 ARS1226 ARS1325 ARS603.5 ARS729 ARS1332 ARS1006 ARS220 ARS216 ARS1330 ARS1415 ARS1618	1000-2000
ARS417.5 477kb – null ARS406 ARS907 ARS1107 ARS1514 ARS229 ARS707 ARS1005 296kb null ARS107 ARS1018.5 ARS1508 ARS512 ARS207.5 ARS1620.5 ARS717 228kb null ARS1219 ARS815 ARS512	2000-3100

Table 7.1 Range of size of the replication ΔOrigin